STUDIES ON SOME SUPPORTED COBALT(II), NICKEL(II) AND COPPER(II) COMPLEXES OF O-PHENYLENEDIAMINE AND SCHIFF BASES DERIVED FROM 3-HYDROXYQUINOXALINE-2-CARBOXALDEHYDE

THESIS SUBMITTED TO
COCHIN UNIVERSITY OF SCIENCE AND TECHNOLOGY
IN PARTIAL FULFILMENT OF THE REQUIREMENTS FOR THE
DEGREE OF

DOCTOR OF PHILOSOPHY

IN

CHEMISTRY

UNDER THE FACULTY OF SCIENCE

By

SUJA N. R

DEPARTMENT OF APPLIED CHEMISTRY
COCHIN UNIVERSITY OF SCIENCE AND TECHNOLOGY
KOCHI- 682 022, INDIA

APRIL 2002

CERTIFICATE

This is to certify that the thesis entitled *"Studies on some supported cobalt(II), nickel(II) and copper(II) complexes of o-phenylenediamine and Schiff bases derived from 3-hydroxy-quinoxaline-2-carboxaldehyde"* submitted for the award of the Degree of Doctor of Philosophy of Cochin University of Science and Technology, is a record of bonafide research work carried out by Ms. Suja.N.R under my supervision in the Department of Applied Chemistry.

Prof. K.K. Mohammed Yusuff

PREFACE

Transition metal complexes have played a significant role in the enormous growth of the field of catalysis. The reactivity as well as selectivity of transition metal complexes depends on the ligand environment of the metal. So the selectivity towards a reaction can be tuned by using suitable ligands. In spite of the advantages, the application of such metal complexes into large and small scale chemical processes is limited. This is due to their homogeneous nature which makes their separation from the reaction medium and reuse difficult. Attempts made on overcoming the above disadvantages led to the field of study of supporting transition metal complexes. Such supported systems are interesting due to their potential to be used for wide range of application like catalysis, gas purification, enzyme mimics, fine chemical synthesis and phase transfer catalysis.

Homogeneous catalysts have often been found to have limited commercial application on a large scale owing to the economic debts of batch type operation and expense of catalyst recovery and recycle. Anchored catalysts maintain the high selectivity of their homogeneous counterpart for many reactions. By using such anchored catalyst the practical advantage of heterogeneous catalyzed reaction can be utilized along with the advantage of high selectivity characteristics of homogeneous catalyzed reaction. Zeolite encapsulation and polymer supporting are the usual methods employed for heterogenization of homogeneous catalysts. Encapsulation of coordination compounds in porous solids like zeolites combines the characteristics of the support-pore diameter, cavity size and electrostatic potential with the electronic and stereochemical properties of complex and could lead to highly selective formation of certain products with a precise structure.

The thesis deals with our studies on certain zeolite encapsulated complexes and few polymer supported complexes. The thesis is divided into seven chapters. Chapter I of the thesis is an introduction to the field of heterogenized homogeneous systems. Chapter II deals with the preparation and purification of the ligands. The various physicochemical techniques used for the characterization are also discussed in this chapter. Chapter III presents our studies on the synthesis and characterization of zeolite encapsulated cobalt(II), nickel(II), and copper(II) complexes of o-phenylenediamine. Chapter IV of the thesis is on the

preparation and characterization of zeolite encapsulated cobalt(II), nickel(II) and copper(II) complexes of Schiff bases of N,N'-bis(3-hydroxyquinoxaline-2-carboxalidene) ethylenediamine,(QED), N,N'-bis(3-hydroxyquinoxaline-2-carboxalidene)o-phenylenediamine, (QPD), 3-hydroxy-quinoxaline-2-carboxaldehyde hydrazone, (QHD) and N,N'-bis(3-hydroxyquinoxaline-2-carboxalidene)diethylenetriamine, (QDT). Chapter V deals with the synthesis and characterization of polymer supported cobalt(II), nickel(II) and copper(II) Schiff base complexes. The catalytic activity studies using the zeolite encapsulated complexes and a comparison with their neat analogues are presented in Chapter VI. The final chapter, Chapter VII is divided into two parts: the Part I is on the kinetic study of the oxidation of catechol to o-benzoquinone, (using the neat as well as zeolite encapsulated copper complex of o-phenylenediamine), Part II is on the kinetic study using the neat as well as zeolite encapsulated copper complex of o-phenylenediamine in the oxidation of 3,5,di-tert-butylcatechol to 3,5,di-tert-butyl-1,2-benzoquinone.

CONTENTS

SUMMARY AND CONCLUSIONS

CHAPTER I

INTRODUCTION

1.1 GENERAL INTRODUCTION

Catalysis is an area of research which still continues to be a premier frontier area of chemistry. It plays a key role in modern chemical technology; in fact, it is the backbone of chemical industry. During the last three decades, there has been a shift from phenomenological approaches in this field to structural and mechanistic investigation at the molecular level using a powerful combination of instrumentation, quantum mechanical calculation and computational methods.

Chemical industries are often criticized for the environmental problems, they create. With further advance of catalysis science and engineering, chemical technologies are expected to become more safe and pure ecologically and consume less energy and raw materials. Catalytic technologies are now extensively used for the purification of waste gases and water from chemical industry. Furthermore these technologies used in the industries provide us with various materials, fuels, fertilizers, medicines and food additives.

Wonderful example of catalysis in life process are given by biological catalysts called enzymes, which are responsible for most complicated chemical reactions in living systems. With better

1

understanding of mechanism of enzymatic catalysis new non-biological catalyst mimicking enzymes can be developed and used as medicines and as substituents of enzymes in biotechnologies.

In catalytic reactions the key role is played by chemical interactions of reactant molecules with definite functional groups (active sites) of homogeneous, heterogeneous or biological (enzymes) catalysts. These interactions, which are neither too strong nor too weak, facilitate the rupture of the chemical bonds in reactants and thus lead to decrease in activation energy for the catalytic reaction route in comparison with the non-catalytic one.[1] More and more, new ideas emerging from basic research in catalysis promise break through that may change the profile of industries in future.

1.2   HOMOGENEOUS CATALYSIS BY METAL COMPLEXES

The most impressive examples of catalyst designs can be found today in the area of homogeneous catalysis by metal complexes.[2-4] An important role in catalysis by metal complex is played by elementary reactions such as oxidative additions of reactants, reductive elimination of products, as well as by numerous but well classified rearrangement of atom and chemical bonds in the coordination sphere of metal atoms.[5] This has demonstrated simultaneously the features of an experienced science and fine art. Thus all reactions catalyzed by metal complexes proceed through a sequence of some simple transformation catalyzed by metal complexes and is associated with the changes in oxidation state of the central metal atom, its coordination number and the nature of the ligand surroundings.

There are numerous examples of reactions catalyzed by homogeneous transition metal complexes. For example, palladium complexes have been used as catalysts for the conversion of CO to CO_2 (water gas shift reaction) and for the synthesis of glycols, H_2O_2 etc. An example of homogeneous process used in the industry is the Oxo-process using the catalyst $Co_2(CO)_8$. The process is used for the hydroformylation of olefins in the presence of CO and H_2 to obtain the aldehyde.[6] Another example is the development of Wacker process for the production of acetaldehyde from ethylene which also makes use of the palladium catalyst.[7] Recently many new chiral Schiff base complexes have been synthesized and have been used in asymmetric synthesis. A chiral Schiff base complex of copper is used for the asymmetric cyclopropanation of styrene.[8] Enantioselective ring opening of meso aziridines has been catalyzed by tridentate Schiff base chromium(III) complexes derived from 1-amino-2-indanol.[9] Asymmetric cycloaddition reaction using chiral transition metal Schiff base complexes have been studied by Jacobsen *et al.*[10] Enantioselective electrocatalytic epoxidation of olefins, such as cis-stilbene, trans-stilbene and styrene by chiral manganese Schiff base complexes has also been studied.[11]

The main disadvantages of such homogeneous transition metal complex catalysts are that they cannot withstand high temperature and they cannot be separated from the reaction. So there is a greater interest for heterogenizing such homogeneous metal complexes.

1.3 HETEROGENIZATION OF HOMOGENEOUS CATALYSTS

Heterogenization of homogeneous catalysts is a very interesting and relatively new area of research. Heterogenization is a term which is often used to refer to the process of immobilizing homogeneous transition metal complex to an inert polymer or inorganic support. When metal complexes are anchored to solid surface, it is possible to prepare structurally organized catalytically active sites. Such complexes exhibit much higher activity and selectivity when compared to structurally disorganized active sites present in their homogeneous counter parts. Activation of small molecules like dioxygen, CO, NO, etc. has been achieved by using heterogenized homogeneous catalysts. Nature performs the important task of uptake, activation and utilization of small molecules by means of metalloenzymes and proteins. The activation of dioxygen involves change in the oxidation state of both metal and the small molecules. Oxygen is reduced from coordinated dioxygen to superoxo or peroxo species. Complexes with σ-donating ligands are most suitable for this. In homogeneous medium the dioxygen capability of the metal complex decreases by forming μ-oxo complexes. Such deactivation is avoided by heterogenizing the homogeneous catalyst since the active metal centers are isolated and chances of deactivation are minimized.

Inorganic supports usually employed for anchoring metal complexes are silica, alumina, zeolites and clays. Organic supports employed are mainly polymers such as polystyrene, poly(4-vinyl pyridine) etc. Inorganic anchored and polymer anchored catalysts are sufficiently different from each other in chemical and physical properties.

Polymer supports possess enough flexibility to permit interaction of polymer bound anchoring groups with the metal complex. Such catalysts are not susceptible to poisoning by impurities, since the catalytic sites are protected by the polymer matrix. They can maintain their catalytic activity over a wide range of concentration. The ability to maintain virtually any desired concentration enables direct control of rate of reaction. Furthermore, selectivity may arise from the steric hindrance of the chemical environment of the polymer matrix. Some polymer metal complex contains incomplete complexes due to steric hindrance. In other case the coordinate bond between the polymer ligand and metal ion is relatively weak and substrate coordinates with high frequency. Chain decomposition of substrate proceeds rapidly because the concentration of the catalytic site is locally enhanced in polymer anchored metal complex systems.

Inorganic supports are known to have several advantages over other supports. They have a rigid structure which circumvents the deactivation process like intermolecular condensation and chelation by multiple anchored ligand coordination.[12] Better control over short-range interactions and better uniformity of distribution of ligand sites can be achieved in these cases. Thermal stability of the anchored complex catalysts is dependent mainly on the stability of metal complex. Anchored catalysts are known to act as bi-functional catalysts. One of the catalytic functions in these systems is associated with the support. For example, zeolite plays the role of support and as one of the active component in the hydroisomerisation catalysts. The other active component is the platinum metal, which in this case functions as

5

hydrogenation component. The support acts as the acidic isomerization component in the hydro-isomerization reaction.

Inorganic anchored catalysts have the unique potential to tailor the catalyst structure to maximize selectivity and activity due to its preparative flexibility and stability. Among the various inorganic supports used, zeolites are particularly interesting since they themselves are active for certain reaction and are relatively rigid inorganic matrices with cavities and channels of molecular dimensions of different sizes and shape. This porous structure provides the shape selectivity for certain reactions.

1.4 ZEOLITES

Zeolite was discovered by Swedish scientist Axel Frederick Cronstedt. When he heated the new mineral he discovered gas bubbles were released and he named it as zeolite (meaning boiling stone.) The zeolites have intracrystalline space. These spaces are occupied by water molecules which can be removed by heating. The general formula of the zeolite is given as $M_{x/n}(AlO_2)_x(SiO_2)_y.wH_2O$. The M^{n+} cation neutralize the charge carried by the tetrahedral framework aluminium.[13] Zeolites are thus a class of crystalline aluminosilicates containing silica and alumina tetrahedra joined through oxygen bridges.
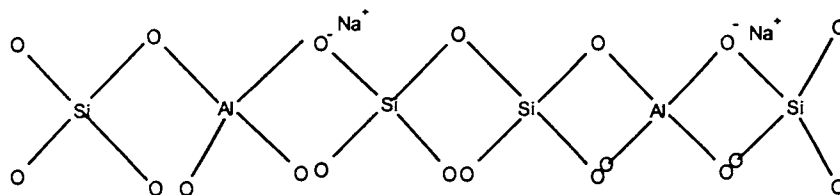
Figure I.1 Schematic representation of SiO_4, AlO_4^- Tetrahedra units in zeolites

When the tetrahedral silica framework is substituted by trivalent aluminium ion to form the zeolite, the aluminium ion gains an excess negative charge thus creating Bronsted acid sites which is compensated by charge balancing cations such as H^+, Na^+ etc (Figure I.1). The formation of the zeolite framework is considered to be as a result of interaction of some initial set of molecules such as acid and $Si(OH)_4$, $Al(OH)_3$, NaOH and H_2O, which yield more complex molecular structure that build the zeolite framework. Stable fragments of the framework correspond to such sequence of interactions of initial molecules which ensures a minimum energy of whole molecular system with a given chemical composition.

60 atom sodalite cage
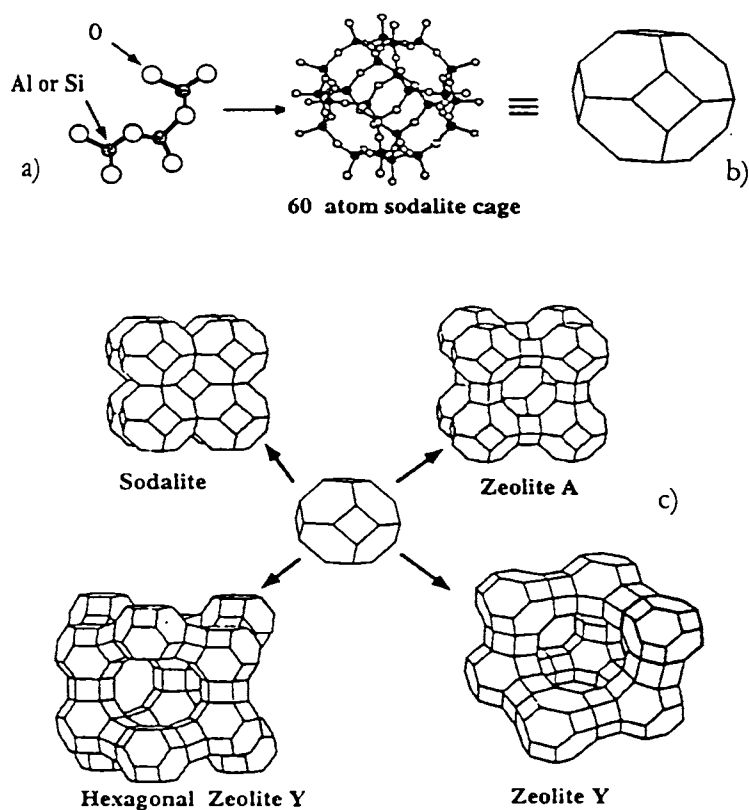
Figure I.2 a) SiO_4, AlO_4^- Tetrahedra units b) Sodalite unit

c) Zeolite A and Zeolite Y
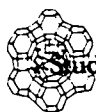
There are large varieties of zeolites present. Zeolites A, X, Y are a group of zeolite which belongs to the faujasite type of zeolites. The aluminosilicate framework of zeolite A contains two types of polyhedra, a simple cubic arrangement of eight tetrahedra, (D4R) and other a truncated octahedron of 24 tetrahedra (sodalite unit). The zeolite X and Y contain a D6R secondary building units (double 6 ring, containing twelve silica alumina tetrahedral) and a sodalite unit. The sodalite unit has six 4-membered ring and eight 6-membered rings. Zeolite A is formed when the sodalite units are joined through the 4-membered ring (square) faces and Zeolite X, Y are formed by joining of the hexagonal 6-membered faces of sodalite unit. Zeolite X and Y differ in their Si/Al ratio which varies from 1.5 to 3 for zeolite Y and 1 to 1.5 for zeolite X. Zeolites have well defined pore system. The cavity of the sodalite unit is known as the β-cage while the large cavity (supercage) formed by the joining of the sodalite unit gives rise to the α cage. The α cage diameter for zeolite Y is 13A° and the α cage aperture is about 8 A°. (see Figure I.2)

There are five common positions occupied by the cations in zeolites. These are represented in the Figure I. 3
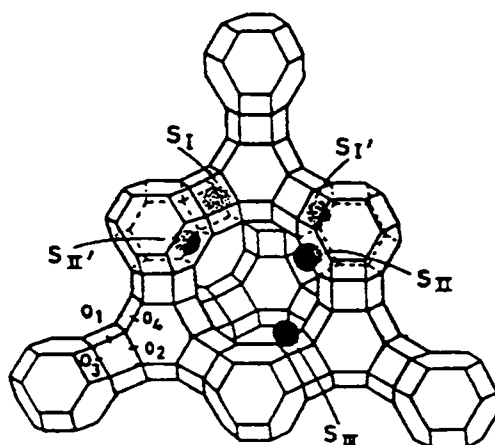
Figure I.3 Cation positions in zeolite Y

Site I-Centre of D6R

Site I'-Inside of β-cage adjacent to D6R

Site II'- Inside of sodalite cage at the centre of single -6-ring

Site II-Near the single 6 ring but lies outside the sodalite in the large cavity

Site III-Wall of the large cavity(12 ring aperture)

1.4.1 Catalysis by zeolites

Zeolites as well as the metal exchanged zeolites are used on a vast scale for separation of gases, for softening hard water and as catalyst in the petroleum and chemical industry. The most important use is in shape selective catalysis.[14-17] Isomerisation and alkylation reactions are few examples, in which shape selective property of zeolites has been made use of. Zeolite X, zeolite Y and mordenite are used for the synthesis of several organic compounds.[18-20] Zeolites are also employed

for carrying out certain nucleophilic substitution reactions of aliphatic compounds. For example, zeolites are used in the production of methyl amines from methanol and ammonia. The selectivity towards dimethylamine was increased to 73% when using Na-mordenite treated with $SiCl_4$ (was used).[21] Acetalisation, ester formation, transesterification are also catalysed by acid zeolites.[22] Electrophilic substitution of aromatics is another reaction catalysed by zeolites. Aromatics such as toluene, phenol and heteroaromatics can be acylated using carboxylic acids, acid anhydride or acid chloride.[23]

Several addition and elimination reactions such as dehydration of alcohols, ethers and hydration of olefins are carried out using zeolites.[24] Iron incorporated into ZSM-5 zeolites is active in methanol conversion and in toluene alkylation. Transition metal incorporation via ion exchange is known to influence the acidity of zeolite. These metal exchanged zeolites catalyze certain important reaction. For example, cobalt exchanged and nickel exchanged zeolites are active for n-butene isomerization. Cadmium, zinc, cobalt and nickel exchanged zeolites bring about the oligomerization of olefins. Acetylene hydration is catalyzed by late transition metal cation exchanged zeolites.[25] There are several reports of oxidation reactions[26] catalyzed by zeolites. Yu and Kevan studied the partial oxidation of propylene to o-acrolein over Cu^{2+} exchanged X and Y zeolites and mixed Cu^{2+}/alkali and alkaline earth exchanged zeolites.

Another application of zeolites is in the light induced electron-transfer mechanisms[27] to mimic artificial photosynthesis. Several studies to understand the influence of cation size in rearrangement and disproportionation of alkyl-dibenzyl ketones have been carried out. The selectivity of products in these cases was influenced by both the zeolite

10

structure and the nature of cation present. Zeolites are also employed as phosphate substituent in detergents and as absorbents for the separation and purification of substances. New potential application of zeolites is in semi conductor, optical sensor technology,[28] optical storage devices and as components of plastics.[29]

In short, zeolites have been used for the following potential applications. Improvement of existing process can be achieved by simple exchange of conventional catalysts. By using zeolites, commercially viable reactions can be introduced in industry which has been unsuccessful previously owing to insufficient activity, selectivity and catalyst life. Another potential application is heterogenization i.e., immobilization of homogeneous catalyst to avoid separation problem. Thus zeolites stand for clean chemistry and for protection of our environment.

1.5 ZEOLITE ENCAPSULATED METAL COMPLEXES

The supercages (α cages) of the zeolite catalyst serve as a sort of reaction flask with molecular dimension for encapsulation of metal complex. The potential for coupling the shape selectivity associated with well defined cages and channels of zeolite with the reactivity of metal complex makes these molecular sieves particularly attractive as active solid supports. The distinct advantage of zeolite over conventional support materials is that a metal complex can be physically trapped in the pores and not necessarily bound to the oxide surface. Another advantage of zeolites is the high thermal stability, well defined and large internal surface area and potential to impose size and shape selectivity on the

product distribution due to the molecular sieving effect. Zeolites supports have their own disadvantage like pore plugging poisoning, migration, leaching and structural defects involving reactants, products, catalytic guest and zeolite host.

Transition metal complex encapsulated in zeolite contains in its first coordination sphere one or more ligands other than lattice oxide ions of the zeolite framework. Depending on whether or not lattice oxide ions is in the first coordination sphere, the zeolite can be considered as an anionic ligand or as an anionic solvent. Zeolite guest molecules are referred to as "ship in a bottle" complexes.

There are different methods adopted for the preparation of zeolite encapsulated metal complexes. A wide variety of metal clusters, organometallic compounds and coordination compounds have been encapsulated in a range of different zeolite hosts. Different methods used for the encapsulation of transition metal complexes are

1.5.a Flexible ligand method

In this method a multidentate ligand diffuses into the zeolite pores where it coordinates with previously exchanged metal ion.[30-34] This approach is based on the principle that free ligand can enter the cavities easily as they are flexible enough to pass through the restricting windows. Many of the zeolite encapsulated salen complexes are prepared using this method.
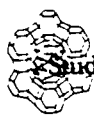
1.5.b Zeolite synthesis method

This method involves the incorporation of transition metal complexes by synthesizing the molecular sieve structure around the preformed complexes.[35-38] Conditions for this method are the stability of the complex under conditions of zeolite synthesis and sufficient solubility in synthesis medium to enable random distribution of the complex in the synthesis mixture and also in the final zeolite.

1.5.c Template synthesis.

This method involves the diffusion of ligand precursor into the zeolite pores where they assemble around an intrazeolite metal ion that acts as a template.[39-41] This is the method adopted for the preparation of phthalocyanine complexes by reacting transition metal exchanged zeolite with 1, 2 dicyanobenzene at 250°C.

1.5.1 Zeolite encapsulated metal phthalocyanine complexes

One of most stable and well characterized intrazeolite organometallics are the phthalocyanine complexes[42-44] of transition metals. The complexes are synthesized by ship in a bottle method.[45] It involves the introduction of metal ion via ion exchange or pre-adsorption of a labile metal complex, such a carbonyl or metallocene, followed by reaction with 1, 2 dicyanobenzene at temp from 250°C to 350°C. Phthalocyanine complexes with almost all of the transition metal complexes have been studied. Cobalt phthalocyanine in zeolites[46] and

13

copper[47], manganese and nickel[48] and ruthenium[49] and rhodium phtalocyanines in the cavities of faujasite, and VPI – 5, and zeolite EMC-2 etc. are some of the complexes studied. The reaction takes place as follows.

$$M^{2+}Y + 4DCBZ + H_2O \rightarrow MPcY + \frac{1}{2} O_2 + 2H^+$$
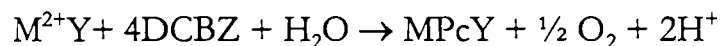
Water is an essential component for complexation since it is the electron source in this reaction. So complexation does not take place, if the zeolite is completely dehydrated. The surface complexes are removed by soxhlet extraction with acetone, pyridine or DMF. Uncomplexed transition metal ions occupy cation position in zeolites.[50] Bronsted acid sites produced during the complexation step and the uncomplexed metal ions present can interfere in catalytic application by catalyzing undesirable side reactions. The synthesis of phthalocyanine molecule by adsorption of metal carbonyl can be achieved by two methods, either by decomposing the metal carbonyl by thermal or photochemical process or by direct ligand exchange of the carbonyl. It is reported that by using the first method only only one phthalocyanine complex is formed per supercage.

Several substituted metal phthalocyanine have also been synthesized in the supercage of faujasite with an aim to enhance the stability of the complex. Bulky substituents protect the meso atom of the phthalocynaine ring. Introduction of election withdrawing groups[51] increases the catalytic activity. Increased activity has been observed in the case of perfluorophthalocyanins of iron, cobalt, copper and manganese and tetranitrophthalocyanine of iron. Transition metal

exchange levels higher than 40% were found to be necessary for successful encapsulation.[52]

Metal phthalocyanins have also been encapsulated inside large pore materials like MCM-41. The complexes are found to be more stabilized in MCM-41. The complexes retain its planar structure in MCM-41, while they are distorted in zeolite Y.[53] The catalytic performance of novel MPc MCM-41 for cyclohexane oxidation was compared with that of the same unsupported complexes as well as that encaged within Y zeolite. The perfluorophthalocyanine encapsulated in the MCM-41 was found to be more active than unsupported and that encapsulated in zeolite Y. It is more active than the unsupported complex. But the phthalocyanine shows higher activity in zeolite Y. These studies indicate that the void dimensions of the porous host can play a role in the performance of metallophthalocyanines as oxidation catalyst.[54]

1.5.2 Zeolite encapsulated porphyrin complexes

Microorganism transforms substrates into products without wasting reagents and energy. This is accomplished through a complicated interplay of a well defined geometry of an active center and the concomitant positioning of chemical species. Enzymes are formed by proteins with definite and complicated structure. When a metal is the part of the active center of the enzyme, it possesses a well defined coordination and is surrounded by polymeric segments which give a precise shape in the cavity. Development of so called fine chemistry requires the development of new catalyst with sophisticated molecular

architecture like that of enzymes to selectively transform reactant into product with specific structures. Many attempts have been made to imitate natural enzymes by encapsulating a coordination compound in a network of porous solid. An interesting class of enzymes contains a metal coordinated in a porphyrin type ring.[55-56] So the synthesis of zeolite encapsulated porphyrin type complexes combine the characteristics of the pore diameter and electrostatic potential of the support, with the electronic and stereo chemical properties of the complexes and thus are found to mimic enzymes.

Zeolite encapsulated tetraphenyl porphyrins have been synthesized from pyrrole and benzaldehyde by using ship in a bottle synthesis. Such porphyrins encapsulated in zeolites mimic cytochrome P-450. Iron – porphyrins containing electron withdrawing substituent on the β-pyrrole positions are highly active for alkane hydrolysis.[57]

1.5.3 Zeolite encapsulated metal carbonyls

The anchoring and catalytic potential of intrazeolitic organometallics have been extensively studied.[58-61] Hexacarbonyl group VI metals $M(CO)_6$ (M=Cr, Mo, W) occluded in zeolite were efficient for Fischer-Tropsch metathesis, hydrogenation, hydrodesulphurization process etc. Several metallocenes Cp_2Fe^+, Cp_2Cr^+ etc has been encapsulated in zeolites by sorption of $M(CO)_6$ into the faujasite. Treatment of metal carbonyls with arenes in solution gives arene metal carbonyl complexes. $M(CO)_n$ complexes within the void space of faujasite zeolite is an active species for hydrogenation and isomerization of olefins. This has been attributed as due to their ability to coordinate

16

substrates at the expense of Mo-O bonds.[62-63] In this case however availability of open coordination sites does not appear as the rate determining step[64] of the catalytic reaction. The catalytic pathways in the above mentioned case includes the sequential complexation, functionalization and liberation of unsaturated hydrocarbon which constitute one of the most important reaction sequences in catalytic organometallic synthesis. Organometallic complexes are good catalysts for water gas shift reaction, carbonylation of methanol and aromatic compounds.

1.5.4 Zeolite encapsulated metal complexes of Schiff bases and other amines

Schiff base metal complexes represent an important and interesting class of coordination compounds. One of the most studied complexes encapsulated in zeolites is the Schiff base complexes of N,N'-bis(salicylidene)ethylenediimine, commonly referred to as Salen complexes.[65-67] Such ligands are able to diffuse through the zeolite pore and are synthesized by flexible ligand method. Copper, cobalt[68] nickel, iron and manganese complexes of the above ligand have been synthesized.[69-71] Various substituted complexes of the above ligand have also been synthesized .Comparative study of the EPR spectra of the zeolite encapsulated copper(Salen) and copper(5-Cl-Salen) with the neat analogues revealed interesting results.[72] EPR spectra of neat complexes showed broad spectra due to nearest neighbour spin-spin interaction whereas the zeolite encapsulated metal complex showed well resolved hyperfine features indicating encapsulation of monomeric Salen complexes. Molecules absorbed on the external surface exhibit spectra

similar to those of the neat complexes. Calculated ground state molecular orbit coefficients suggest an increase in the in-plane covalency of the copper ligand bond and depletion of electron density at copper on encapsulation thereby facilitating the attack of incoming nucleophiles such as tert-butyl hydroperoxide anion at copper atom.

Zeolite encapsulated copper and manganese complexes of Salen and substituted Salen or octaazamacrocylic ligand have been synthesized. Such catalysts are found to be active for the catalytic oxidation of methane to methanol. Methane conversion is of great economic potential due to the large reservoir of natural gas. Furthermore, it is of great importance from the environmental point of view due to the removal of a gas which contributes to the global warming.[73]

Five coordinate Schiff base complexes have been prepared and characterized in both EMT type zeolite and zeolite Y. The Schiff bases were bis(3-salicylideneamino)propylmethylamine and bis(salicylidene)-ethylenediamine. The study indicated that formation of square planar geometry was very difficult in EMT while 6-coordinate Co(smdpt) with normal coordination is easily formed. This study shows that addition of tertiary nitrogen in the ligand provides the donor strength required to remove the Co^{2+} from the zeolite coordination environment. This is reported to be the first example of chelating multidentate ligand inside a zeolite cavity and the first example of a single coordination compound that displays structural difference when encapsulated in two different zeolite cages.[74] Similar studies were done for tetradentate cobalt(II) complexes of bis(acetylacetone)ethylenediimine [acacen] and bis(pyridene-2-carboxaldehyde)ethylenediimine [pyren], bis(salicyl-

acetone)methylnitrilodipropyldimine [smdpt] and it was found that support influences the structure of Schiff base complexes.[75]
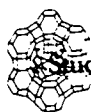
Another most studied system is the bipyridine complexes encapsulated in zeolites. The [(Ru^{II}(bipy)$_2$complex are prepared by allowing zeolite NaY, exchanged with [(Ru^{III}(NH$_3$)$_4$]$^{3+}$ to react with bipyridine and then reducing it.[76-77] Iron, manganese and copper bipyridyl complexes have also been extensively studied and they possess several interesting properties[78] especially in photochemical reactions and thereby in solar energy conversion schemes. The bisterpyridine complex, [Ru(tpy)$_2$]$^{2+}$ in free solution have a very short excited state lifetime and is practically nonluminiscent. The entrapment within the zeolite super cages results in dramatic increase in emission intensity and excited state lifetime at room temperature.[79] Ru(bpy)$_3$$^{3+}$ molecules encapsulated within the zeolite brings about the oxidation of H$_2$O to O$_2$.[80] In this case intramolecular electron transfer lead to the formation of a hydroxylated bipyridine radical and the metal is reduced to ruthenium(II). The slow dissociation of this complex to Ru(bpy)$_3$$^{2+}$ and hydroxyl radical takes place and this further reacts with unreacted Ru(bpy)$_3$$^{3+}$. This is an example which indicates that it is possible to isolate reactive molecules in zeolite cages and this leads to the observation of a chemical pathway that do not occur in solution.[81] Thus in zeolite encapsulated complexes the guest-host interaction retard the energy wasting election transfer reaction of initial photoproducts.[82] The bipyridine complexes of cobalt, [Co(bipy)$_3$]$^{2+}$ have also been synthesized and encapsulated in zeolite and characterized.[83-84]

Several amine complexes with ligands like ethylenediamine and ammonia[85-87] as ligands have also been encapsulated in zeolites. The

cobalt ethylenediamine complexes encapsulated in zeolites are found to bind O_2 reversibly and the presence of paramagnetic oxygen adducts in cobalt exchanged X and Y indicates that low spin $[Co^{III}(en)_2O_2^-]^{2+}$ adduct is formed in the large cavities and is stable in the presence of O_2 upto 70°C.[88] Cobalt amine complexes with NH_3, methylamine or n-propylamine (as ligands) also bind oxygen reversibly in the zeolite.

A copper(II)pyridine complex has also been encapsulated in the zeolite Y. The complex was found to be easily reduced to Cu(I) under vacuum at 200°C and reoxidized to Cu(II) upon exposure to O_2 in its reduced state.[89] In the oxidative coupling of 2,6-dimethylphenol using the above catalyst the predominant product was the polymerized compound. The copper(II)pyridine O_2 systems in the homogenous state are useful for oxidative coupling reactions of acetylene, aromatic amines and phenols.[90] Tris(1-nitroso–2–naphthalato)manganese(III) and (2-nitro-2-naphthalato) manganese(II), copper(II) and Zinc(II) complex in zeolite Y are found to be active for the oxidation of phenol.[91]

Zeolite encapsulated vanadium complexes e.g.V(IV)picolinate complexes, are reported to be active catalyst for oxidation reaction. These complexes were prepared by treating $VO^{(2+)}$ NaY with molten picolinic acid. This on treatment with urea – H_2O_2 adduct in methylcyanide generate peroxo vanadium species. This is the active intermediate for several oxidation reactions. In comparison to the homogeneous counter part these complexes showed preferable oxidation of smaller substrate in competitive oxidations, increased selectivity of the oxidation of terminal methyl groups in isomeric octanes and preferable formation of alkyl hydroperoxides in alkane oxidation.[92]

Another complex synthesized in zeolite is copper-dicyanoanthraquinone by ship in a bottle method. From the above study it was found that hydrogen can significantly accelerate the charge transfer kinetics[93] in the above complexes. Copper(II)thiazolylhydrazone[94] complexes and cobalt(II)phenanthroline and 8-hydroxy phenanthroline complexes were found to be good catalysts for catalytic hydroxylation of phenol. The investigation of redox behaviour of cobalt, nickel and tellurium phenanthroline complexes by cyclic voltammetry in acetonitrile indicated a similar behaviour to that of the neat complexes in solution. The bis(bipyridine) nickel complex were active towards reduction of organic halides.[95] Cobalt(II)methyl isocyanides complexes were encapsulated in zeolite. The complex is found to be six coordinate with D_4h symmetry. The study based on this indicated that it is possible to form fully coordinated complexes within the large cavities of the zeolite and that the framework oxygen need not be in the first coordination sphere.[96]

Dinitrogen complexes of ruthenium and osmium in zeolite Y were prepared to study the ideas of providing a model which emulates the low temperature fixation of N_2. $(Ru(II)NH_3N_2)^{2+}$ was synthesized by first exchanging $(Ru(II)NH_3NO)^{3+}$ and reacting this with hydrazine. Zeolite encapsulated bis(dimethylglyoxime) complexes are known to catalyze a variety of organic reactions, especially for the selective oxidation of propene.[97]

Several aminoacid complexes have also been encapsulated in zeolites.[98] Zeolite encapsulated copper histidine complexes were studied as mimics of natural enzymes.[99] Copper complexes of amino acids like glycine, histidine, alanine, serine etc in faujasite has been investigated and

21

their potential for oxidation of alcohols, alkanes and alkenes has been studied

Even though many cationic complexes have been prepared inside the zeolite, very few examples of anionic complexes are known. One example studied is the anionic cobalt(II) cyanide complex inside zeoliteY. This complex is stable in the presence of water and can even be prepared in aqueous solution. This complex can act in reversibly binding oxygen. The cyanide ligand is very stable to oxidation and the zeolite prevents dimerisation to form the μ-peroxo complex.[100]

1.6   APPLICATIONS OF ZEOLITE ENCAPSULATED COMPLEXES

Zeolite encapsulated metal complexes have wide range of applications.[101-105] An important advantage of zeolite molecular sieve over other support is that, it is possible to decide which substrate molecules can enter and reach the active site by choosing a suitable combination of molecular sieve and solvent.

Catalytic applications of zeolite encapsulated metal complexes are immense. They are used as catalyst for a number of chemical reactions which are used industrially. For example oxidation of p-xylene to p-toluic acid, which may be used for the preparation of industrially useful terephtahlic acid was carried out using copper and manganese salen complexes encapsulated in zeolite.[106] Selective oxidation of olefins to form epoxide has been carried out using cobalt phthalocyanine encapsulated in zeolite Y.[107] This study showed that encapsulation besides favoring dispersion and preventing auto oxidation, combines its catalytic activity with favorable influences exerted by matrix. Oxidation

22

of cyclohexanone and cyclohexane to adipic acid which is used in industrial production of artificial resins (nylon), urethane foams, acidulant in baking powder etc. has also been carried out using iron phthalocyanine in Zeolite Y.[108] Methyl trioxorhenium encapsulated in zeolite Y is used as a tunable olefin metathesis catalyst.[109] Rhenium oxo complexes are an exciting family of organometallics exhibiting versatile catalytic behaviour. Metathesis is an attractive reaction from which undesired products must be recycled.

Oxy halogenation like oxychlorination and oxybromination under near ambient conditions of benzene, toluene, phenol, aniline, anisole and resorcinol using copper, iron and cobalt encapsulated in zeolite X,Y,Z.[110] Hydrochloric acid and alkali chloride/bromide were sources of halogens and H_2O_2 and O_2 were used as oxidants. Salen and substituted Salen Schiff base complexes of cobalt(II) catalysis the oxidation of p-cresol into p-hydroxy benzaldehyde. Zeolite encapsulated complexes have been referred to as enzymes or model compounds for enzyme mimicking. Iron porphyrin is found to mimic cytochrome P-450. The catalytic properties of zeolite encapsulated transition metal complexes have been explored in various selective oxidation and hydrogenation reactions.

Difference in activity and interesting selectivity changes are also observed upon immobilization. When oxidation of cyclohexane and cyclodecane mixture with iodosobenzene was studied it was found that cyclohexane is preferentially oxidized.[111] An example of regioselectivity is that, over free iron phthalocyanine the oxidation of n-octane occurs with equal selectivities in 2,3,4 position while in the zeolite encapsulated one oxidation occurs at 1-position. An example of stereoselectivity is

23

that in the case of norbornene as reactant, the C-H bond which extends along the molecular axis is preferred for oxidation.[112] Zeolite encapsulated metal complexes are also used in hydrogenation reactions.[113-114] Selective oxidation of styrene using zeolite encapsulated manganese salen complexes has been reported.[115] Schiff base complexes with five coordinate cobalt are used as dioxygen activating sites in zeolites.[116]

Another application of zeolite encapsulated metal complexes is the use in zeolite modified electrodes. For e.g. Ni(bpy)^0 encapsulated in Y-type zeolite can be selectively implicated in the electro-assisted catalytic reduction of organic halides. This indicates that Ni(II)/Ni(0) redox process is taking place during the reaction and zeolite framework serves as a relay between the host species.[117]

Enantioselectivity is very important in organic synthesis. For many applications especially for biochemical and pharmaceutical only one of the enantiomers is required. Asymmetry cannot be created in a symmetric environment. In chiral metal complex catalyst, the alkene is attached to the metal preferably in one orientation controlled by the chirality of the ligands and cis addition of hydrogen takes place selectively to one face of the double bond leading to a single enantiomer. The advantage of chiral metal complex over chiral stochiometric reagent is that a single molecule of chiral catalyst can bring about the asymmetric synthesis of a large number of product molecules. They can also be recovered and reused if they are hetereogenized by supporting them to polymer or by encapsulating them in zeolites.

Several zeolite encapsulated metal complexes are used in enantioselective synthesis. Rhodium and nickel complexes with nitrogen-based chiral ligands were introduced into a modified Y zeolite. These complexes were used as catalyst for the enantioselective hydrogenation of N-acyl-dihydrophenylalanine derivatives. The zeolite was found to show a cooperative effect on the reaction rate and enantioselectivity of the reaction, increasing the enantiomeric excess.[118]

Zeolite as support has therefore the following advantages like;

1. Metal ions may be uniformity distributed and polynuclear clusters can be avoided.

2. The dimensions of the cages are roughly equivalent to that encountered in enzymes making their comparison easy.

3. They can function both as a solvent and the counter-ion in the formation of metal complexes.

However, there are certain disadvantages for zeolite to be used as a support

1. The size of the ligand is restricted by the size of the window in a zeolite.

2. Encapsulation is generally restricted to cationic complexes, since the zeolite structure is anionic.

3. Another problem is the diffusion, when many of the cavities are nearly filled by large complexes.

1.7 POLYMER SUPPORTED METAL COMPLEXES

Chemistry of polymers containing metallochelate units (PCMU) have received much attention in the last three decades.[119-124] It is a multidisciplinary field involving the efforts of specialists in various fields such as catalysis, polymer, coordination, bioinorganic and analytical chemistry. Polymers containing metallochelate units are used in almost all fields of human activity. For example, in healthcare and pharmacology (for administering of desired metals into organism, such as iron in the case of asiderotic anaemia), removal of harmful particularly radioactive metals in atomic industry and hydrometallurgy (concentration and separation of rare metals and radioactive isotopes) and catalysis (preparation of highly effective immobilized catalysts).

Polymer containing metallochelating units are high molecular weight compounds that incorporate metallochelate cycles. The polymer chain makes them behave like high molecular weight compounds and the presence of metal ion in them is responsible for properties typical of given metal ion. The combination gives them properties related to biological catalytic activity.

Attempts have been made to synthesize metal complexes and compare its activity with the simple monomeric species. The argument for the above study is that the structure within the coordination sphere is uniform in a polymer complex and a monomeric complex and their reactivity ought to be the same. However the steric effect, which is determined by the conformation and density of a polymer ligand chain play a role in its catalytic activity. Systems modeling biological systems
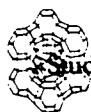
such as haemoglobin chlorophyll and vitamin B_{12} are of great importance in order to construct artificial system for practical use.

Polymer bound metal complexes may be classified into two types according to the mode of attachment to the polymer chain.[125]

1. Coordinative polymer bonded metal chelates.

2. Covalent polymer bonded metal chelates.

1.7.1 Polymer bound porphyrins and phthalocyanine complexes

Naturally occurring porphyrins containing carboxylic acid functions were used in the preparation of polymer attached porphyrins. A synthetic polymer is able to stabilize porphyrins against oxidation. An example of polymer attached metal complex which is analogues to chlorophyll is Mg-octaethyl porphin in solid (1-vinylimidazole co-styrene). This complex is stabilized against oxidation just as the natural protein in chlorophyll against O_2.[126] Porphyrins attached to polymers have immense potential in the removal of mercaptans and other sulfur compounds from cracked gasoline. Polymer supported porphyrins and phthalocyanines and their carboxylate derivatives are useful as thiol oxidation catalysts.[127,128] Phthalocyanines are related to porphyrins and have the advantage that they are more stable. In phthalocyanine the bridging atom is nitrogen in place of carbon in the porphyrin and the pyrrole residues in a square planar symmetry are replaced by benzopyrrole moieties. Metallophthalocyanine are attached to a polymer support via an axial ligand. In thiol oxidation the amino group of the polymer backbone serves the purpose of the base, and H_2O_2 generated during the process brings out further oxidation. Polymer bound

phthalocyanine is of industrial interest in terms of desulphurization of hydrocarbon streams.

Another application of polymer bound porphyrin complexes is the epoxidation. Manganese(III)tetraphenylporphyrin epoxidise cyclohexane using dioxygen. When mononuclear and dinuclear polymer pophyrins were tested as sensitizer in the photoreduction of fast red with L-ascorbic acid as reducing agent it was found that dinuclear porphyrins were more active than mononuclear ones.[129-131] Polymer bound porphyrins were also used for cyanide ion removal.[132]

1.7.2 Polymer supported metal carbonyls

Polymer supported metal carbonyls can be prepared by the polymerization of monomers containing metal carbonyls and groups which undergo vinyl polymerization. This method is used in the preparation of polymers containing first row transition metal carbonyls. Another method of preparation is refluxing under pressure polymers containing arene π electrons with metal carbonyl. They can also be immobilized using cyclopentadienyl linkages.

Polymer supported metal carbonyls have several applications. For example $Cr(CO)_6$ supported on styrene-divinyl benzene resin has been reported to catalyzehydrogenation of methylsorbate in cyclohexane.[133] Another catalyst prepared by refluxing $Mo(CO)_6$ and polystyrene beads catalyzes the alkylation and arylation of aromatic substrates.[134] Polymer immobilized $(\eta^5$–cyclopentadienyl)cobalt dicarbonyl catalysts has been employed for olefine hydro-formylation and they are also used as Fischer–Tropsch catalyst.[135] Polymer immobilized analogues of

28

$In_4(CO)_{11}PPh_3$ are active for ethylene hydrogenation at 313K and $1x10^5$ N/m^2. Catalysts based on $Co_2(CO)_8$ and phosphinated polymers have shown to possess significant activity for olefine hydroformylation.

Alkene epoxidation reaction is another field where metal complexes supported on polymers find application. Transition metal complexes capable of attaining high oxidation state (e.g. $Mo(CO)_6$) seem to be the best catalyst for the above reaction. Oxomolebdenum(VI) and oxovanadium(V) catalysts supported on polystyrene resins carrying bis(phophonomethyl)amino are found to be active catalysts for the above reaction. Vanadium species are more active for allylic alcohol substrates while molybdenum species are active for cyclohexene.

1.7.3 Polymer supported Schiff bases and other amines

The first polymer supported Schiff base chelate was synthesized on a macroporous glycidyl methacrylate-ethylene dimethylacrytate copolymer. Nucleophilic addition of ethylenediamine led to polymer amine which is condensed with salicylaldehyde to form Schiff base ligand, and this was then with treated with copper(II) and cobalt(II) to form the chelates.[136,137]

Another interesting polymer bound Schiff base nickel(II) chelate was prepared by treating chloromethylated polystyrene and pentane-2,4-dione and then reacting with 1,2-diaminoethane and nickel(II). Such low molecular weight Schiff base chelates are well known for phenol oxidaton reaction. Polymer Schiff base ligands containing a nitrogen atom in the bridge are easily synthesized by N-alkylation from

29

crosslinked chloromethylated polystyrene and low molecular weight N_3O_2 ligand.

Poly(4-vinylpyridene)copper(II) catalyst are active for the oxidation of ascorbic acid, salicylic acid etc. Polymer metal complexes behaves as a polycation in aqueous solution and the reaction is sensitive to charge of low molecular weight species .The electrostatic effect due to the poly-cationic domain of a polymer metal catalyst is predominant in the oxidation of charged substrates.

Polymer supported and zeolite encapsulated Schiff base complexes of biologically impoant ligands like Embelin and 2-aminobenzimidazole has also been studied and their use in catalyzing hydrogen oxygen reaction to give H_2O has been studied.[138]

Synthesis and characterization of polymer supported copper(II), nickel(II), iron(III), zinc(II), cadmium(II) and zinc(IV), molybdenum(V and VI) and uranium(VI) complexes of polystyrene supported Schiff base derived from 3-formylsalicylic acid and o-aminophenol have been reported.[139] Polymer bound Schiff base manganese complexes prepared from polystyrene bound salicylaldehyde and phenylalanine is found to be a good catalyst for the oxidation of cyclohexene, linear aliphatic olefines and styrene by O_2. Mechanism of this oxidation is reported to be a radical chain mechanism.[140] A styrene-divinyl benzene copolymer with (5% and 15%cross linking) containing palladium(II)diaminopropane complexes were found to be active catalyst for hydrogenation.[141]

Polymer bound 2,2' dipyridylamine has been prepared. Like naphthyridine and bipyridine this ligand can be bound to polymer support smoothely.[142] Studies on these complexes revealed that polymer
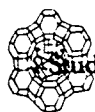
bound dipyridyl amine ligand have important application in quantitative and qualitative removal of metal ions like Fe^{3+} in organic media

1.7.4 Other interesting polymer supported reagents

A polymer carrier with cobalt-carbon bond is synthesized by reacting poly(chloromethylstyrene–co-styrene) with cobaloximes[143] in benzene. The cobalt-carbon bond in this compound is similar to that in coenzyme B_{12}.

Merrifield has demonstrated the use of polymers as supports for chelates and catalysts by demonstrating their use in peptide synthesis. In the above method, the amino acid corresponding to the carboxyl end of a peptide chain is attached to a supporting polymer matrix and the chain is extended to the amino end by coupling with activated aminoacids or peptide regiments.

Polymer supported mixed carboxylic-dithiocarbamic anhydride(PCDA) serves as a new class of solid acylating reagents for the amino groups in different environment. They are characterized by ease of handling, quantitative acyl group transfer, specificity for the amino group, mild reaction condition and ease to recycle. Even though many polymer supports are used, most widely used is polystyrene-crosslinked with divinylbenzene .
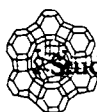
1.8   APPLICATIONS OF POLYMER SUPPORTED CATALYSTS

Polymer bound metal complexes have several applications in analytical chemistry like extraction of toxic metals[144] from drinking water. Metal ions are selectively adsorbed using polymeric ligands which permit the construction of a binding mode with respect to the nature of the metal ion. An example is extraction of about 78% of Uranium from sea water[145] using polyallylamine modified with phosphoric acid and formaldehyde

Polymers containing metallochelate units are stable upto 473-523K. Even small addition of metal ion to cross linked polymers enhances[146] the stability of the polymer and its resistance to organic solvent. For example, thermal stability is increased by immobilizing metallochelates of the β-dicarbonyl and acylhydrazone type on chlorine containing polymers. This property is used in titania containing polymers for the production of various coatings frequently with enamel like surface.[147].

The thermal treatment of polymeric chelates of silver(I), copper(II), titanium(IV) with Schiff bases from β -hydroxy-γ-amines [148] at 140°C enhance softening point and thermostability, and also imparts to them semiconductive properties due to electronic and ionic contributions.

Another application is in organic synthesis.[149]Many organic synthesis can be carried out on polymer support. Advantage of such process is the possibility of catalyst regeneration, automated waste free process, easy extraction of final products and better environmental

control. Such systems can also be used in laser microchemical industries for direct information recording.[150]

Immobilised catalysts couple a high activity of homogeneous catalyst and a good workability of heterogeneous system. For example, a rhodium complex with styrene-crosslinked-DVB containing dipyridine fragments, were found to be effective catalyst for olefine hydrogenation for more than 300 cycles.[151] Schiff base complexes of nickel(II) immobilized on the polyethylene surface are active in alkylene dimerization for over 40 h, whereas a homogeneous analogue loses its useful activity after 2 h.[152] Another application of PCMU is as biologically active substances. A number of metallochelate polymers display fungicidal and antibacterial properties and make many products resistant to attack by mold and putrefactive microorganisms.

Polymeric porphyrins have the interesting property such as visible light energy conversion and catalytic activity due to multiple porphyrin centers. Polymeric cobalt containing porphyrins can be used for photochemical power storage in a norbornadiene quadicyclam system.[153]

A number of highly active and selective asymmetric catalyst are available today. An important asymmetric epoxidation catalyst are the optically active manganese(III)salen[154] complex. They are active in the enantioselective epoxidation of cis-internal alkenes.

Polymer bound metal chelates containing metal phthalocyanines, porphyrins or Schiff base chelates can bring about electro catalysis in fuel cells.[155] The cathodic reduction of O_2 and the anodic oxidation of N_2H_4, H_2, CH_3OH needs active catalysts which must fulfill the following requirements like high open circuit cell voltage, reduced polarization in

33

the working function of cell and long time stability. The most common catalyst is platinum which is expensive and has the disadvantage of being active for the cathodic and anodic side. So mixed potential reduces the half cell voltage. The polymer bound metalchelates have a definite advantage in this case.

Polymer metal complexes exhibit high efficiency in the catalytic decomposition of H_2O_2. Polymer supported metal complexes are found to act as hydrogenation catalysts, although only a few examples have been reported. One example is poly(acrylic acid)rhodium(II)[156] complexes. When a comparison of this polymer supported catalysts was made with that of homogeneous catalyst, the rate was found to be 10^3 times higher in the case of polymer supported complex. Asymmetric hydrogenation[157,158] is catalysed by poly(L-methyleneimine)-ruthenium(III) complexes. In reduction reactions polymer metal complexes are sensitive to moisture and the catalyst decomposes in the presence of air and water. Thus they are carried out under artificial conditions like organic solvent under high pressure and temperature while oxidative reaction proceeds under mild condition.

Another type of reaction is the catalytic hydrolysis of oligophosphates by poly(L-lipine)copper(II)[159] complexes. This complex is active in attacking attacked pentaphosphate exclusively thus producing the orthophosphate as the main product. Polymer metal complexes that can carry O_2 have been reported. Such complexes may be used to isolate pure O_2 from air and they may eventually find application in formation of artificial blood. They can also be utilized as photo responsive materials and develop into electron transfer reagents. Polymer-supported metal complexes are also used as alkene epoxidation chiral catalysts, the

34

concentration on the support so as to block reactant access to support surface. Another approach is to block the hydroxyl surface by silylating agent to form a lipophilic organic layer on the surface.

1.10 SCOPE OF THE PRESENT INVESTIGATION

A search through the literature has clearly revealed that there is a continuing interest in the field of immobilizing transition metal complexes on different supports. Attempts of anchoring metal complexes on different supports are even now extensively studied. Such heterogenized catalysts have advantages and limitations, when compared to their homogeneous counterparts. Exploring the potential of using supported transition metal complexes as catalysts in industrially important reactions is always a challenge for coordination chemists.

Scope of the present investigation involves:

1. Synthesis and characterization of zeolite encapsulated cobalt(II), nickel(II) and copper(II) complexes of *o*-phenylenediamine.

2. Synthesis and characterization of zeolite encapsulated cobalt(II), nickel(II) and copper(II) complexes of Schiff bases derived from 3-hydroxyquinoxaline- 2 -carboxaldehyde.

3. Synthesis and characterization of polymer supported cobalt(II), nickel(II) and copper(II) complexes of Schiff bases derived by

    a. Condensing polymer bound benzaldehyde and *o*-phenylenediamine.

    b. Condensing polymer bound benzylamine and 3-hydroxyquinoxaline-2-carboxaldehyde.

4. Catalytic activity studies of above complexes in phenol hydroxylation.

5. Detailed kinetic study of oxidation of catechol and 3,5-di-tert-butylcatechol with the most active complexes and proposing a possible mechanism for this reaction.

The above mentioned studies have been incorporated in the thesis.

REFERENCES

1. G. K. Boreskov, *Heterogeneous Catalysis*, Nauka, Moskva **(1986)**.

2. A. Nakamura, M. Tsulsui, *Principles and applications of Homogeneous catalysis*, Wiley, New York **(1980)**.

3. C. Masters; *Homogeneous transition metal catalysis*, Chapman and Hall-London, New York **(1981)**.

4. G. H. Olive, S. Olive, *Coordination and catalysis*, Verlag Chemie, New york **(1977)**.

5. R.S. Nyholm, *Proc. 3rd Internat.Congr. Catalysis*, North-Holland Publ.Co, Amsterdam **(1965)**.

6. D. Antolovic, E.R. Davidson, *J.Am.Chem.Soc.* 109 **(1987)** 5828.

7. J. Smidt, W. Hafner, R. Jira, J. Sedlneier, R. Sieber, R. Rulttinger, H. Kojer, *Angew.Chem.* 71 **(1959)** 176.

8. Z. Li, G. Lui, Z. Zheng, H. Chen, *Tetrahedron* 56(37) **(2000)** 7187.

9. Z. Li, M. Fernandez, E. N. Jacobsen, *Org.Lett.* 1(10) **(1999)** 1611.

10. E. N. Jacobsen, S. E. Schaus, A. G. Dossetter, T. F. Jamison, *US Patent*-1999-255480

11. G. Peng, W. K. Yin, *Electrochem.Commun.* 1. 11 **(1999)** 559.

12. L.L. Murrell, *Advanced materials in catalysis*, Academic Press, New York **(1977)**.

13. W.M Meir, D.H Olson.; *Atlas of zeolite structure types*, 2nd edition, Butterwork, London, **1987**.

14. N.Y. Chen, W.E. Garwood, F.G. Duyer, *Shape selective catalysis in industrial applications*, Marcel Dekker Inc., New York **(1996)**.

15. R.J. Argauer, G.R Landolt, US 3 702 886, Mobil Oil Corp, P.B.Weisz, *Pure.Appl.Chem.* 52 **(1980)** 2091.

16. W.F. Hoelderich, E. Gallei, *Ger.Chem.Eng.* 8 **(1985)** 337.

17. N.Y. Chen, W.E. Garwood, *Catal.Rev.-Sci.Eng.* 28 **(1986)** 185.

18. P.S. Landis, P.B. Venuto, *J.Catal.* 6 **(1966)** 245.

19. P.B. Venuto, P.S. Landis, *Adv.Catal* 18 **(1968)** 259.

20. P.B. Venuto, *Chem.Tech.* **(1971)** 215.

21. K. Segawa, A. Sugiywa, M. Sakaguchi, K. Sakurai, *Proc.Int.symp. Acid base catalysis*, Sapporo, Japan **(1988)**.

22. W.F. Hoelderich, M. Hesse, F. Naeumann, *Angew.Chem.Int.Edit.Engl* 27 **(1988)** 226.

23. B.H. Chiche, A. Finiels, C. Gautheir, P. G. Graille, D. Pioch, *J.Org.Chem.* 51 **(1986)** 2128.

24. M. Iwamoto, M. Tajima, S. Kagawa, *J.Catal.* 101 **(1986)** 195.

25. D. Kallo, G.Onyeslyak., *J.Mol.Catal.A:Chem.* 62 **(1990)** 307.

26. D.R.C. Huybrechts, R.F. Pareton, P.A Jacobs, *Chemistry of Microporous Crystals*, Elsevier Science Pub., Amsterdam **(1991)**.

27. J.S. Kruger., C. Loi., Z. Li, J.E. Moyer., T.E. Mallouk, *J.Incl.Phenom.* Plenum Press, New York **(1990)**365.

28. G.A. Ozin, A. Kupermonn, A. Stein, *Angew.Chem.* 101 **(1989)** 373.

29. H.K. Beyer, G. Borbely, P. Miasnikov, P. Rozsa, *Stud.Surf.Sci.Catal.* 46 **(1989)** 635.

30. N. Herron, *Inorg.Chem* 25 **(1986)** 4714.

31. D.E. De. Vos, P.A. Jacobs, *Proceedings from the ninth international zeolite conference*, Boston, 2 **(1994)** 615.

32. K.J. Balkus, A.A. Welch, B.E. Gnade, *Zeolites* 19 **(1990)** 722.

33. S. Kowalak, R.C. Weiss, K.J. Balkus, *J.Chem.Soc.Chem.Commun.* **(1991)** 57.

34. F. Bedioni, L. Roue, J. Devynck,K.J. Balkus-*Stud.Surf.Sci.Catal.* 84-B **(1994)** 917.

35. V.Y. Zakharov, B.V. Ramanovsky, *Vest mask Univ*, Khim Ser 2. 18 **(1977)** 143.

36. B.V. Romanovsky, A.G. Gabrielov, *Stud.Surf.Sci.Catal.* 72 **(1992)** 443.

37. K.J. Balkus(jr), J.P. Ferraris, A. Schade, *J.Incl Phenom.* 14 **(1992)** 163.

38. K.J. Balkus (jr), J.P.P. Ferraris, *J.Phys.Chem.*94 **(1990)** 8019.

39. L.A. Rankel, E.W. Yalyocsik, *US Patent* 4500503, **1985.**

40. L.A. Balkus jr, S. Kowalak, K.T. Ly, D.C Hargis, *Stud.Surf.Sci.Catal.* 69 **(1991)** 93.

41. S. Kowalak, K.J. Balkus jr, *Collect.Czeck.Chem.Commun.* 57 **(1992)** 774.

42. G. Meyer, D. Wohrle, M. Mohl, G. Schulz-Ekloff; *Zeolites* 4 **(1984)** 30.

43. N. Herron, G. Stucky, C. Tolman; *J.Chem.Soc.Chem.Commun* **(1986)** 1521.

44. A.G. Gabrieloc, A.N. Zakharov, B.V. Romanovsky, O.P.Tkachenko, E.S.Shpiro, K.M.Minachev, *Koord.Chem.* 14 **(1988)** 821.

45. S. Schulz-Ekloff and S. Ernst, "*Handbook of Heterogeneous Catalysis*", G. Ertil, J. Knozinger and J. Weitramp(Eds), Wiley-VCH **(1997)** 374.

46. E. Paez-Mozo, N.G. Abriunas, R. Maggi, D. Acosta, P. Ruiz, B. Delmon. *J.Mol.Catal.* 91 **(1992)** 251.

47. K.J. Balkus Jr, J.R. Ferrarris, *J.Phy.Chem.* 94 **(1990)** 8019.

48. B.V. Romanosky, A.G. Gabrielov, *J.Mol.Catal.* 74 **(1992)** 293.

49. F. Bedioui, L .Roue, l. Gaillon, J. Devynck, S. L .Bell, K.J. Balkus Jr *Prepr.Div.Petrol.Chem*, ACS38, 3 **(1992)** 529.

50. H.G Karge, H. Pferfer, W. Holderich, *Stud.Surf.Sci.Catal.* Elsevier, Amsterdam, 84B **(1994)** 925.

51. K.J. Balkus Jr., A.G. Gabrielov, S.L. Bell, F. Bediou, L. Rone, J. Devy, *Inorg.Chem.* 33 **(1994)** 67.

52. A. Elvera, C. Avelino, F. Vicente, G. Hermenegildo, P. Jaimo, *Appl. Catal A.*181(2) **(1999)** 305.

53. S. Ernest, M. Selle, *Microp.Mater.* 27 **(1999)** 355.

54. P. E. Ellis Jr, J. E. Lyons, *Coord.Chem.Rev.*, 105 **(1990)** 181.

55. Y. Chan, R. Wilson, ACS *Prepr.Div.Petrol.Chem* 33 **(1988)**453.

56. N. Nakamura, T. Tatsumi, H. Tominaga, *Bull.Chem.Soc.Jpn.* 63 **(1990)** 3334.

57. S. Deshpande., D. Srinivas, P. Ratnasamy, *J.Catal.*188(2) **(2000)** 261.

58. D.C. Bailey, S.H. Langer, *Chem.Rev.* 81 **(1981)** 109.

59. J.E. Maxwell, *Adv.Catal.* 31 **(1982)** 32.

60. B.C. Gates, L. Guczi, H. Knozinger, *Metal cluster in catalysis*, Elsevier, Amsterdam **(1986)**.

61. J. Goldwasser, S.M. Fang, M. Houalla, W.K. Hall, *J.Catal.* 115 **(1989)** 3.

62. Y. Okamoto, H. Kane, T. Imanakai, *Catal.Lett.* 2 **(1989)** 335.

63. Y. Okamoto, H. Onimatsu, M. H.Inui, T. Imanaka, *Catal.Lett.* 12 **(1992)** 239

64. C. Bremard, *Coord.Chem.Rev.* 178-180 **(1998)** 1647.

65. F. Bedioui, L. Roue, J. Devynck, K.J. Balkus; *Stud.Surf.Sci.Catal* 84 **(1994)** 917.

66. K.J. Balkus, A..A.Welch, B.E. Gnade, *Zeolites* 10 **(1990)** 722.

67. S. Kowalak, R.C.Weiss, K.J.Balkus Jr, *J.Chem.Soc. Chem.Commun.* **(1991)** 57.

68. C.A. Bessel, D. R. Rolison; *J.Am.Chem.Soc* 119 **(1997)** 12673.

69. F. Bedioui, E. De. Boysson, J. Devyuck, K.J. Balkus Jr, *J.Chem.Soc Faraday Trans.* 87 **(1991)** 3831.

70. L. Gaillon, N. Sajot, F. Bedioui, J. Devyuck, K.J. Balkus jr; *J.Electoanal.Chem* 34 **(1992)** 157.

71. S. P. Varkey, C. R. Jacob, *Ind.J.Chem.*37A **(1998)** 407.

72. S. P. Varkey, C. R. Jacob, *Ind.J.Chem.*38A **(1999)** 320

73. De. Vos, E. Dirk., T. Starzyk, Frederic, P.A Jacobs. *Angew. Chem.Int.Ed.Engl.* 106(4) **(1994)** 431.

74. D.E. Devos, E.J.P. Feijen, R.A. Schoonheydt, P.A Jacobs *J.Am.Chem.Soc.*116 **(1994)** 4746.

75. K. Maruszeuski, P.A. Strommen, K. Handrich, J.R. Kincaid, *Inorg. Chem.* 30 **(1991)** 4579.

76. J.A. Incavo, P.K. Dutta, *J.Phys.Chem.* 94 **(1990)** 3075.

77. W.H. Quale, J.H. Lunsford, *Inorg.Chem.*21 **(1982)** 97.

78. A. A. Bhuiyan, J.R. Kincaid , *Inorg.Chem.* 37 **(1998)** 2525.

79. M.Ledney, P. K. Dutta, *J.Am.Chem.Soc* 117 **(1995)** 7687.

80. W. Turbeville, D. S. Robins, P. K.Dutta, *J.Phys.Chem.* 96 **(1992)** 5034.

81. M Borja., P.K Dutta., *Nature* 362 **(1993)** 43.

82. P.K. Dutta, R.E. Zaykoshi, *Inorg.Chem.* 24 **(1985)** 3490.

83. S.K. Tiwary, S. Vasudevan, *Chem.Phys.Lett.* 84 **(1997)** 2779.

84. S.K. Tiwary, S. Vasudevan, *Inorg.Chem.* 37 **(1998)** 5239.

85. D.R. Henlge, J.H. Lunsford, P.A. Jacobs, J.B. Uytterhoeven., *J.Phys.Chem.* 40 **(1975)** 354.

86. W.D. Wilde, R.A. Schooheydt, .J.B Uytterhoeven, *ACS Symp.Series* 40 **(1977)** 132.

87. D.R. Flentge, J.H. Lunsford, P.A. Jacobs, J.B. Uytterhoeven, *J.Phys.Chem.* 79 **(1975)** 354.

88. R.F. Howe, J.H. Lunsford, *J.Phys.Chem.* 79 **(1975)** 17.

89. Y. Ukisu, A. Kazusaka, *J.Mol.Catal.* 70 **(1991)** 165.

90. A.S. Hay, H.S. Blanchards, G.F. Endres, J.W. Eustance, *J.Am.Chem.Soc.* **(1959)** 6335.

91. N. Hiroshi, S. Hideaki, Y.Mayumi, K. Kazu, *J.Chem Soc.Perkin Trans.2.* 9 **(1999)** 1919.

92. K. Alexandar, K. Anguelin, A. Kiyotaka, K. Yasuhiro *J.Mol.Catal:A.Chem* 137(1-3) **(1999)** 223.

93. C. J. Shang, L. L. Kao, W. C. Mow, *J.Chin.Chem.Soc*, 44(4) **(1997)** 431.

94. L. David., O. Cozar., L. Sumalan, R. Tetean, C. Cracium, N. Pop., *Stud.Univ.Babes-Bolyai, Phys.* 41(1) **(1996)** 43.

95. M. Khalidi, C. Bernad, B. Tethi, D. Jacques, *J.Mater.Chem.* 3(8) **(1993)** 873.

96. J.H. Lunsford,.*Catal.Rev.Sci.Eng.* 12(2) **(1975)** 137.

97. P.J. Hegruber, C. Platho., Schlulz-Ekloff., *J.Mol.Catal.* 24 **(1984)** 115

98. R. Grammen, P. Manikandan, *J.Am.Chem.Soc.* 122 (**2000**) 11488

99. B. M. Weckhuysen *Angew.Chem.Int.Engl.* 34 **(1995)** 2652

100. R. J. Taylor, R. S. Drago, J. E. George, *J.Am.Chem.Soc.* 111 **(1989)** 6610

101. R.Parton, D.De.Vos, P.A.Jacobs in *Zeolite Microporous solids synthesis structure, reactivity* , Kluwer academic publishers, sordrecht, Netherland, **(1992)** 555

102. D.e.Devos, P.P.Knopps-gerrits, R.F. Parton, P.A. Jacobs *Macromol.Symp.* 80 **(1994)** 157

103. B.V.Romanovsky, *Macromol.Symp.*80 **(1994)** 185

104. B.V.Romanovsky: *Proc 8th Int Congr. Catal*-Verlag Chemie Weinheim 4 **(1984)** 657

105. B.V.Ramovsky; *Acta.Phys.Chem.* 31 **(1985)** 215

106. C.R. Jacob, S.P. Varkey, P. Ratnasamy, *App.Catal:A.Gen.*182 **(1999)** 91

107. E. P. Mozo, N. Gabriunas, R. Maggi, D. Acosta, P. Ruiz, B. Delmon, *J.Mol.Catal.* 91 **(1994)** 251.

108. F. Thibault-Starzyk, R.F.Parton, P.A.Jacobs, *Stud.Surf.Sci.Catal.* 84B **(1994)** 1419.

109. T. Bein, C. Huber, K. Moller, Chun-guey Wu, L. Xu, *Chem.Mater.* 11 **(1997)** 2253.

110. R. Raja, P. Ratnasamy, *J.Catal.*170 **(1997)** 244.

111. N. Herron, *J.Coord.Chem.* 19 **(1988)** 25.

112. B.H.Weckhuysen et al. *J.Phys.Chem.* 100 **(1996)** 9456.

113. S. Kowalak, R.C. Weiss, K.J. Balkus, *J.Chem.Soc. Chem.Commun.* **(1991)** 57.

114. T. Kimura, A. Fukuoka, M. Ichikawa, *Catal.Lett.* 4 **(1990)** 279.

115. S.P.Varkey, C.R.Jacob, *Ind.J.Chem.* 37A **(1998)**407.

116. D.De. Vos, F. Thibault-Stalzyk, P.A. Jacobs, *Angew. Chem.Int.Ed.Eng* 4 **(1994)** 33.

117. M. Khalid, C. Bernad, B Fethi, D. Jacques, *J.Mater.Chem. 3(8) (1993) 873*

118. A. Corma, M. Iglesias, C. Depino, F. Sanchez. *Stud.Surf.Sci.Catal.* 75 **(1993)** 2293.

119. M.S. Scurrel, in *Catalysis.Chem.Soc. Specialist Periodical Reports,* London, 2 **(1978)** 215.

120. S. Bhaduri, H. Khuaja, V. Khanualkar, *J.Chem..Soc. Dalton.Trans.* **(1982)** 445.

121. L.R Melby, *J.Am.Chem.Soc.* 97 **(1975)** 4044.

122. L.D Rollman, *J.Am.Chem.Soc.* 97 **(1975)** 2132.

123. C.J. Pedersen., H.K. Frendorff,. *Angew Chem.Int.Ed.Engl.* 11 **(1972)** 16.

124. R.S Drago, J. Caul., A. Zombeck, D.K Staub, *J.Am.Chem.Soc.*102 **(1980)** 1063.

125. D.Wohrle, *Adv.Polym.Sci.* 10 **(1972)** 35.

126. J.H Fuhrhop, *Angew.Chemie.* 88 **(1976)** 616.

127. Y.I.Yermakov, *Cat.Rev.Sci.Eng.* 13 **(1976)** 77.

128. J. Villadsen, H. Livbjerg, *Cat.Rev.Sci.Eng.* 17 **(1978)** 203.

129. M.J. Kamogawa,.*J.Polym.Sci:Polym.Chem.Ed.* 12 **(1974)** 2317.

130. M.J Kamogawa, *J.Polym.Sci:Polym.Lett.* 10 **(1972)** 711.

131. M Kamogawa., H. Inoue, M.J. Nanasawa, *J.Polym.Sci:Polym.Chem.Ed.* 18 **(1980)** 2209.

132. E. Kokufuta, H. Watanabe, I. Nakamura, *Polym.Bull.* 4 **(1981)** 603

133. C.U. Pillmann.Jr., B.T. Kim., W.H. Douglas., *J.Org.Chem.* 40 **(1975)** 590.

134. C.P. Tsonis, M.T. Farona., *J.Organomet.Chem.* 101 **(1976)** 3985.

135. B.H. Chang, R.H. Grubbs, C.H. Brubaker. Jr, *J.Org.Chem.* 40 **(1975)** 590.

136. E. Kalalova., J. Kalal., F. Svec . *Angew.Makromol.Chem.* 89 **(1980)** 201.

137. E. Svec., *Acta.Polym.* 31**(1980)** 68.

138. Rani Abraham, Ph.D. *Thesis, Cochin University of Science and Technology, November* **(1999).**

139. A. Syamal, M.M. Singh, *Ind.J.Chem.*32A **(1993)** 42.

140. R.H. Wang., C. Hao, Y. Ho, C. Guxia, J. Ren Wang, Y. P. Wang *J.Appl.Poly.Sci.* 75 **(2000)** 1138

141. J. Jacob, M.K. Dalal., R.N. Ram., *J.Mol.Catal: A.Chem.* 137(1-3) **(1999)** 183

142. M. R. Kratz D.G. Hendricker, *Polymer* 27 **(1986)** 1641

143. E Tsuchida, Y Kurimura., *J.Polym.Sci:Polym.Chem.Ed.* 16 **(1978)** 2453.

144. S.K .Sahni, J Reedijk, *Coord.Chem.Rev.* 59 **(1984)** 1

145. S. Koboyashi., M.Tokunoh. *Macromolecules.* 18 **(1985)** 2357.

146. A.D. Pomogaito, I.E. Uplyand, *Adv.Polym.Sci.*, Springer-Verlag 97 **(1990)** 63.

147. O. Josino, S. Tamotsu, K. Syu, F. Tomoaki, *Japan Pat* 59-217746, *Japan Pat* 60-79010.

148. Jaguar-Grodzinsk,. *J.Macromol.Chem.* 181 **(1980)** 2441.

149. P Hodge., D.C Sherrington, *Polymer supported reactions in Org. Synthesis* – Wiley London **(1981)**.

150. .D.J Ehrlich., J.Y Tsao *.J.Vac.Sc., Techn.* Sec.B 9 **(1983)** 1

151. R.S Drago., E.D Nyberg., A.G. El A'mma , *Inorg.Chem.* 20 **(1981)** 2461.

152. I.E.Uflyand., A.D Pomogailo, M.O. Gorbunolva., A.G. Starikou., V.N. Sheinker., *Kinetics and Catalysis* 28 **(1987)** 613.

153. R.B. King, E.M.C. Sweet, *J.Org.Chem.* 44 **(1979)** 386.

154. E.N. Jacobson, *Asymmetric catalytic epoxidation of unfunctionalised olefines* VCII , New York 12 **(1995)** 1097.

155. H Jahnke, *Chimia* 34 **(1980)** 58.

156. Y Nakamura, H Hirai, *Chem.Lett.* 645 **(1974)** 809.

157. H Hirai, T. J Furuta, *Polym.Sci.Lett* 9 **(1971)** 459.

158. G.Meyer, D Wohrle., *Mater.Sci.* 7**(1981)** 265.

159. Y Moriguchi, *Bull.Chem.Soc.Japan* 37 **(1966)** 2656

160. D.C. Sherrington, *Catal.Today* 57(1-2) **(2000)** 87.

161. A.V Artemoce, E.F Vainstein. *Int.J.Polym.Mater.* 43(1-2) **(1999)** 137.

CHAPTER II
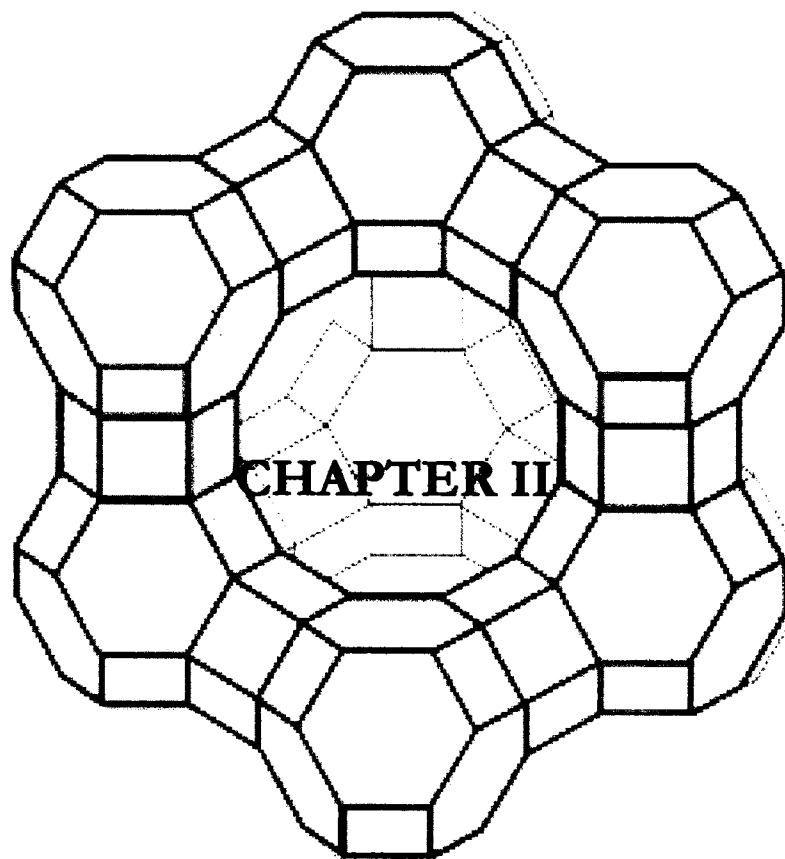
EXPERIMENTAL TECHNIQUES

2.1 INTRODUCTION

General reagents used in the preparation and characterization of ligands and various analytical and physico-chemical methods employed in the characterization of the metal complexes are presented in this chapter.

2.2 REAGENTS

Metal salts used were $CoCl_2.6H_2O$ (E.Merck, G.R), $NiCl_2.6H_2O$ (BDH, GR), $CuCl_2.2H_2O$(E.Merck, GR).

2.3 LIGAND SYNTHESIS

O-Phenylenediamine (Loba chemie) was used as one of the ligand. It was used as such after purification. Purification was done by dissolving o-phenylenediamine in water. Activated charcoal was added to this. The solution was then boiled, filtered and recrystallised. Other ligands used in the present study were prepared according to the following procedures:
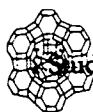
2.3.1 Preparaton of Schiff bases of 3-hydroxyquinoxaline-2-carboxaldehyde.

Sodium pyruvate (SRL), *o*-phenylenediamine (Loba chemie), Br_2 (Merck), glacial acetic acid (99% Merck), $CaCO_3$precipitated (E.Merck) were used for the preparation of aldehyde. The aldehyde 3-hydroxyquinoxaline–2–carboxaldehyde was prepared according to the reported procedure[1]. The amines used for the synthesis of the Schiff bases are ethylenediamine (BDH), hydrazine hydrate, diethylenetriamine (SRL, Technical Grade) and *o*-phenylenediamine (Loba Chemie).

2.3.2 N,N'-bis(3-hydroxyquinoxaline-2-carboxalidene) ethylenediamine-(QED)

To the solution of 3-hydroxyquinoxaline-2-carboxaldehyde (5 g in 1 litre of H_2O) about 2 to 3 drops of concentrated hydrochloric acid was added. An alcoholic solution of ethylenediamine (2 ml in 20 ml alcohol) was added to this drop by drop until precipitation was complete. The yellow precipitate was filtered washed with methanol and dried in vacuum over anhydrous calcium chloride.

2.3.3 N,N'-bis(3-hydroxyquinoxaline-2-carboxalidene) *o*-phenylenediamine (QPD)

To the aldehyde solution (5 g in 1 litre H_2O) 2 to 3 drops of concentrated hydrochloric acid was added and to this solution of o-phenylenediamine (2 g in 20 ml H_2O) was added drop by drop while the solution was stirred. The orange yellow solid obtained was filtered washed and dried over anhydrous calcium chloride.
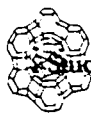
2.3.4 N,N'-bis (3-hydroxyquinoxaline -2-carboxalidene)hydrazone-(QHD)

To the aldehyde solution (5 g in 1 litre H_2O) 5 drops of concentrated hydrochloric acid was added and an aqueous 90% hydrazine hydrate (2 ml in 20 ml H_2O) was added to this drop by drop with stirring. The fluorescent bright yellow Schiff base was filtered and washed with methanol and dried over anhydrous calcium chloride.

2.3.5 N,N'-bis(3-hydroxyquinoxaline–2carboxalidene)diethylenetriamine (QDT)

Aldehyde solution (5 g in 1 litre H_2O) was made acidic with 1 or 2 drops of concentrated hydrochloric acid and an alcoholic solution of diethylenetriamine (2 ml in 20 ml alcohol) was added to this drop by drop with stirring. The amine solution was added till the precipitation of Schiff base was complete. The yellow compound was separated, filtered, washed with methanol and dried over anhydrous calcium chloride.

2.4 SUPPORTS USED

2.4.1 Polystyrene beads

Chloromethylated polystyrene beads of 200-400 mesh size, crosslinked with 2% divinyl benzene and contaning 12.9% chlorine (Fluka) was used as the starting material for the study. This was then functionalized into the aldehyde-bound and amino-bound polystyrene

2.4.1.1Preparation of polymer bound benzaldehyde.

A mixture of chloromethyl polystyrene (20.0 g), dimethylsulphoxide (300 ml) and sodium bicarbonate (19.0 g) was stirred at 138-140°C for 12 hours.[2] The resultant resin was filtered, washed with hot, ethanol, methylene chloride and benzene and dried in vacuum over anhydrous calcium chloride.

2.4.1.2 Preparation of amino-methyl polystyrene

Chloromethyl polystyrene (11.0 g) was suspended in 200 ml DMF and hexamethylene triamine (11.2 g) and potassium iodide (13.3 g) was added to this suspension.[3] The solution was heated with stirring under reflux at 100°C in an oil bath for 10 hours. The resin was filtered and washed with 6N hydrochloric acid and water. It was then stirred with sodium hydroxide (10% for 2 h) filtered, washed several times with water and methanol and dried in vacuum to constant weight. The prepared resin containing amino-methyl group gives a deep blue colour with ninhydrin reagent, which is a positive test for the presence of amino group.

2.4.2 Zeolite Y

Synthetic Y type zeolite was obtained from Süd-Chemie India (P) Ltd., Baroda.

2.4.2.1 Preparation of metal exchanged Zeolite Y

The synthetic Y type zeolite was stirred in 0.1 mol dm^{-3} solution of sodium chloride for 24 hours to convert any other ions if present into Na$^+$ ions. The sodium exchanged zeolite was then made chloride free by washing with distilled water.[4] It was then dried at 100°C. The sodium ions are now replaced with bivalent transition metal ions, Co^{2+}, Ni^{2+} or Cu^{2+} by stirring with 0.01 mol dm^{-3} solution of the respective metal chloride for 24 hours. It was then filtered and dehydrated at 450°C for 4 hours.

2.5 REAGENTS FOR CATALYTIC ACTIVITY STUDY AND KINETIC STUDY

Phenol (Merck) and hydrogen peroxide (30% aqueous solution, E.Merck) catechol (E.Merck) and 3,5-di-tert-butylcatechol (Aldrich Chemicals) were used for the catalytic activity as well as kinetic study. Details of the above study are presented in Chapters VI and Chapter VII.

2.6 ANALYTICAL METHODS

The characterization techniques were employed to answer the following queries.

1. How is the complex distributed in the host crystal?

2. What is the degree of complexation?

3. What is the type of coordinaton compared to that in liquid solvent?

4. How does the host-guest interaction influence the structure of the encapsulated complex?

5. What is the stability in the solid state compared to that in the dissolved state?.

6. Does it exhibit free coordination site for chemisorption and catalysis?

2.6.1. Analysis of Si, Al, Na and transition metal ion in the zeolite

Zeolite encapsulated metal complexes was accurately weighed ('x'g) and transferred to a beaker. Concentrated sulphuric acid (about 40 ml) was added and heated until it just fumes. It was diluted with 200 ml water after cooling and filtered through an ash less filter paper. The residue was dried at 1000°C in a platinum crucible, cooled and weighed ('a' g). Then hydrofluoric acid (10 ml) was added when all the silica is removed as SiF_4 and the remaining solid finally ignited to 1000°C('b' g).[4] From this the percentage of silica (SiO_2) was calculated using the equaton.

$$\% \ SiO_2 \quad = \frac{(a-b)}{x} x100$$

The residue in the platinum crucible was then fused with potassium persulphate until a clear melt was obtained and this was dissolved in water again filtered and combined with earlier filtrate. The Na, Al and transition metal ions in the solution were determined by ICP-AES. From the metal percentages obtained the ion exchange capacity was calculated and derived the unit cell formula.[5]
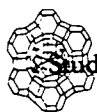
2.6.2 Analysis of metal content of polymer

The polymer samples were accurately weighed into a beaker. The polymer was decomposed with 4N acetic acid and heated on a water bath for 2 h.[6] The resin was filtered and washed with acetic acid and metal ion concentration in the solution was determined by ICP-AES.

2.6.3 CHN Analysis

Microanalysis for carbon, hydrogen and nitrogen in the polymer as well as the zeolite samples were done at Central Drug Research Institute, Lucknow.

2.6.4 Estimation of chlorine

Polymer supported complexes were analysed for their chlorine content by Volhards method.[7] For this polymer supported metal complexes are digested in pyridine for 2 hours at 100°C. The mixture was then quantitatively transferred to a conical flask containing 50% acetic acid (30 ml) and concentrated nitric acid (5 ml). To this, standard silver nitrate solution was added with stirring and this mixture was allowed to stand for 5 minutes. Afterwards water (~50 ml) was added to this followed by toluene (5 ml.). The solution was mixed thoroughly using a stirrer. The unreacted silver nitrate was determined by titration with standard thiocyanate solution.

2.6.5 Magnetic moment measurements

Magnetic susceptibility measurements provide a complementary means for investigation of site preference of transition metal ion and coordination geometry of the ligand. However, magnetic susceptibility measurement data can be taken as a qualitative guide in predicting the structure in the case of zeolite and polymer supported complexes.

Magnetic susceptibility measurements were done at room temperature using a guoy balance. The reference used for standardization was $Co[Hg(CNS)_4]$ as recommended by Figgis and Nyholm.[8] The effective magnetic moment is calculated using the equation.

$$\mu_{eff} = 2.84(x_m^{corr}T)^{1/2} \text{ B.M.}$$

Where T is the absolute temperature and x_M^{corr} is the molar susceptibility corrected for the diamagnetism of the atoms in the complex using Pascals constant and the molecular weight of zeolite was determined from the unit cell formula.

For the polymer samples magnetic susceptibility was calculated by following the method by Shyamal et.al[9] after finding out the molecular weight of the repeating units.

2.6.7 Surface area analysis and pore volume

Total surface area of porous structures is measured by adsorption of particular molecular species from a gas or liquid on to the surface. The

most common method is that of the Brunauer, Emmett and Teller (B.E.T. method).[10] The equation used in the determination is:

$$\frac{P}{V(Po-P)} = \frac{1}{VmC} + \frac{(C-1)P}{VmCPo}$$

V = Volume of gas adsorbed at Pressure P

Vm = Volume of gas in the monolayer

Po = Saturation P of adsorbate gas at the expt temp

C = a constant related to heat of adsorption and liquefaction of gas.

Surface area analysis of the prepared complex and parent zeolite and polymer were measured using B.E.T. method using a Micromeritics Gemini 2360 surface area analysis. Nitrogen gas was used as the adsorbate at liquid N_2 temperature.

B.E.T Surface Area is calculated using

$$S_{BET} = X_m \, N \, A_m \, 10^{-20}$$

N = Avagadro s number

A_m = cross-sectional area of the adsorbate molecule in Å^2

Pore volume of the sample at P/Po $\approx$ 0.9 is computed by converting the volume of N_2 adsorbed at P/Po $\approx$ 0.9 to volume of liquid equivalent to it using the equation given below

$$V_{tot} = V_{ads} \, D$$

where

$$V_{tot} = \text{total pore volume at P/Po} \approx 0.9$$

$$V_{ads} = \text{volume of gas adsorbed at relative pressure } 0.9$$

$$D = \text{density conversion factor}$$

2.6.8 Infrared spectra

Infrared spectra of the ligands and supported complexes were obtained in the region from 4600-400cm^{-1} using KBr pellet technique using Shimadzu 8000 Fourier Transform IR spectrophotometer. The mid IR region of the spectrum is very useful in structural analysis of zeolite as it contains the fundamental vibrations of the framework and each zeolite exhibit a typical IR pattern. FTIR was used to complement structural information on zeolite framework and to detect the formation of nitrogen containing organic compound.

2.6.9 Electronic spectra

The electronic spectra[11-12] of the zeolite and polymer samples were recorded on a Carry Win spectrophotomer in the diffuse reflectance mode at Regional Sophisticated Instrumentation Centre, IIT Chennai, SICART, Vallabh Vidyanagar, Gujarat. The UV-Visible spectroscopy gives evidence about the coordinaton environment and about other compounds present.

The location and coordination taken up by charge balancing cation in zeolites has been a problem. Reflectance spectroscopy is a useful technique to study the coordination since the extinction coefficient for different coordinations are different.

A Kubelka-Munk equation is used

$$\text{Log} \frac{(1 - r_\alpha)^2}{2r_\alpha} = \text{Log } k - \text{Log } S$$

$r_\alpha = R_\alpha(\text{sample}) / R_\alpha(\text{Std})$. The standard is usually sodium form of the zeolite. (sometimes MgO is also used). $R\alpha$ is taken as 1 for the standard. K = absorption coefficient and S=scattering coefficient.

$$F(R) = \frac{(1 - r_\alpha)^2}{2r_\alpha} = \frac{k}{S}$$

F(R)is the Kubelka Munk factor

A plot of $(1-r_\alpha)^2/2r_\alpha$ as a function of wavelength gives the corrected absorption curve.

2.6.10 EPR spectra

EPR is also a useful technique to find out the co-ordination environment. But above 4K, due to spin lattice relaxation effects the signals becomes broad and useful information can be obtained only by going below this temperature.
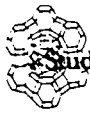
The EPR spectra of the powdered samples were recorded at liquid N_2 temperature using a Varian E-109 X/Q band spectrometer. The standard used was TCNE (tetracyanoethylene g = 2.0027). Magnetic moment (μ_{eff}) values were also determined from EPR by substituting $g_\perp$ and g_{11} in the following equations.[13]

$$\mu^2_{eff} = g_{II}{}^2/4 + g_\perp{}^2/4 + 3KT/\lambda_o(g\text{-}2)$$

where λ_o is the spin-orbit coupling constant for the free metal ion.

The density[14] of the unpaired electron at the central atom can be computed from the equation.

$$\alpha^2 = (A_{II}/0.036) + (g_{II} - 2) + 3/7\ (g_\perp - 2) + 0.04$$

where $1\text{-}\alpha^2$ measures the covalency associated with the bonding of metal ion to the ligand .

The bonding parameter P can be calculated using the equation given below

$$P = (A_{II} - A_\perp)/(g_{II}\text{-}2) \text{-}5/14(g_\perp\text{-}2)\text{-}6/7$$

2.6.11 X-Ray Diffraction

In a crystalline material an infinite number of lattice planes with different miller indices exist and each set of plane will have a particular separation d_{hkl}. Combining Braggs equation[15] and expression of d-spacing

$$\mathrm{Sin}^2\theta = \frac{\lambda^2(h^2 + k^2 + l^2)}{4a^2}$$

In powder XRD, there will be all possible orientation of the crystal. Each lattice spacing will give rise to a cone of diffraction. Each cone consists of a set of closely spaced data each one of which represents a diffraction from a single crystallite within the power sample. Detector used in powder XRD is sensitive to X-rays. Scanning of the detector around the sample along the circumference of a circle cuts through the diffraction cones at various diffraction maxima. The intensity of X-rays detected as a function of detector angle 2θ is obtained.

Metal exchanged zeolite and zeolite encapsulated complexes were analyzed by powder X-ray diffraction for comparing their crystallinity. X-ray diffractometer used in the present study is Rigaka-D. Max.C measurements were done with a stationary X-ray source, Ni filtered CuKα radiation (λ = 1.5404) and a movable detector which scans the intensity of the diffracted radiation as a function of the angle 2θ between the incident and diffracted beam.

2.6.12 TG Analysis

Thermogravimetric analysis was done on a Shimadzu TGA-50 at a heating rate of 20°C min^{-1} in an inert atmosphere using a platinum crucible.

2.6.13 Scanning Electron Microscopy

The morphology of the samples was investigated using scanning electron microscopy. The samples were coated with a thin film of gold to prevent surface charging and to protect the zeolite material from
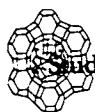
thermal damage by electron beam. This method was used to determine whether there are any surface adsorbed materials.

2.6.14 Gas Chromatography

Catalytic activity studies were performed using a Chemito 8510 gas chromatograph (SE-30 column) equipped with a flame ionization detector.

2.6.15 Kinetic studies

Kinetic studies were performed by using a Shimadzu UV-visible spectrophotometer 160A.
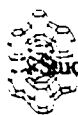
REFERENCES

1. Jose Mathew, *Ph.D Thesis*, Cochin University of Science and Technology, November **(1995)**.

2. J.M.J. Frechet, K.E. Haque, *Macromolecules*.8 **(1975)** 130.

3. K.S. Devaki, V.N.R. Pillai, *Eur.Polym.J.* 24 **(1988)** 209.

4. Rani Abraham, *Ph.D Thesis*, Cochin University of Science and Technology, November**(1999)**.

5. C. Tollmann, N. Herron, *Symposium in Hydroc. Oxidation* 194th National meeting of American Chemical Society., New Orleans, LA, Aug 30-Sep.4 **(1987)**.

6. A. Syamal and M.M. Singh, *Ind.J.Chem.* 31A **(1992)** 110.

7. G.H. Jeffery, J. Bassett, J. Mendham, R.C. Denney, *Vogel's Textbook of Quantitative Inorganic Analysis*-5th Edition-Elbs-Longman Singapore publishers **(1991)**.

8. B.N. Figgis, R.S. Nyholm, *J.Chem.Soc.* **(1958)** 4190.

9. A. Syamal, M.M. Singh, *Ind.J.Chem. 32A* **(1993)** *42.*

10. C.N. Satterfield, *Heterogeneous Catalysis in Industrial Practice*, 2nd Edition, Mc.Graw-Hill, Singapore **(1993)**.

11. S.K. Tiwary, S. Vasudevan, *Inorg.Chem.* 37 **(1998)** 5239.

12. G. Kortum, *Reflectance spectroscopy Principles, Methods, Applications*, *Springer-Verlag-Berlin* **(1969)**.

13. B.V. Agarwala, *Inorg.Chim.Acta.* 36 **(1979)** 209.

14. D. Kivelson, R. Neiman, *J.Chem.Phys.* 35 **(1961)**149.

15. D.L. Bish, J.E.Post, *Modern Powder diffraction-Structures and structure determination*, H.G.Karge and J.Weitkam eds, Springer **(1999)**.

CHAPTER III
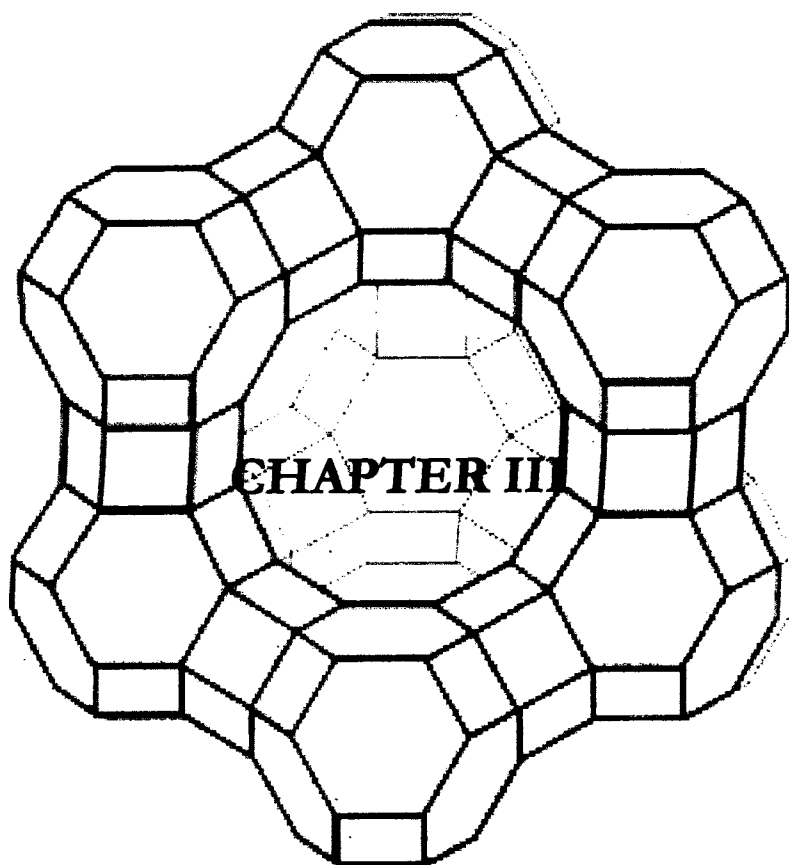
ZEOLITE ENCAPSULATED COBALT(II), NICKEL(II) AND COPPER(II) COMPLEXES OF *O*-PHENYLENEDIAMINE

3.1 INTRODUCTION

Studies on the complexes of ligand *o*-phenylenediamine have been going on since many years.[1-4] The preparation of complexes of aromatic diamines is of special interest, since the use of nitrogen atoms for coordination to a single cation is directly related to its location in the ortho, meta or para position.[5] When *o*-phenylenediamine is used as ligand, the proximity of the nitrogen atoms permit their coordination to the same metal cation leading mainly to monomeric species. Aromatic amine ligands differ from their aliphatic analogues in several aspects. Unlike the aliphatic amines[6], the aromatic amines are less basic due to the delocalization of the electron pair on the nitrogen atom towards the aromatic ring. Aliphatic amines are flexible, whereas aromatic amines are rigid and prefer a planar arrangement. Thus aromatic amines are an interesting class of ligand.

Studies on the complexes of *o*-phenylenediamines with various metal ions have been reported in literature. The dichloro-(*o*-phenylenediamine)platinum(II) complexes possess antitumour activity[7-8] Complexes of *o*-phenylenediamine with copper(II), cadmium(II)[9-11], nickel(II)[12-14] and with iron(II)[15] have been widely

61

studied. The interaction of WCl_6 with o-phenylenediamine in propanol results in the formation of a binuclear compound[16]. Several new complexes of Re(VII) and Re(VI) with o-phenylenediamine has also been prepared[17].

Composition and structure of the simple complexes of o-phenylenediamine are found to vary with the method of preparation. Their encapsulation inside the zeolite cages may alter the structure and may in turn lead to lower coordinated structures. Such lower coordinated structures are expected to be more active as catalysts. A systematic study was therefore carried out on the zeolite encapsulated complexes and the properties have been compared with the already reported simple complexes. The results of this study are presented in this chapter.

3.2   EXPERIMENTAL

Details regarding the purification of the ligand are presented in chapter II. The simple complexes were prepared according to the procedure reported earlier.[18]

3.2.1 Synthesis of metal exchanged zeolites

The following general procedure was used to synthesize the complexes. Zeolite Y (10 g) was Na exchanged with 0.1 mol dm^{-3} NaCl to obtain Na-Y which was then made chloride free. This was then heated to 110°C for 2-3 hours. About 5 g of Na-Y was taken and stirred overnight in a solution containing 0.01 mol dm^{-3} metal chloride solution. It was then filtered and heated to 450°C.

3.2.2 Preparation of zeolite encapsulated metal complexes of *o*-phenylenediamine

Zeolite encapsulated cobalt(II), nickel(II), copper(II) complexes of *o*-phenylenediamine were prepared from the metal exchanged zeolite using the flexible ligand method.[19] *o*-Phenylenediamine (OPD) corresponding to a ligand to metal ratio of approximately 2:1 was taken and dissolved in ethanol. The solution was refluxed with metal exchanged zeolite (5 g) on a water bath for 6 hours. The complexes were then filtered and soxhlet extracted with ethanol and acetone till the washings were colourless. It was then back exchanged with 0.1 mol dm^{-3} NaCl to replace the uncomplexed metal ion with Na$^+$.

3.3 ANALYTICAL METHODS

Stability of complexes in the cages and channels play a major role in ion exchange of transition metal complexes. The stability depends on the microenvironment i.e. the residual water molecules, Si/Al ratio of the framework, residual Na$^+$ ion. The various physico-chemical characterization techniques were employed to characterize the prepared metal complexes. Details of the analytical methods used are given in chapter(II).

3.4 RESULTS AND DISCUSSION

3.4.1 Metal exchanged zeolites

The analytical data for the metal exchanged zeolites is given below in the Table III.1. The Si/Al ratio of NaY is 2.49 which is found to be

retained even after the metal exchange indicating the absence of any dealumination.

Table III.1:

Analytical data of metal exchanged zeolites

Metal exchanged zeolite	%Si	%Al	%Na	%Cu
NaY	19.7	7.9	6.69	-
CuY	19.45	7.85	5.81	4.13
CoY	19.72	7.80	4.7	6.02
NiY	19.73	7.20	4.28	3.35

The unit cell formula of the metal exchanged zeolites is given below in Table III.2.

Table III.2.

Composition of metal exchanged zeolites

Metal Exchanged Zeolite	Unit Cell Formula	Ion exchange capacity
NaY	$Na_{56}(AlO_2)_{56} (SiO_2)_{136}nH_2O$	
CoY	$Na_{16}Co_{20}(AlO_2)_{56} (SiO_2)_{136} nH_2O$	57
NiY	$Na_{34}Ni_{11}(AlO_2)_{56} (SiO_2)_{136} nH_2O$	39
CuY	$Na_{24}Cu_{16}(AlO_2)_{56} (SiO_2)_{136} nH_2O$	71

From the metal percentage it can be seen that maximum ion exchange capacity is for CoY. The order of ion exchange capacity is CoY > CuY > NiY.

The coordination of transition metal ion to lattice oxide ion is governed by the number of lattice oxide ions in the first coordination sphere, the ligand field strength, the symmetry of the ligand field and number of d-electrons. Lattice oxide ions are weak ligands and hence the transition metal ions are expected to be in their high spin configuration. The spectroscopic characteristics of the Co^{2+}, Ni^{2+}, Cu^{2+} coordinated to the lattice oxide ions of the zeolite framework have been reported (see Table III.3). The active surface of the zeolites can create an electric field in the cages which varies rapidly with distance. This is due to the presence of exchangeable cations and it is reported that zeolite exchanged with divalent cations are stable than those with monovalent cations.

Table III.3

Electronic spectra and EPR parameters of metal exchanged zeolites

Zeolite Y	Cation position	d-d absorption bands	g_{II}	A_{II}	$g_{\perp}$	$A_{\perp}$
Co^{2+}		6000, b/w 15000 and 20000, 25000				
Ni^{2+}	I	6100-6400,19000-20000				
	I'	4900,9300,21500-				
	II	23500				
Cu^{2+}	I'	10700, 12900, 14800	2.34	15.7	2.07	1.9
	II	10400, 12400, 14700	2.39	12.4	2.07	1.3

Asym. stretch	Sym. stretch	Dbl. ring	T-O bend	Pore
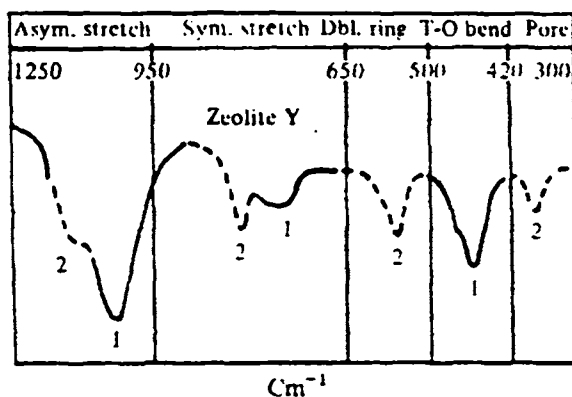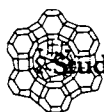
FigureIII.1

FTIR Spectra of NaY

1-internal tetrahedra structure

2-external linkages

The major infrared bands in the zeolite have been reported to occur in the IR region (200-1300 cm^{-1}) as it contains the fundamental vibration of framework alumina or silica. The zeolitic vibrations are grouped into two: Those due to internal vibrations of the tetrahedra and those due to the linkages between the tetrahedra. The IR spectra of zeolite Y is given in the Figure III.1. All the metal exchanged zeolites exhibit almost the same IR spectrum as that of zeolite Y. This also shows that the zeolite framework remains intact on metal exchange. The IR spectra of the metal exchanged zeolites are given in the Figure.III.2.

3.4.2 Analytical data of zeolite encapsulated complexes

Zeolite encapsulated o-phenylenediamine complexes of cobalt(II), nickel(II) and copper(II) prepared using the flexible ligand method was characterized using chemical analysis, SEM, XRD, surface area, pore volume, magnetic moment, diffuse reflectance spectroscopy, FTIR and EPR spectroscopy . The thermal stability of the complexes were determined using the thermogravimetric analysis.

66
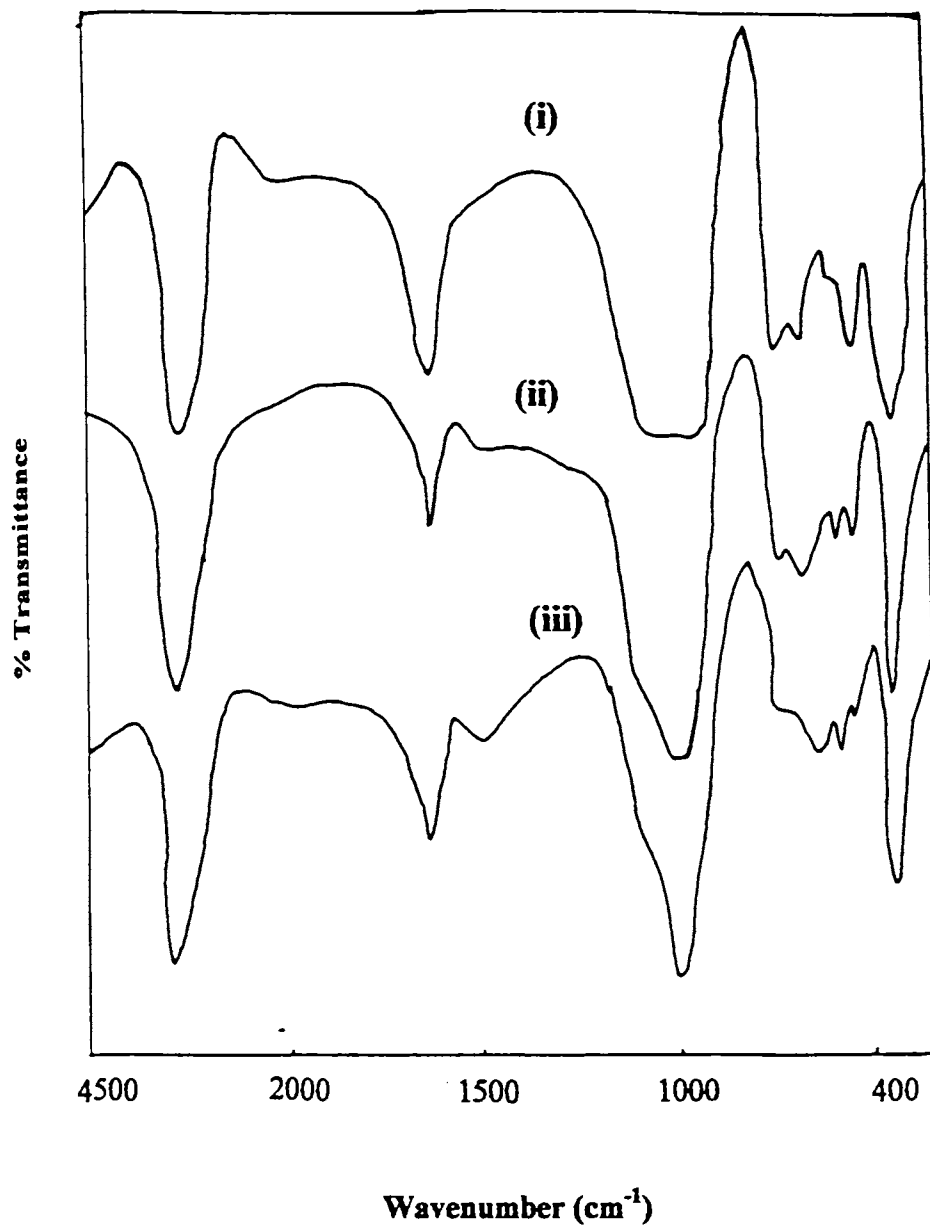
Figure III. 2 IR spectra of i) CoY ii) NiY iii) CuY
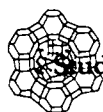
3.4.2.1 Elemental analysis

The carbon, hydrogen and nitrogen percentage of the zeolite encapsulated complexes indicate the presence of metal complex in the zeolite. The complexes can be considered to be placed inside a dilute framework of the zeolite. The percentage silica was determined according to the procedure described in chapter II and metal percentages were determined by ICP-AES analysis. The silica-alumina ratio of the zeolite encapsulated complexes was in the range typical of zeolite Y. The maximum complexation was observed in the case of copper exchanged zeolite Y. The elemental analysis results are presented in the Table III.4. The unit cell formula of complexes has been calculated based on analytical data.[20] The exact percentage of metal which is in the complexed state cannot be determined since some uncomplexed metal may still remain in the zeolite cage even after back exchange.

Table III.4.

Analytical data of encapsulated complexes of o-phenylenediamine

Complexes	%Si	%Al	%Na	%M	%C	%N
YCoOPD	19.35	7.5	6.60	1.07	0.49	0.28
YNiOPD	19.60	7.30	5.13	2	0.37	0.32
YCuOPD	19.70	7.91	6.70	0.91	1.09	0.49

3.4.2.2 Surface area and pore volume

The surface area and pore volume data for the zeolite encapsulated complexes are given in the Table III.5. This was determined using B.E.T. adsorption isotherms. There is not much difference in surface area of NaY and metal exchanged zeolite but the surface area decreased drastically in the case of the encapsulated complexes.

Table III.5 .

Surface area and pore volume data of zeolite encapsulated complexes of
o-phenylenediamine

Metal ion	Surface Area (m^2/g)		Pore Volume (CC/g)	
	Uncomplexed (MY)	Complexed (MLY)	Uncomplexed (MY)	Complexed (MLY)
Co	450	296	0.2604	0.1751
Ni	420	306	0.2494	0.1801
Cu	380	287	0.2198	0.1566

The surface area of porous solids like zeolite is mainly internal surface area and blocking of the pores due to the formation of metal complexes decreases the surface area.[21] The surface area ranges from 450 m^2/g to 380 m^2/g in the case of metal exchanged zeolites which decreased further by 100m^2/g on encapsulation of the metal complexes.
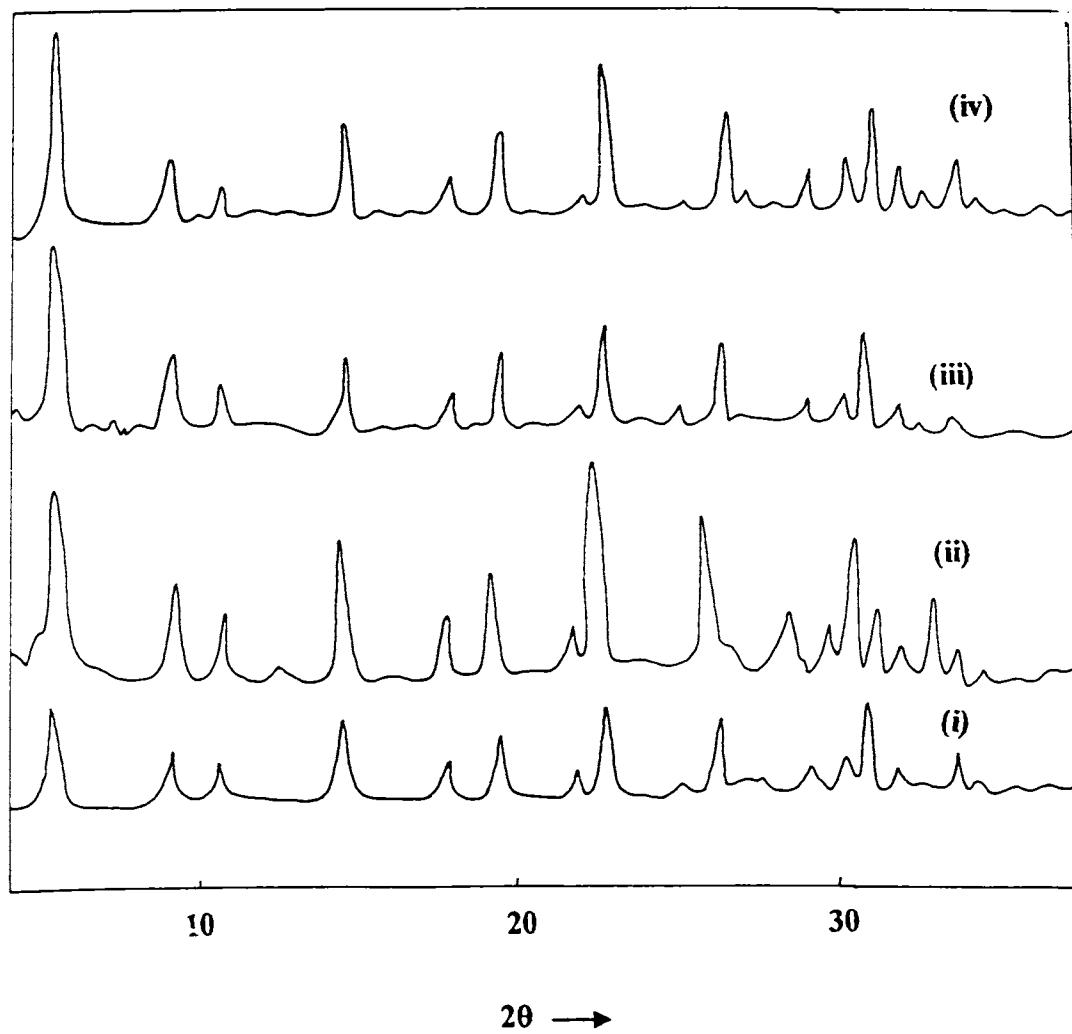
Figure III. 3 XRD patterns i) NaY ii) YCoOPD iii) YNiOPD
iv) YCuOPD

3.4.2.3 X-ray diffraction and SEM analysis

The XRD patterns of the encapsulated complexes, exactly match with that of the metal exchanged zeolite as well as NaY. This shows the retention of crystallinity and the absence of any dealumination. The zeolite structure is retained as such on encapsulation. The XRD patterns of the zeolite encapsulated complexes as well as NaY are given in the Figure III.3. The absence of any extraneous material on the zeolite is evidenced by scanning electron microscopic studies. The SEM of the zeolite encapsulated complexes taken before and after soxhlet extraction with ethanol shows the removal of the surface adsorbed species. Soxhlet extraction with a suitable solvent can thus be successfully employed for removing the surface complexes. The complexes formed inside zeolite cages remain trapped and are not able to come out. Scanning Electron micrographs of the zeolite encapsulated copper complexes of o-phenylenediamine at different magnifications are given in the Figure III.4 and Figure III.5.

3.4.2.4 Magnetic moment measurements

Magnetic moments of the zeolite encapsulated complexes were determined at room temperature using the Guoy method. The determination of magnetic moment of the zeolite encapsulated complexes is very difficult due to the high diamagnetic contribution from zeolite framework and the presence of iron impurities. The molecular weight of the zeolite encapsulated complexes were determined based on the unit cell formula calculated using the elemental analysis. This method cannot be considered as accurate; however it gives a qualitative idea
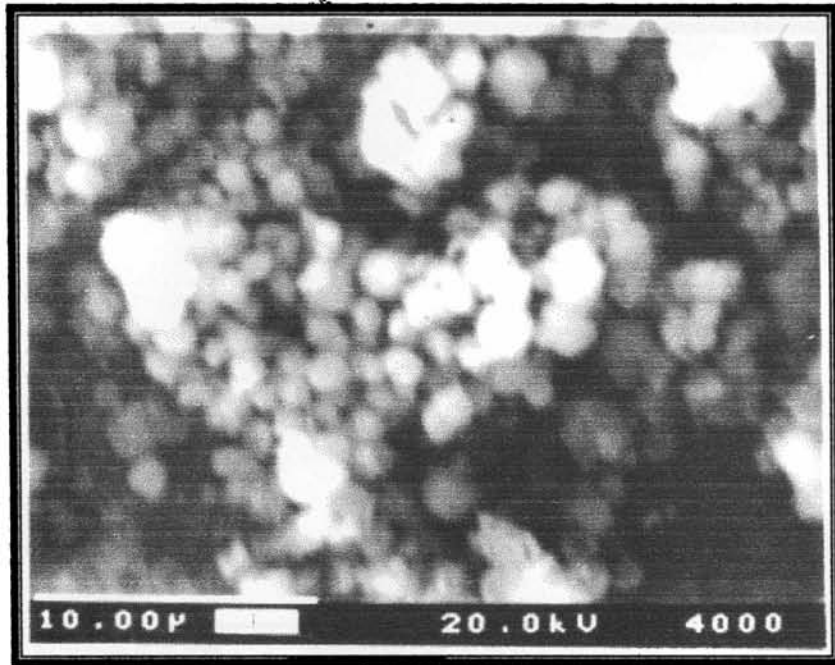
(i)
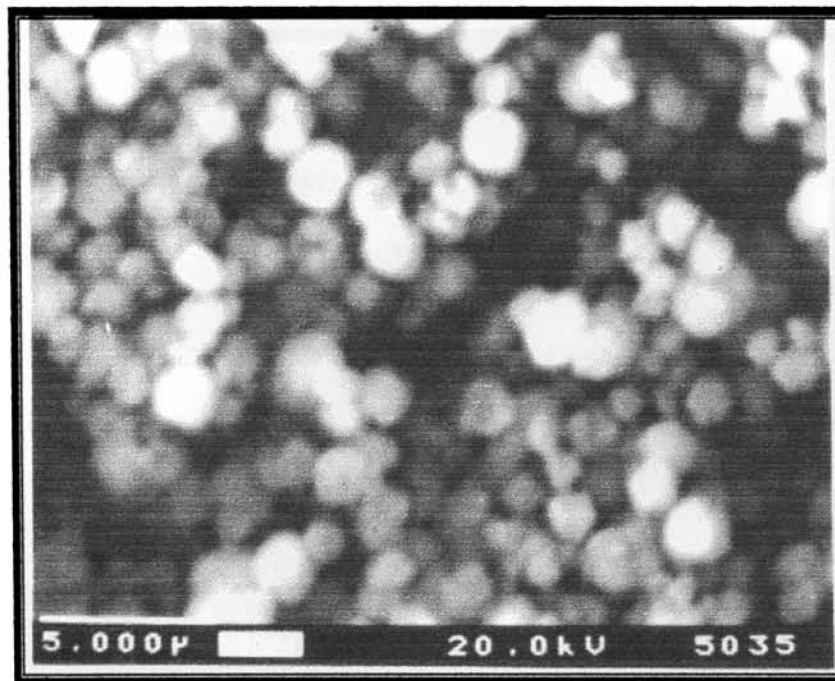
(ii)

Figure III.4 Scanning Electron Micrographs of YCuOPD (i) before and
(ii) after soxhlet extraction
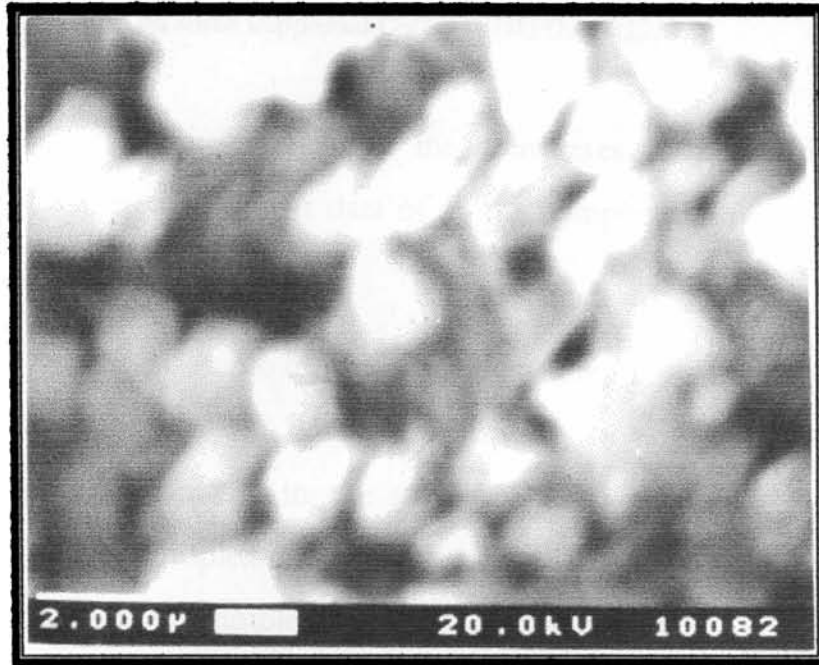
(i)
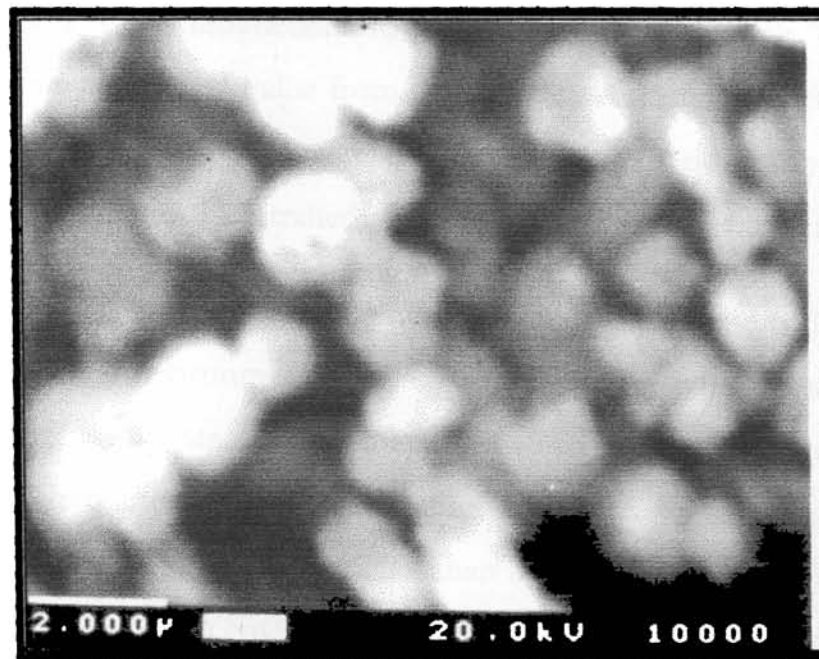
(ii)

Figure III.5 Scanning Electron Micrographs of YCuOPD (i) before and
(ii) after soxhlet extraction

about magnetic moment of the complexes formed inside the zeolite. The magnetic moment data of all the complexes are presented in Table III.6

The magnetic moment of the zeolite encapsulated cobalt complex is obtained as 4.80 BM As octahedral cobalt(II) complexes exhibit a magnetic moments in the range of 4.8-5.2 BM, the encapsulated cobalt(II) complexes may be assigned a six coordinated octahedral structure. The simple cobalt(II) complexes with o-phenylenediamine were reported to have a magnetic moment of 5.0 BM[18] A magnetic moment value of 4.3 BM is obtained for cobalt(II) exchanged in zeolite Y indicating tetrahedral structure (tetrahedral cobalt ions show a magnetic moment value from 4.3-4.8 BM). Octahedral aqua complex of cobalt entering the super cage during the metal exchange may be converted into the tetrahedral species during the dehydration.[22]

The electronic configuration of the ground state of $Ni^{2+}(d^8)$ in an octahedral environment is $t_{2g}^6 eg^2$. This ground state mixes with the first excited triplet state $(^3T_{2g})$ having the electronic configuration $t_{2g}^5 e_g^3$ and this leads to orbital contribution to magnetic moment. Therefore magnetic moment values higher than the spin only value of 2.83 BM are expected. The YNiOPD complex is having a magnetic moment of 3.2.BM which suggests an octahedral geometry for the complex. The fifth and sixth co-ordination may be provided by the water molecules or the zeolite framework oxygen atoms.

The copper complexes cannot be assigned stereochemistry based on magnetic moment value alone. Copper complexes usually exhibit magnetic moment in the range from 1.7-2.2 BM The magnetic moments

of both the simple as well as the zeolite encapsulated copper(II) complexes are 1.86 BM Any conclusion regarding the structure of copper(II) complexes cannot be arrived from this data.

Table III.6

Magnetic moment data of encapsulated OPD complexes

Complexes	Magnetic Moment(BM)	Unit cell
YCoOPD	4.80	$Na_{43}Co_{6..5}(AlO_2)_{56}(SiO_2)_{136}.nH_2O$
YNiOPD	3.20	$Na_{49}Ni_{3.5}(AlO_2)_{56}(SiO_2)_{136}.nH_2O$
YCuOPD	1.86	$Na_{50}Cu_3(AlO_2)_{56}(SiO_2)_{136}.nH_2O$

3.4.2.5 EPR spectra

EPR spectra of the complexes were recorded at liquid N_2 temperature. The EPR technique enables us to determine the electronic state and the symmetry of the ligand field which provides information on the immediate environment. The EPR spectra of the neat and zeolite encapsulated copper complex and that of CuY are given in Figure III.6. The EPR parameters for the CuY is $g_\perp=2.08$ and $g_{II}=2.37$ and $A_\perp$ and A_{II} are 66.66 and 136.66 x 10^{-4} cm^{-1}. The $g_\perp$ and the g_{II} values of the zeolite encapsulated copper complexes are found to be 2.076 and 2.395 respectively and the $A_\perp$ and A_{II} values are 103.33 x10^{-4} and 110 x 10^{-4} cm^{-1}. The g_{II} value is greater than the $g_\perp$ value indicating a tetragonal

71
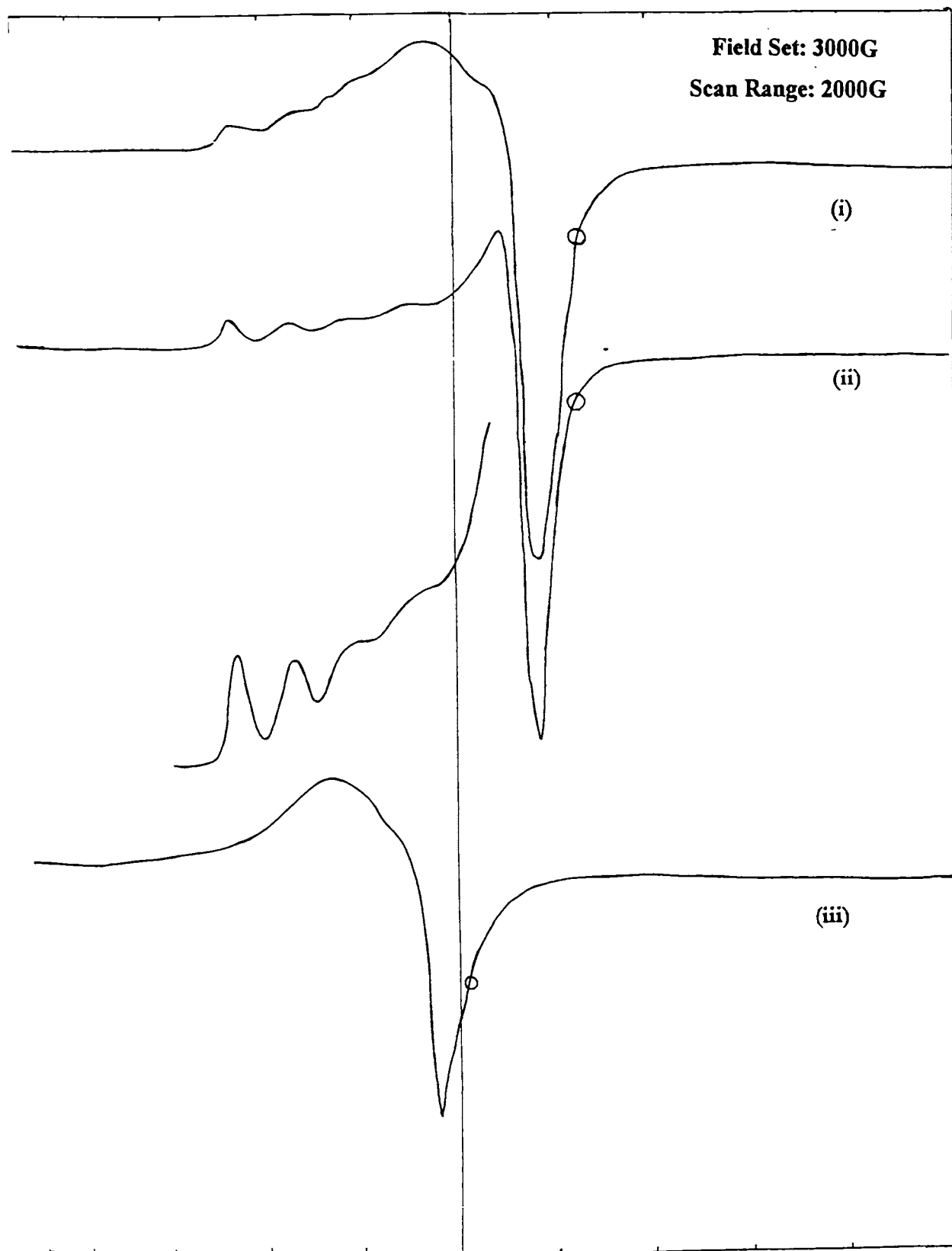
Figure III. 6 EPR Spectra of i) CuY ii) YCuOPD iii) Cu(OPD)$_2$

geometry for the copper complex. The in-plane covalence parameter, α^2 and bonding parameter, P are 0.7698 and 0.8826 respectively. The α^2 values give information about the nature of bonding. The smaller the square of α, the more covalent is the bonding, α^2 value of 1 suggests complete ionic bonding while α^2 value of 0.5 suggests complete covalent bonding. The α^2 value of 0.7698 for the zeolite encapsulated complex indicates that the metal ligand bond is intermediate between an ionic and covalent bond.

The change in the EPR parameters of metal exchanged zeolite (YCu) on complexation with the ligand indicates the encapsulation in the zeolite cavities. The EPR parameters of the neat, zeolite encapsulated complexes and CuY are tabulated in the Table III.7. The EPR spectrum of the neat copper complex of o-phenylenediamine was recorded in the solid state in order to compare it with that of the encapsulated complex. The hyperfine splitting is not observed in the neat complex even at liquid nitrogen temperature. The broad EPR spectrum in the case of the neat copper complexes is due to nearest neighbour spin-spin interactions. The well resolved hyperfine features similar to that in dilute solution in the case of the encapsulated complexes indicate the encapsulation of the monomeric complex in the zeolite. The g_{II} in the case of zeolite encapsulated complex as well as metal exchanged zeolite is higher than the usually reported value. Such higher value for g_{II} was observed by Sakaguchi and Addison.[23] They have attributed it to tetrahedral distortion of a square planar chromophore or due to increasing positive charge on donor atom. The higher value of g_{II} is also an indication of the decreased covalence of the metal-ligand bond due to increased delocalization. The

higher g_{II} value obtained in the present may be due to the distortion caused by the ligand and the zeolite oxygen atom on coordination.

Both the neat as well as the zeolite encapsulated nickel complexes are EPR inactive. This may be because of octahedral-square planar equilibrium present in the zeolite encapsulated nickel complexes and the freezing of the geometry into the square planar one at liquid N_2 temperature. Cobalt complexes gave very broad EPR signals due to low spin-lattice relaxation time, which is expected for high spin cobalt(II) in octahedral geometry.

Table III.7:

EPR parameters of the CuY, zeolite encapsulated and neat
o-phenylenediamine complexes

Compound	$g_{\perp}$	g_{II}	$A_{\perp}$	A_{II}
MY	2.08	2.37	66.66	136.66
Zeolite encapsulated complexes	2.076	2.39	103.33	110
Neat complexes	2.09	2.19	116.66	73.33

3.4.2.6 Infrared spectra

The IR spectra, is the technique which is most often used to get information about the donor atom which is coordinated to the metal. The IR spectra of the neat complexes are given in Figure III.7. The N-H stretching frequencies of the unbonded amine group usually occurs in

73
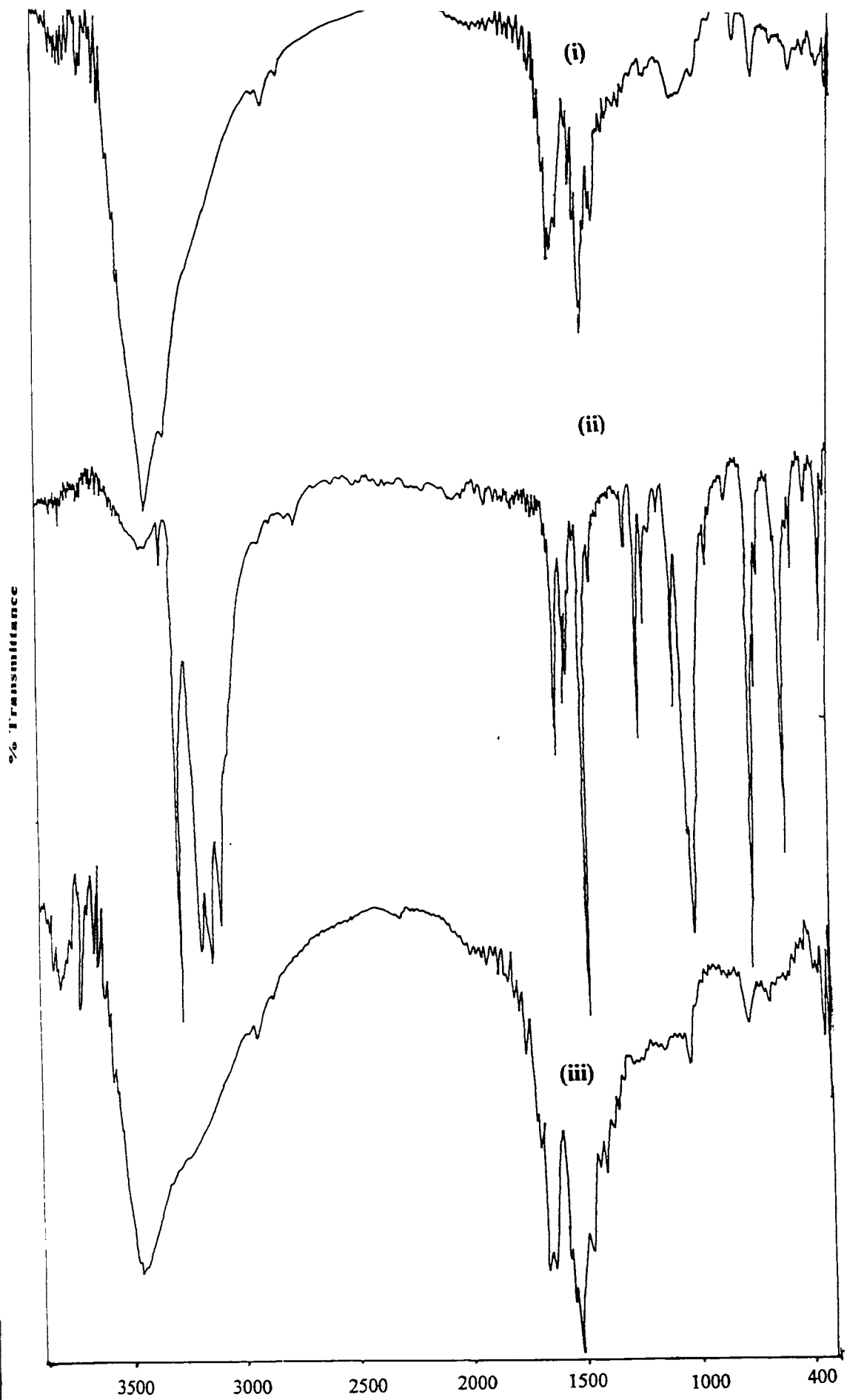
Figure III. 7 IR Spectra of i) Co(OPD)$_2$ ii) Ni(OPD)$_2$ iii) Cu(OPD)$_2$

the region 3500-3400 cm^{-1}. In the case of neat nickel(II) complex of
o-phenylenediamine, the N-H stretching frequencies are observed at
3350 and 3293 cm^{-1} which indicates the involvement of
benzoquinonediimine type linkage to the metal. This is also supported by
the increase in C=N stretching frequencies from 1210 cm^{-1} to 1253 cm^{-1}.
The IR spectra of the neat cobalt and copper complexes were found to
be similar and shows some differences from the spectra of nickel(II)
complex. A similar observation was made earlier for the 1:2 complexes
of the nickel.[24] There is only a small decrease in the N-H stretching
frequency (from 3460 cm^{-1} to 3450cm^{-1} in the case of cobalt(II) complex
and to 3424 cm^{-1} in the case of copper(II) complex) and N-H bending
frequencies indicating that the bonding is through the free amino group
and not through the imino group in these complexes.

The IR spectra of the zeolite encapsulated complexes are given in
the Figure III.8 and the IR frequencies are represented in the Table III.8.
The spectra are dominated by the peaks due to the zeolite. The
stretching due to the zeolite OH group is spread over the region from
3500-3700 cm^{-1}. The bands due to the N-H can be assigned in the
region from 3300 to 3500 cm^{-1}. Among the zeolite encapsulated
complexes the cobalt complex exhibit a triplet N-H stretch as found in
many of the neat complexes. The C-N stretching bands are masked by
the zeolite peaks in the region 1200 cm^{-1}. Therefore evidence for
benzoquinonediimine linkage in the zeolite encapsulated nickel complex,
could not be obtained. There is an additional band below 2400 cm^{-1}. This
type of band is present in amino acids and primary amine salts. This may
be due to interaction of amino group of o-phenylenediamine with the
zeolite hydroxyl and formation of NH$_3^+$. Some of the zeolite framework
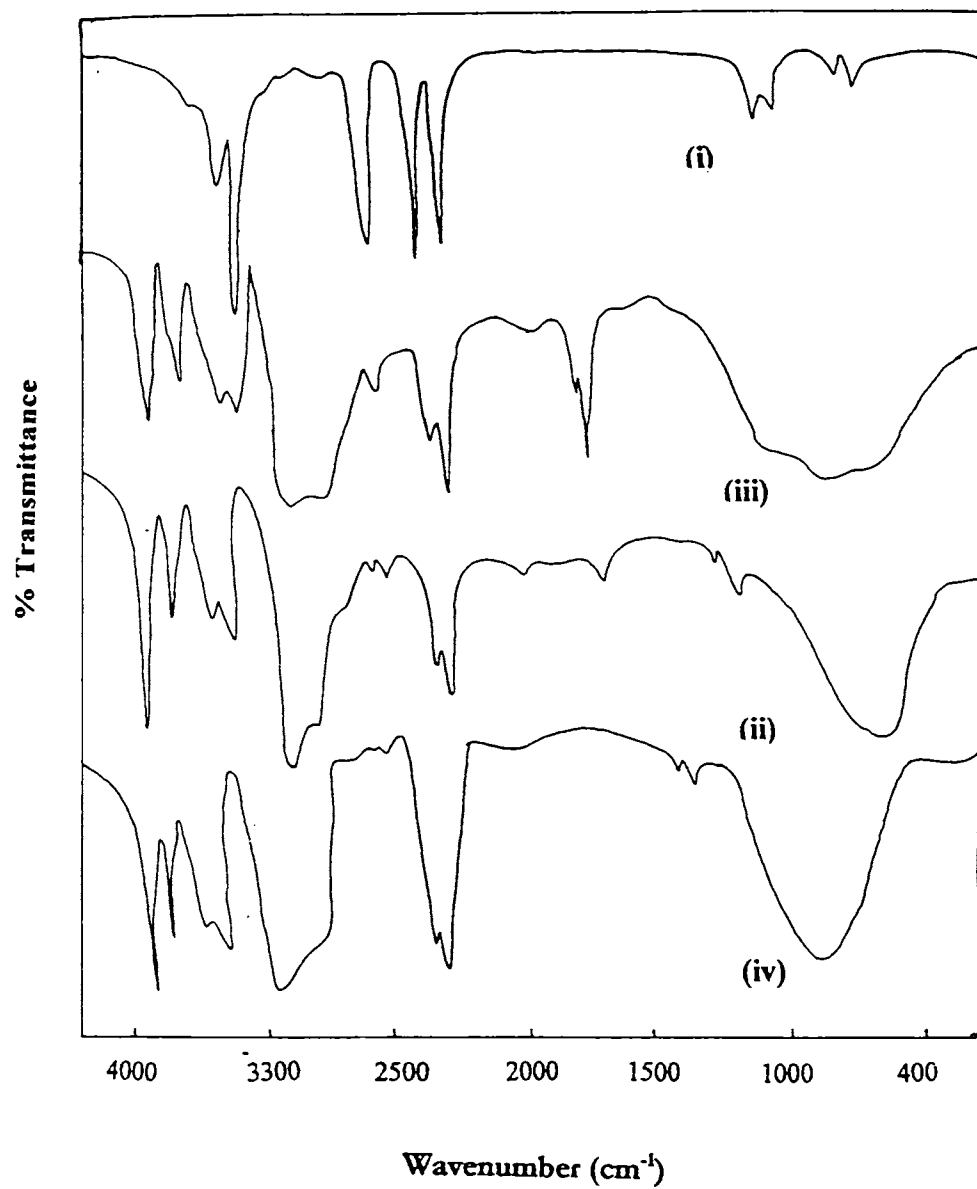
Figure III. 8 IR Spectra of i) OPD ii) YCoOPD iii) YNiOPD
iv) YCuOPD

peaks are also showing a shift indicating the electrostatic interaction with the metal complex. The N-H bending frequencies are shifting to lower frequencies indicating the coordination of nitrogen to the metal.

Table III.8.

FT-IR data of the encapsulated OPD complexes

Complexes	N-H Strech	N-H bend	Vibartions due to linkages between tetrahedra in zeolite		
OPD	3440, 3350	1680	-	-	-
CuY	-	-	752	692	465
YCoOPD	3542, 3373,3140	1654	769	667	456
YNiOPD	3474	1640	764	670	447
YCuOPD	3400	1650	778	697	461

3.4.2.7 TG analysis

TG analyses of the encapsulated complexes were performed in an inert atmosphere at a heating rate of 20°C. TG Curves of the zeolite encapsulated complexes is given in Figure III.9 and the DTG curves in Figure III.10. TG data indicates (Table III.9) a continuous weight loss in the temperature 30-400°C for all the complexes. Thermal stability of the complexes are as follows:
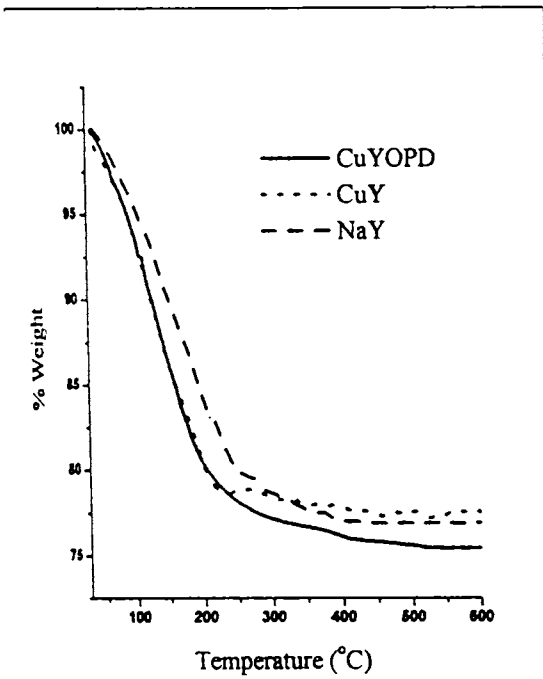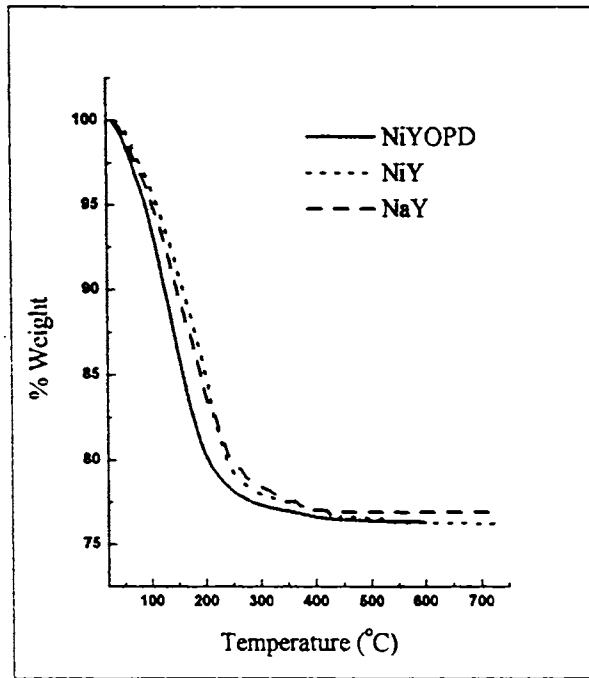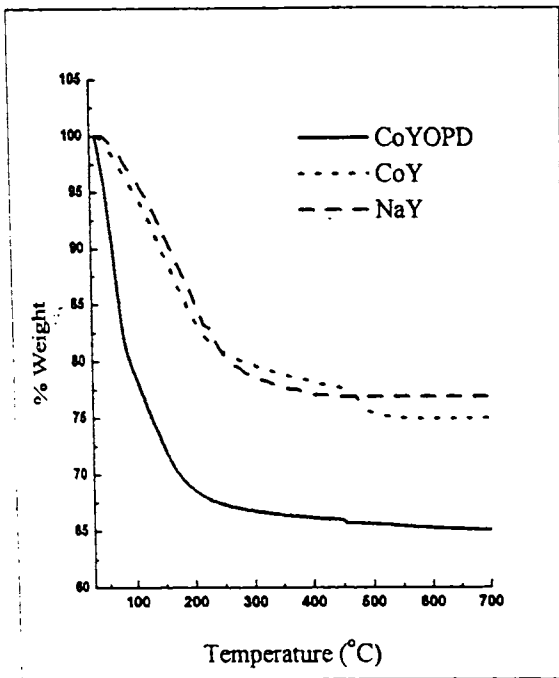
Figure III.9

TG Curves of zeolite encapsulated complexes of OPD, metal exchanged zeolite and NaY
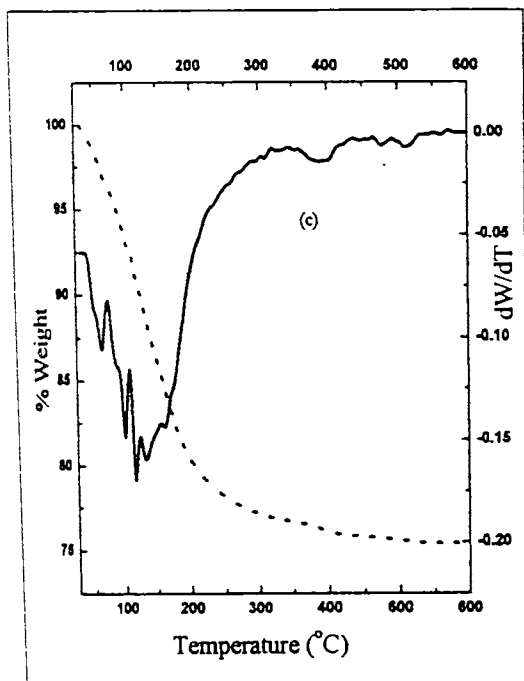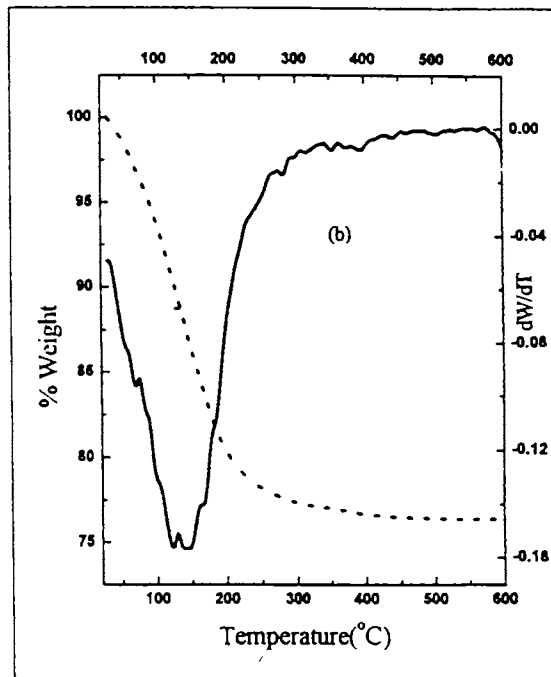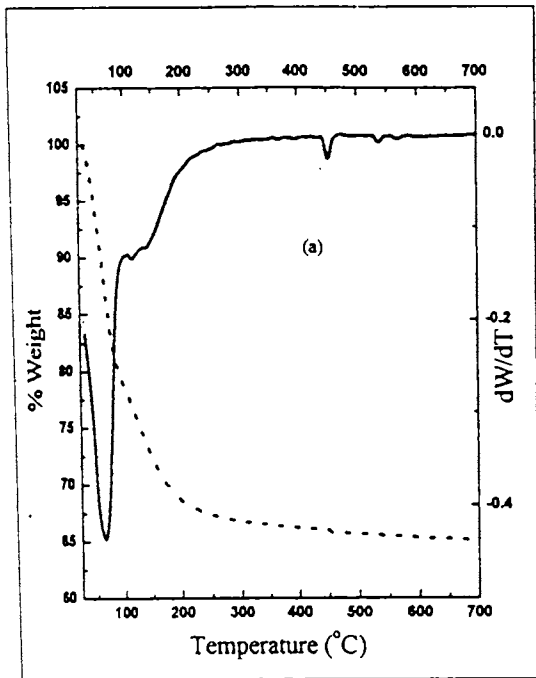
Figure III.10

TG/DTG Curves of zeolite
encapsulated OPD Complexes
  (a) Cobalt
  (b) Nickel
  (c) Copper

YCuOPD > YNiOPD > YCoOPD

Thus the removal of water as well as the decomposition of the complex is taking place in the same temperature range.

Table III.9

Thermogravimetric analysis data of the encapsulated complexes

Complex	Temperature range (^{o}C)	% weight loss
YCuOPD	30-400	24%
YNiOPD	30-400	22%
YCoOPD	30-400	33%

3.4.2.8 Electronic spectra

Electronic spectroscopy gives information about the d-orbital splitting through the d-d transitions and of the ligand-metal interactions through the ligand to metal charge transfer transitions. Information about the coordination bond is obtained qualitatively by comparison of the spectra with spectra of known complexes.[25] Diffuse reflectance spectroscopy was used to study the geometry of the complexes in zeolite cages since the complexes are insoluble. A Kubelka-Munk analysis was (details of which are given in Chapter II) used for the data interpretation. The diffuse reflectance spectra of neat as well as the encapsulated

complexes are given in Figure III.11. The diffuse reflectance data of the zeolite encapsulated complexes is given in the Table III.10.

a)   Cobalt Complex

The electronic spectra of cobalt(II) complex provide reliable structural information. Most six coordinate cobalt(II) complexes are reported to be high spin. Three transitions are usually predicted for octahedral complexes, $^4T_{2g}\leftarrow {}^4T_{1g}(F)$, $^4A_{2g}\leftarrow {}^4T_{1g}$, and $^4T_{1g}(P)\leftarrow {}^4T_{1g}(F)$. Additional bands may arise due to the further splitting of any of these terms due to distortions. The zeolite encapsulated complex show peaks at 13840, 15630, 17850, 25970 and 32540 cm^{-1}. This is characteristic of tetragonally distorted octahedral structure. This is also supported by the magnetic moment values. The neat complexes prepared have almost the same spectra as reported by the earlier studies[18]. The electronic spectra of the neat cobalt complex show absorption maxima at 33410, 28220, 18460, 15950, 15360 and 13280 cm^{-1}. These are typical for an octahedral o-phenylenediamine complex of cobalt.

b)   Nickel complex

Octahedral nickel(II) complexes are reported to have three absorption bands in the regions 8000 to 13000 cm^{-1}, 15000 to 19000 cm^{-1} and 25000 to 29000 cm^{-1}. The exact position of the peaks is found to depend on the strength of the ligand field. Zeolite encapsulated YNiOPD complex shows peaks (at 13480, 15980, 17750, 21560 and 25150 cm^{-1}) corresponding to six coordinate tetragonal complex. The electronic spectra of the neat complex shows peaks (35640, 26970, 17540, 15930 cm^{-1}) characteristic of octahedral complex with the o-

phenylenediamine ligands in a square planar environment and two axial positions occupied by the anions. Earlier studies indicated that there is some amount of distortion.[26]

c) Copper Complex

The diffuse reflectance data for the zeolite encapsulated copper complexes suggests a six coordinate structure with a tetragonal distortion. The tetragonal distortion of the copper(II) complexes with bidenatate ligands is smaller than that with monodentate ligands due to the long bond being part of the bidentate ligand in the equatorial plane. The t_{2g}-e_g level occur in a regular octahedron and in the case of tetragonal distortions the e_g level splits resulting in separation between the z^2 and x^2-y^2 transitions. Magnetic moment values of 1.86 BM cannot distinguish between octahedral and tetrahedral geometry in the case of copper complexes. The peaks in the case of zeolite encapsulated copper complex occurs at 31620, 23350, 14500, 12640 cm^{-1}. The neat complexes give absorptions at 37880, 35000, 22610, 21800, 14150 cm^{-1}. The data almost agree with that reported for the octahedral copper complexes of o-phenylenediamine.

Thus a comparison of the structure of zeolite encapsulated o-phenylenediamine complexes with that due to the simple complexes indicates that even though the structure of the complex remains to be six coordinate in both cases, the fifth and sixth coordination in the case of zeolite encapsulated complexes may be provided by the zeolite framework oxide ions or by water molecules present in the zeolite whereas in the case of the simple complexes it is provided by anions.
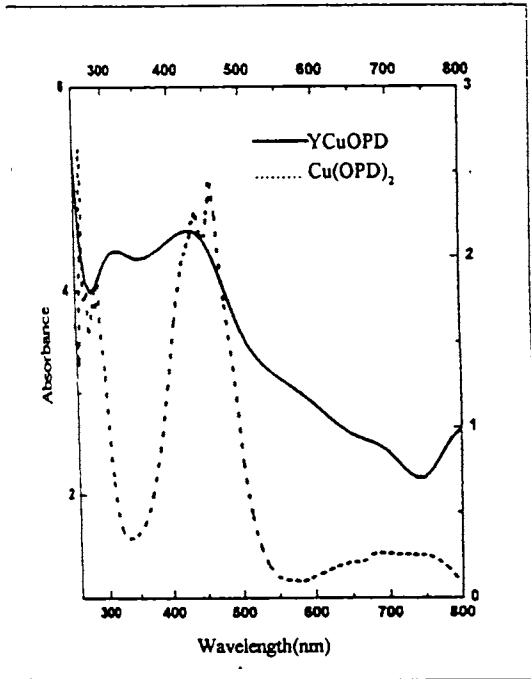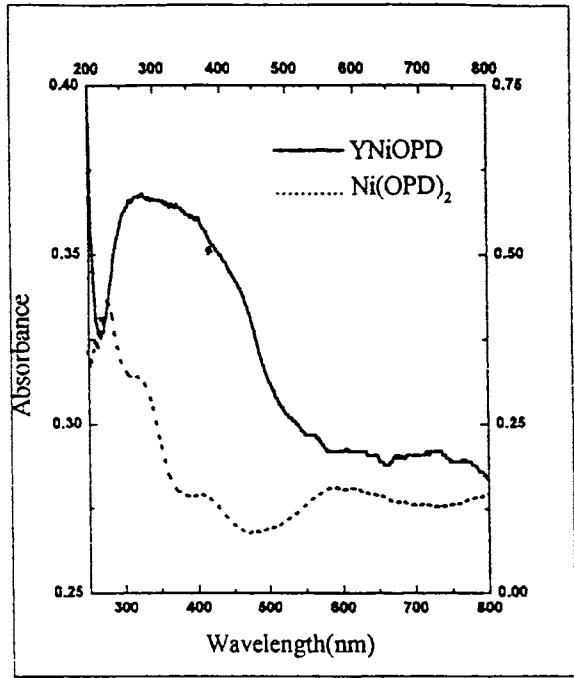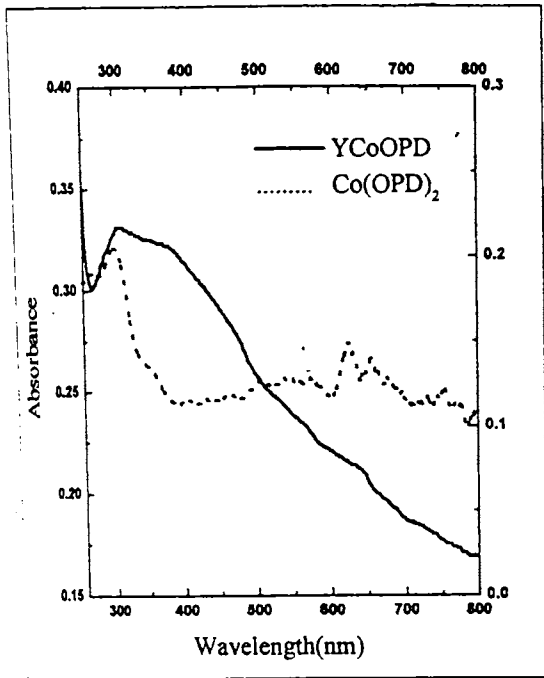
Figure III.11

Electronic spectra of neat
and zeolite encapsulated
OPD complexes
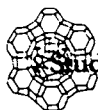
Table III.10

Diffuse reflectance data of the encapsulated complexes

Complexes	Absorption (cm^{-1})	Tentative assignments
YCoOPD	13840	$^4T_1g(P) \leftarrow {}^4T_1g(F)$
	15630	$^4A_2g(F) \leftarrow {}^4T_1g(F)$
	17850	$^4T_2g(F) \leftarrow {}^4T_1g(F)$
	25970	Charge Transfer
	32540	Charge Transfer
YNiOPD	13480	$^3T_1g(P) \leftarrow {}^3A_2g$
	15980	$^3T_2g(F) \leftarrow {}^3A_2g$
	17750	$^3T_1g (F) \leftarrow {}^3A_2g$
	21560	Charge transfer
	25150	Charge Transfer
YCuOPD	12640	$z^2 \ldots\ldots x^2-y^2$
	14500	$xy,yz\ldots x^2-y^2$
	23350	Charge transfer
	31620	Charge Transfer

Conclusions

Cobalt(II), nickel(II) and copper(II) complexes of o-phenylenediamine was successfully encapsulated in the Zeolite Y. The parent zeolite NaY used has the formula $Na_{56}(AlO_2)_{56}(SiO_2)_{136}.xH_2O$. The unit cell formula of all the metal exchanged zeolite was determined from the elemental analysis. Based on the XRD and SEM studies it was found that all the metal exchanged zeolites as well as the encapsulated complexes retained their zeolite structure. Flexible ligand method can thus be employed for encapsulation of o-phenylenediamine without any dealumination. Surface area and pore volume results provide evidence for encapsulation of the complexes. The probable structure of the complexes was assigned as six coordinate with some distortion based on the magnetic moment, EPR and electronic spectral data of encapsulated complexes. The structures are almost similar to that reported for the simple complexes. The evidence for coordination of amino group was obtained from FTIR spectra. Thermogravimetric analysis even though could not provide much information gave a comparative evaluation of stability and showed that both the complex as well as the ligand was removed in the same temperature range.

REFERENCES

1. A.L. Batch, H. Holm, *J.Am.Chem.Soc.* 88 **(1966)** 5201.

2. W. Heiber, R. Weisboeck, *Chem.Ber.* 91 **(1958)** 1146.

3. D.R. Marks, D.J. Phillips and J.P. Redfern, *J.Chem.Soc.(A)* **(1968)** 2013.

4. G. Wilkinson, R.D. Gillard, J.A. McCleverty., *Comprehensive Coordination Chemistry*, Volume 2, *Ligands*, First Edition, Peragamon Press, Oxford **(1987).**

5. A. Mederos, S. Dominguez, R.Hernandez-Molina, J. Sanchiz, T. Brito, *Coord.Chem.Rev.*193-195 **(1999)** 857-911.

6. A. Mederos, S. Dominguez, R. Hernandez-Molina, J. Sauchiz, F. Brito, *Coord.Chem.Rev.*193-195 **(1999)** 913-939.

7. T.A. Connors, M. Jones, W.C.J. Ross, P.D. Braddock, A.R Khokhar, M.L. Toba, *Chem.Biol.Interact.* 5 **(1972)** 415.

8. S.J. Meischem, G.R. Gale, L.M. Lake, C.J. Frangakis, M.G. Rosemblum, F.M. Walker, L.M.Atkins, A.B smith, *J.Natt.Cancer Inst.* 57 **(1976)**841.

9. W. Heiber, C. Schielssmann, K. Ries, *Z.Anorg.Chem.* 180 **(1929)** 89.

10. W. Hieber, R. Wiesboeck, *Chem.Ber.* 91 **(1958)** 1146.

11. M.D. Barbinok, I.S. Bukhareva, *Zhur.Neorg.Khim.*10 **(1965)** 861.

12. D. Bandopadhayay, *J.Indian Chem.Soc.* 34 **(1957)** 798.

13. S. Prasad, V. Krishnan, *J.Indian Chem.Soc.* 35 **(1958)** 352.

14. S. Prasad, Y.M. Reddy, M.S. Seethapathy, *J.Indian Chem.Soc* .42 **(1965)** 46.

15. G.A. Renovitch, W.A. Baker, *J.Chem.Soc(A)* **(1969)** 75.

16. C. Redshaw, G. Wilkinson, B. Hussain Bates, M.B. Hursthouse *J.Chem.Soc Dalton Trans.***(1992)** 1803.

17. A.A. Danopoulos, A.C.C. Wong, G. Wilkinson, M.B. Hursthouse, B. Hussain, *J.Chem.Soc.Dalton Trans.* **(1991)** 2051.

18. E.J. Duff, *J.chem.Soc.* (A) **(1968)** 434.

19. R. Parton, D.De. Vos, P.A. Jacobs — *Proceeding of NATO Advanced study institute on Zeolite Microporous Solids, Synthesis, Structure & Reactivity,* Kluwer, Dodrecht, 555 **(1992)** 578.

20. C. Tollman, H. Herron — *Symposium on Hydroc. Oxidation National Meeting of American .Chemical .Society,* New Orleans **(1987).**

21. E.P. Mozo, N. Gabriunas, F. Lucaccioni, D.D. Acosta, P. Patrono, A.L. Givestra, P. Reiz, B. Delmon, *J.Phys.Chem.* 97 **(1993)** 12819.

22. 22.T.A. Egerton, A. Hagan, F.S. Stone and J.C. Wickerman, *J.Chem.Soc.Faraday Trans I,* 68 **(1972)** 723.

23. U. Sakaguchi, A.W. Addison, *J.Chem.Soc.DaltonTrans.* **(1979)** 600.

24. G.S. Hall, R.H. Sodelberg, *Inorg.Chem.* 7 **(1968)** 2300.

25. A.B.P. Lever, *Inorganic Electronic spectroscopy",* Elsevier, Amsterdam **(1968).**

26. G. Maki, *J.Chem.Phys.*29 **(1958)** 162.
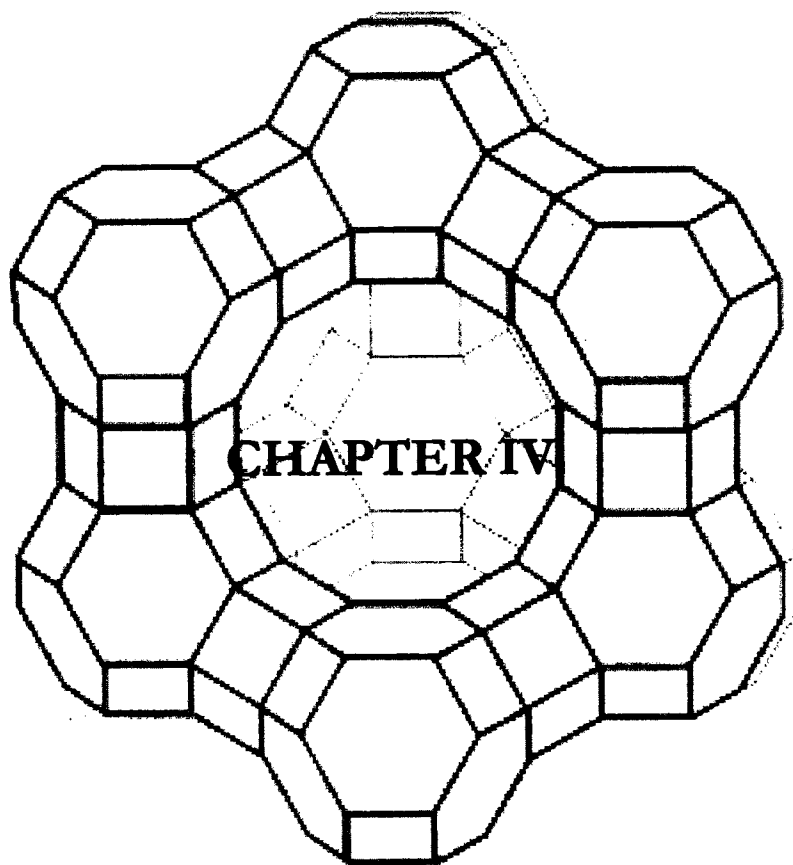
CHAPTER IV

ZEOLITE ENCAPSULATED COBALT(II), NICKEL(II) AND COPPER(II) COMPLEXES OF SCHIFF BASES DERIVED FROM 3-HYDROXYQUINOXALINE-2-CARBOXALDEHYDE

-

4.1 INTRODUCTION

Schiff bases are compounds containing an azomethine group and its preparation procedure was first reported by Schiff[1]. Metal complexes derived from Schiff base ligands have wide applications. Many of them are found to have immense catalytic and bio-mimetic property. Schiff base complexes are generally prepared by the interaction of metal ions and concerned Schiff base in suitable solvent[2]. By introducing electron releasing or election withdrawing substituent or an aromatic ring as an integral part to stiffen the ligand or by attaching a group which can provide a fifth coordination etc. one can tune the electronic and magnetic properties of metal complexes of Schiff bases, especially of tetradentate Schiff bases. The ligand properties and conformational aspects are mutually related in these type of complexes. In metal complexes with tetradentate Schiff bases, the ligands are in their ionized form with the four donor atoms which are nearly coplanar. The relative flexibility of such ligands allows distortion in the structure of complexes. The extent of distortion depends on the nature of metal and the bulkiness of the apical and axial ligands and also on the interaction of the ethylene bridge substituent with apical ligands. Such distortions play a

83

significant role in reversible oxygenation[3] exhibited by Schiff base complexes.

Schiff bases derived from 3-hydroxyquinoxaline-2-carboxaldehyde are expected to be weaker than those derived from salicylaldehyde. As a result there exists the possibility for spin cross over. Some of the neat complexes of the above ligand have been reported earlier to show this interesting property[4]. Further, many of them were reported to be dimeric complexes. It was therefore considered worthwhile to encapsulate the metal complexes of Schiff bases derived from 3-hydroxyquinoxaline-2-carboxaldehyde inside zeolite Y cages and study whether there is any structural change imposed due to the confinement inside the zeolite framework and also to assess the influence of encapsulation on their spin properties.

4.2 EXPERIMENTAL

4.2.1 Materials

The metal salts used for the preparation of the complexes and the various reagents used for the preparation of ligands are given in chapter II.

4.2.2 Preparation of metal exchanged zeolite

Metal exchanged zeolite Y was prepared by partially exchanging NaY with metal ion by stirring overnight with a solution of metal ion (0.01 mol dm^{-3}) according to the procedure described in Chapter II.

4.2.3 Preparation of ligands

All the ligands were prepared by condensing 3-hydroxy-quinoxaline-2-carboxaldehyde with various amines. They were prepared according to the procedures reported in chapter II. The structures of Schiff base ligands used in the present study are given in the Figure IV.1a-1d.

4.2.4 Preparation of zeolite Y encapsulated complexes

The encapsulation of metal complexes in zeolite Y was achieved by flexible ligand method[5-9]. A general procedure was adopted for the synthesis of the complexes. Metal exchanged zeolite Y (~5 g) was mixed with the ligand dissolved in 50 ml ethanol (the concentration of the ligand was adjusted to have 1:1 metal:ligand mole ratio) and was refluxed on a water bath for about 8 h. The complexes thus formed were then soxhlet extracted with ethanol and dichloromethane for several days until the extract was colourless. This process removes the any surface complexes formed on the zeolite. Uncomplexed metal ions present in the zeolite were removed by back exchanging with (0.1 mol dm^{-3}) NaCl solution for 24 h. The zeolite containing the metal complexes was then made chloride free by washing with distilled water and dried in vacuum. The resulting zeolite encapsulated metal complexes are denoted as YMQED, YMQPD, YMQHD and YMQDT where M = Co^{2+}, Ni^{2+} or Cu^{2+} and Y stands for zeolite-Y.

85
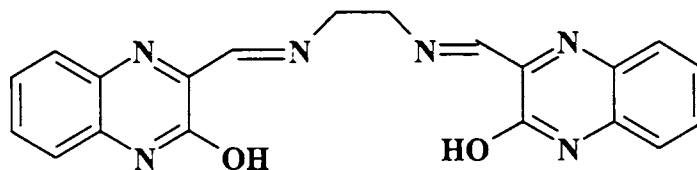
Figure IV.1a N,N'-bis(3-hydroxyquinoxaline-2-carboxalidene)
ethylenediamine(QED)
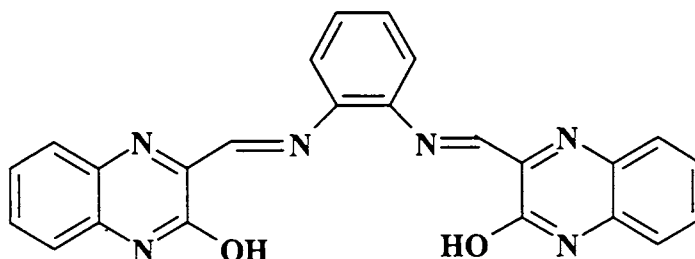
Figure IV.1b N, N'-bis(3-hydroxyquinoxaline-2-carboxalidene)
*o*-phenylenediamine, (QPD)
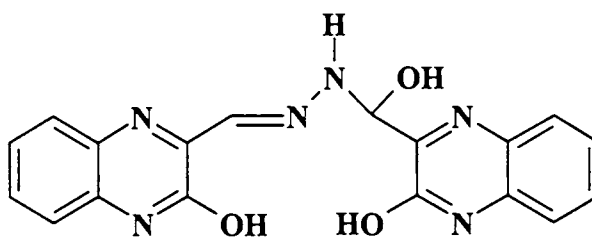
Figure IV.1c 3-hydroxyquinoxaline-2-carboxaldehyde
hydrazone, (QHD)
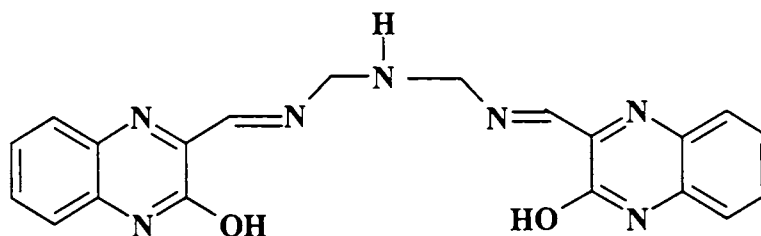
Figure IV.1d N, N'-bis(3-hydroxyquinoxaline-2-carboxalidene)
diethylenetriamine,(QDT)

4.3 PHYSICO-CHEMICAL METHODS

The details of the various physicochemical techniques used in the study are given in the chapter II.

4.3.1 Chemical analysis

Chemical analysis were done to obtain information about the bulk composition of the samples, in particular, to quantify the degree of exchange. The percentage of silica in the metal exchanged as well as zeolite encapsulated complexes was determined by converting the silica into SiF_4 as described in Chapter II. The metal percentage was determined using ICP-AES technique. For NaY, the usually observed Si/Al ratio of ~2.5 was obtained. The same ratio was retained as such even after the metal exchange indicating the absence of any dealumination during the exchange reaction. From the metal analysis, (Table IV.1-3) the unit cell formula of the metal exchanged zeolite was calculated.

4.3.2 C H N analysis

The details of the C, H, N analysis are given in Chapter II. The CHN analysis data obtained in the present case are presented in Table IV.1-3. The data confirm the formation of the metal complexes in the zeolite cavities. The metal percentage and CHN analyses suggest that 1:1 complex is formed inside the zeolite.

In order to understand the location of complex inside zeolite cages, an understanding on the position of cation in zeolite–Y is required. According to the earlier reports, different metal ions have preference for certain sites in the zeolite. During the exchange process, the metal(II) ions enters the zeolite in the form of a hexa-aqua complexes, which are localized in the supercage. This complex behaves in the same manner as metal(II)ions in solution. On dehydrating the metal exchanged zeolites, the coordinated water molecules are removed and the resulting vacant coordination sites may be occupied by lattice oxygen. Rehydration of the samples produces a back migration of the cation towards the supercage. Thus, the metal ions in a zeolite can be considered to be in dynamic system, where the metal migrates to the most favourable position to fulfill the best coordination. However, if the ligand is large enough it cannot enter the smaller cages. In such cases, supercage is the most probable site for complex formation. The metal(II) ions migrate to the supercage for complexation. In some cases the metal-oxygen bond (lattice) may be broken and new bond with the ligand will be formed.[10-14]

The analytical data for the complexes suggest that the percentage of metal is slightly in excess over what is required for formation of 1:1 complexes. This excess metal is not removed even after back exchange with Na^+ ions. The uncomplexed metal ions in the smaller cages can usually be removed during the back exchange. The excess metal ion concentration may be due to the occupation of more than one metal ion in the same cage of the zeolite. The complex formed with one of the ions may hinder the approach of the ligands for complex formation with other metal ions.

Table IV.1

Elemental analysis data for NaY, YCo and zeolite encapsulated cobalt complexes

Compound	%Si	%Al	%Na	%Co	%C	%N
NaY	19.70	7.90	6.69	-	-	-
YCo	19.72	7.80	4.70	6.02	-	-
YCoQED	19.60	7.71	5.30	4.10	2.14	0.79
YCoQPD	19.71	7.60	5.15	3.75	2.19	0.64
YCoQHD	19.76	7.80	5.26	5.43	1.34	0.47
YCoQDT	19.45	7.24	4.90	4.00	2.68	1.03

Table IV.2

Elemental analysis data for YNi and zeolite encapsulated nickel complexes

Compound	%Si	%Al	%Na	%Ni	%C	%N
YNi	19.73	7.20	4.28	3.35	-	-
YNiQED	19.60	7.50	6.4	2.58	0.35	0.12
YNiQPD	19.30	7.43	4.48	2.01	1.39	0.41
YNiQHD	20.1	8.2	5.45	2.35	2.70	0.97
YNiQDT	19.8	7.8	5.30	2.4	3.015	1.14

Table IV.3

Elemental analysis data for YCu and zeolite encapsulated copper complexes

Compound	%Si	%Al	%Na	%Cu	%C	%N
YCu	19.45	7.85	5.81	4.13		
YCuQED	19.30	7.70	5.13	1.18	1.46	0.48
YCuQPD	19.50	7.90	5.75	2.63	4.04	1.26
YCuQHD	19.60	7.73	5.88	2.95	2.28	0.86
YCuQDT	19.65	7.80	6.60	2.1	1.90	0.73

4.3.3 Surface area and pore volume

Surface area analyses provide a strong evidence for encapsulation. A decrease in surface area on encapsulation of metal complexes indicates that the pores of the zeolite are filled by metal complexes. This is also supported by a decrease in pore volume. In the case of zeolites the surface area is largely internal. Hence the inclusion of guest molecules should reduce their absorption capacity. The BET surface area of the metal exchanged zeolite-Y as well as the encapsulated complexes is given in Table IV.4. It can be seen that surface area of the zeolite encapsulated metal complex is considerably lower than the corresponding metal exchanged zeolite.

Table IV.4

Surface area and pore volume data of the metal exchanged and encapsulated complexes

	Surface Area (Sq.m/g)			Pore volume(cc/g)		
	Co	Cu	Ni	Co	Cu	Ni
Y	450	380	420	0.2604	0.2198	0.2494
QED	201	246	277	0.1157	0.1375	0.1621
QPD	330	300	320	0.1818	0.1736	0.1796
QHD	291	306	184	0.1558	0.1886	0.1053
QDT	273	164	328	0.1558	0.0963	0.1859

4.3.4 X-ray diffraction

XRD provides valuable information on crystallinity[15-17] as well as any change in unit cell parameters that might arise due to the encapsulation. The XRD pattern obtained for all the complexes were similar in nature. As a specimen, XRD patterns of the zeolite encapsulated copper complexes and those of the copper Y zeolite are given in the Figure IV.2. The patterns reveal that there is no change in the overall crystallinity of the zeolite Y host lattice on encapsulation. Thus the zeolite framework remains intact during encapsulation.

4.3.5 SEM analysis

Purification of the encapsulated complexes was done by soxhlet extraction using ethanol and dichloromethane. SEM[18] of the zeolite
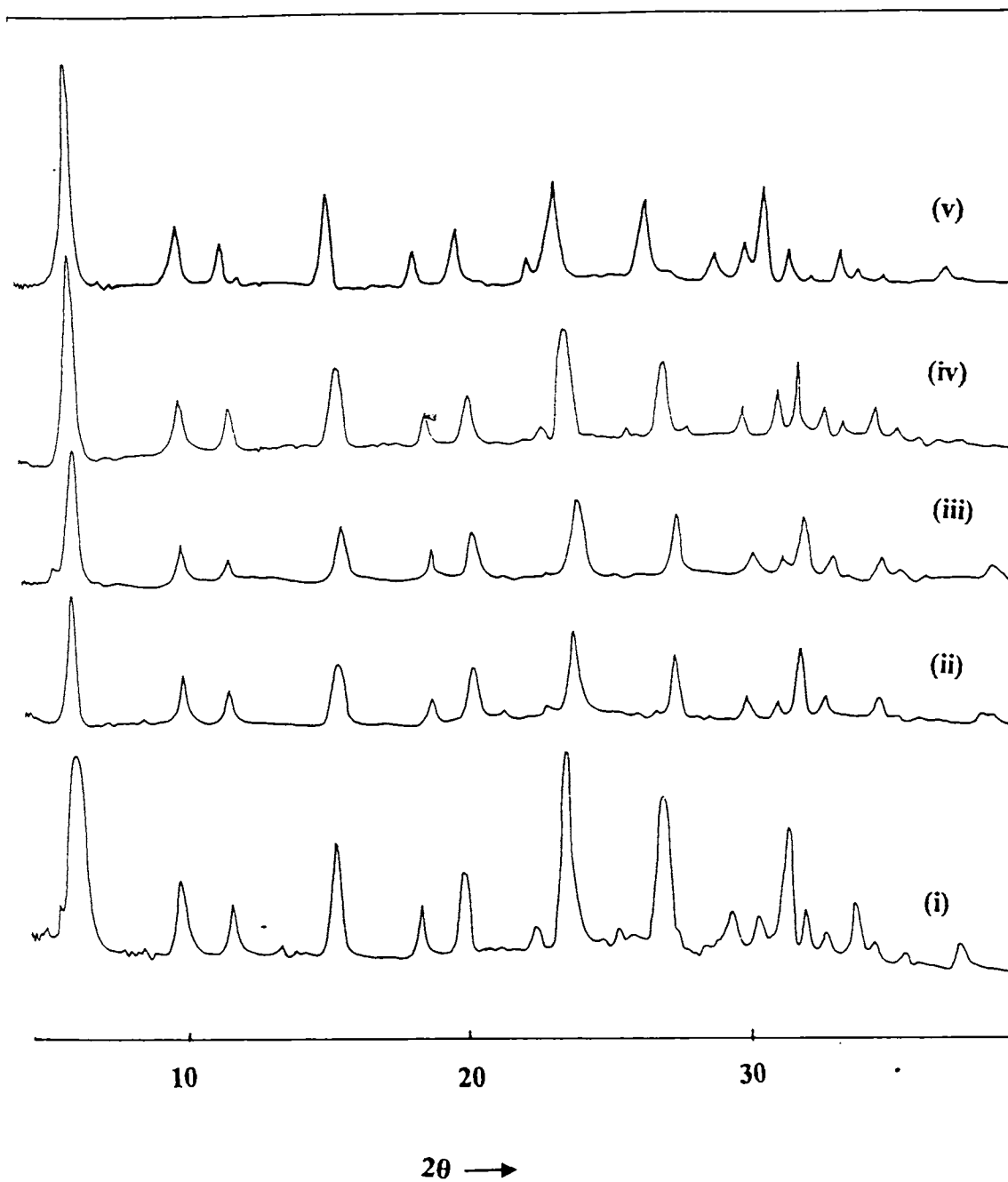
Figure IV.2 XRD spectra of i) YCu ii) YCuQED iii) YCuQPD iv) YCuQHD v) YCuQDT

10   20   30

$2\theta \longrightarrow$
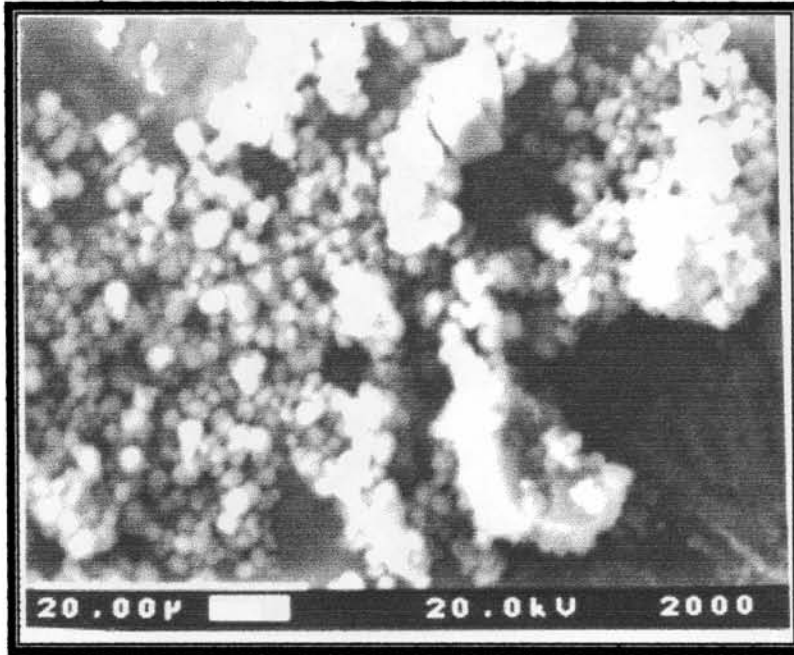
(i)
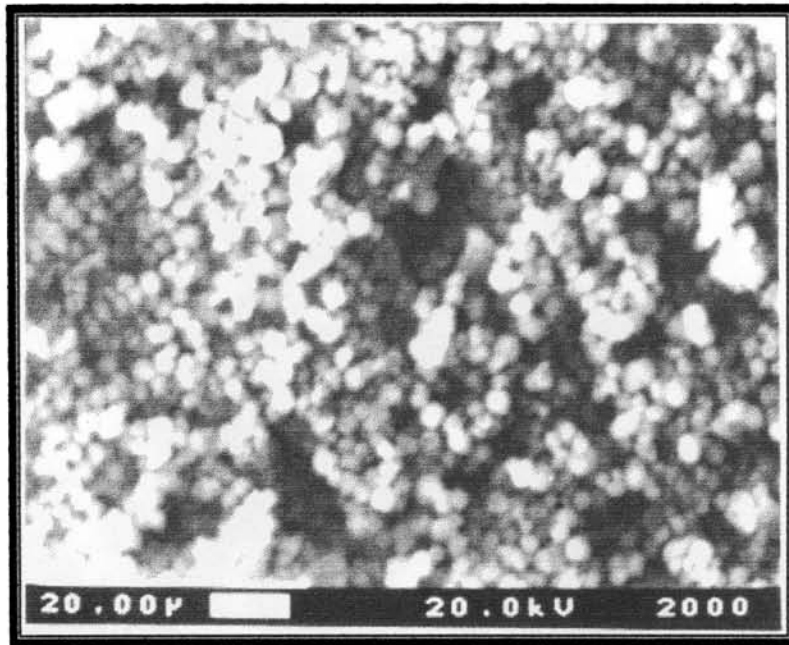
(ii)

Figure IV.3 Scanning Electron Micrographs of YCoQED (i) before and
(ii) after soxhlet extraction
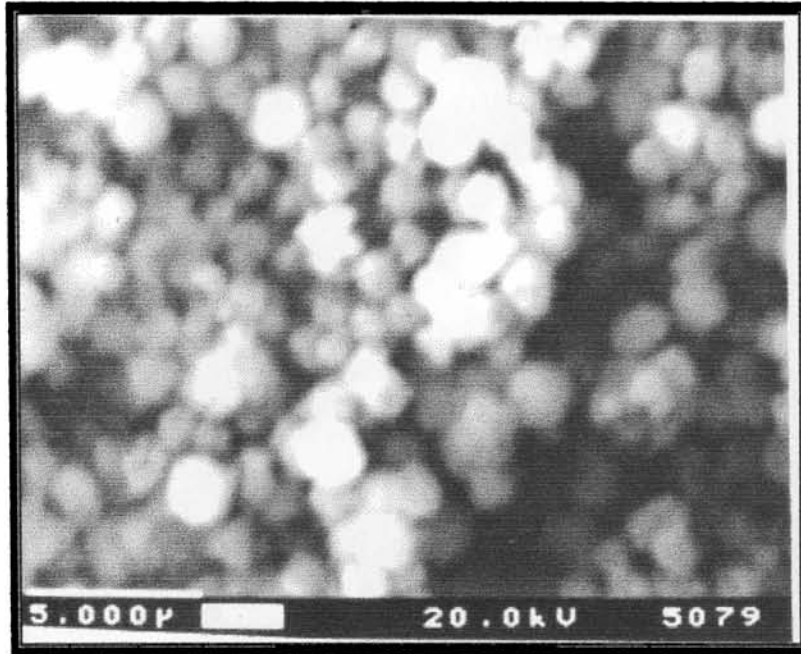
(i)
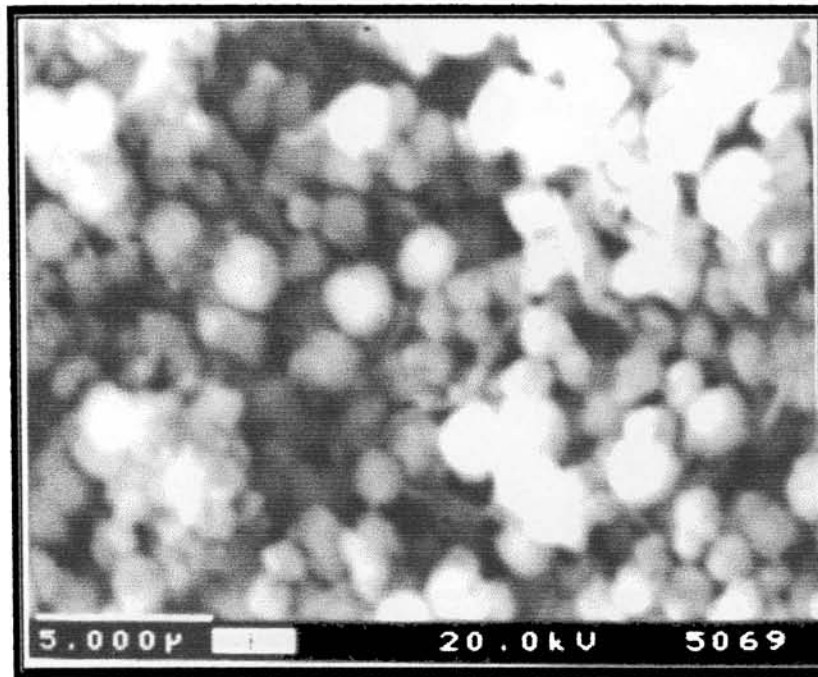
(ii)

Figure IV.4 Scanning Electron Micrographs of YCoQED (i) before and
(ii) after soxhlet extraction
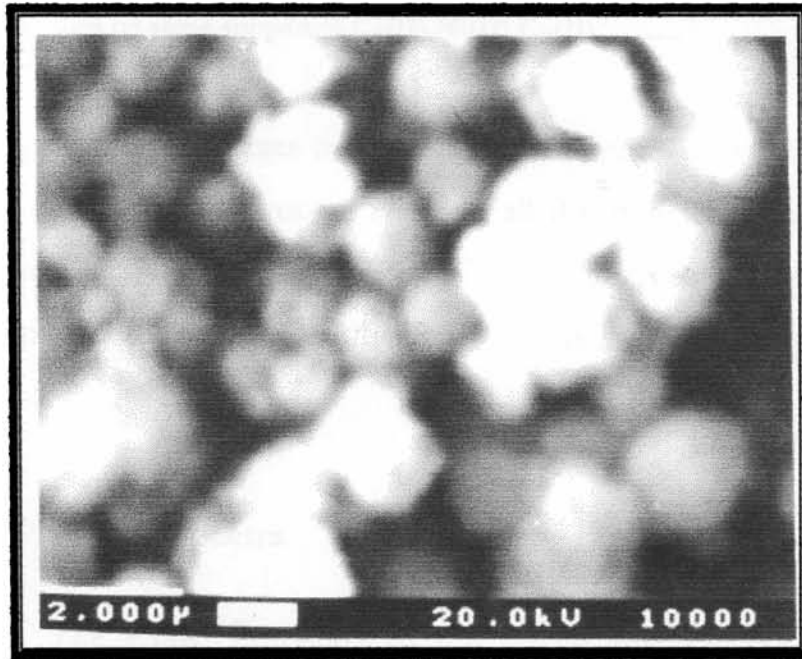
(i)
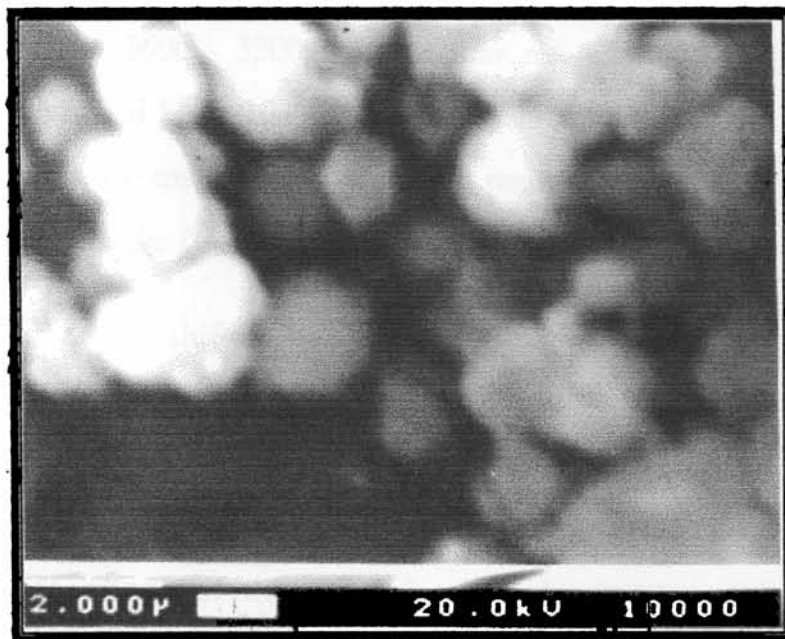
(ii)

Figure IV.5. Scanning Electron Micrographs of YCoQED (i) before and
(ii) after soxhlet extraction

% Transmittance (y-axis)

(iv)

(iii)

(ii)

(i)

Wavenumber (cm⁻¹) (x-axis)

4000 3500 3000 2500 1500 1000 400
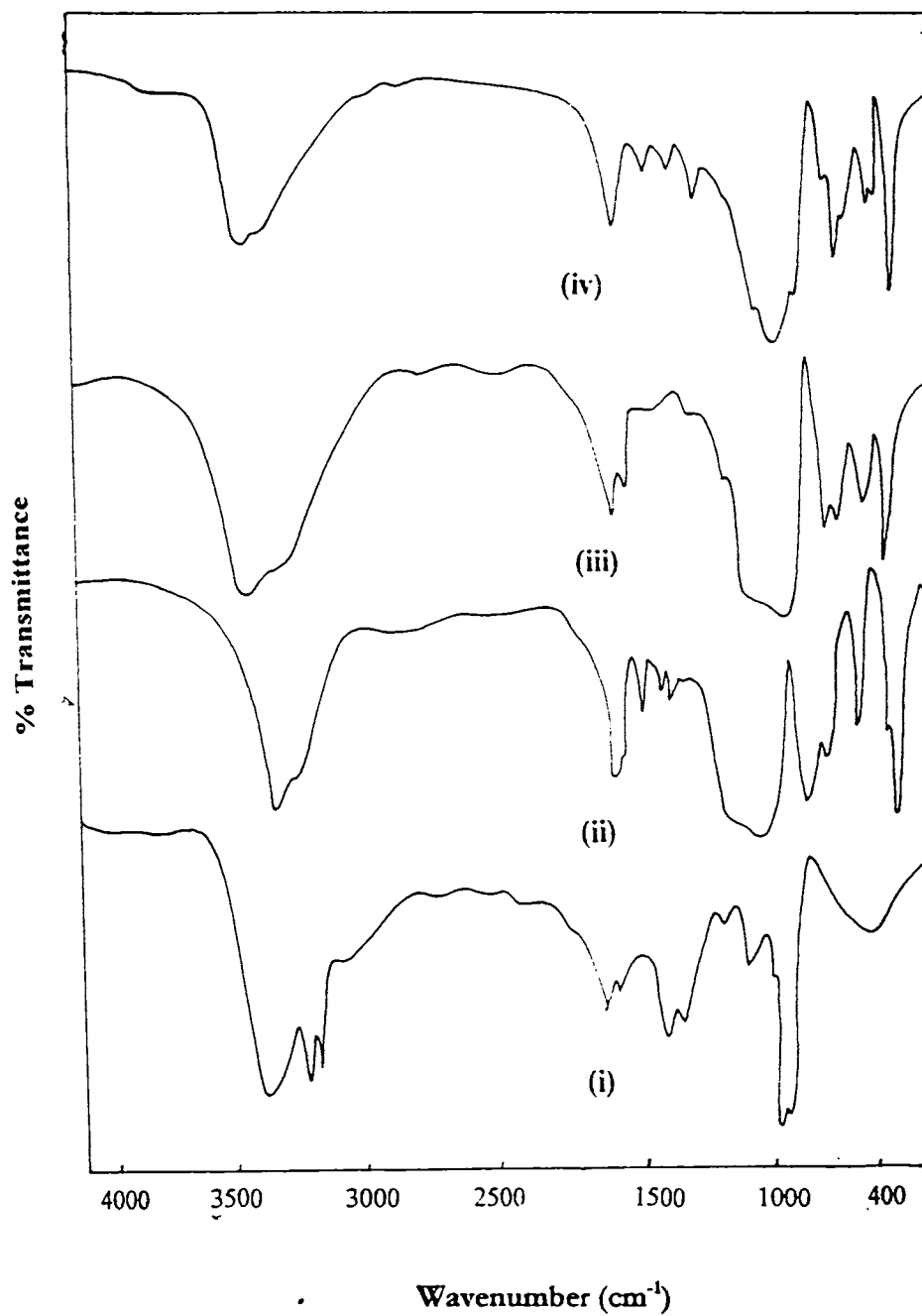
Figure **IV.6** IR Spectra of i) QED ii) YCoQED iii) YNiQED iv) YCuQED
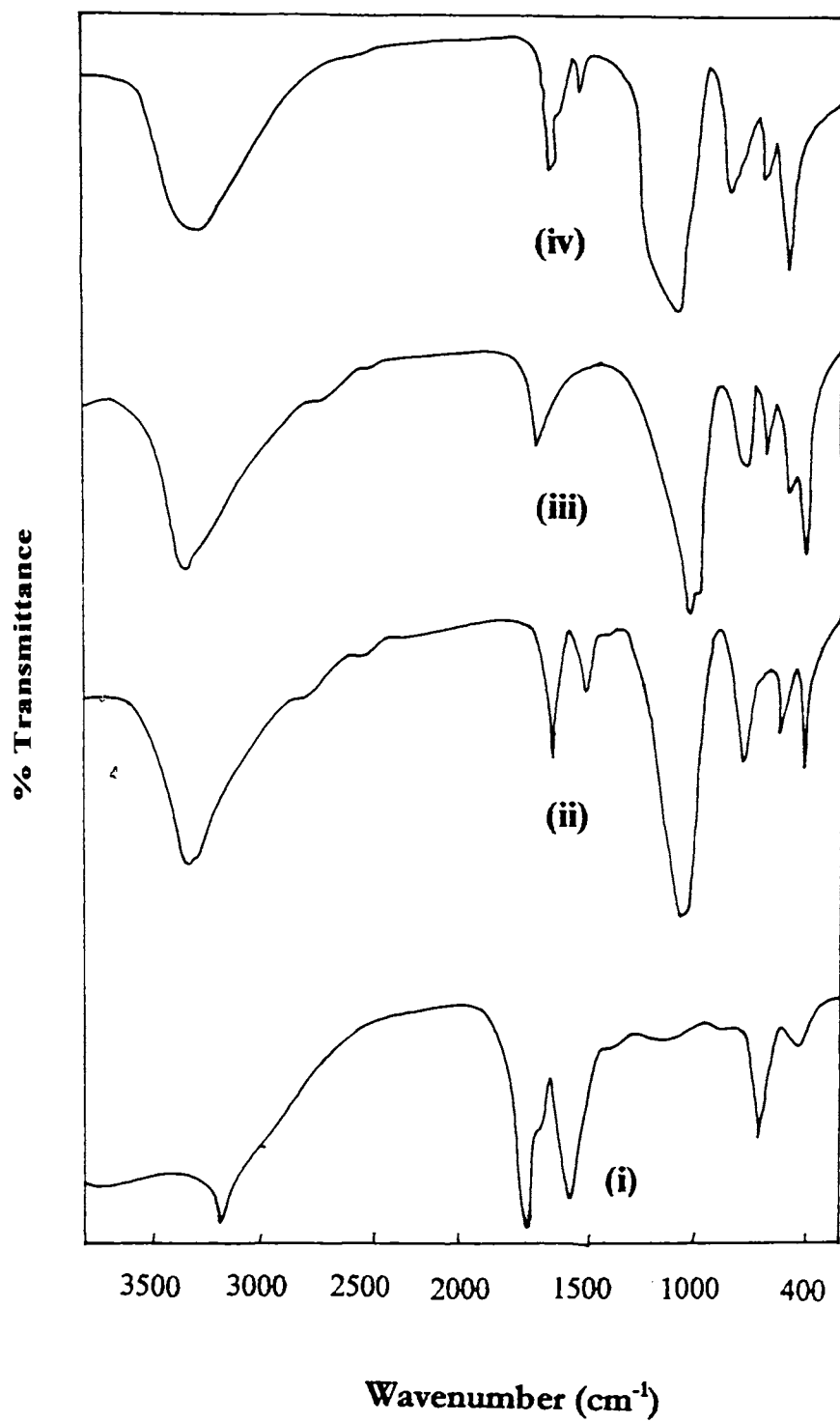
Figure IV.7 IR Spectra of i) QPD ii) YCoQPD iii) YNiQPD iv) YCuQPD
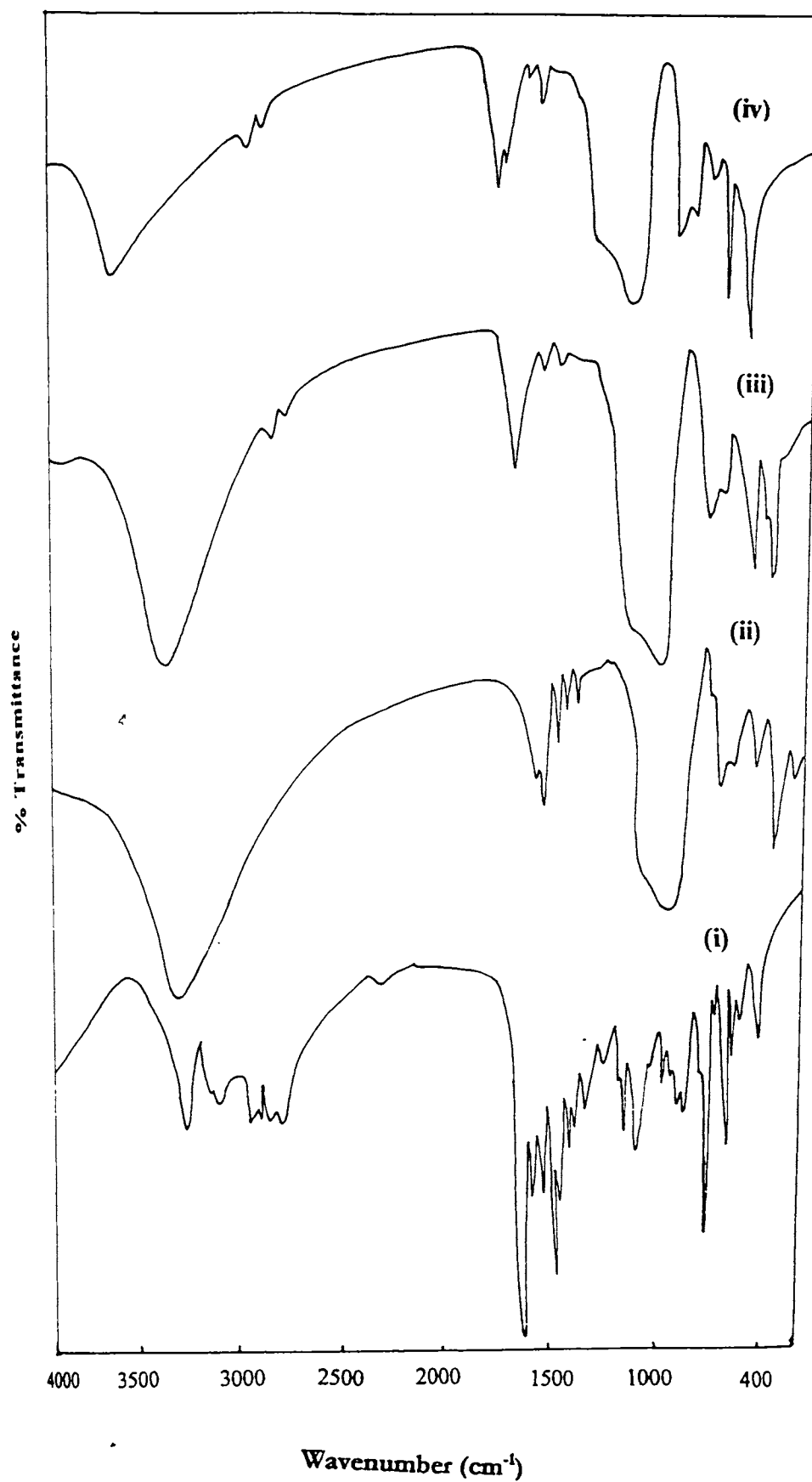
Figure IV.8 IR Spectra of i) QHD ii) YCoQHD iii) YNiQHD iv) YCuQHD
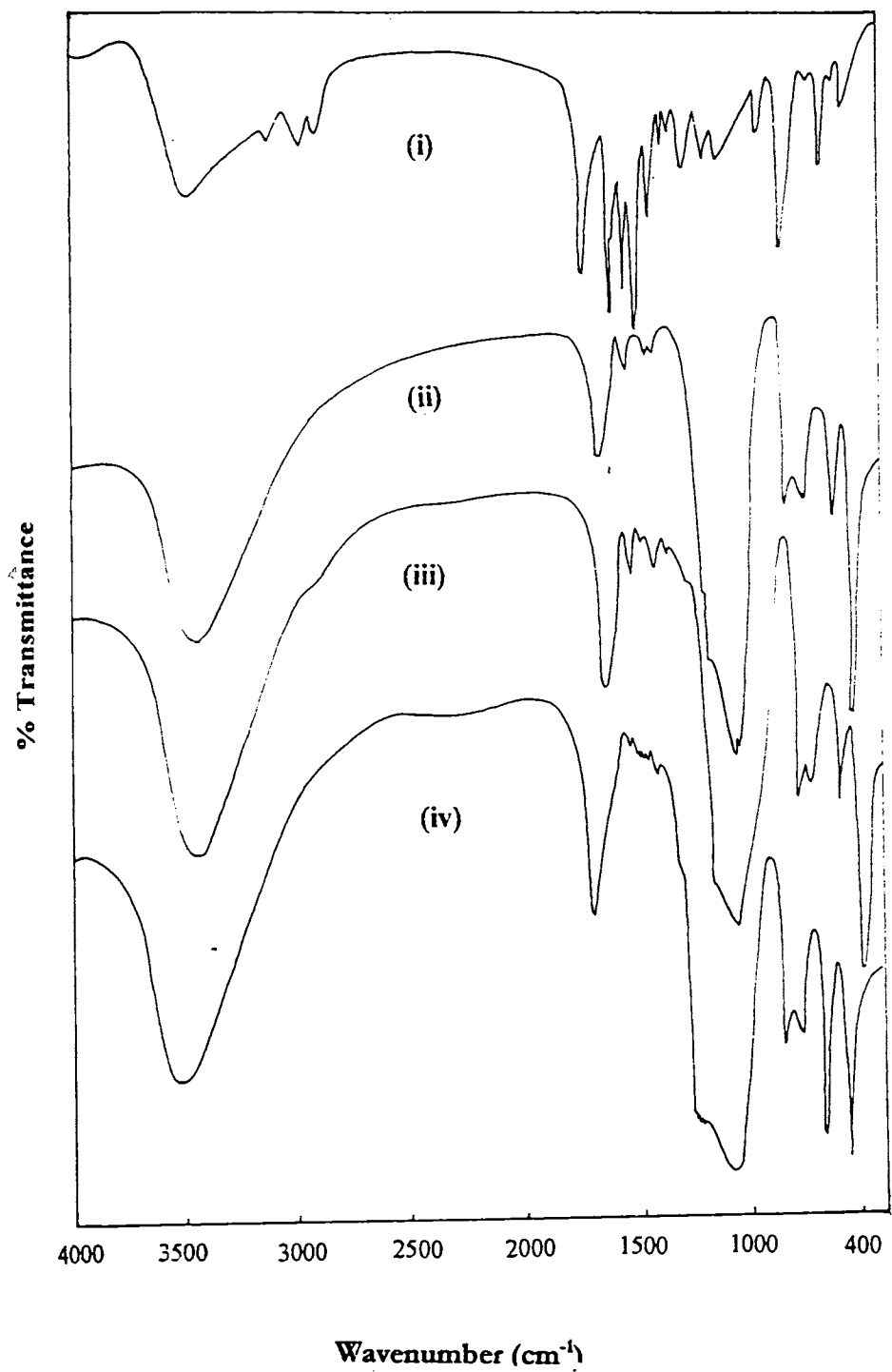
Figure IV.9 IR spectra of i) QDT ii) YCoQDT iii) YNiQDT iv) YCuQDT

4.3.7 EPR Spectra

Electron paramagnetic resonance spectroscopy[21] is a powerful tool to study the geometry of the paramagnetic complexes. The EPR technique enables us to determine the electronic state and the symmetry of the ligand field in metal exchanged zeolites. Several studies on the EPR of the zeolite encapsulated cobalt [22,23] and copper [24,25] complexes have been carried out. The EPR spectra of the present complexes were obtained at liquid nitrogen temperature.

4.3.7.1 Cobalt Complexes

The EPR of Co^{2+} is very sensitive to coordination. The bands obtained for zeolite encapsulated YCoQED and YCoQPD complexes were very broad. Usually spin transition or thermal vibrations decrease the life time of the excited state and due to this EPR spectrum becomes broad. But square pyramidal as well as square planar cobalt complexes are known to exhibit good EPR spectra The YCoQHD and YCoQDT complexes show EPR spectra with hyperfine splittings (See Figure VI.11-12). The g_{II} and $g_{\perp}$ values are found to be 2.07 and 2.12 respectively for YCoQHD and 2.07 and 2.11 for YCoQDT. A square pyramidal or square planar structure may therefore be assigned for these complexes.

4.3.7.2 Nickel Complexes

The EPR spectra obtained for the nickel(II) complexes, YNiQED and YNiQPD did not provide any valuable information. However the

EPR spectra of YNiQHD as well as YNiQDT showed hyperfine splitting (see Figure IV.11-12). The g_{II} and $g_{\perp}$ values, for YNiQHD are 2.06 and 2.05 respectively and for YNiQDT the values are 2.10 and 2.12. The spectra indicate an octahedral structure for these complexes.

4.3.7.3 Copper Complexes

EPR parameters of the copper complexes are given in the Table.IV.6. The $g_{\perp}$ and g_{II} values of all the complexes were determined. The in plane covalence parameter α^2 and bonding parameter P are determined from the EPR spectra. The details regarding the calculation of the above parameters are given in the chapter II. The EPR spectra of copper complexes YCuQED and YCuQPD are given in Figure IV.10 and that of YCuQHD and YCuQDT are presented in the Figure. IV.11.

All the complexes have $g_{II} > g_{\perp}$, indicating an axial geometry. Copper(II) complexes are unlikely of having a regular octahedral geometry due to Jahn-Teller distortions. Sakaguchi and Addison[26] has reported that the quotient g_{II}/A_{II} is an indication of extend of tetragonal distortion. The quotient ranges from 105 to 135 cm for square planar structures. A value of 130 cm obtained for YCuQED, therefore support a square planar structure for the complex. The higher g_{II}/A_{II} values for YCuQHD and YCuQDT suggest a six coordinate structure with a large amount of tetragonal distortions. The value of α^2 gives an indication about the extent of covalent or ionic bonding. The α^2 value of 0.75 for YCu is increasing to higher value (closer to ~1) indicating the ionic nature of the bond in all the cases.

Field Set: 3000G

Scan Range: 2000G

(i)

(ii)
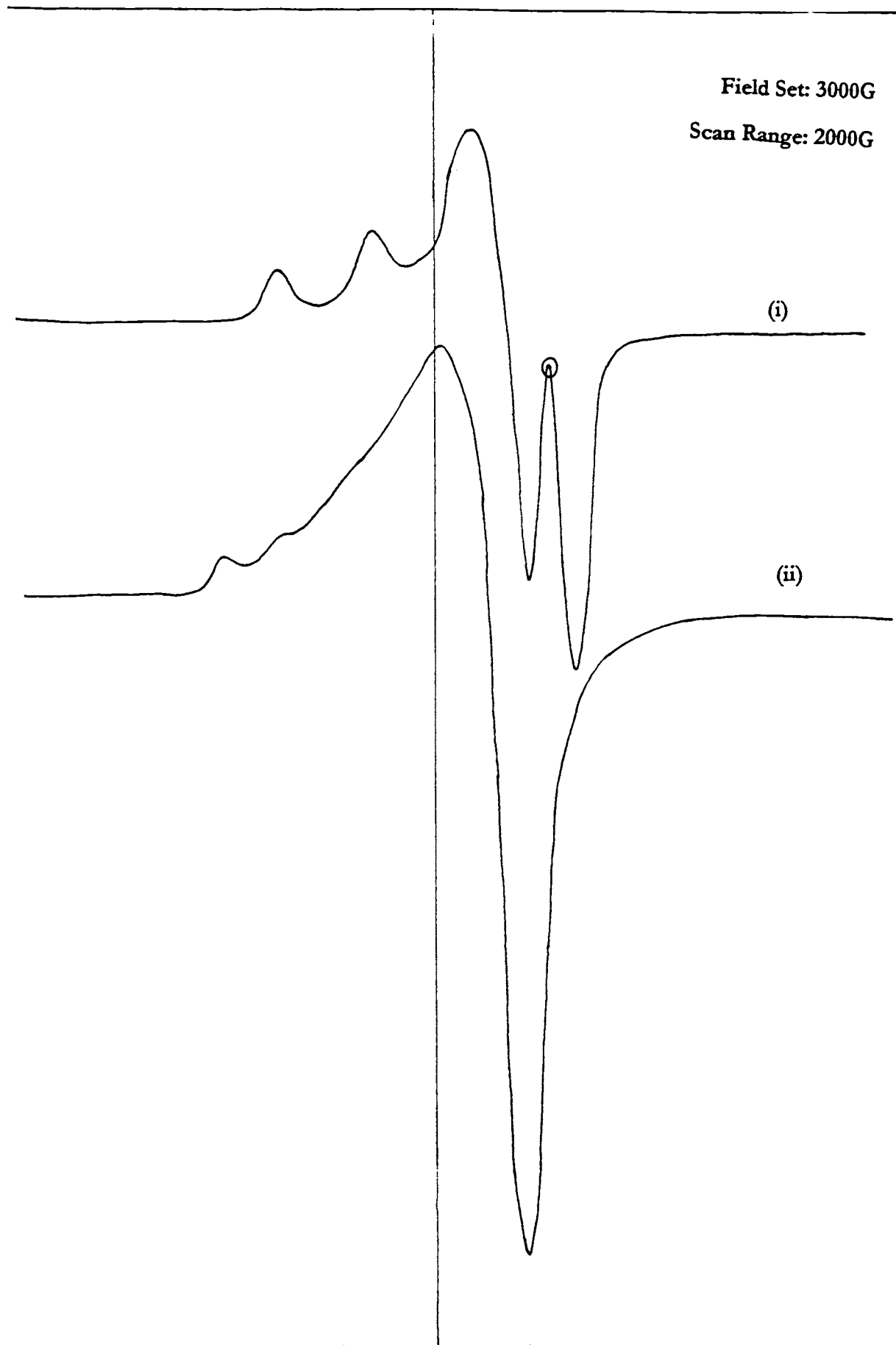
Figure IV.10 EPR spectra of i) YCuQED ii) YCuQPD
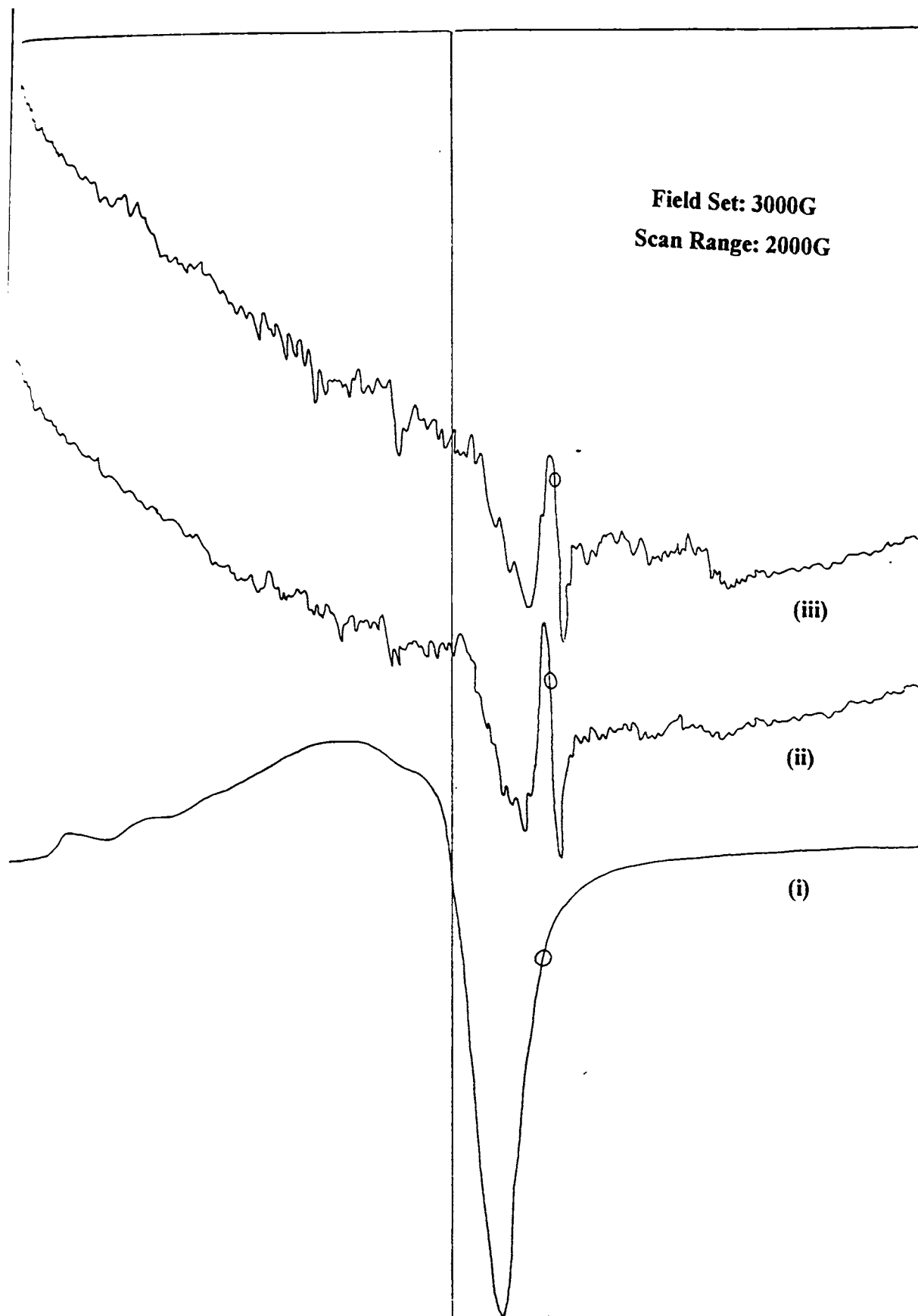
Figure IV.11 EPR spectra of i) YCuQHD ii) YNiQHD iii) YCoQHD
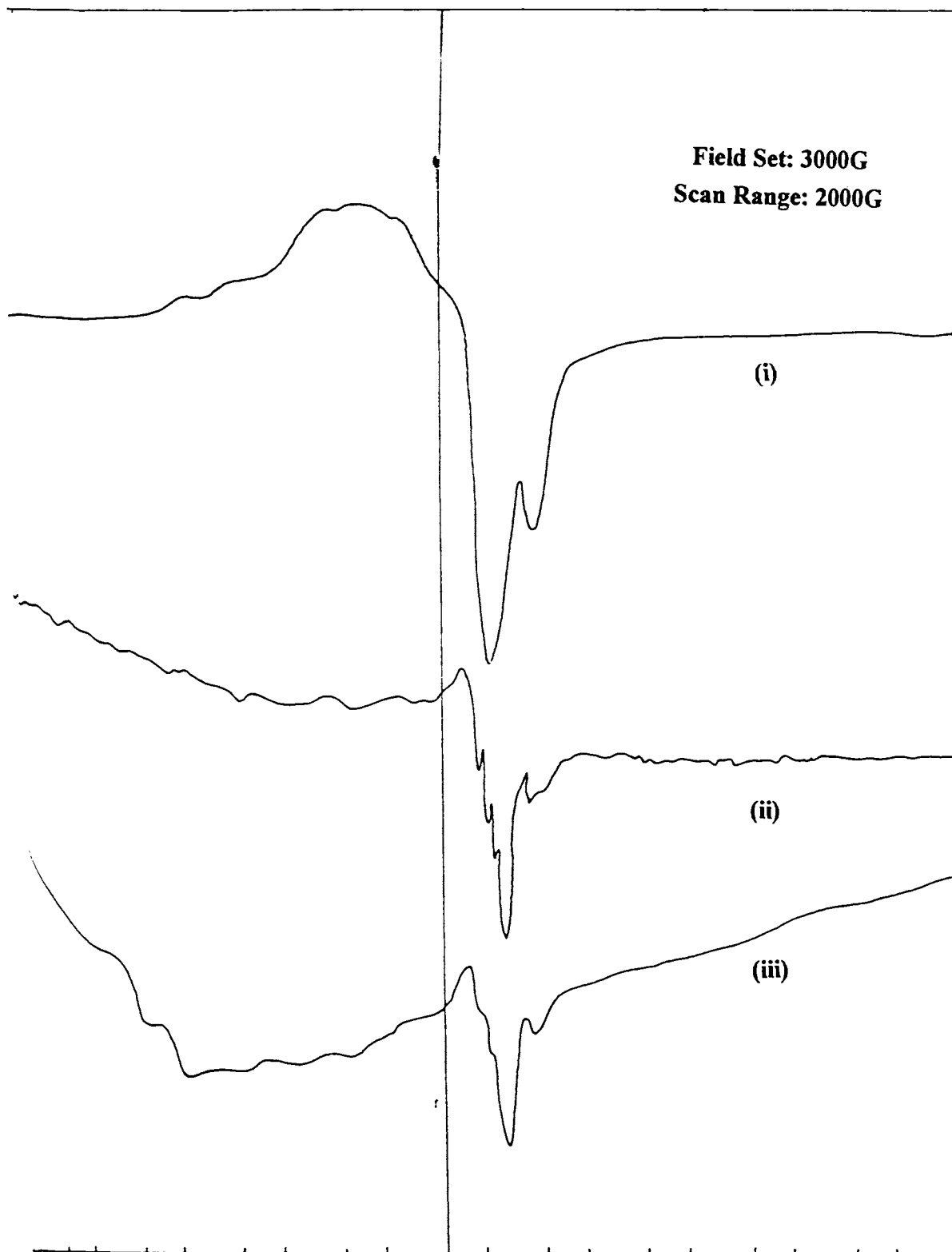
Figure IV.12 EPR spectra of i) YCuQDT ii) YNiQDT iii) YCoQDT

Table IV. 6

EPR Parameter of the copper Y and encapsulated copper complexes

Compound	$g_\perp$	$A_\perp$	g_{II}	A_{II}	α^2	P	g_{II}/A_{II}
YCu	2.08	66	2.37	136	0.75	-0.88	173
YCuQED	2.05	113	2.22	170	0.85	-0.85	130
YCuQPD	2.07	120	2.34	160	0.94	-0.87	146
YCuQHD	2.15	83	2.46	136	0.94	-0.90	180
YCuQDT	2.26	91	2.50	88	0.90	-0.96	283

It was anticipated that a variation of copper concentration in the zeolite may affect the structure and properties of the zeolite encapsulated complexes. Therefore a study was undertaken to know the changes in the EPR spectral properties that may arise when the zeolite Y containing various concentration of copper(II) ions are treated with the ligand, QED.

The variation in the concentration of the copper(II) ion in the zeolite was done by co-exchanging with various concentration of NaCl. YCuQED with various ratio of Cu^{2+}: Na^+(1:20, 1:10, 1:5, 1:1 or 2:1) was prepared as follows:

A solution containing Cu^{2+}: Na^+ of 1:20, was prepared by adding sodium chloride (10 mol dm^{-3}) to 100ml of copper(II) chloride solution (0.5 mol dm^{-3}). To this solution, zeolite Y (5 g) was added and stirred for

96

24 h. The metal exchanged zeolite thus obtained was filtered and washed free of chloride using distilled water. This was then calcined at 450°C. The ligand, QED (0.01 mol dm^{-3}) was dissolved in ethanol and added to the YCu samples containing varying concentrations of copper. The samples were then soxhlet extracted with ethanol and dichloromethane. Similar procedure was adopted for the preparation of 1:10, 1:5, 1:1 and 2:1 using 5.0 mol dm^{-3}, 2.5 mol dm^{-3}, 0.5 mol dm^{-3}, 0.25 mol dm^{-3} of sodium chloride respectively. For elemental analysis data see Table IV.7

Table IV.7

Elemental analysis data of YCuQED complexes containing various concentration of copper.

Ratio of Cu^{2+} to Na^{+} taken for preparation of YCuQED	%Na	%M	% composition of Unit cell
1:20	6.0	2.8	$Na_{47}Cu_{4.4}(AlO_2)_{56}(SiO_2)_{136}$ nH$_2$O
1:10	4.8	6.0	$Na_{38}Cu_{9.2}(AlO_2)_{56}(SiO_2)_{136}$ nH$_2$O
1:5	3.8	9.0	$Na_{28}Cu_{13.8}(AlO_2)_{56}(SiO_2)_{136}nH_2$O
1:1	2.9	10.0	$Na_{25}Cu_{15.5}(AlO_2)_{56}(SiO_2)_{136}nH_2$O
2:1	1.9	11.0	$Na_{22}Cu_{17}(AlO_2)_{56}(SiO_2)_{136}$ nH$_2$O

EPR spectra of the various samples are recorded at LNT and are presented in the Figure IV.13. The following observations were made from the study.

The spectrum of the 1:20 complex exhibits hyperfine splitting. The spectra broadened and hyperfine splitting disappeared with increase in concentration of the copper(II) ions in the complexes. The g_{II} values (Table IV.8) are remaining almost the same in all the complexes but the g values are varying slightly. The constancy of g_{II} value, points that there is no change occurring in the ligand environment (xy plane) with varying copper concentration. The variation in $g_{\perp}$ is attributed to change in the interaction with neighbouring copper(II) ions or lattice oxide or water molecules. The hyperfine splitting observed in the case of 1:20 complexes is due to lower concentration of copper ions (table). Extensive exchange leads to multiple occupancy of copper ions in the cages. This leads to interaction between neighbouring cations. The A_{II} and $A_{\perp}$ values are also varying. In all the complexes, the $g_{II} > g_{\perp}$ indicating an axial geometry.

Field Set: 3000G

Scan Range: 2000G
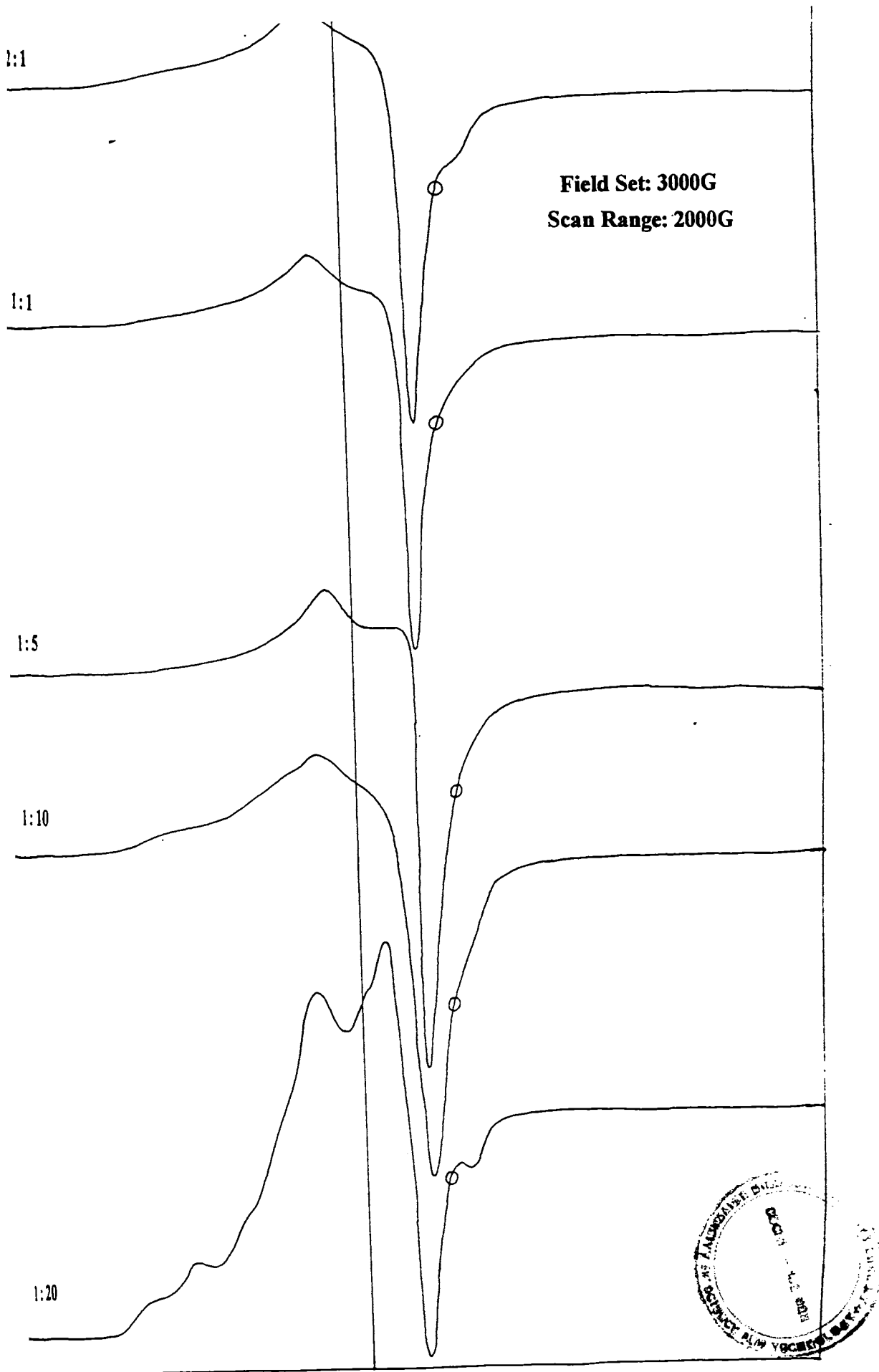
Figure IV.13 EPR spectra of YCuQED containing varying amounts of copper
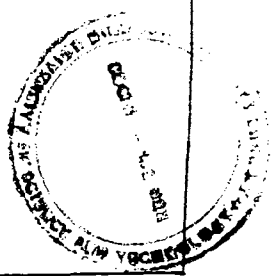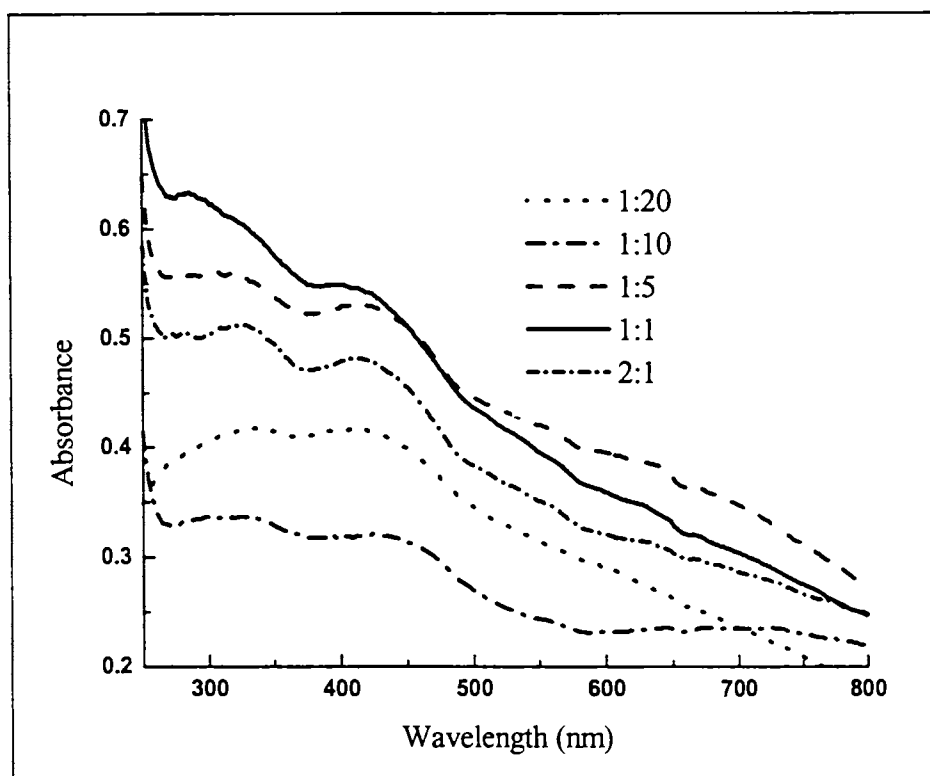
Figure IV.14 Diffuse reflectance spectra for the QED complexes containing different amounts of copper

. Surface area of the complexes was found to decrease with increase of copper(II) concentration, which might be due to larger blocking of the pores. The diffuse reflectance spectra of the complexes are given in Figure IV.14. The spectra shows slight variation is absorption peaks which suggest small changes in the geometry resulting from the interaction from neighbouring copper(II) ions

Table IV.8

EPR and diffuse reflectance data for the QED complexes containing different amounts of copper

Ratio of Cu^{2+} to Na^+ taken for preparation of YCuQED	$g_\perp$	g_{II}	$A_\perp$ $(x10^{-4}cm^{-1})$	A_{II} $(\bar{x}10^{-4}cm^{-1})$	Absorption (cm^{-1})
1:20	2.07	2.40	65,	100	30395, 24015, 16756
1:10	2.08	2.40	56.66	93.3	30000, 22768, 13827
1:5	2.06	2.40	66.66	98.33	31486, 23764, 15733
1:1	2.07	2.41	63.33	100	31055, 24615,16170, 14459
2:1	2.08	2.40	61.66	103.33	30769, 23769,18328, 15625

4.3.8 Magnetic moment measurements

In the present study, magnetic susceptibility[27] measurements were done using a Guoy balance and the values were obtained after applying necessary diamagnetic correction. The magnetic moments of the samples were then calculated using the weight of the unit cell (calculated form elemental analysis) of zeolite as the molecular weight. Reports on the magnetic study of zeolite encapsulated complexes are few because

most of the complexes behave as diamagnetic due to the large zeolite framework. The results obtained from the magnetic moment measurements are presented in the Table IV.9-11 and some useful inferences are drawn from this study. These inferences can be taken only as a qualitative guide in suggesting the structure.

4.3.8.1 Cobalt Complexes

Magnetic susceptibility measurement as a function of dehydration has been studied in detail for the cobalt exchanged zeolite Y.[10] Such systems are attractive choice for magnetic study because of the large difference in magnetic susceptibility shown by cobalt ions in different coordination. The earlier studies have indicated that in case of fully hydrated YCo, magnetic moment (μ_{eff}) suggests an octahedral coordination. Cobalt ions in the supercages (α cages) have different coordination to that in sodalite (β cage). Both four and six coordinate cobalt may be present in the cage. Paramagnetic susceptibility of Co^{2+} in Zeolite Y often becomes complicated due to a small field dependence arising from ferromagnetic impurities (0.18 atoms of Fe per unit cell).[28] Therefore the magnetic susceptibility of NaY was measured and this value was used for diamagnetic correction. The magnetic moment values of the zeolite encapsulated cobalt complexes are given in Tables IV.9. The magnetic moment values of the neat complexes are also included in this table for the sake of comparison.

Table IV.9

Magnetic moment data of the zeolite encapsulated and neat cobalt complexes

Cobalt Complexes	Magnetic moment of zeolite-Y encapsulated complexes(BM..)	Magnetic moment of neat complexes(BM.)[4]
QED	5.0	3.97
QPD	4.9	3.89
QHD	3.0	3.95
QDT	3.2	4.26

The neat complex of cobalt with ligand QED is a dimer with the formula $[Co(QED)]_2$. This complex has a magnetic moment of 3.97 BM. The zeolite encapsulated complex of the same ligand has a μ_{eff} value of 5.0 BM, which suggest an octahedral geometry for the complex. The YCoQPD also may have an octahedral geometry as its magnetic moment value is 4.9 BM. YCoQHD and YCoQDT exhibit μ_{eff} values of 3.0 and 3.2 BM respectively. These values are lower than expected for octahedral and tetrahedral complexes of cobalt. As these complexes are EPR active a low spin square pyramidal geometry can be assigned for these complexes. The simple complexes CoQPD and CoQDT are monomeric with magnetic moment of 3.89 and 4.26 BM respectively. The $Co(QHD)_2$ complex is dimeric and has magnetic moment of 3.97 BM The magnetic moment of QHD and QDT zeolite encapsulated

complexes are lower, and those of QED and QPD are higher, when compared to the magnetic moment values of the neat complexes. Thus there is a change in the structure of complexes on encapsulation.

4.3.8.2 Nickel Complexes

The magnetic moment values of the zeolite encapsulated and neat nickel complexes are given in the Table IV.10

The spin only magnetic moment for nickel(II) is 2.83 BM. For tetrahedral nickel complexes the magnetic moment values lie between 3.2-4.1 BM. and for octahedral complexes the magnetic moment value is between 2.9 – 3.3 BM. YNiQED has a magnetic moment value of 4.3 BM indicating a tetrahedral coordination, and magnetic moment value of 3.1 BM for YNiQPD hints towards an octahedral structure for this complex. YNiQHD and YNiQDT have magnetic moment value of 3.0 and 3.2 BM respectively resembling that of octahedral complexes. The simple complexes [Ni(QED)]$_2$ and [Ni(QHD)]$_2$ are reported to be dimers and NiQPD and NiQDT are monomers. All these complexes are showing somewhat lower magnetic moment value than the spin only value of 2.83 BM. This has been attributed to reduced singlet-triplet transition in the case of simple complexes. The values are higher in the case of the encapsulated complexes and the results of this study suggest change in the structure of all the nickel complexes on encapsulation.

Table IV.10

Magnetic moment data of the zeolite encapsulated and neat nickel complexes

Nickel Complexes	Magnetic moment of zeolite-Y encapsulated complexes(BM)	Magnetic moment of neat complexes(BM)[4]
QED	4.3	2.30
QPD	3.1	2.10
QHD	3.4	1.90
QDT	3.2	2.70

4.3.8.3 Copper Complexes

Magnetic moment values of the copper complexes lies in the range of 1.75-2.20 BM regardless of the stereochemistry. YCuQED has a magnetic moment of 2.0 BM. This may be because of the higher spin orbit coupling in the case of the above complex. These values suggest distorted square planar structure. Magnetic moment value of 1.95 BM is reported for the simple complex $Cu(QED)_2$. The magnetic moment data for the complexes are given in the Table IV.11.

Table IV.11

Magnetic moment data of the zeolite encapsulated and neat copper complexes

Copper Complexes	Magnetic moment of zeolite-Y encapsulated complexes(BM)	Magnetic moment of neat complexes(BM)[4]
QED	2.00	1.95
QPD	1.75	1.70
QHD	1.90	1.40
QDT	1.85	1.96

Zeolite encapsulated YCuQDT and YCuQPD complexes exhibit magnetic moment values of 1.85 and 1.75 BM respectively. This suggests an octahedral structure for these complexes. YCuQHD complex has a magnetic moment value of 1.90 BM. The simple complex $Cu(QHD)_2$ has a value of 1.40 BM. The lower magnetic moment of the neat complex is reported to be due to the antiferromagnetic coupling of copper atom. Such a coupling is absent in the encapsulated complex, YCuQHD, as its magnetic moment value is 1.90 BM.

4.3.9 Electronic spectra

The electronic spectra of all the zeolite encapsulated complexes were measured in the diffuse reflectance mode because of the insolubility of the zeolite encapsulated complexes. The location and coordination

taken up by the charge balancing cations and the complexes in the zeolite could be obtained from the electronic spectra of the complexes[29]. The spectra combined with the EPR data and magnetic measurements can be used to predict the probable structure of the zeolite encapsulated metal complexes. The UV-visible diffuse reflectance spectra of the zeolite encapsulated as well as the simple complexes are given in the Figure IV.15-18.

4.3.9.1 Cobalt Complexes

The electronic spectral data of the zeolite encapsulated cobalt complexes are given in the Table IV.12. YCoQED shows absorptions at 29820, 23920, 17830 and 15480 cm^{-1}. These values suggest a six coordinated octahedral coordination. Moreover, the complex is EPR silent indicating an octahedral structure with the ligand in a planar symmetry and the other coordination sites occupied by zeolite oxygen or water molecules. The YCoQPD complex also exhibits transitions characteristic of octahedral complexes. The absorptions are obtained at 28520, 23400, 17670 and 13500 cm^{-1}. In the case of YCoQHD the bands are seen at 28940, 24440 and 15690 cm^{-1} and for YCoQDT, the bands are at 30280, 23700, 15700 12970 cm^{-1}. As the already reported square pyramidal complexes, Co(ttp)I$_2$, Co(AP)$_2$I$^{+30,31}$ exhibit bands at similar positions, the present zeolite encapsulated complexes, may be considered to have square pyramidal geometry. Such a possibility is higher for these ligands, as they can act as pentadentate ligands. Furthermore, these complexes are EPR active which also supports square pyramidal structure.
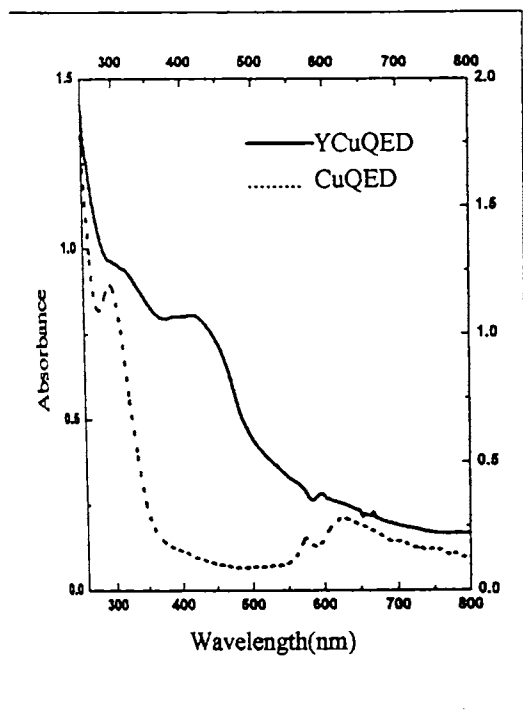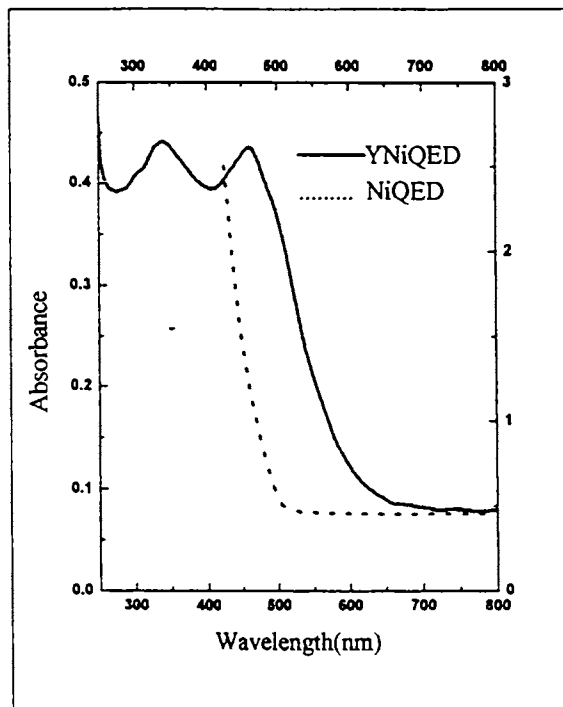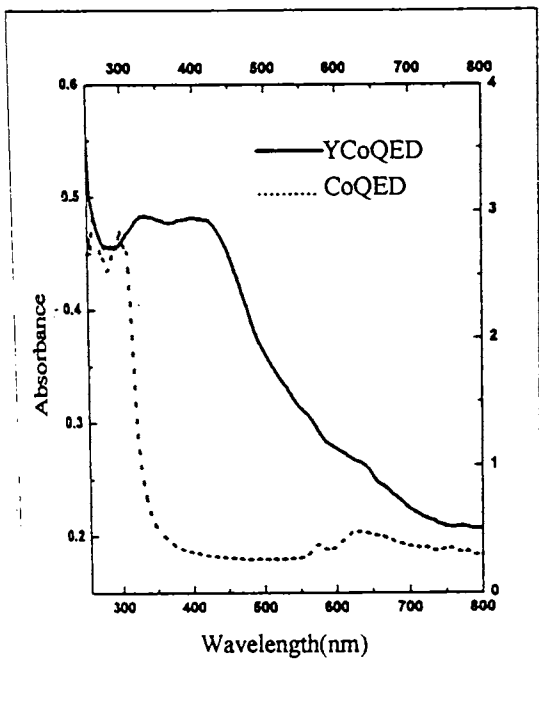
Figure.IV.15.

Electronic spectra of neat and zeolite encapsulated QED complexes
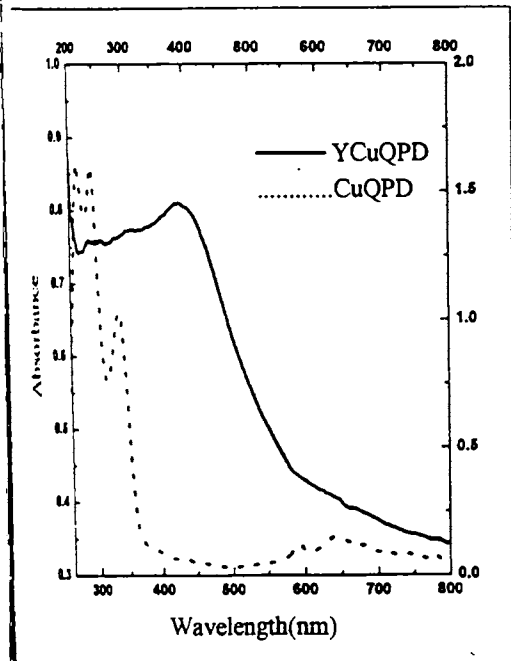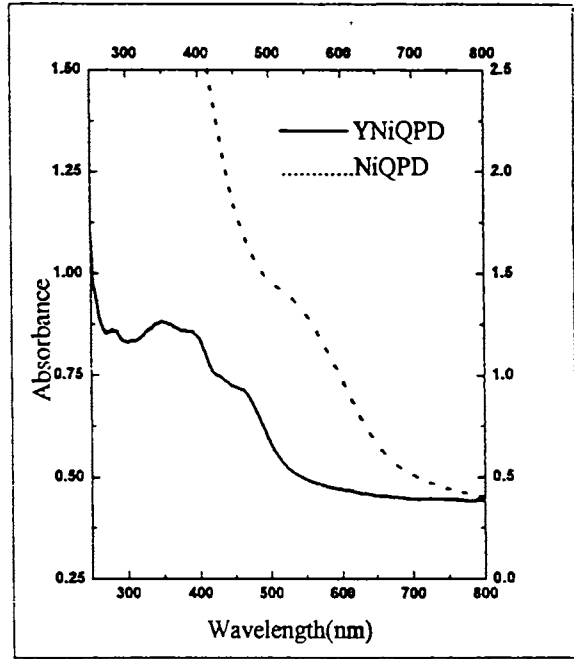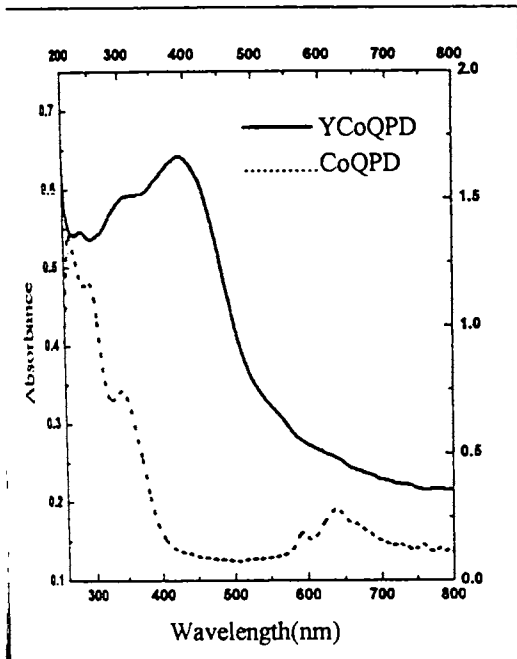
Figure. IV.16

Electronic spectra of neat
and zeolite encapsulated
QPD complexes

Table IV.12

Electronic spectral data for the zeolite encapsulated cobalt complexes

Complexes	Absorptions (cm^{-1})	Tentative Assignments	Magnetic Moment
YCoQED	29,820 23,920 17,830 15,480	$^4T_1g(P) \leftarrow {}^4T_1g(F)$ $^4A_2g(F) \leftarrow {}^4T_1g(F)$ $^4T_2g(F) \leftarrow {}^4T_1g(F$	5.0
YCoQPD	28520 23400 17670 13500	$^4T_1g(P) \leftarrow {}^4T_1g(F)$ $^4A_2g(F) \leftarrow {}^4T_1g(F)$ $^4T_2g(F) \leftarrow {}^4T_1g(F)$	4.9
YCoQHD	28,940 24,440 15,690	Charge Transfer $^2E \leftarrow {}^2A_1$ $^2B_2 \leftarrow {}^2A_1$	3.0
YCoQDT	30280 23700 15700 12970	Charge Transfer $^2E \leftarrow {}^2A_1$ $^2B_2 \leftarrow {}^2A_1$	3.2

4.3.9.2 Nickel Complexes

The YNiQED complexes exhibit bands characteristic of tetrahedral complexes (Table IV.13). The complex has bands at 14390, and 13400 cm^{-1}. The tetrahedral complex, [32] $NiBr_4^{2-}$, also has bands at 13230, 14140 cm^{-1}. Therefore YNiQED may also have a tetrahedral structure.

Table IV.13

Electronic spectral data for the zeolite encapsulated nickel complexes

| Complexes	Absorptions (cm^{-1})	Tentative Assignments	μ_{eff}
YNiQED	13400 14390 21670 29600 33510	$^3T_2$ (F) $\leftarrow$ $^3T_1$(F) $^3A_2$(F) $\leftarrow$ $^3T_1$(F) $^3T_1$(P) $\leftarrow$ $^3T_1$(F) Charge transfer	4.3
YNiQPD	16500 21500 23000 28230 35000	$^3T_{1}g$(P) $\leftarrow$ $^3A_{2}g$ $^3T_{2}g$(F) $\leftarrow$ $^3A_{2}g$ $^3T_{1}g$ (F) $\leftarrow$ $^3A_{2}g$ Charge transfer	3.1
YNiQHD	14600 15550 18300 25470 34700	$^3T_{1}g$(P) $\leftarrow$ $^3A_{2}g$ $^3T_{2}g$(F) $\leftarrow$ $^3A_{2}g$ $^3T_{1}g$ (F) $\leftarrow$ $^3A_{2}g$ Charge transfer	3.35
YNiQDT	13500 15600 18820 24800 30160	$^3T_{1}g$(P) $\leftarrow$ $^3A_{2}g$ $^3T_{2}g$(F) $\leftarrow$ $^3A_{2}g$ $^3T_{1}g$ (F) $\leftarrow$ $^3A_{2}g$ Charge transfer	3.2

Figure IV.17

Electronic spectra of neat
and encapsulated
QHD complexes
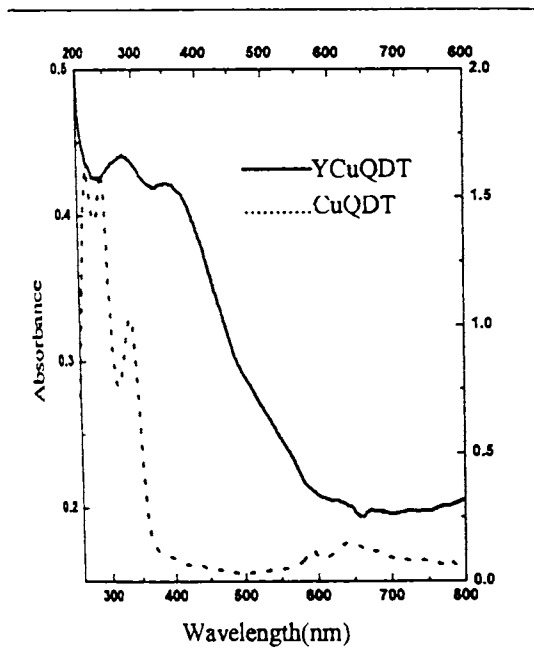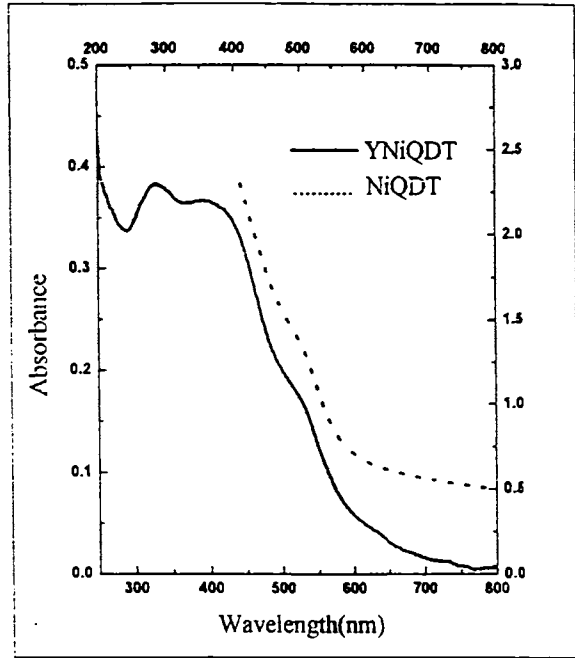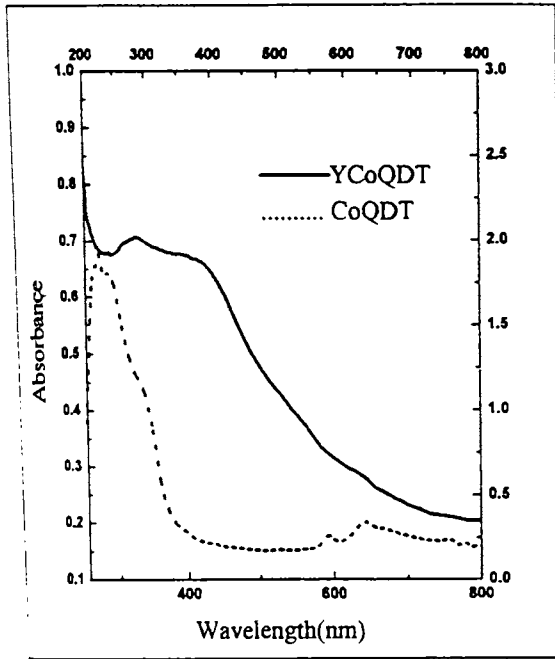
Figure IV.18

Electronic spectra of neat
and zeolite encapsulated
complexes of QDT

The absorption maxima in the case YNiQPD were at 35000, 28230, 23000, 21500, 16500 cm^{-1}. These values suggest an octahedral coordination. This compound did not give EPR spectra. Therefore the complex may exist as a square planar complex at LNT. This can be expected as the ligand QPD has a rigid structure. YNiQHD and YNiQDT complexes exhibit transitions at 34700, 25470, 18300, 15550, 14600 cm^{-1} and 30160, 24800, 18820, 15600, 13500 cm^{-1} characteristic of octahedral complexes. These complexes were EPR active. Usually octahedral complexes of nickel give EPR spectra at LNT. This also supports octahedral structure for YNiQHD and YNiQDT. The bands above 24000 cm^{-1} in all the complexes may be due to charge transfer. This is evident from the high intensity of the bands observed in the spectra (Figure IV.15-18)

4.3.9.3 Copper Complexes

YCuQED complex exhibit transitions at 31100, 23300, 16700 and 14980 cm^{-1}, indicating a pseudotetrahedral structure (Table IV.14). Tetrahedral copper(II) complexes are invariably distorted. Four coordinate square planar structure is strongly favoured for a d^9 electronic configuration. The distortion from the tetrahedra involves flattening to square planar geometry. YCuQPD, YCuQHD and YCuQDT may be assigned a tetragonally distorted octahedral geometry. A regular octahedral geometry is rare in the case of copper complexes due to Jahn-Teller distortions. For a regular octahedral geometry only one transition should be observed $^2E \leftarrow {}^2T$

Table IV.14

Electronic spectral data for the zeolite encapsulated copper complexes

Complex	Absorptions (cm^{-1})	Tentative Assignments	μ_{eff}
YCuQED	14980	$^2E \leftarrow {}^2B_2$	2.0
	16770	$^2B_1 \leftarrow {}^2B_2$	
	23300	$^2A_1 \leftarrow {}^2B_2$	
	31100		
YCuQPD	13106	$z^2 \ldots x^2-y^2$	1.75
	15698	$xz,yz \ldots x^2-y^2$	
	22 000	Charge Transfer	
	28116		
	35165		
YCuQHD	14285	$z^2 \ldots x^2-y^2$	1.90
	22200	$xz,yz \ldots x^2-y^2$	
	24000	Charge Transfer	
	29875		
YCuQDT	15873	$z^2 \leftarrow x^2-y^2$	1.85
	17482	$xz,yz \leftarrow x^2-y^2$	
	33898	Charge Transfer	

4.3.10 TG Analysis

Thermal analysis is an useful tool to study the decomposition pattern of metal complexes.[33] The TG of NaY, metal exchanged zeolite as well as the zeolite encapsulated complexes is given in Figure IV.19-22 and DTG plots are given in Figure IV.19a-22a. A weight loss of about 15-16% is observed in the temperature range 30-300°C (Table IV.15). Such a weight loss is observed in the case of the metal exchanged zeolite

also. Therefore, this may be due to the loss of intrazeolite water molecules. IR spectra of the complexes obtained after heating to 300°C is found to be exactly similar to that of the original complex indicating that there is no decomposition of the complex taking place in this range. Further decomposition of the complexes takes place in a single step. However, small weight loss is observed later in certain cases. In the case of YNiQPD the loss of intrazeolite water and ligands could not be distinguished as they occur in the same range. The variation in the thermal decomposition pattern exhibited by the different complexes is an indication of formation of metal complexes. The amount of intrazeolite metal complex can be roughly calculated from the weight loss. It is seen from the Table IV.15 that about 5% weight loss occurs during the second stage of decomposition. Probably this weight loss might be due to the decomposition of the complex within the zeolite. Therefore for comparing the stabilities of the complexes the peak temperature in the second stage of decomposition was considered. For all the complexes, there was about 20-25% weight loss in the temperature range from 50°C-600°C. Zeolite framework is seen to be destroyed only above 793°C. Among the copper complexes the order of stability was as follows: YCuQPD >YCuQED > YCuQDT >YCuQHD .The order of stability of cobalt, nickel and copper complexes is as follows

YNiQED > YCuQED> YCoQED

YCoQPD > YCuQPD >YNiQPD

YCoQHD >YCuQHD > YNiQHD

YCuQDT > YNiQDT > YCoQDT
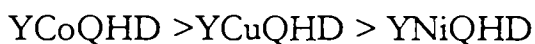
Table IV.15

TG/DTG data of the encapsulated complexes

Compound	Weight loss- Stage I			Weight loss- Stage II		
	Temp. range (°C)	Peak temp. (°C)	% Mass loss	Temp. range (°C)	Peak temp. (°C)	% Mass loss
YCoQED	50-250	127	15	310-600	298	4.5
YNiQED	50-300	143	16	350-500	606	3
YCuQED	50-250	116	14	300-650	450	7
YCoQPD	50-350	117	16	355-600	552	4.1
YNiQPD	50-320	161	16	-	-	-
YCuQPD	50-350	104	16	350-500	4610	4.6
YCoQHD	50-220	133	17	230-600	552	4.4
YNiQHD	50-230	116	15	240-550	499	4.2
YCuQHD	50-240	125	16	250-630	451	7
YCoQDT	50-200	125	16	210-500	413	7
YNiQDT	50-220	123	15	230-540	446	3.8
YCuQDT	50-250	115	15	255-450	458	4.2
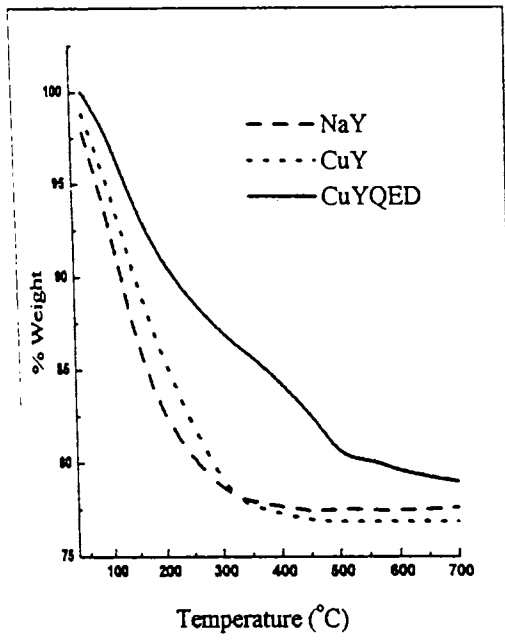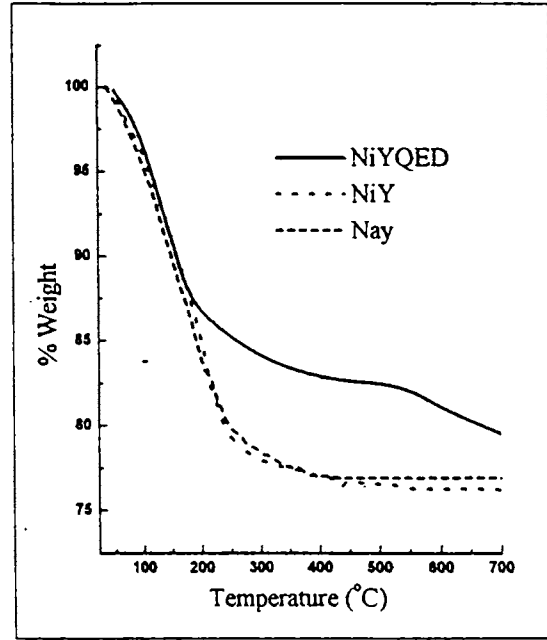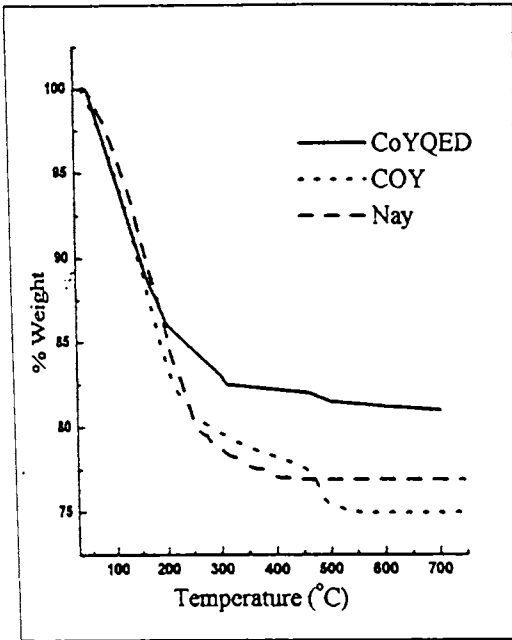
Figure IV.19

TG Curves of zeolite encapsulated
complexes of QED, metal exchanged
zeolite and NaY
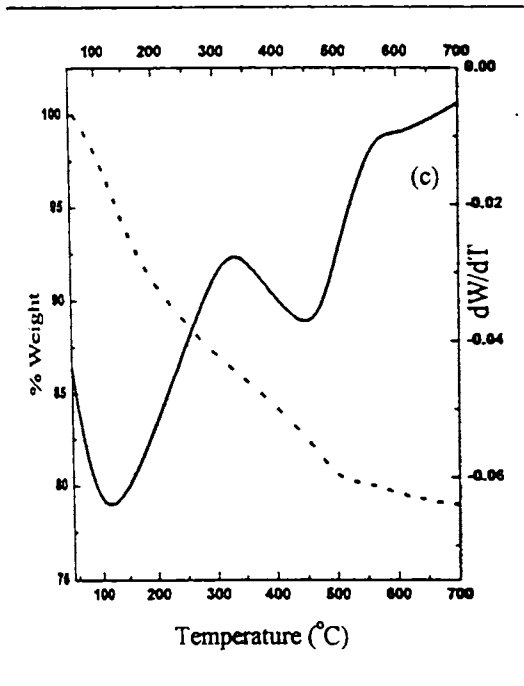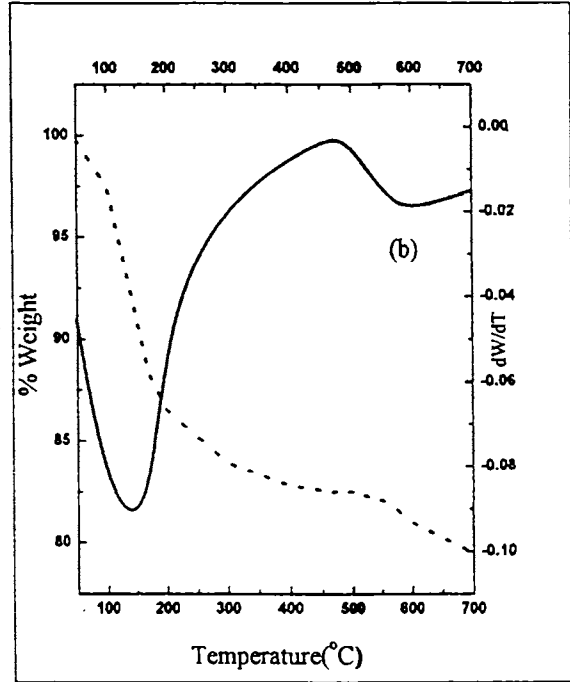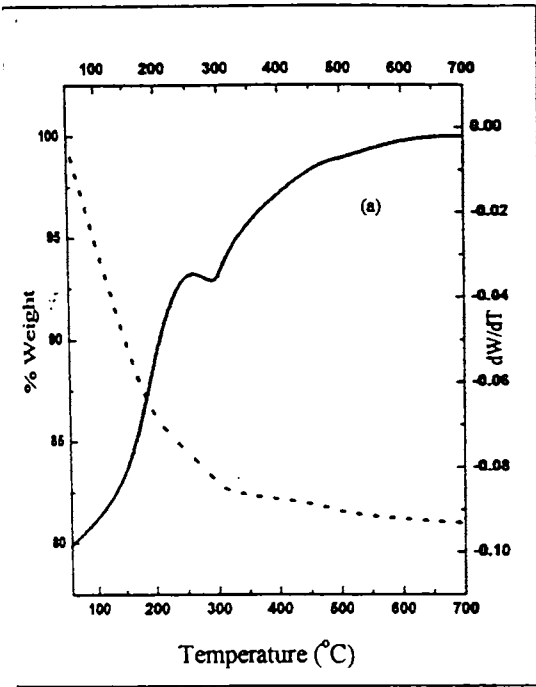
Figure IV.19a

TG/DTG curves of zeolite
encapsulated QED complexes
(a) Cobalt
(b) Nickel
(c) Copper
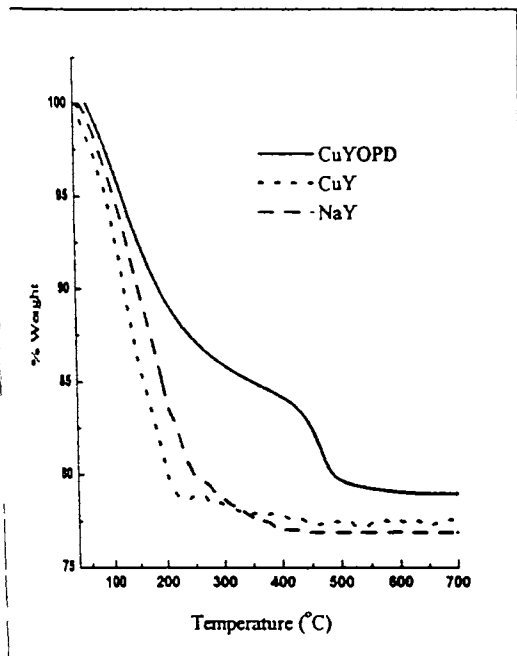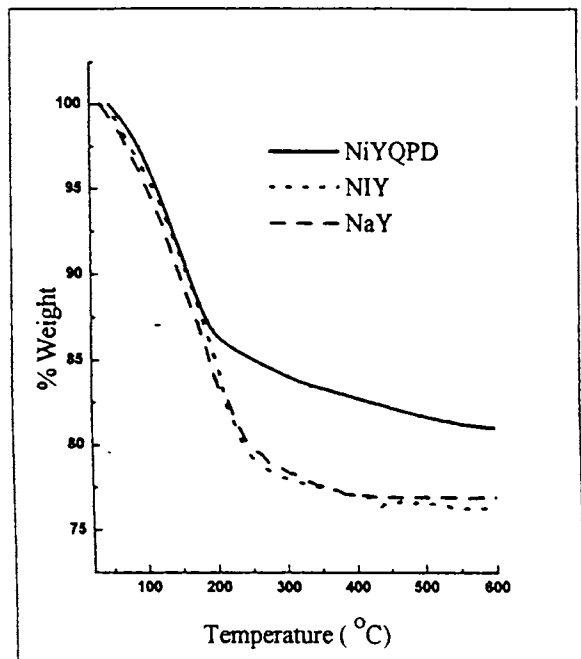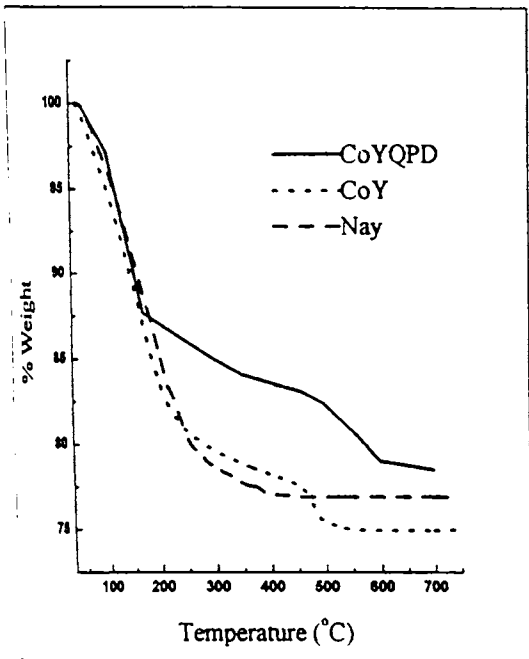
Figure IV.20

TG curves of zeolite encapsulated complexes of QPD, metal exchanged zeolite and NaY
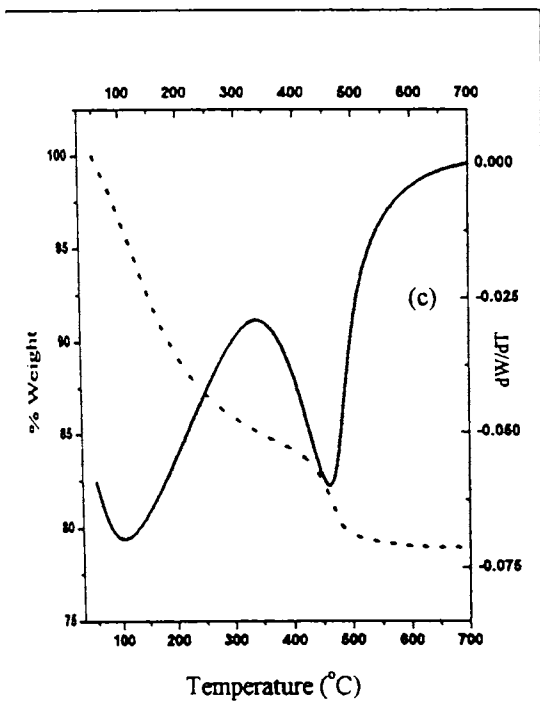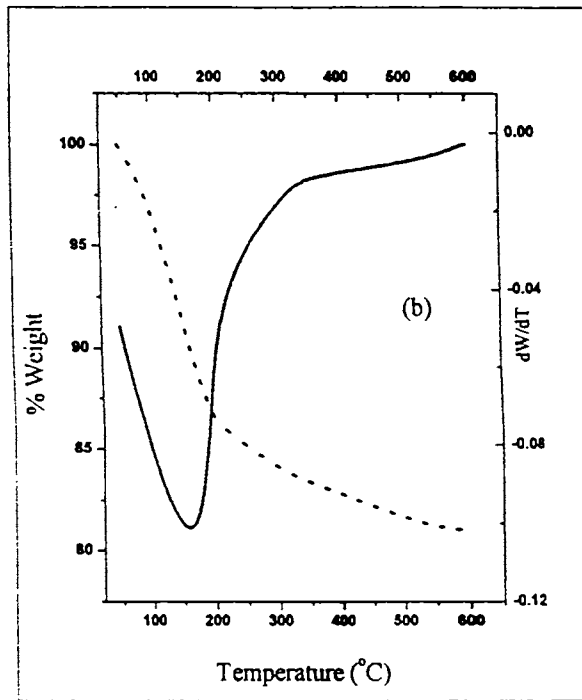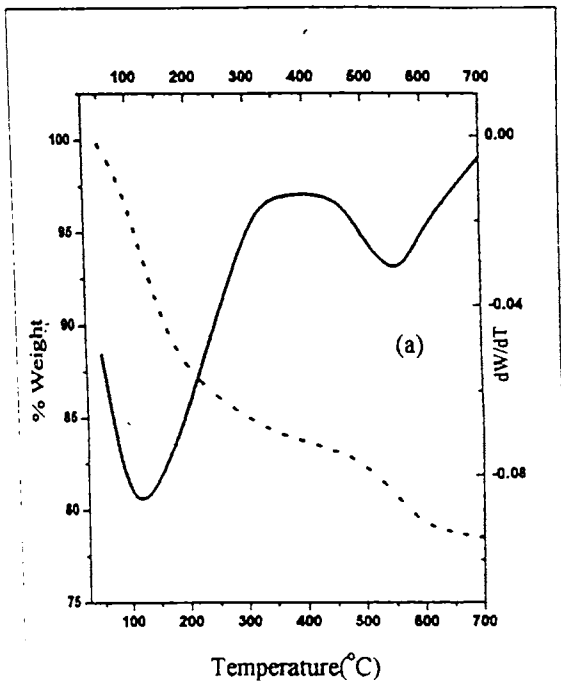
Figure IV.20a

TG/DTG curves of zeolite
encapsulated QPD complexes
(a)Cobalt
(b)Nickel
(c)Copper
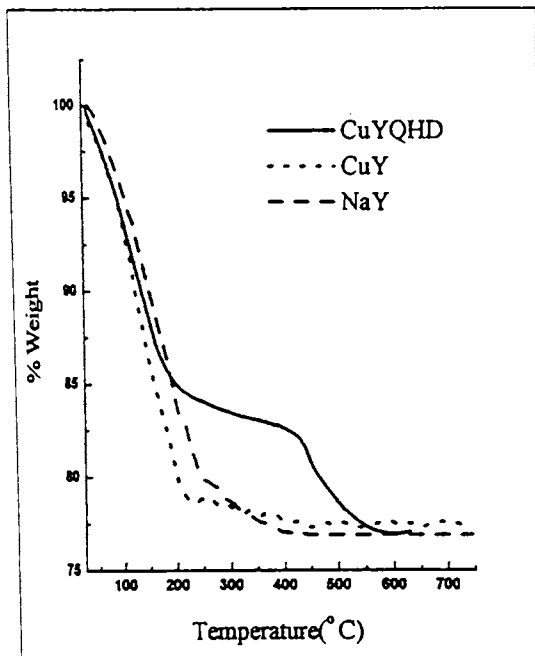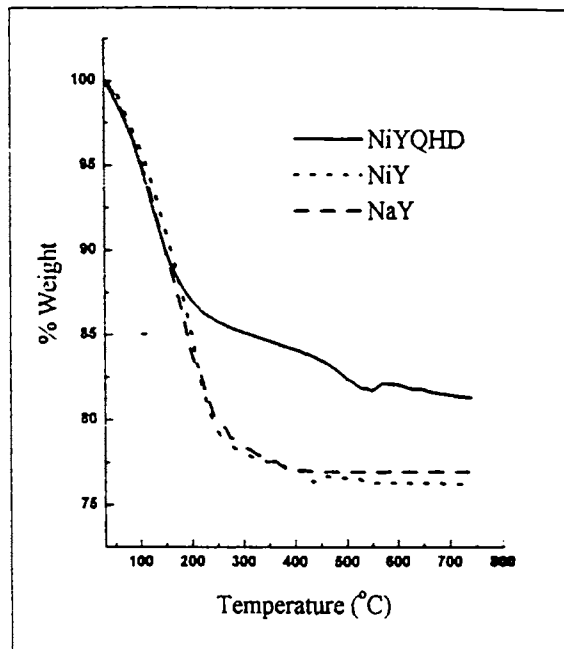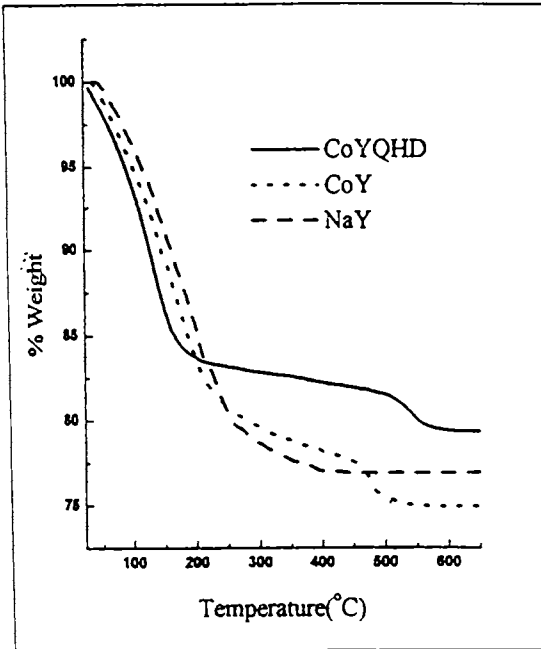
Figure IV.21

TG Curves of the zeolite encapsulated complexes of QHD, metal exchanged zeolite and NaY
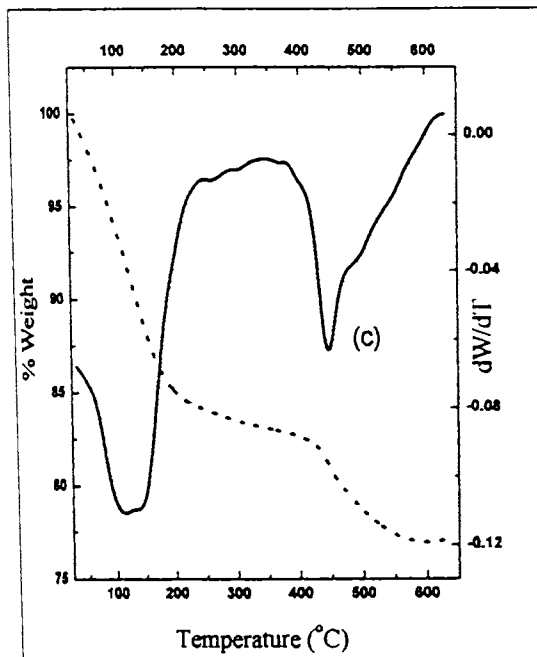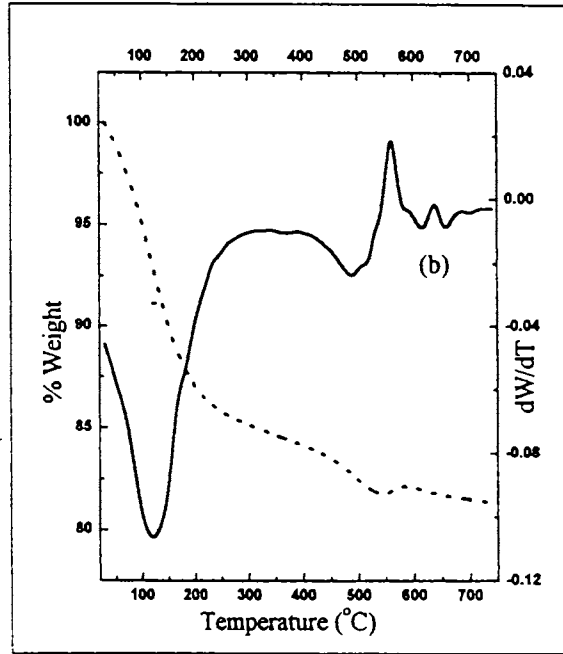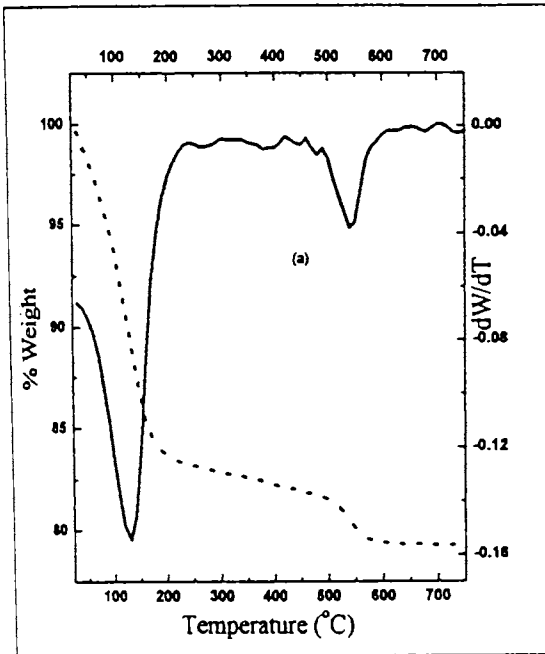
Figure IV.21a

TG/DTG curves of zeolite
encapsulated QHD complexes
    (a)Cobalt
    (b)Nickel
    (c)Copper
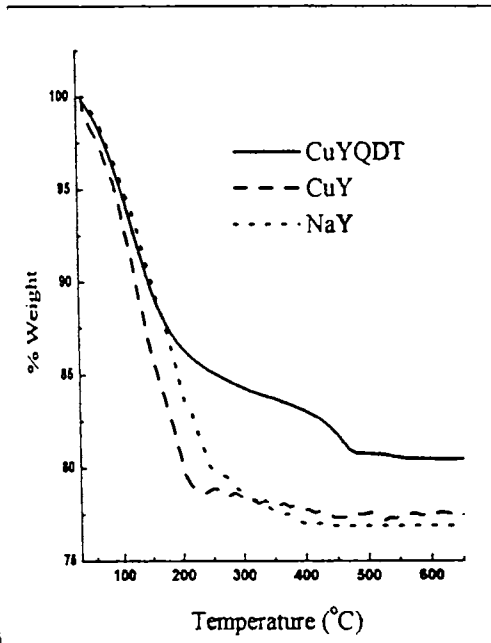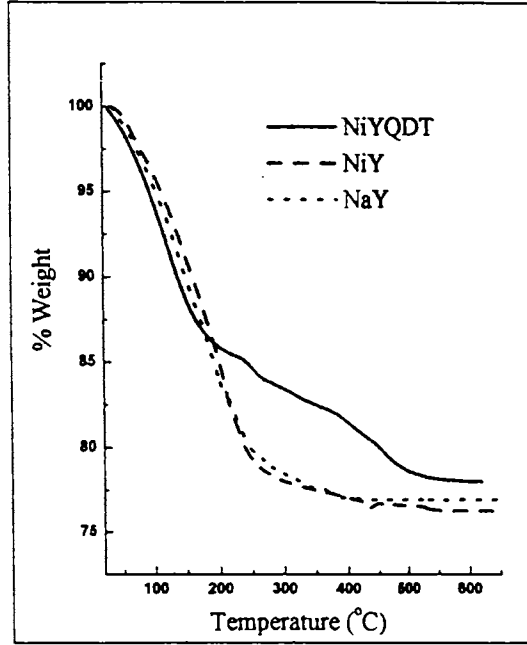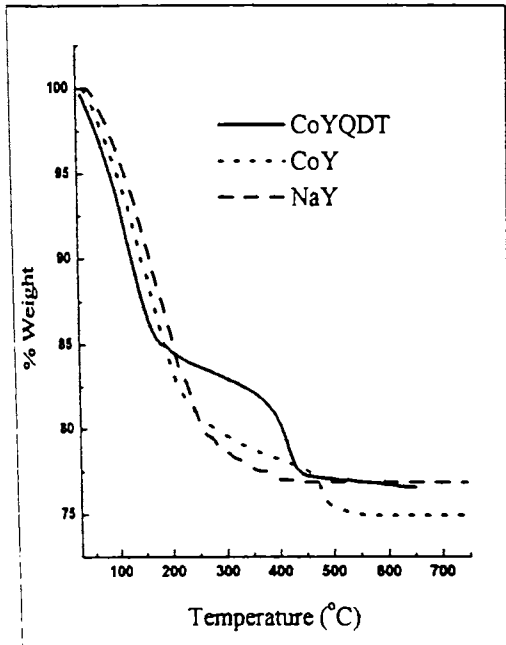
Figure IV.22

TG Curves of zeolite encapsulated
complexes of QDT,metal exchanged
zeolite and NaY
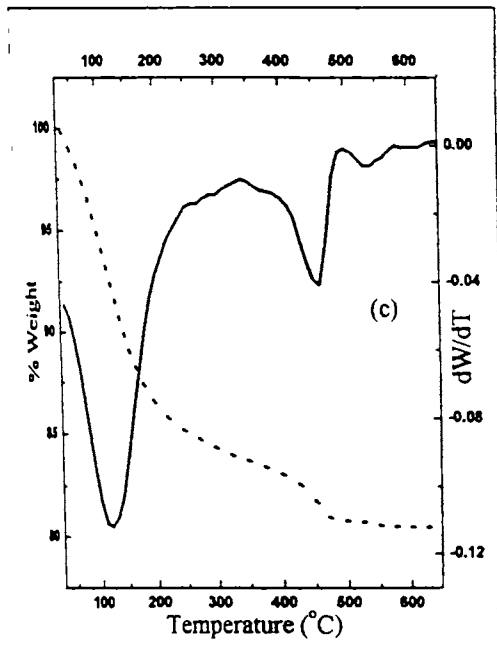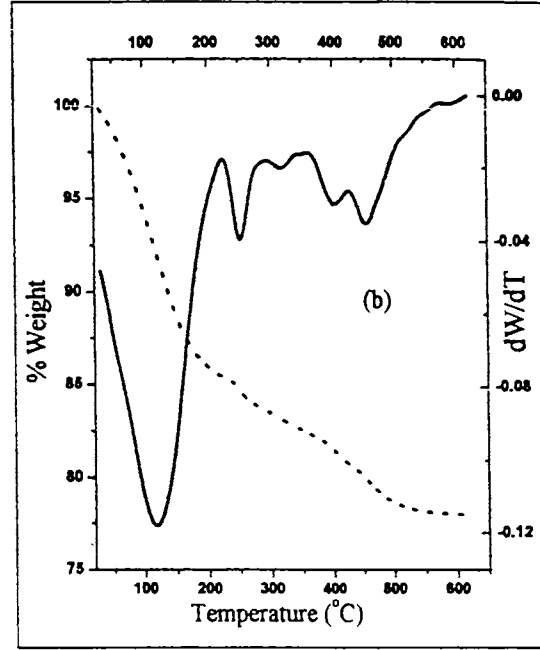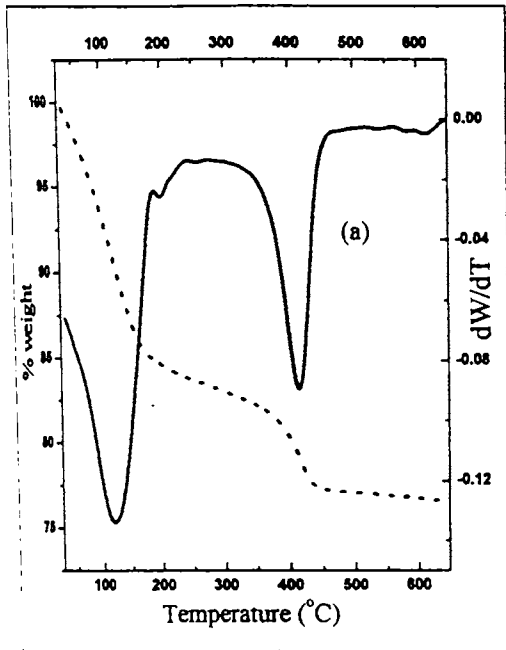
Figure.IV.22a

TG/DTG curves of zeolite
encapsulated QDT complexes
(a) Cobalt
(b) Nickel
(c) Copper

Conclusions

Zeolite encapsulated cobalt(II), nickel(II) and copper(II) complexes of Schiff bases derived from 3-hydroxyquinoxaline-2-carboxaldehyde has been successfully encapsulated in the zeolite Y. The unit cell formulae of the complexes were determined from the elemental analysis. The XRD and SEM studies indicated that there is no surface complexes remaining and the zeolite framework is retained as such without dealumination. The surface area and pore volumes were decreasing indicating the encapsulation of metal complexes inside the pores. Among the cobalt complexes, the electronic spectral values and magnetic moment values suggested an octahedral structure for YCoQED and YCoQPD, QHD and QDT are ligands capable of acting as pentadentate ligand and the complexes YCoQHD, YCoQDT are EPR active. The magnetic moment values of 3.0 and 3.2 BM repectively and the electronic spectral values supports a five coordinate structure for these complexes. The NiYQED was assigned a tetrahedral geometry. NiYOPD complex was EPR silent hinting the possibility of square planar-octahedral equilibrium in this case. NiYQHD and NiYQDT are having an octahedral structure. This is evident from the magnetic moment, spectral as well as EPR spectral values. The CuYQED complex is assigned a pseudotetrahedral structure based on the electronic spectra, EPR and magnetic moment value of 2.0 BM. The CuYQPD, CuYQDT, CuYQHD complexes have been assigned a six coordinate structure. The FTIR data could suggest the coordination of azomethine nitrogen and hydroxyl group on the quinoxaline ring of the ligands in all the complexes. Thermal analysis could give an inference about the relative stability of the different complexes.

REFERENCES

1. H.Schiff, *Ann.Chem.* Paris 113 **(1864)** 241.

2. S. Dayagi, Y. Degani "*Chemistry of Carbon-Nitrogen double bond*" Wiley Interscience, New York **(1970).**

3. G. Wilkinson, R.D. Gillard, J. A. McCleverty *Comprehensive Coordination Chemistry*, Volume 2, Ligands,. First Edition, Peragamon Press, Oxford**(1987).**

4. Jose Mathew, *Ph.D.Thesis*, Cochin University of Science and Technology, November **1995.**

5. C.R. Jacob, S.P. Varkey,. P. Ratnasamy, *Appl.Catal.A.Gen* 1568 **(1988)** 3453.

6. S. Schulz-Ekloff and S. Ernst, *Handbook of Heterogeneous Catalysis*", G. Ertil, J. Knozinger and J. Weitramp(Eds), Wiley-VCH **(1997)** 374.

7. C. Bowers, P.K. Dutta, *J.Catal.*122 **(1990)** 271.

8. S. Kowalak, R.C. Weisis, K.J. Balkur Jr, *J.Chem.Soc.Chem.Commun.* **(1991)** 57.

9. D.E. Devos, E.J.P. Feijen, R.A. Schoonheydt, P.A. Jacobs, *J.Am.Chem.Soc.*116 **(1994)** 4746.

10. T.A. Egerton, A. Hagan, F.S. Stone, J.C. Vickerman, *J.Chem.Soc.Faraday Trans.* 168 **(1972)** 723.

11. E.F. Vansant, J.H. Lunsford, *J.Phys.Chem.*76 **(1972)** 2860.

12. J.H. Lunsford, E.F. Vansant, *J.Phys.Soc.,Faraday.Trans II.,* 69 **(1973)** 1028.

13. J.W. Jermijn, T.J. Johnson, E.F. Vansant, J.H. Lunsford, *J. Phys.Chem* 77 **(1973)** 2964.

14. P.K. Dutta, J.H. Lunsford, *J.Chem.Phys.* 6(10) **(1977)** 4716.

15. P. Gallezot, Y. B. Taarit, B. Imelik, *J.Catal.* 26 **(1972)** 205.

16. H.D. Simpson, H. Steinfink, *J.Am.Chem.Soc.* 91 **(1969)** 6225.

17. H.D. Simpson, H. Steinfink, *J.Am.Chem.Soc.* 91 **(1969)** 6229.

18. J.M. Thomas, C.R.A. Calton, *Prog.Inorg.Chem.* 35 **(1988)**1.

19. M.J. Wilson, *Clay Minerology, Spectroscopy and chemical determination method,* Chapman & Hall **(1994).**

20. K.Nakamoto, "*Infrared spectra and Raman of Inorganic and coordination Compounds*", Part B, 5th Ed, John Wiley and Sons **(1997).**

21. J.E. Wertz, J.R. Bolton, *Electron Spin Resonance Elementary theory and Practical Applications,* McGraw-Hill **(1972).**

22. M.A. Heilbron , J.C. Vickerman, *J.Catal.* 3 **(1974)** 434.

23. E.F. Vansant, *Catalysis: Heterogeneous and Homogeneous,* Elsevier, B. Delmon & G. James Ed, Amsterdam **(1975)** 171.

24. H. Li, D. Biglino, R. Erickson, A. Lund, *Chem.Phys.Lett.* 266 **(1977)** 417.

25. C. Naccache, Y.B. Taarit, *Chem.Phys.Lett.* 111(**1971)** 11.

26. U. Sakaguchi, A. W. Addison, *J.Chem.Soc.Dalton Trans.* **(1979)** 600.

27. A. Earnshaw, "*Introduction to Magnetochemistry*" Academic Press, London**(1968).**

28. T.I. Barry, L.A. Lay, *J.Phys.Chem..Solid* 29 **(1968)** 1395.

29. G. Kortum, *Reflectance Spectroscopy Principles, Methods, Applications,* Springer-Verlag-Berlin **(1969).**

30. E. Nappier (Jr)., D.W.Meek, *Inorg.Chim.Acta.* 7 **(1973)** 235.

31. J.F. White and M.F. Farona, *Inorg.Chem* 10 **(1971)** 1080.

32. M. Goodgame, D.M.L. Goodgame, F. A. Cotton, *J. Am.Chem.Soc.* 83 **(1961)**4161.

33. T. Hatakeyama, Z. Liu, *Handbook of Thermal Analysis,* John Wiley and Sons, New York**(1998).**

CHAPTER V
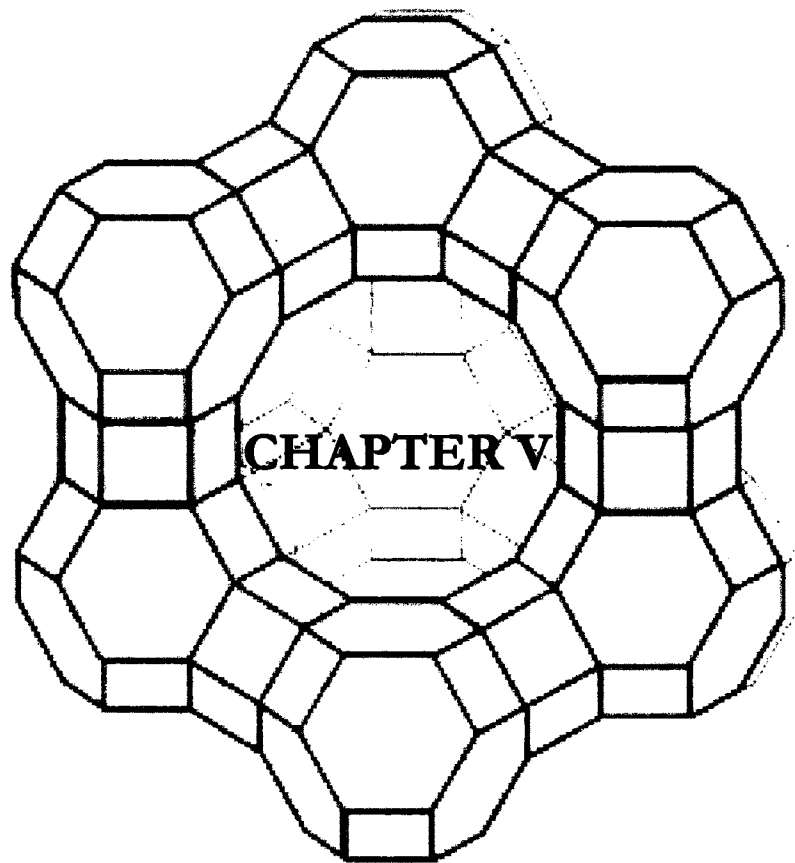
COBALT(II), NICKEL(II) AND COPPER(II) COMPLEXES OF POLYSTYRENE SUPPORTED SCHIFF BASES

5.1 INTRODUCTION

Anchoring metal complexes to polymer supports is done to give an organic polymer inorganic function[1] Such complexes may show a specific type of catalytic activity reflecting the properties of polymers. In metalloenzymes, such as haemoglobin and oxidase, where the metal complex is the active site, the organic part plays a significant role in the reactivity.[2-4] Such catalysts are now extensively used in new fields like triphase catalysis.[5] The insoluble polymer supported complex have the advantage of easy separation from the reaction mixture leading to operational flexibility, facile regenerability and higher stability. Such polymer supported complexes are used for a wide variety of industrial reactions. In this case, the reactants must diffuse into a swollen polymer matrix to reach a bound catalyst site and reaction rate may be lowered and become rate limiting. Another characteristics of polymer bound complex is that the concentration of reactants at the catalytic site can be different from that in solution. This occurs because of the difference in solvation energies between bulk solution and the inside of the swollen polymer matrix. This leads to different concentration gradient for various reactants to enter into the matrix. Polymer anchoring may also stabilize coordinatively unsaturated mononuclear reaction centers. While
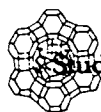
preparing polymer bound complexes, the following factors have to be taken into consideration. Polymer matrix should be rigid so that adjacent metal centers are unable to approach each other. Similarly covalent link between polymer and metal centres must be sufficiently strong to remain intact during the course of the reaction. The commonly used polymer support is polystyrene. It can be made rigid by increasing the degree of cross linking with divinyl benzene.

This chapter deals with the study of cobalt(II), nickel(II) and copper(II) complexes of the polymer anchored Schiff base PS-HQAD(1) and PS-OPD(2). Polymer bound aldehyde was condensed with o-phenylenediamine to prepare Schiff base PS-OPD and polymer bound amine was condensed with 3-hydroxyquinoxaline-2-carboxaldehyde to prepare the Schiff base PS-HQAD. All the complexes have been characterised and the possible geometry of the complexes has been suggested using elemental analysis, diffuse reflectance UV, FT-IR, thermal studies, surface area studies and magnetic measurements.

(1)   (2)
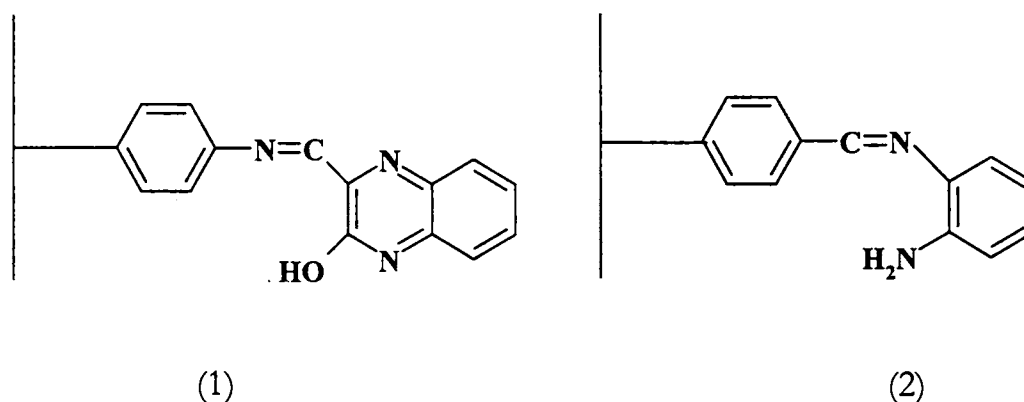
Figure V.1 Structure of (1)PSHQAD and (2) PSOPD

5.2 EXPERIMENTAL

Chloromethylated polystyrene (3.1mmol Cl/g) (Merck) crosslinked with 2% divinyl benzene was used as the starting material. Amine bound[6] and aldehyde[7] bound polystyrene was synthesised from the chloromethylated polystyrene according to procedure described in Chapter II. o-Phenylenediamine was purchased from CDH laboratories and 3-hydroxyquinoxaline-2-carboxaldehyde was prepared following a reported procedure.[8] A. polymer anchored Schiff base of o-phenylenediamine (PS-OPD) was prepared from polymer bound aldehyde (scheme-1) and polymer anchored Schiff base of 3-hydroxyquinoxaline-2-carboxaldehyde (PS-HQAD) was prepared from polymer bound amine (scheme-2) according to the procedure reported in Chapter II.

5.2.1 Synthesis of cobalt (II), nickel(II) and copper(II) complexes of PSOPD

The polymer bound Schiff base, PS-OPD (3 g) was swelled in chloroform (25ml) for 1 hour. It was then filtered and refluxed with a solution of metal chloride (2.37 g of $CoCl_2.6H_2O$, 2.37 g of $NiCl_2.6H_2O$, 1.70 g of $CuCl_2.2H_2O$ in 100ml ethanol) on a water bath for about 6 hours. All these complexes were then washed several times with ethanol and dried in vacuum over anhydrous calcium chloride.

118
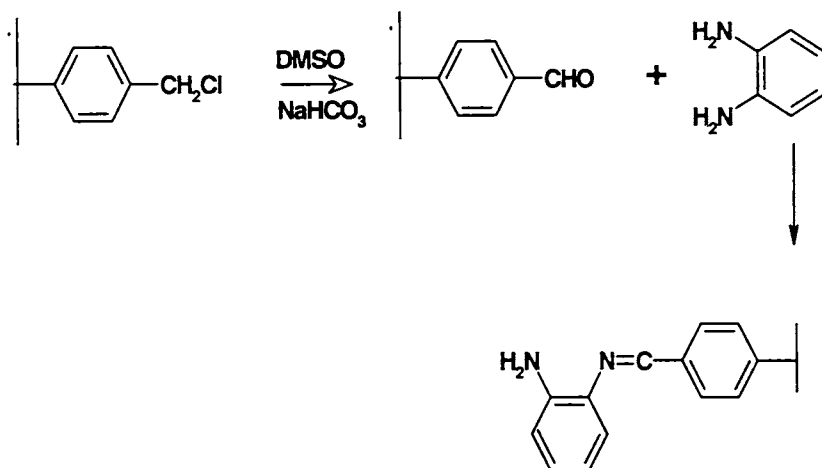
Scheme-1

5.2.2 Synthesis of cobalt(II), nickel (II) and copper(II) complexes of PSHQAD

The polymer bound Schiff base PSHQAD (3g) was swelled in chloroform for 1 hour. After swelling it was filtered and refluxed with a solution of metal chloride (2.37g of $CoCl_2.6H_2O$, 2.37g of $NiCl_2.6H_2O$, 1.70 g of $CuCl_2.2H_2O$ in 100ml ethanol) for about 6 hours. The complexes thus formed were washed with ethanol several times, filtered and dried in vacuum over anhydrous calcium chloride.
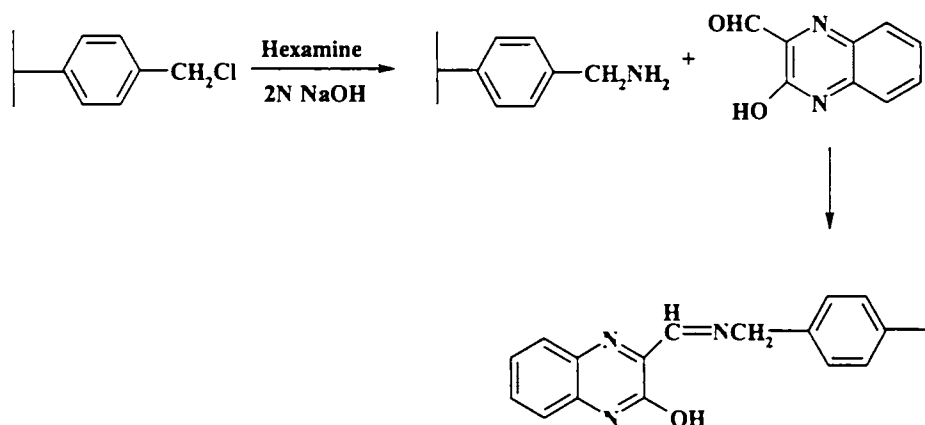
Scheme - 2
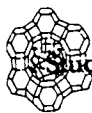
5.3 RESULTS AND DISCUSSION

The starting material used for the preparation of polymer bound Schiff base was chloromethylated polystyrene containing about 13% Cl, which on treating with dimethyl suphoxide and sodium bicarbonate yielded polymer bound benzaldehyde (Scheme 1). The formation of the aldehyde was evidenced by the positive test with Borsche's reagent. The chlorine content of the polymer bound aldehyde was negligible indicating almost complete conversion of the chloromethylene groups into aldehyde. Amino methyl polystyrene was prepared through the polymer analogue of delepine reaction (scheme 2). The compound thus prepared gave a deep blue colour with ninhydrin reagent (the positive test for formation of amino group). The percentage of nitrogen indicates that there is only 14% conversion. The polymer bound amine was condensed with 3-hydroxyquinoxaline-2-carboxaldehyde to form the Schiff base, PSHQAD. Percentage of nitrogen in the Schiff base indicates that the Schiff base units are about 7-8 units apart and there may be possibility of formation of intra-polymer complex by twisting or bending of the polymer chain. The metal binding capacity was found to be highest for the cobalt complex (Table V.1).

Table V.1

Elemental analysis data of the polymer support and polymer bound complexes

COMPOUND	%C	%H	%N	%M	%Cl
PSOPD	77.76	7.36	3.32 ·	-	-
CoPSOPD	74.66	6.58	2.88	2.2	2.5
NiPSOPD	77.59	7.11	2.48	1.5	-
CuPSOPD	74.45	7.04	2.61	1.5	-
PSHQAD	77.57	6.80	4.43	-	-
CoPSHQAD	72.36	6.70	3.00	2.3	3
NiPSHQAD	76.35	6.79	3.77	1.3	3
CuPSHQAD	73.91	6.73	3.31	1.1	-

5.3.1 Surface area and pore volume

Porous structure of the polymer appears to be blocked, after the formation of the complex. A drastic decrease in surface area of polymer bound Schiff base on complex formation was observed (See Table V.2). A similar trend is observed in the case of pore volume values.
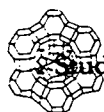
Table V.2.

Surface area analysis results of polymer support and metal complexes

Compound	Surface area (m^2/g)	Pore Volume(cc/g)
PSCHO	154	0.0950
CoPSOPD	47	0.0348
NiPSOPD	54	0.0403
CuPSOPD	50	0.0384
PSNH$_2$	265	0.1640
CoPSHQAD	41	0.0326
NiPSHQAD	36	0.0277
CuPSHQAD	41	0.0320

5.3.2 Magnetic moment measurements

For calculation of magnetic susceptibility, Guoy method was used. Magnetic susceptibility of all the complexes showed a negative value probably due to the low concentration of the metal and the very large diamagnetic susceptibility of the atoms present in the polymer complex. However approximate molecular weight and empirical formula of the repeating complex unit containing one metal atom was calculated using a reported procedure.[9] The magnetic moment μ_{eff} of the different complexes are given in the Table IV.3. In the case

PSOPD complexes, the cobalt complex Co(II)PSOPD has a magnetic moment of 2.46 BM Magnetic moment values of 2.0-2.5 are usually reported for square planar cobalt(II) complexes. This higher magnetic moment value (when compared to that expected for one unpaired electron) for low spin square planar complexes corresponds to the spin only value for one unpaired electron multiplied by a factor of (1+(2A/Δ). Here, A is the single electron spin-orbit coupling constant, and Δ is the separation between the d_{xy} orbit and its neighbouring levels. The red crystals of the compound Co(PEt$_3$)$_2$(NCS)$_2$ has a magnetic moment of 2.3 BM and is having a square planar geometry.[10] Cobalt complexes of ligand Salen are also planar with a magnetic moment value of 2.2 BM. Thus the present Co(II)PSOPD complex, can be considered to have a square planar structure. Ni(II)PSOPD has a μ_{eff} = 3.3 BM which suggest an octahedral structure and Cu(II)PSOPD has a magnetic moment of 1.8 BM. indicating a distorted octahedral structure.

Among the complexes of PSHQAD, the PSCo(II)HQAD has a magnetic moment of 2.2 BM. hinting towards a square pyramidal geometry for the complex. The Ni(II)PSHQAD exhibits a magnetic moment value of 3.0 BM. and therefore may be have an octahedral structure. Cu(II)PSHQAD has a magnetic moment value of 2.1 BM. indicating a tetrahedral geometry for this complex.

5.3.3 EPR spectra

EPR spectra of the complexes were recorded at liquid nitrogen temperature. EPR parameters of the complexes are given in the Table V. 3.

All the complexes of PSOPD are seen to be EPR active (See Figure V.2). For the Co(II)PSOPD complex, g_{II}=2.004 and $g_\perp$ =2.20. These values suggest a square planar structure. The assignment of this geometry is supported by the magnetic moment value of 2.46 BM. The Ni(II)PSOPD is EPR active and $g_\perp$ and g_{II} values for this complex are 2.004 and 2.076 respectively. This suggests an octahedral structure for this complex. The EPR spectra of the polymer anchored Cu(II)PSOPD complex shows two g values (g_{II} = 2.28 and $g_\perp$ = 2.08) indicating a tetragonal symmetry or a distorted octahedral structure. The A_{II} and $A_\perp$ values for Cu(II)PSOPD are found to be $150 \times 10^{-4} cm^{-1}$ and $66 \times 10^{-4} cm^{-1}$.

The EPR spectra of all the complexes of PSHQAD are depicted in Figure V.3. The EPR spectra of Co(II)PSHQAD gives two g values, g_{II} =2.70 and $g_\perp$=2.02 indicating a square pyramidal structure. The EPR spectra is observed in the case of nickel complex, Ni(II)PSHQAD and gives a g value of 2.023. This may be due to the octahedral structure for the complex. Cu(II)PSHQAD complex also exhibit two g values, g_{II} =2.26 and $g_\perp$=2.06 . and the A_{II} and $A_\perp$ values are $133 \times 10^{-4} cm^{-1}$ and $60 \times 10^{-4} cm^{-1}$.

The polymer anchored complexes exhibit a covalent environment as indicated by a g_{II} value less than 2.3.[11] Strength of the

Field Set: 3000G

Scan Range: 2000G

(iii)

(ii)

(i)
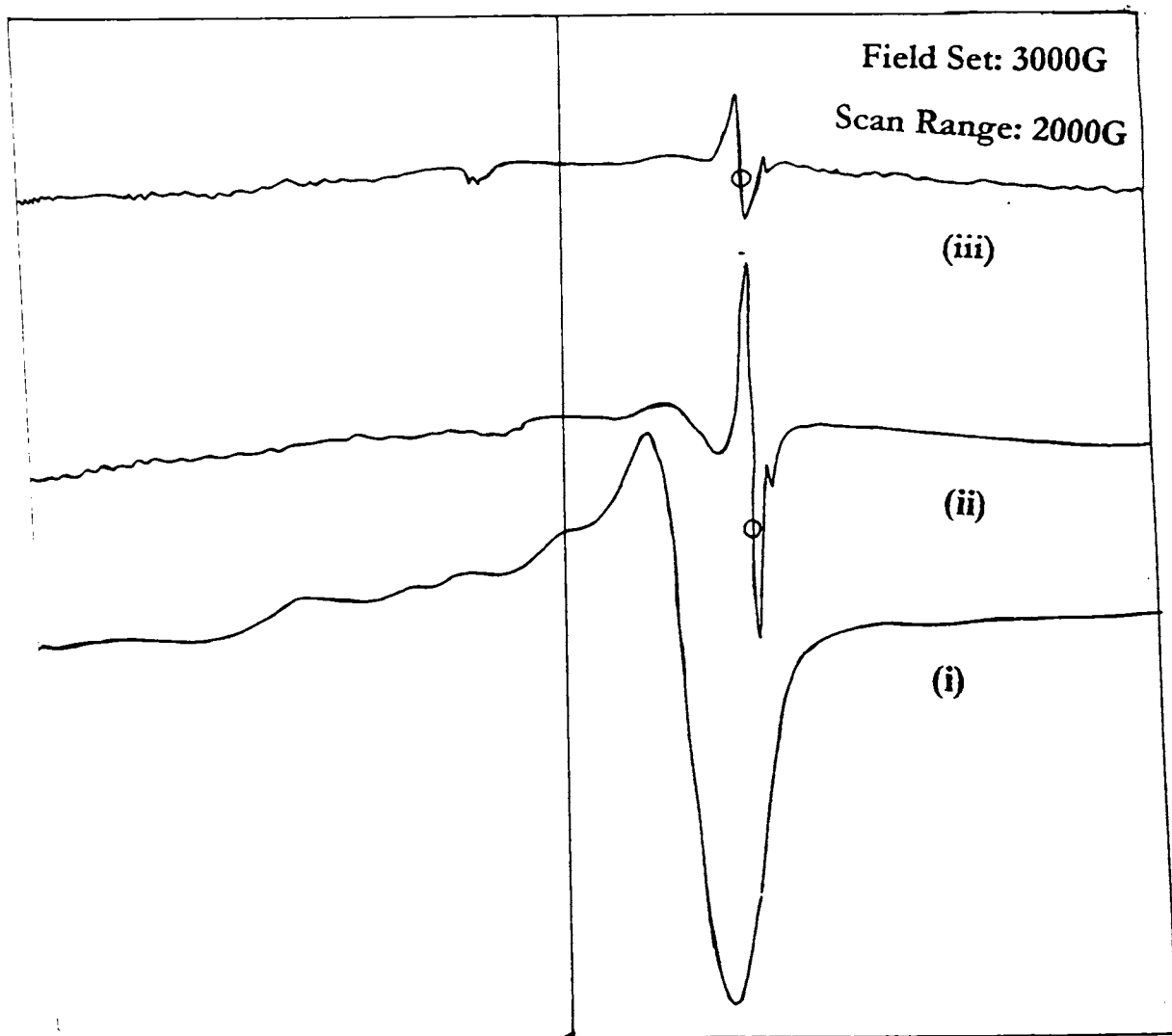
Figure V.2 EPR spectra of Polymer bound OPD complexes
(i) CuPSOPD   (ii) NiPSOPD   (iii) CoPSOPD

Scan Range: 2000G
Field Set: 3000G

(i)

(ii)

(iii)
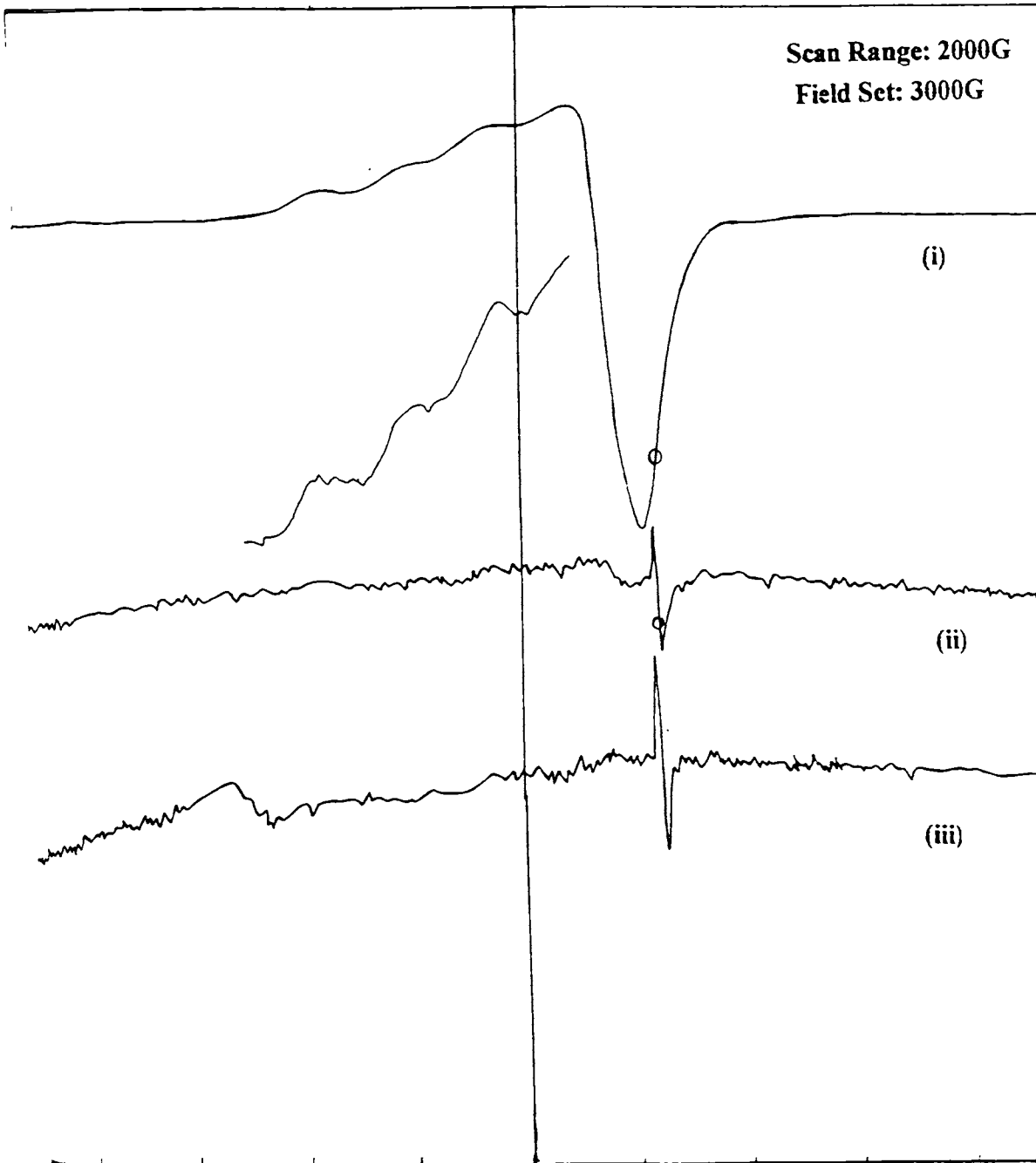
Figure V.3 EPR Spectra of Polymer bound HQAD complexes
(i) CuPSHQAD (ii) NiPSHQAD (iii) CoPSHQAD
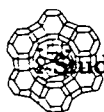
ligand can be assessed from the G^{12} value which can be calculated using the following equation:

$$G = g_{II} -2.002/ g_{\perp}-2.002$$

If it is less than 4, the ligand forming the copper(II) complex is regarded as a strong field ligand. In the present case, it was observed to be less than 4 (G value is 3.79 for Cu(II)PSHQAD and G = 3.56 for Cu(II)PSOPD) indicating the strong field nature of the ligands. The in-plane covalence parameter $\alpha^2 Cu$ were found to be 0.7676 and 0.6992 for Cu(II)PSOPD and Cu(II)PSHQAD respectively which also supports covalent nature.

Table V.3:

EPR and magnetic moment data for the complexes

Complexes	$g_{\perp}$	g_{II}	Magnetic moment
CoPSHQAD	2.20	2.70	2.2
NiPSHQAD	2.023		3.0
CuPSHQAD	2.07	2.27	2.1
CoPSOPD	2.004	2.20	2.5
NiPSOPD	2.004	2.076	3.3
CuPSOPD	2.06	2.20	1.8

5.3.4 TG analysis

Thermal Analysis of the PSHQAD complexes was carried out to find the stability of the complexes. The TG and DTG plots of the complexes are presented in the Figure.V.4 All the complexes were
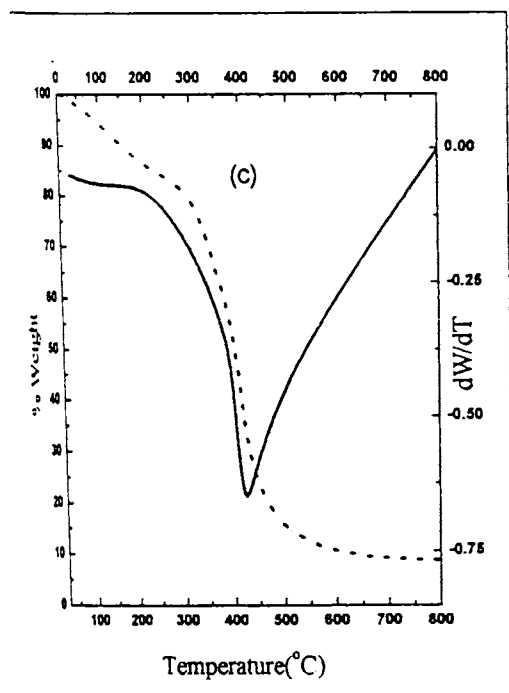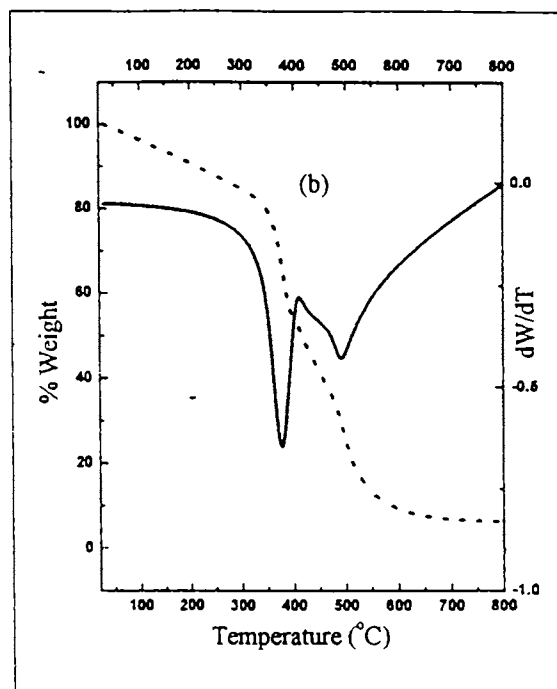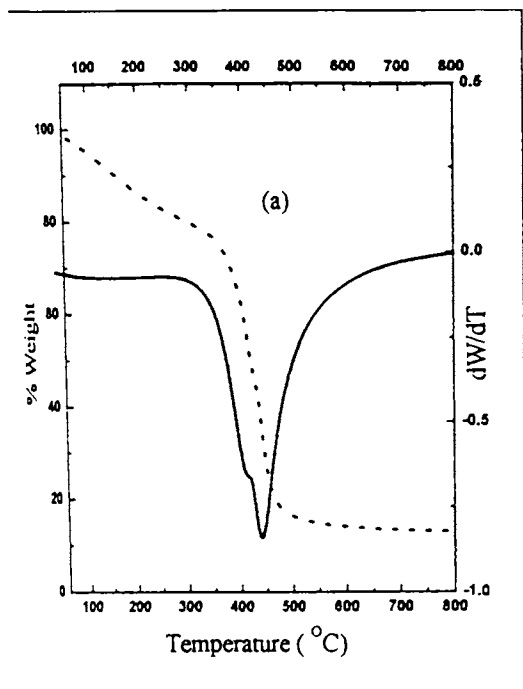
Figure V.4

TG/DTG Curves of Polymer
supported HQAD Complexes
(a) Cobalt
(b) Nickel
(c) Copper

stable upto 300°C. Below 300°C there appears to be a small decrease in weight corresponding to weight loss of 4%. This may be due to the loss of physisorbed water. Therefore, the complexes can be considered to decompose in two stages (Table V.4). There was about 40% weight loss during the second stage of decomposition. The decomposition of the Schiff base PSHQAD is almost complete at 600°C whereas the decomposition of the complexes was found to happen at a lower temperature. The lower decomposition temperature in the case of the complexes may be due to the catalytic activity of the metal ion in the decomposition of the polymer part.

Table V.3:

Thermogravimetric data of PSHQAD Complexes

Compound	Temperature range	Weight Loss
PSHQAD	50-405	39.5
	410-600	53.7
CoPSHQAD	50-406	38.4
	410-500	47.5
NiPSHQAD	50-405	41.6
	410-538	47.2
CuPSHQAD	50-385	41.1
	385-447	48.24

The TG and DTG plots of the PSOPD complexes are presented in the Figure V.5 and the data are given in Table V.4. The PSOPD complexes are stable upto 250^{0}C. Upto 250^{0}C there is only 6-8% weight loss due to adsorbed water or solvent molecules. Further decomposition of the complexes occurs in a single stage. Among the complexes, the cobalt complex, PSCo(II)OPD was found to be of lower stability. This may be due to the lower coordinated square planar structure of this complex. It may be seen that the PSHQAD complexes were more stable than the PSOPD complexes.

Table V.4:

Thermogravimetric Analysis data of PSOPD and metal complexes

Compound	Temperature Range	%Weight loss
PSOPD	265-600	25
	600-800	48
CoPSOPD	50-250	8
	266-800	79
NiPSOPD	50-260	7
	273-600	44
CuPSOPD	50-240	6
	240-512	52
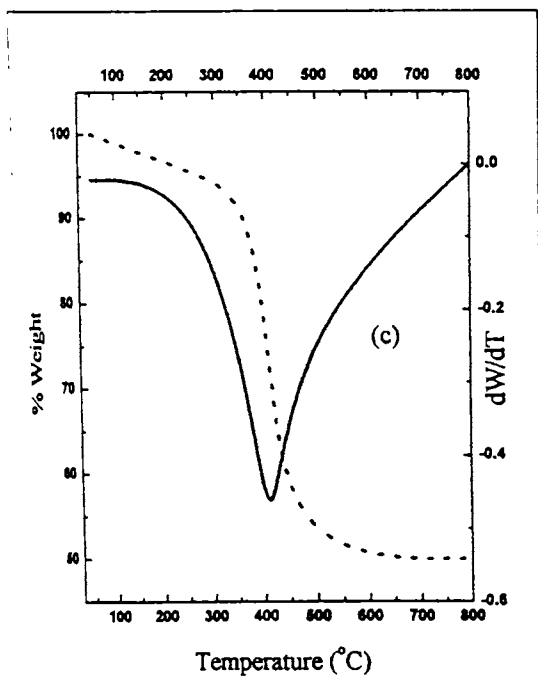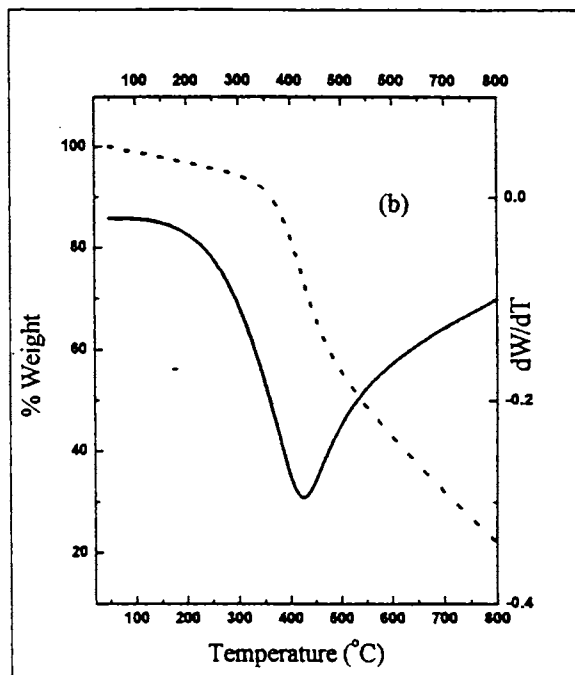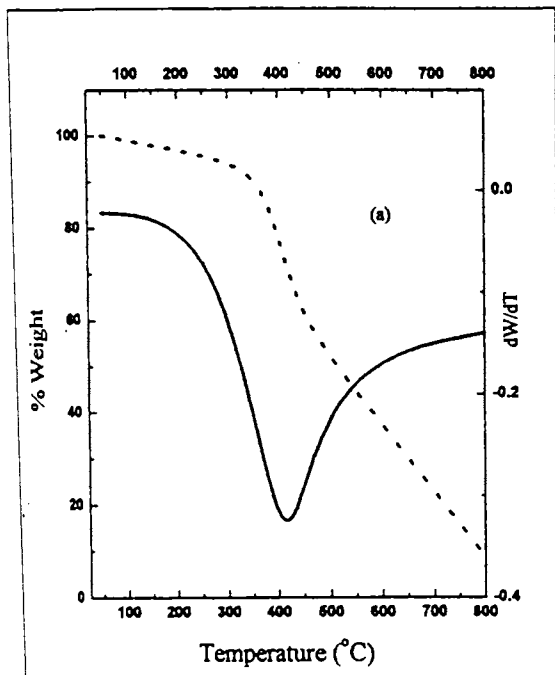
Figure. V.5

TG/DTG Curves of Polymer
supported OPD complexes.
  (a) Cobalt
  (b) Nickel
  (c) Copper

5.3.5 Infrared spectra.

Infrared spectra of the ligands and the polymer supported complexes were taken as KBr pellets in the region, 400-4000 cm^{-1}. The IR frequencies of PSOPD and its complexes are given in the Table V.5 and the spectra are depicted in Figure V.6. It is seen that PSOPD exhibit a band at 1650 cm^{-1}. This can be assigned to the[13] azomethine C=N linkage of the Schiff base. This band is observed to show a negative shift by 10-25cm^{-1} in the complexes. This indicates the coordination of this nitrogen to the metal in the complexes. The bands at 1268, 1162 cm^{-1} due to stretching of C-N bond between the aromatic ring and the free amino group seems to be shifted to higher frequency. This is probably due to the shift in electron density from the benzene ring through resonance as the nitrogen is coordinated to the metal. The bands observed at 552 cm^{-1} for the cobalt complex, at 539 cm^{-1} for the nickel complex and at 569 cm^{-1} for the copper complex may be due to M-N stretching modes.

The spectral data for PSHQAD and its complexes are given in the Table V.6 and the spectra are represented in the Figure V.7. In the case of PSHQAD complexes also, the azomethine band at 1660 cm^{-1} for PSHQAD is undergoing a red shift on complexation. This indicates the coordination of nitrogen. In the case of cobalt complex, Co(II)PSHQAD there is an additional peak at 3549 cm^{-1} due to O-H stretching. The hydroxyl proton may be retained in this case while in all the other cases -OH group is getting deprotonated (during the complex formation). The C-O stretching frequencies at 1573 cm^{-1} shift towards a lower frequency indicating the coordination of oxygen to the metal. The C-N stretching of the aromatic ring nitrogen at

128
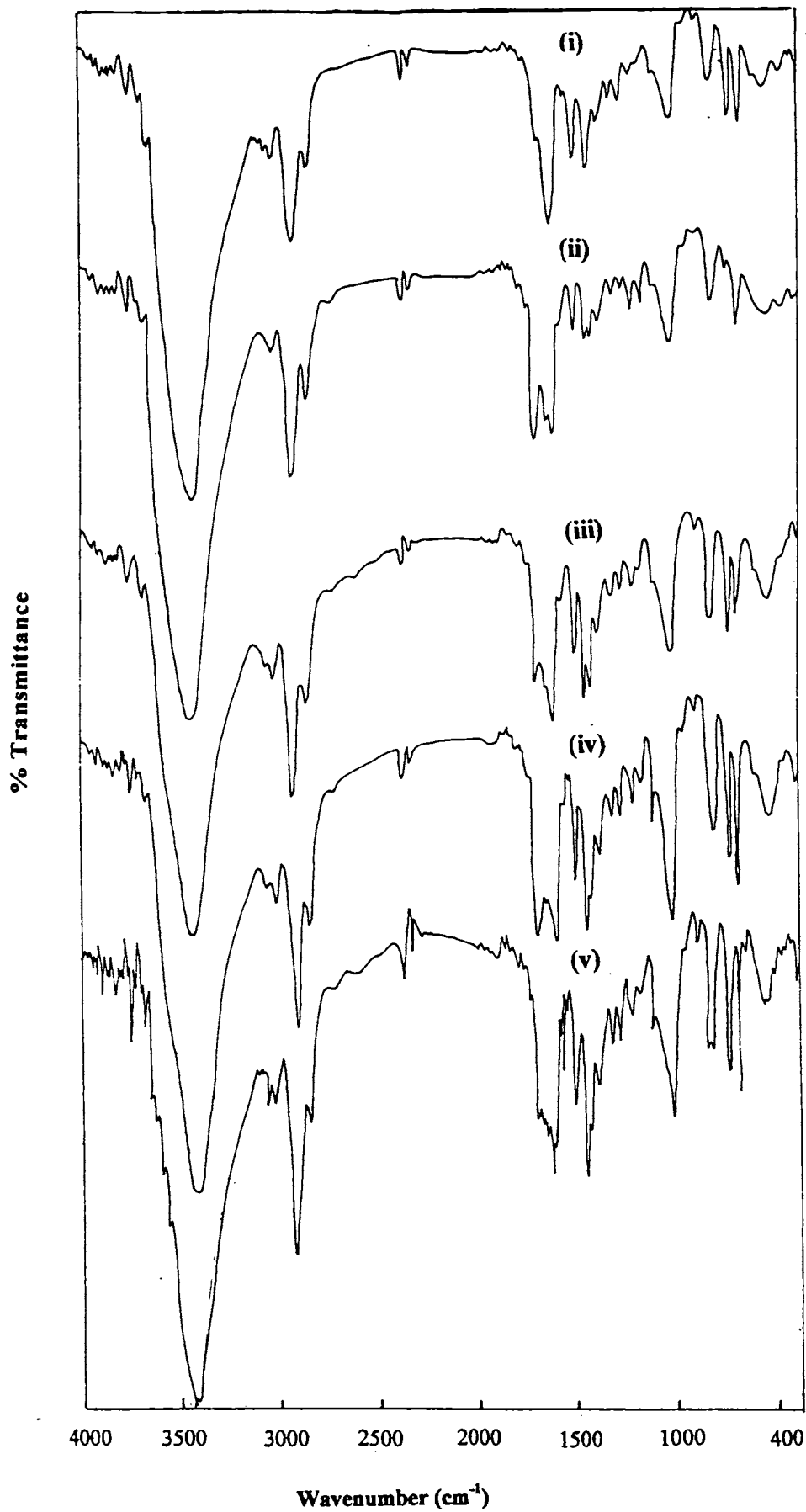
Figure V.6 FTIR data of polymer bound OPD complexes (i) PSCHO
(ii) PSOPD (iii) CoPSOPD (iv) NiPSOPD (v) CuPSOPD

1460 cm^{-1} is also showing a shift towards lower frequencies. This may be due to the shift in the electron density from the quinoxaline ring as a result of the coordination of oxygen and nitrogen to the metal. The metal oxygen stretching frequencies are at 691, 590 and 698 cm^{-1} for cobalt, nickel and copper complexes respectively.

Table V.5

FTIR Spectral data of PSOPD and metal complexes

| Compound	N-H Stretching	Azomethine C=N Stretching	C-N Stretching	M-N Stretching
PSOPD	3436	1650	1268 1162	
CoPSOPD	3436	1635	1275 1175	552
NiPSOPD	3436	1640	1275 1175	539
CuPSOPD	3436	1626	1275 1175	565
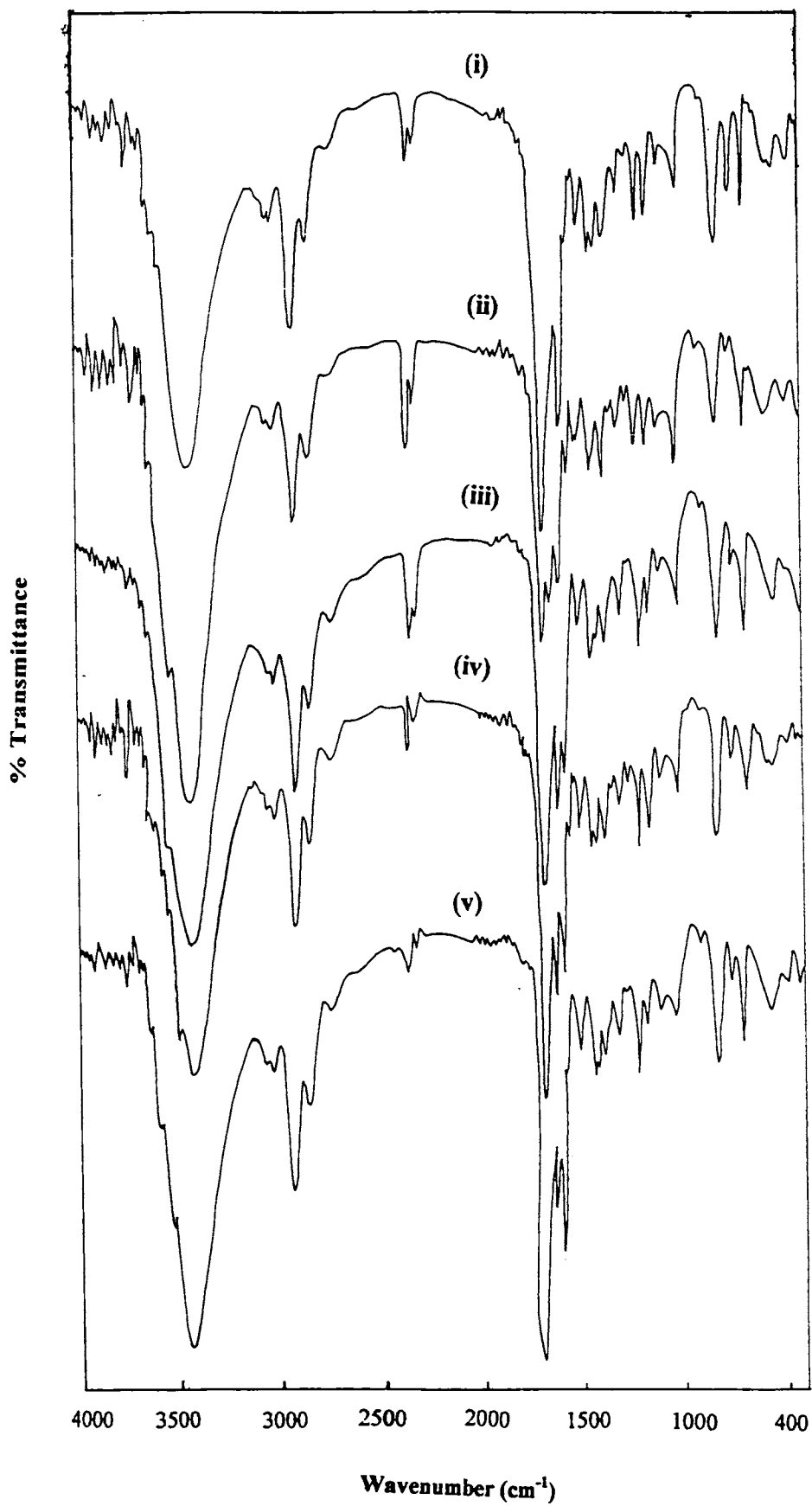
Figure V.7 FTIR data of polymer bound HQAD complexes
(i) PSNH₂ (ii) PSHQAD (iii) CoPSHQAD (iv) NiPSHQAD
(v) CuPSHQAD

Table V.6:

FTIR spectral data of PSHQAD and the metal complexes

Compound	O-H stretching	Aliphatic C-N stretching	C-O stretching	Azomethine C=N stretching	Aldehydic C-H stretching	Aromatic Ring C-N stretching
PSHQAD	-	1029	1573	1660	2740	1460
CoPSHQAD	3549	1023	1560	1645	2727	1454
NiPSHQAD	-	1023	1566	1650	2733	1454
CoPSHQAD	-	1016	1566	1650	2727	1447

5.3.6 Electronic spectra

Since the polymer samples were not soluble the spectra was recorded in the diffuse reflectance mode[14]. The diffuse reflectance spectrum is a plot of %R versus wavelength. A Kubelka Munk analysis was performed on the reflectance data.

The diffuse reflectance spectra of PSOPD complexes are presented in Figure V.8. Copper complexes of PSOPD, exhibit bands at 9500, 8300, 13,330 cm^{-1}. A copper complex,[15] $Cu(bipy)_2(ONO)^+$ having absorption maxima at 9500 and 14000 cm^{-1} has been reported to be having a cis distorted octahedral structure. In the present case the copper complex may be assigned such a structure. The complex, Co(II)PSOPD exhibit bands at 8000 cm^{-1} and 11,500 cm^{-1} characteristic of square planar complexes. The complex is also EPR active. The nickel complex showed bands at 8000 and 13000 cm^{-1} characteristic of octahedral nickel complexes.

130

Among the complexes of PSHQAD, the copper complex exhibits bands (see Figure V. 9) at 16000, 10500, 9500, 8000 and 5000 cm^{-1} resembling that of a pseudo tetrahedral complex reported earlier.[16] The nickel complex exhibits several bands in the region 4000-8000 cm^{-1}, one at 9500 cm^{-1} and 12,000 cm^{-1} characteristic of tetragonally distorted octahedral nickel complex. The cobalt complexes exhibit band at 5300, 8000, 10500, 13300 and 17000 cm^{-1} indicating low spin square pyramidal geometry. The complex is EPR active, and has a magnetic moment value agreeing with this geometry.

Table V.7:

Diffuse reflectance data for the P-OPD Complexes

Complexes	Absorption (cm^{-1})	Tentative assignments
CoPSOPD	8000	$xz....z^2$
	11,500	$xy....z^2$
NiPSOPD	7200	$^3T_{1g}(P) \leftarrow {}^3A_{2g}$
	8000	$^3T_{2g}(F) \leftarrow {}^3A_{2g}$
	13000	$^3T_{1g}(F) \leftarrow {}^3A_{2g}$
CuPSOPD	8300	
	9500	$z^2.....x^2-y^2$
	13,330	$xz,yz,xy....x^2-y^2$
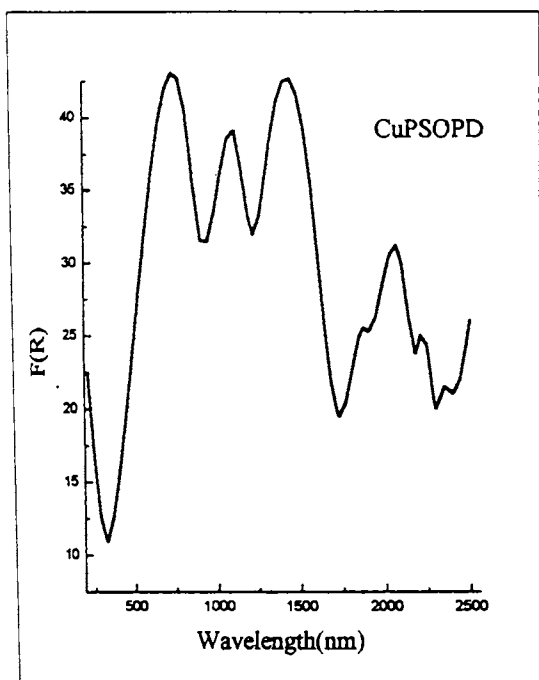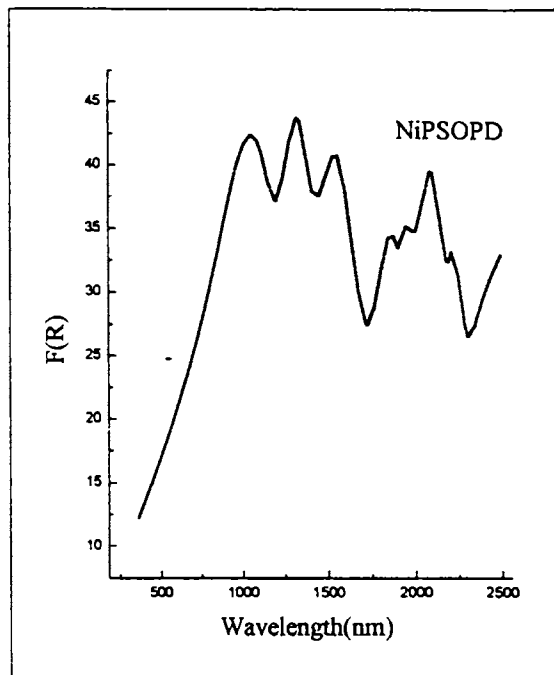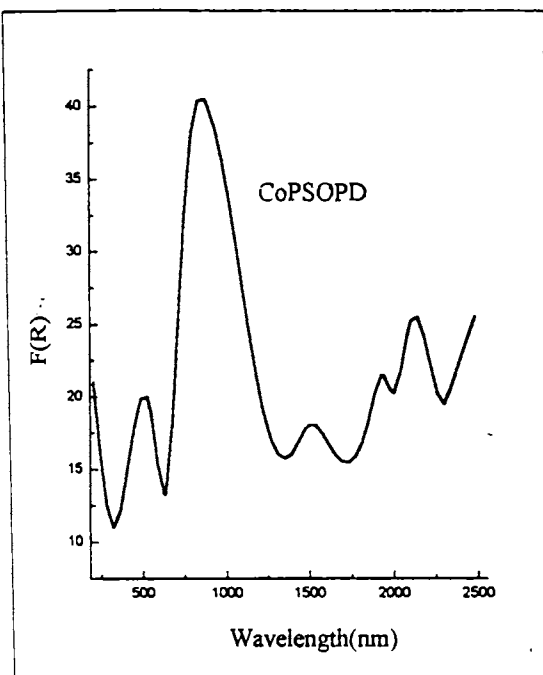
Figure V. 8

Electronic spectra of polymer supported OPD complexes

Table V.8 :

Diffuse reflectance data for the P-HQAD complexes

Complexes	Absorption (cm^{-1})	Tentative assignments
CoPSHQAD	5300	d-d transition
	8000	d-d transition
	10,500	$^2B_1 \leftarrow ^2A_1$
	13,300	$^2E \leftarrow ^2A_1$
	17000	
NiPSHQAD	4000-8000	$^3T_1g(P) \leftarrow ^3A_2g$
	9500	$^3T_2g(F) \leftarrow ^3A_2g$
	12,000	$^3T_1g (F) \leftarrow ^3A_2g$
CuPSHQAD	5000	xz, yz .....xy
	8000	z^2, x^2-y^2.....xy
	9500	
	10,500	

CoPSHQAD
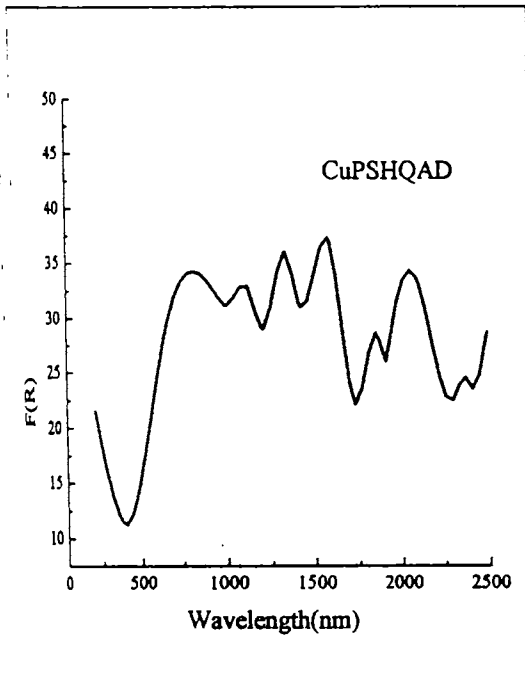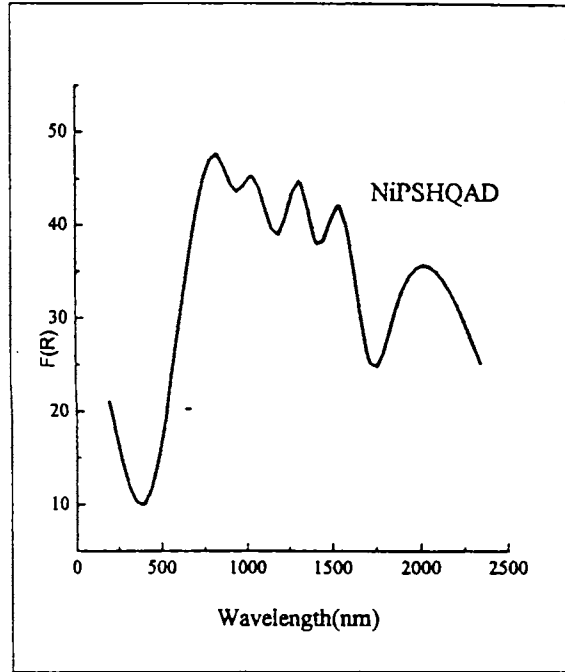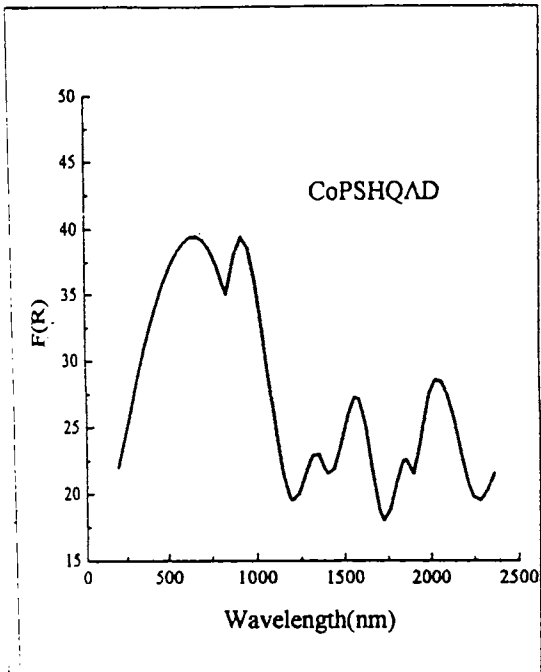
NiPSHQAD

CuPSHQAD

Figure V.9

Electronic spectra of polymer
supported HQAD Complexes

Conclusions

Cobalt(II), nickel(II) and copper(II) complexes of polymer supported Schiff bases, PSOPD and PSHQAD was prepared . The structural assignments of the complexes were made based on the EPR and diffuse reflectance studies. The cobalt complex of Schiff base PSHQAD is found to have square pyramidal geometry and that of PSOPD has a square planar geometry. Square planar complexes are found to act a catalyst in a number of reactions through reversible binding of oxygen. Nickel complex of PSHQAD and PSOPD has an octahedral structure while copper complexes, Cu(II)PSOPD and Cu(II)PSHQAD are having a cis-distorted octahedral and pseudotetrahedral structure respectively. Thus a series of Schiff base complexes, which have the potential of being used as catalyst, was synthesised and characterised using the above techniques.

REFERENCES

1.   E. Tsuchida,. N. Nishide, *Advances in Polymer Science*, Springer-verlag Berlin, 24 (1977).

2.   D. Wohrle,. *Advances in Polymer Science*, Springer-Verlag Berlin (1983) 50.

3.   M. N. Hughes, *The inorganic chemistry of Biological process*, 2nd Edition, Wiley chechester (1981)

4.   W. Hay, *Bioinorganic Chemistry*, Horwood, England (1984).

5.   V. Sasson, R. Newmann, *Handbook of Phase transfer catalysis*, Chapmann and Hall (1997).

6.   J.M.J Freuchet, K.E Hague, *Macromolecules* 8 (1975)130.

7.   K.S. Devaki, V.N.R. Pillai, *Eur.Polym.J.* 24 (1988) 209.

8.   Jose Mathew, *Ph.D thesis*, Cochin University of Science and Technology, November (1995).

9.   A Syamal, M.M.Singh, *Ind.J.Chem*, 32A (1993)42.

10.   A.Turco, C. Pecile, M. Nicolini, M. Martelli, *J.Am.Chem.Soc.* 85 (1963) 3510.

11.   D. Kivelson, R Neiman, *J.Chem.Phy.* 35 (1961) 149.

12.   I.M Proctor., B.J Hathaway, P Nicholls, *J.Chem.Soc A* (1968) 1678.

13.   K.K Mohammed Yusuff. and R.Sreekala, *J.Polym.Sci:PartA, Polym.Chem.* 30 (1992) 2595.

14.   A.B.P Lever, I*norganic electronic spectroscopy*, Elsevier, Amsterdam (1984)

15.   W. Fitzgerald, B. Murphy, S. Tyagi,, B. Walsh and B. J. Hathaway, *J.Chem.Soc.Dalton Trans.* (1981) 271.

16.   J. Ferguson, *J.Chem.Phys.* 40(1964)3406.

CHAPTER VI
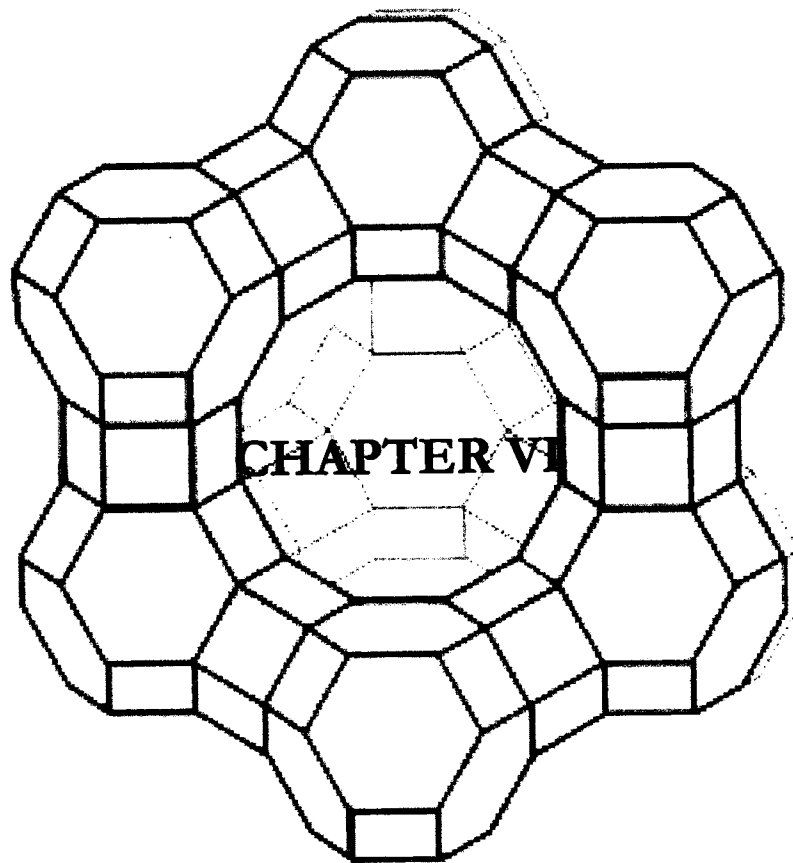
CATALYTIC HYDROXYLATION OF PHENOL

6.1 INTRODUCTION

Industrial effluents especially from pharmaceuticals, chemical and petrochemical industries contain many organic pollutants. Different methods for treating industrial waste water containing organic pollutants have been developed.[1] Phenol, is one such environmentally toxic industrial by product which is poorly biodegradable. The choice of treatment for phenol containing waste water is dependent on the level of phenol concentration, economical and easy control of the process, reliability and treatment efficiency. Many processes have been employed such as chemical oxidation,[2] electrochemical treatment,[3,4] wet oxidation, photocatalytic oxidation etc.

Reaction conditions such as higher temperature (500-700K) and pressures (70-200 bar) required for oxidation to take place in these cases are too vigorous to be implemented. So the attention of industrialists has now been directed to the development of inexpensive and efficient processes for waste water treatment to dispose phenol. Further, development of eco-friendly technologies is one of the major goals of chemists. One method of disposal of phenol is its conversion to useful products. Several industrial applications developed during this century are based on diphenols. The
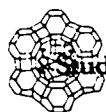
increasing demand for these products was the driving force to discover new technologies for the conversion of phenol to diphenols.

Homogeneous catalysts such as metal complexes are generally very efficient for catalytic wet peroxidation reaction but their recovery from the treated effluent is rather difficult and requires additional separation steps which induce an increase in the treatment costs. All these drawbacks can be overcome by using heterogeneous catalysts. Among all the oxidants the catalytic wet peroxidation process using H_2O_2 was the most widely employed one since it allows one to work at ambient conditions. Catalytic wet peroxidation process was first adapted from the classical Fentons reagent which allows efficient oxidation under mild conditions. (0.1 – 0.5 MPa, T≤ 100°C) with Fe^{2+} catalyst and H_2O_2. Various materials have been proposed as catalysts for the oxidation of phenols at atmospheric pressure. Some examples of these are Cu/Fe supported on Al_2O_3, Fe and ZSM-5, and supported metallo-porphyrins[7,8,9]. The catalytic efficiency of the process can be improved by combining a porous support like zeolite and an active site for the adsorption of organic compound. This causes activation of H_2O_2 and leads to complete oxidation[10,11]. Various aspects of phenol hydroxylation reaction such as the reaction mechanism, contribution of external surface and diffusion of reactant and product are not fully understood.

We have synthesized certain zeolite encapsulated metal complexes of o-phenylenediamine and Schiff bases derived from 3-hydroxyquinoxaline -2-carboxaldehyde and the efficiency of these supported complexes and the neat complex in catalytic wet hydroxylation of phenol was tested. The results of the study are presented in this chapter.

6.2   MATERIALS

The details of all the materials used for catalytic study are given in chapter II.   The zeolite encapsulated metal complexes were prepared according to the procedure reported in Chapters III and IV. All the simple complexes were prepared according to a reported procedure[12] and metal content in all these complexes have also been determined as described in chapter II.

6.3   PROCEDURE : CATALYTIC REACTION

Hydroxylation of phenol was conducted in a 100 ml batch reactor fitted with a magnetic stirrer. For the general reaction phenol (2 ml), H_2O_2 (5 ml) and H_2O (5 ml) were taken and the catalyst (about 0.1 g) was added. The reaction mixture was stirred for 4 h. The reactions were done at three different temperatures.   For reactions at higher temperature, oil bath was used.

6.4   PRODUCT ANALYSIS

The products of oxidation were analyzed using a gas chromatograph equipped with FID detection using a SE-30 column. Some of the products were further analyzed using UV-visible spectrophotometer .

6.5   BLANK RUN

When the phenol hydroxylation reaction was carried out in the absence of any catalyst, there was no appreciable conversion even after 4 hours.

137

6.6   SCREENING STUDIES

Zeolite encapsulated complexes of copper, cobalt and nickel with *o*-phenylenediamine and Schiff bases derived from 3-hydroxyquinoxaline– 2– carboxaldehyde, like QED, QPD, QHD and QDT were screened for their activity for phenol hydroxylation. The reactions were carried out in water solvent at 80°C, keeping phenol to H_2O_2 volume ratio at 2:5. The percentage conversion of phenol was noted after 4 hours of reaction. The percentage conversion obtained with various catalysts is given in Table VI.1 and represented graphically in Figure VI. 1
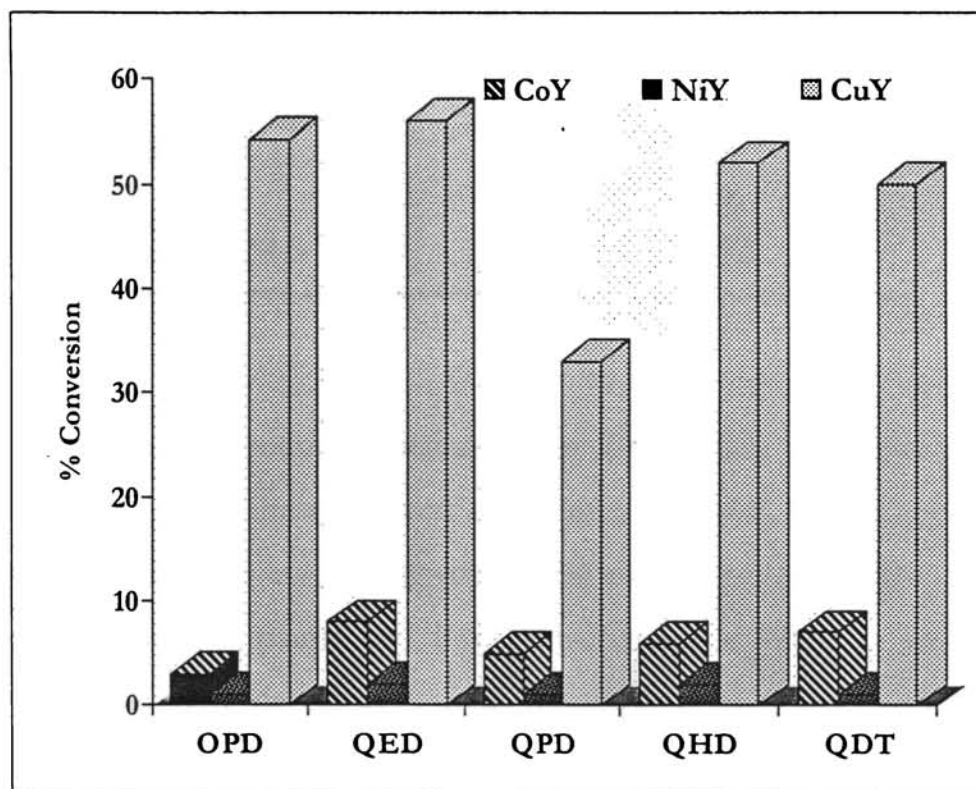
Figure VI. 1 Percentage conversion for the various zeolite-Y encapsulated cobalt(II), nickel(II) and copper (II) complexes at 80^0C (Phenol:H_2O_2 ratio 1:2.5)

These screening studies indicated that the copper complexes were most active . The higher catalytic activity of copper may be due to tuning of its redox potential by the ligands to match the requirement for the reaction of phenol hydroxylation.

Table VI. 1

Results of the screening studies, Phenol : H_2O_2 = 1:2.5

Reaction time = 4 h. Temp 80°C

	% conversion					
	OPD	QED	QPD	QHD	QDT	QPD
CoY	3	8	5	4	6	7
NiY	1	2	1	1	2	1
CuY	54.3	56	33	42	52	50

The major products obtained from the reaction are hydroquinone and catechol. Both these products are industrially useful. Catechol (CAT) is an antioxidant and is used to prepare guaicol and veratrole. It is also used in the preparation of paints and inks. Hydroquinone (HQ) is used as a photographic film developer. It is an antioxidant and it retards the oxidation of fats and milk powders.
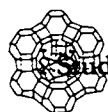
The results obtained may be described as follows.

6.7.1 Phenol-H₂O₂ ratio

The results obtained during the variation of phenol to H_2O_2 ratio are given below in Table VI.2 and VI.3

Table VI.2

Effect of phenol/H_2O_2 ratio on percentage conversion of phenol in the case of zeolite encapsulated complexes

Catalyst	Volume ratio (Phenol:H_2O_2)								
	1:1			1:2.5			1:5		
	%Con	CAT	HQ	%Con	CAT	HQ	%Con	CAT	HQ
YCuOPD	9	99	1	27	98	2	29	94.7	5.3
YCuQED	18	54	46	36.5	50	50	61	41	58.9
YCuQPD	21	53.3	46.6	48.7	52	48	57	45.2	54.8
YCuQHD	26.5	83.6	16.4	38	76	24	54	44	56
YCuQDT	14.8	78.8	21.2	30.2	68	32	56.7	49.4	50.6

Table VI.3

Effect of Phenol/H_2O_2 ratio on percentage conversion of phenol in the case of neat complexes

| Catalyst | Volume ratio (Phenol:H_2O_2) | | | | | | | | |
| | 1:1 | | | 1:2.5 | | | 1:5 | | |
	% Con	CAT	HQ	% Con	CAT	HQ	% Con	CAT	HQ
CuOPD	8	67	33	24	99	1	Only tarry products		
CuQED	2	39.7	34.7	28	63	37	44	89.5	10.5
CuQPD	2.5	99	1	34	66	34	37	99	1
CuQHD	5.7	71.5	28.5	9.4	56	44	46.7	92.	8
CuQDT	3.68	87.7	12.3	29.1	53	46	41.26	95	5
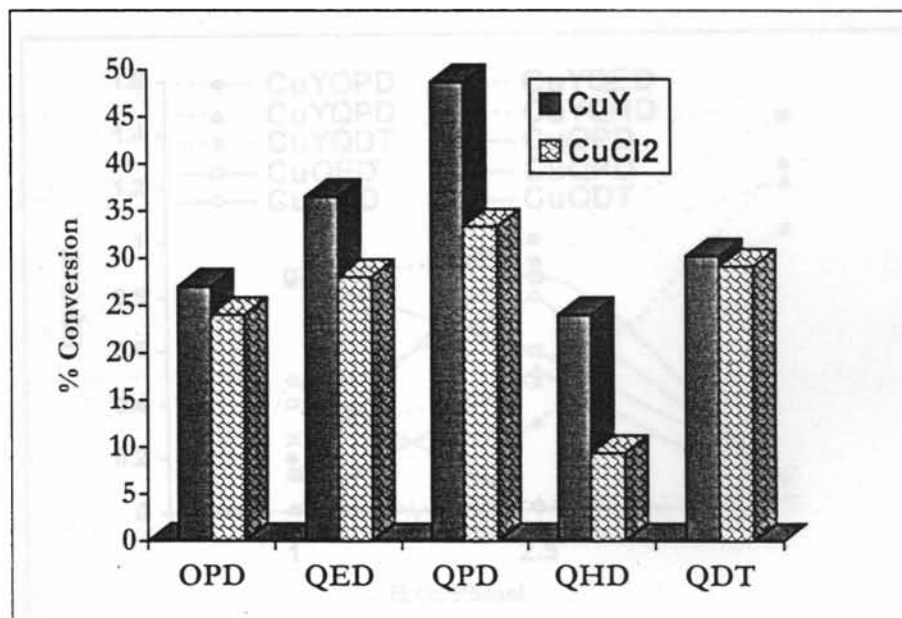
Figure. VI.2 Graph showing the %Conversion for neat as well as

zeolite encapsulated complex(Phenol:H_2O_2:1:2.5)

Comparison between the catalytic activity of zeolite encapsulated as well as neat complexes indicated that the zeolite encapsulated complexes were more active than the neat complexes. From the Table VI.2 it can be seen that in the case of zeolite encapsulated complexes the conversion % increases with increase in H_2O_2/phenol ratio. It was also seen that the conversion into the industrially more useful hydroquinone was increasing with increase in H_2O_2/phenol ratio. An interesting fact observed was that in the case of YCuOPD complex there is a preference or selectivity towards catechol. The catechol to hydroquinone ratio which followed a statistical ratio of 2:1 in the case of homogeneous complexes, due to the availability of two ortho positions, approached a ratio close to 1 in the case of zeolite encapsulated complexes Figure VI. 3. This may be due to the shape selectivity of the zeolite pore.
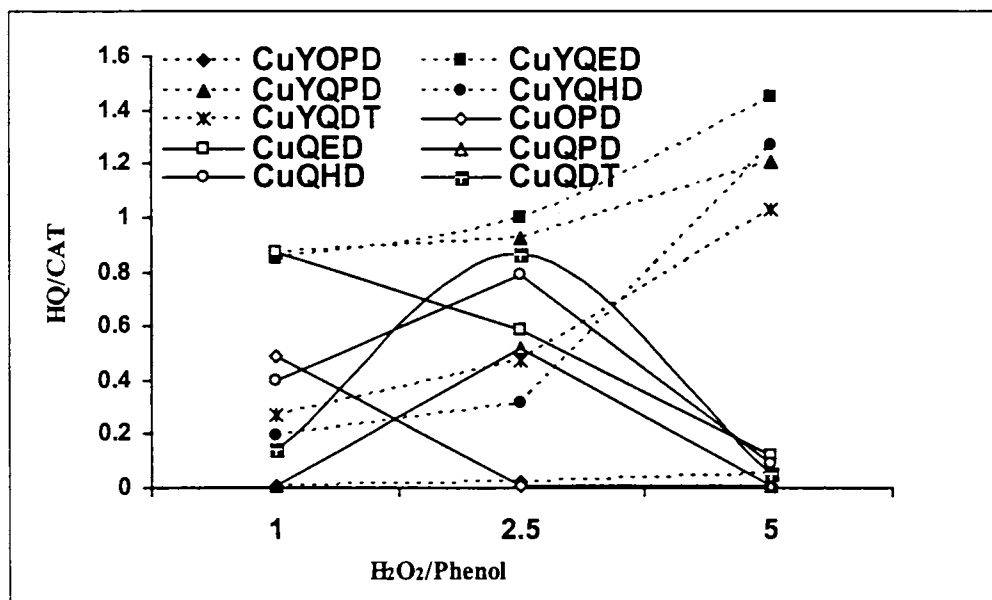

Figure VI. 3 Plot HQ /CAT ratio against H_2O_2 /Phenol ratio.
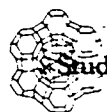
In the case of simple complexes the conversion showed a sharp increase when the H_2O_2/phenol ratio was increased from 1 to 2.5 (see Table VI. 3). But when H_2O_2/phenol ratio increased from 2.5 to 5, even though the conversion % was increased the selectivity towards hydroquinone showed a decrease. This may be due to the conversion of phenol into unwanted tarry products.

Table VI.4

Conversion % per g of metal per hour of the zeolite encapsulated as well as neat complexes of copper

	% Copper		(Conversion % per g of metal per hour) X 10^{-3}	
	Encapsulated Complexes	Neat complexes	Encapsulated complexes	Neat complexes
QED	1.17	14.47	7.76	0.483
QPD	2.63	13.36	4.62	0.636
QHD	2.95	14.87	3.22	0.662
QDT	2.1	13.27	3.59	0.546
OPD	0.91	23.04	7.41	0.260

Inspite of the higher metal percentage of the simple complexes, the conversion percent is higher for zeolite encapsulated complex. When the conversion % per g of metal per hour was calculated for the simple as well as the zeolite encapsulated complexes (Given in the Table VI. 4) it was found the TON was ten times more for the zeolite encapsulated complexes.

The order of reactivity of zeolite encapsulated complexes may be given as

YCuQED > YCuQDT > YCuQHD > YCuQPD > YCuOPD

For simple complexes the order of reactivity.

CuQED > CuQHD > CuQDT > CuQPD > CuOPD

6.7.2 Temperature dependence

The influence of temperature on the conversion was studied by carrying out the reaction at three different temperatures, $30 \pm 2°C$, $80°C$ and $100°C$. The results of the study are given in the Table VI. 5 and Table VI. 6.

For the zeolite encapsulated complexes the conversion was increasing with increase in temperature and the hydroquinone selectivity was also increasing. In the case of simple complex the conversion increased rapidly up to $80°C$ (See Table VI. 5). But as the temperature is increased further to $100°C$, the conversion started decreasing. This may be due to the decomposition of the simple complex at $100°C$. In the case of simple complex, another interesting observation was that even though the conversion decreased at $100°C$, the ratio of CAT/HQ was maintained almost close to 2, same as the expected statistical ratio, whereas in the case of the zeolite encapsulated complex the selectivity towards hydroquinone increased.
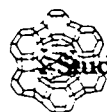
Table VI. 5

Influence of temperature on the conversion percentage of zeolite
encapsulated complexes

Catalyst	30			80			100		
	%Con	CAT	HQ	%Con	CAT	HQ	%Con	CAT	HQ
YCuOPD	27	98	2	54.6	63.2	36.8	52.5	60	40
YCuQED	36.5	50	50	56	66.6	33.4	65.5	37.5	62.5
YCuQPD	48.7	52.1	47.9	53.2	50	50	66	45.4	54.6
YCuQHD	24	76	24	42.3	64.8	35.2	68.7	53.9	46.1
YCuQDT	30.2	68	32	55	56.4	43.6	79	47.3	52.7

Table VI.6

Influence of temperature on the conversion percentage of zeolite
encapsulated complexes of neat complexes

Catalyst	30			80			100		
	%Con	CAT	HQ	%Con	CAT	HQ	%Con	CAT	HQ
CuOPD	34	67	33	37.5	70	30	30	67.6	32.4
CuQED	28	63	37	54	62	38	22	62	38
CuQPD	34	66	34	78.5	64	36	42.5	68.5	31.5
CuQHD	9.4	56	44	73	66	34	45	67.5	32.5
CuQDT	29.1	53	47	54	69	31	39.4	92.6	7.4
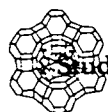
6.7.3 Reaction Time

The conversion was studied with variation of reaction time. Above 4 h, both the catalysts resulted in the formation of tarry products. But the tar formation was much less in the case of zeolite encapsulated complex. The results for YCuOPD are given in the Table VI. 7.

Table VI. 7

Effect of reaction time on the percentage conversion of phenol

Zeolite encapsulated complexes			
Time	%Conversion	CAT %	HQ %
2 h	36	70	30
4 h	48.7	52.1	47.9
6 h	53	65	35 (Tar formed)
8 h	60	80	20 (Tar formed)
10 h		only Tar	
Neat Complexes			
2 h	25	100	0
4 h	34	66	37
6 h		Only Tar formed	
8 h			
10 h			

When the selectivity towards catechol and hydroquinone was studied it was seen that up to 4 h the catechol percentage was decreasing with a corresponding increase in hydroquinone percentage. But after 6 h., the rise in catechol percentage observed may be due to higher percentage of tar formation. In the case of neat complex, no hydroquinone was observed after 2 h indicating complete selectivity for catechol formation. However, after 4 h the statistical ratio of 2:1 was observed and complete conversion into tar resulted after 6 h. This may be because of the higher metal percentage in the neat complexes leading to uncontrollable side reactions. Since no tar formation was observed upto 4 h, it was taken as the optimum reaction time.

6.7.4 Amount of catalyst

Table VI.8 gives the variation in conversion on varying the amount of catalyst i.e. YCuQDT or CuQDT.

It can be seen that even though the catalyst amount was increased from 0.1 to 0.5 g there was not much increase in conversion for zeolite encapsulated complexes, but in the case of neat complexes the conversion increased from 30 to 70 %. But the CAT/HQ ratio remained almost 2 for the neat complexes where as in the case of zeolite encapsulated complexes the percentage of hydroquinone increased. The higher conversion percentage in the case of neat complex may be due to higher metal percentage. The higher selectivity towards hydroquinone in the case of zeolite encapsulated complex is due to shape selectivity induced by the zeolite pores.

Table VI.8

Effect of amount of catalyst on the percentage conversion of phenol

Catalyst	Zeolite Complex			Neat Complex		
(g)	%Con	CAT	HQ	%Con	Cat	HQ
0.1	30.2	68	32	29.1	53	47
0.2	37	64	46	35	60	40
0.3	46	50	50	50	66	34
0.4	50	40	60	60	60	40
0.5	52	40	60	66	68	32

6.7.5 Variation of Solvent

When the reaction was studied in different solvents like water, acetonitrile methanol and acetone, the following results were obtained (see Figure VI. 4 and Figure VI. 5 . Water was found to be the best solvent with a higher conversion percentage and selectivity towards more desirable hydroquinone. Even though the conversion percentage of acetonitrile was comparable with that of water, acetonitrile showed a higher selectivity towards catechol. Methanol and acetone were poor solvents with conversion less than 5% and catechol was the only product formed. The results of this study are presented in the Table VI.9 and Table VI.10.
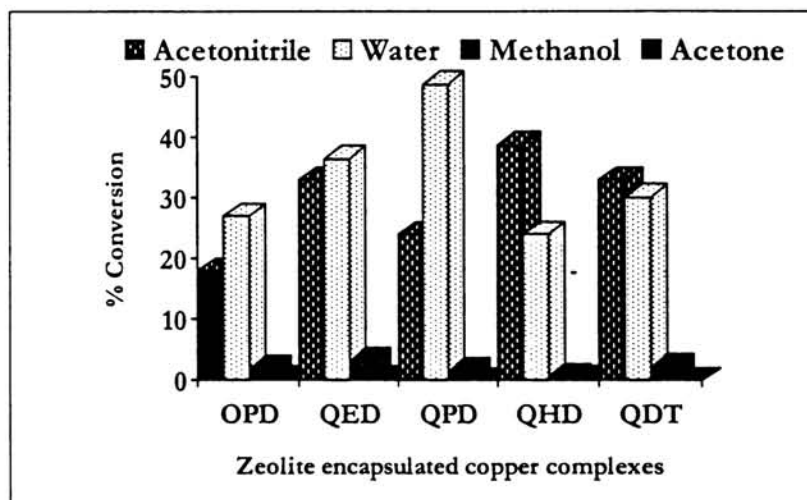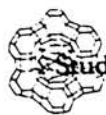
Figure VI. 4 Effect of various solvent on the conversion of phenol in the case of zeolite encapsulated copper complexes.
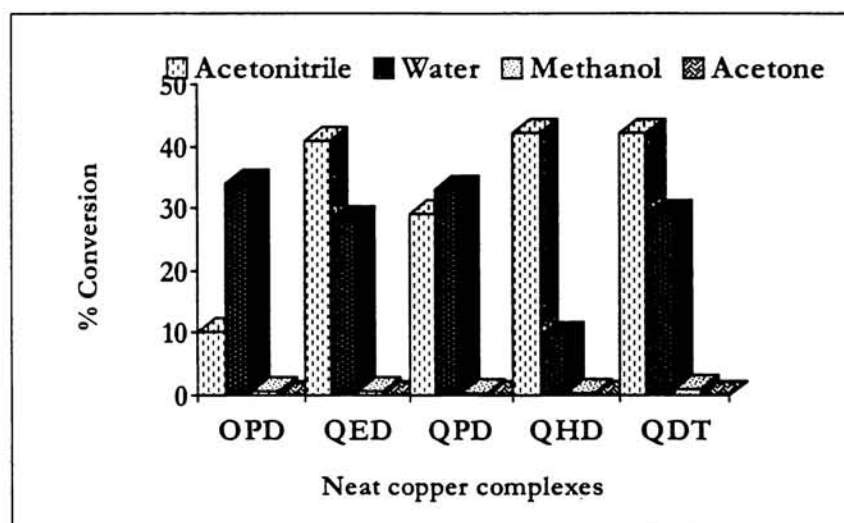

Figure VI. 4 Effect of various solvent on the conversion of phenol in the case of neat copper complexes.
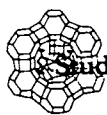
Table VI.9

Effect of solvent variation on phenol conversion for zeolite encapsulated copper complexes

Solvents	OPD	QED	QPD	QHD	QDT
Acetonitrile	18	33	24	38.72	33
Water	27	36.5	48.7	24	30.2
Methanol	1.9	3.15	1.65	0.7	2.17
Acetone	0.2	0.2	0.1	0.2	0.1

Table VI.10

Effect of solvent variation on phenol conversion for the neat copper complexes

|	OPD	QED	QPD	QHD	QDT
Acetonitrile	10	40.71	29	42.3	42
Water	34	28	33	9.37	29.1
methanol	0.8	0.67	0.35	0.32	0.9
Acetone	0.1	0.1	0.1	0.1	0.1
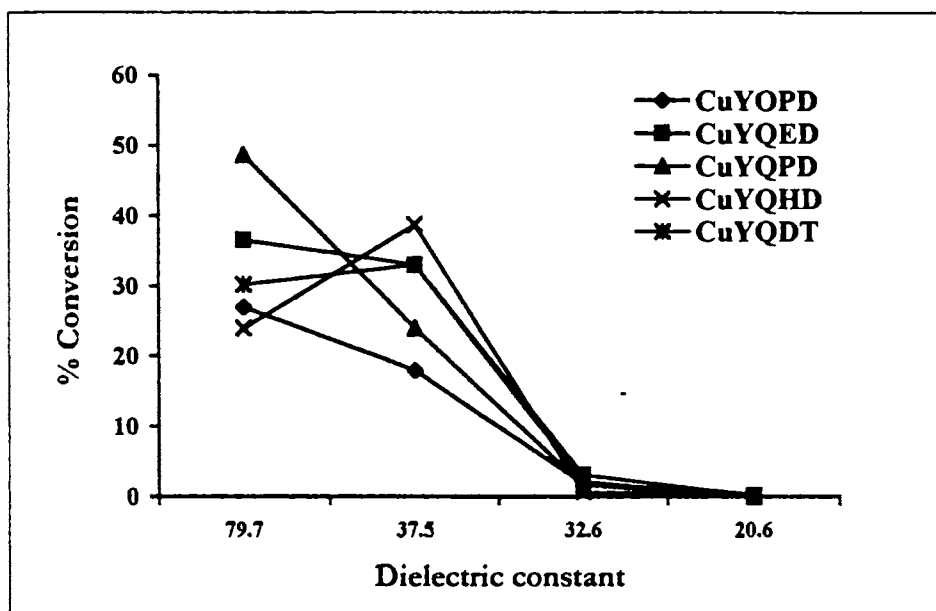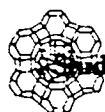
Figure VI.6 Plot of dielectric constant versus the percentage
conversion for zeolite encapsulated complexes
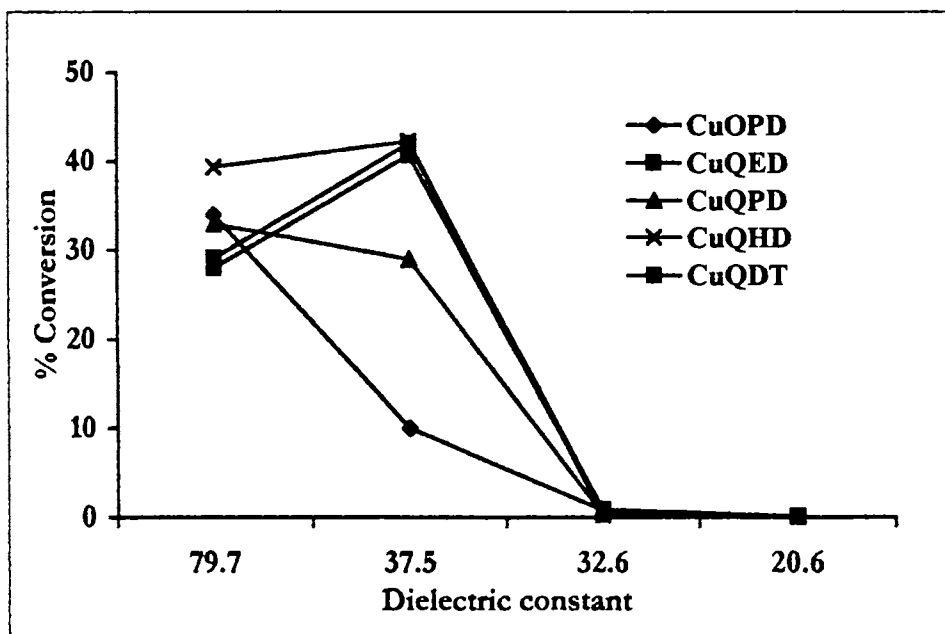
Figure VI. 7 Plot of dielectric constant versus the percentage
conversion for neat complexes

152

6.8 DISCUSSION

The results obtained from the above study showed that temperature, substrate to oxidant ratio, relative diffusion rates of the solvent as well as the substrate, the competition between the substrate and solvent molecules for coordination to the transition metal cation all play a role in the relative ratio of catechol to hydroquinone. In many of the H_2O_2 oxidations, reactive species is reported to be of the type $H_3O_2^+$. Such a species is known to be formed in strongly acidic media and is reported to be a powerful oxidant.

In the present study it was observed that the conversion percentage obtained with the zeolite encapsulated complexes is more than that with the neat complexes in spite of the higher metal content of the latter. This may be explained if we assume a similar species to be active in our case also. In the case of the zeolite encapsulated complex the acidic sites available on the zeolite framework may be supplementing the acidity requirement for the formation of $H_3O_2^+$. We therefore assume the following mechanism for the oxidation of phenol. The first step involves reaction between phenol and the complex in which an electron is transferred to the metal ion. In the process a phenol radical is formed. Ortho attack on the radical by $H_3O_2^+$ leads to catechol while para attack leads to hydroquinone. The mechanism is outlined in the scheme I

$$H_2O_2 \; + \; H^+ \rightleftharpoons H_3O_2^+$$
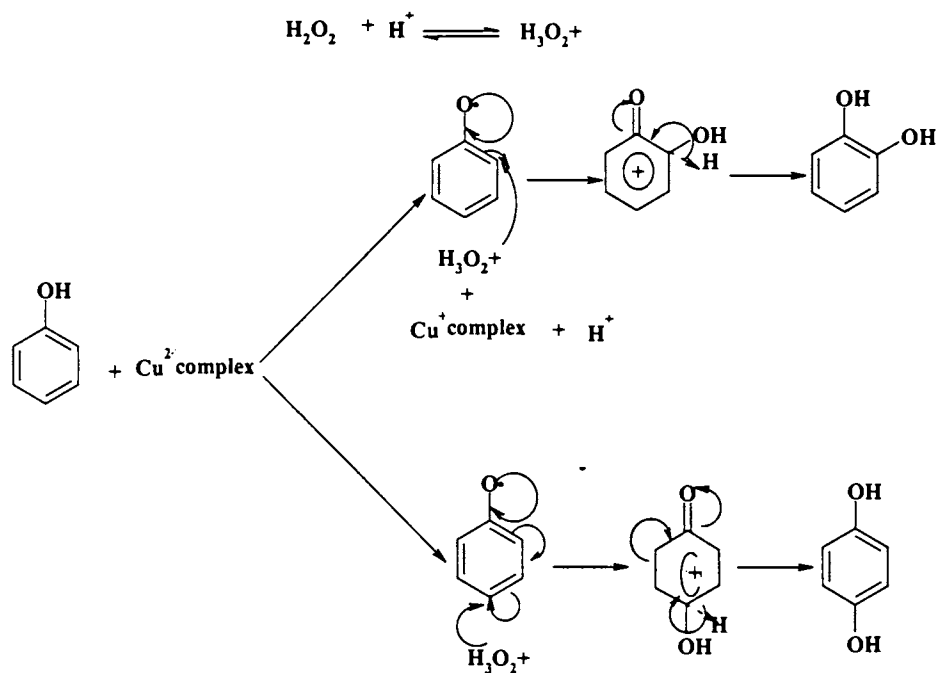
Scheme I

Similar mechanism has been proposed by earlier workers for phenol hydroxylation reaction.[13]. The earlier reports on phenol hydroxylation reaction using similar porous catalysts indicated that the reaction can take place at the external surface as well as in the internal pores. The reaction in the internal pores leads mainly to hydroquinone formation whereas the reaction on the external surface leads to catechol as well as tarry products.

The presence of acid as well as higher concentration of H_2O_2 shift the first equilibrium in the proposed mechanism to the right and this explains the higher conversion observed for higher H_2O_2/phenol ratio. The shape selectivity imposed by the zeolite pores in the case of encapsulated metal complexes allows higher phenol conversion with reduced formation of tars and a lower ortho to para ratio. The lower conversion percentage obtained for the simple complex may be due to the absence of these two factors. In the case of the simple complex the formation of tarry products

may be due to polymerization side reactions taking place. Unwanted side reactions may be resulting from higher metal percentage. The greater preference for catechol formation in the case of YCuOPD may be explained in terms of the pseudo tetrahedral structure which enables the hydroxyl group to attack from the ortho side preferably.

As expected, when the temperature is increased a higher conversion of phenol and higher selectivity towards hydroquinone is observed. The increased diffusion of phenol into the pores of zeolite may also be contributing to the increased conversion.

Although prolonging the reaction time will be beneficial for phenol conversion, increased unavoidable deep oxidation at longer reaction time reduce the selectivity of the phenol oxidation products. Hence the optimum reaction time can be taken as four hours.

The solvents used in the reaction are known to have a profound influence on phenol conversion. Maximum conversion was observed in water. This is due to the fact that phenol and H_2O_2 can reach the active sites more easily with water than with organic solvents. It has been reported that the activity coefficient of phenol in water is much higher than in any other solvent.[14] Methanol is giving only very low conversion. This may be due to the radical scavenging property of methanol which removes the reactive phenol radicals. Conversion is much higher in acetonitrile solvent, it is even comparable with that in water but catechol is the product formed selectively. This may be explained as due to competition between acetonitrile and phenol for the catalyst site inside the pores. As a result, most of the reaction may be taking place on the surface leading to the formation thermodynamically favourable catechol. Diffusion may also be a

factor influencing the conversion of phenol. The earlier studies indicate that diffusion follows the order $D_{HQ} > D_{CAT} > D_{Phenol}$ substantiating the role of internal sites as well external sites in phenol hydroxylation to catechol.

Conclusions

Among the various zeolite encapsulated complexes the copper complexes are found to be more active for phenol hydroxylation. Furthermore, from the above study it may be concluded that the zeolite encapsulation leads to an increase in percentage conversion of phenol hydroxylation reaction, easy separation from the reaction medium and more selectivity towards hydroquinone.

Studies on some supported Co(II),Ni(II),Cu(II)..........

REFERENCES

1. A. Alejandre, F. Medina, P. Salagre, A. Fabregat, J. E. Sueiras. *Appl.Catal.B:Environ.* 18 **(1998)** 307.

2. Y. Yamamato, E. Niki, M. Shiokuwa, *J.Org.Chem.* 44 **(1979)** 2137.

3. D. Kirk, S. Shafirian, *J.Appl.Electrochem.* 15 **(1985)** 285.

4. A. Boudenne, O. Cerelier, J. Galca, E. Vandenllist, *Appl.Cata.A:Gen.* 143(2) **(1996)** 185.

5. K. Fajerweg, H. Debellefontaine, *Appl.Catal.B:Environ.* 19(4) **(1996)** 229.

6. L. Palmisano, M.Schiavello, A. Selafani,. G. Martra, *Appl.Catal B:Environ.* 3(2-3) **(1994)** 117.

7. A.R. Sangen, T.T.K. Lee, K.T. Chuang, *Progress in Catalysis,* **(1992)** 197.

8. C. Pulgarin, D. Peringer, P. Alberts, J. Kiwi , *J.Mol.Catal.A.* 95 **(1995)** 61.

9. C. Labat, J. L. Seris, B. Meunier, *Angew.Chem.Ind.Ed.Eng.* 29(1990)1471.

10. D.E.W. Vangham, *Catal.Today.* 2 **(1988)** 187.

11. F.Figueras, *Catal.Rev.Sci.Eng,* 30 **(1988)** 457.

12. Jose Mathew, *Ph.D. Thesis,* Cochin University of Science and Technology, November **1995.**

13. A.Sadana, J.Katzer *J.Catal.* 35 **(1974)** 140.

14. Ch.subramanyan, B.Louis, B.viswanathan, A.Renken, T.K.Varadarajan *Eurasian Chem.Tech.J.* 3 **(2001)** 5963.

CHAPTER VI
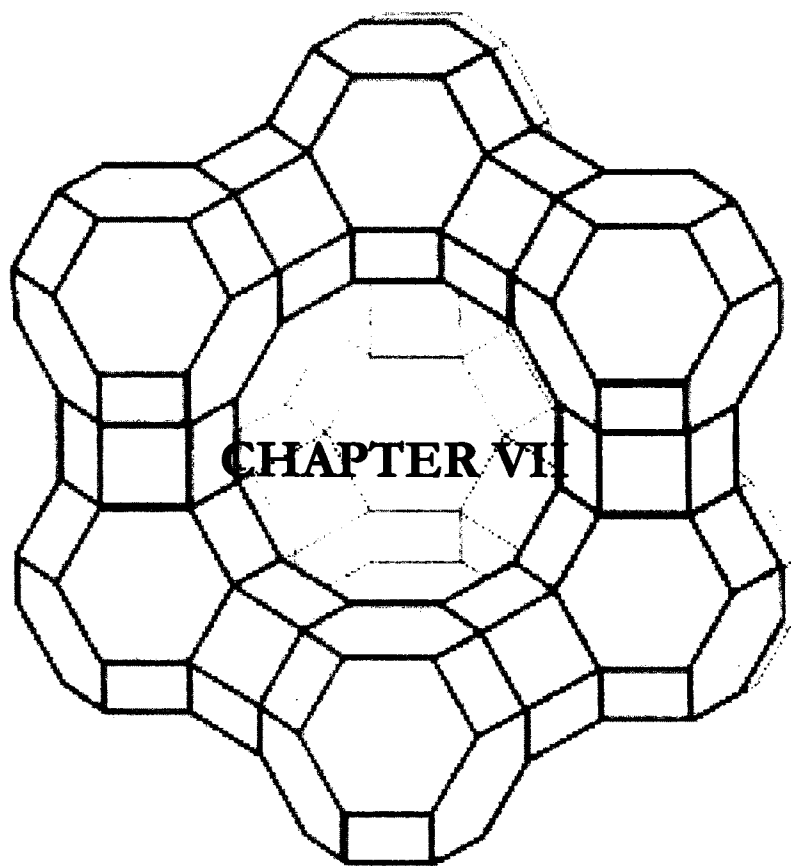
KINETICS OF OXIDATION OF CATECHOL AND 3,5-DI-TERT-BUTYLCATECHOL-A COMPARATIVE STUDY USING ZEOLITE ENCAPSULATED AS WELL AS THE NEAT COPPER COMPLEXES OF O-PHENYLENEDIAMINE

7.1 INTRODUCTION

Many attempts are being made to synthesize metal complexes that model biological systems and to reproduce the structural, spectroscopic and reactivity properties of enzymes. Copper complexes containing the ligands like COO-, NH_2-, CONH- , which are the possible sites of attachment of metal ions in proteins, are studied as models for copper enzymes.[1] The effect of ligands on the catalytic activity indicates that the reduction of Cu(II) coordinated to the two nitrogens is kinetically much faster[2] than that of aquo cupric ion. The enhancement in catalytic activity has been attributed to strain[3] around the metal ion catalyst provoked by the ligand molecules. The redox potential of the metal ion is one of the critical factors determining the activity of a catalyst for the redox reaction. The catalytic activity of ethylenediamine complexes of copper has been correlated with the ability of metal complex to transfer an electron to molecular oxygen.[4] The number of coordinated ligand groups in a Cu^{2+} complex can be deduced from the relation between its structure and catalytic activity.[5]

Metal ion attached to molecular sieve behaves differently from a metal ion or atom in any ordinary metal oxide. In a metal oxide the interaction between different metal atoms is possible whereas in zeolites the

158
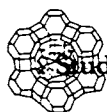
metal ions are more isolated and tend to behave as their homogeneous analogues. Zeolite encapsulated metal complex often exhibit catalytic activity similar to that of enzymes and hence are referred to as zeozymes. The important changes provoked by ligand coordination in the electronic environment around the metal ion in the zeolite, (particularly with regard to redox potential, substitution reactivity and activation of the substrate by metal ion and their complexes) have been investigated extensively in comparison with homogeneous catalysis.

There are at least four possible rate determining steps, a) mass transport across the gas-liquid interface, b) mass transport across the diffusion layer at the surface of the zeolite particles, c) mass transport into the zeolite pores and d) reaction at catalytic sites. If reaction rates were limited by the diffusion of the substrate in to the zeolite, the catalyst may ultimately be poisoned through adsorption of products on to the catalyst.

The exploration of the common roots of heterogeneous and homogeneous catalysis requires the correlation of the catalyst structure, reactivity and the elementary reaction. The activity of the intrazeolitic complexes is compared with that of the enzymes and also with the homogeneous metal complex catalysts.[6] Oxidation of pyrocatechol with molecular oxygen has been carried out using homogeneous metal complex catalyst. The reaction is found to proceed with successive one electron transfers from the metal to oxygen followed by electron transfer from the substrate to the metal ion to give the quinone and regenerate the lower oxidation state of the metal. In spite of diffusion restriction, zeolite encapsulated complexes have a catalytic activity comparable with that of a

homogeneous metal chelate catalyst. The activity of such catalysts is only an order of magnitude less than that of a typical enzyme oxidation catalyst.

One of the classes of catalytic reactions studied widely is those involving hydrogen peroxide. In the disproportionation of H_2O_2 one molecule of H_2O_2 is oxidized and another is reduced.

$$H_2O_2 + H_2O_2 \rightarrow O_2 + 2H_2O$$
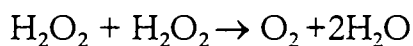
Direct decomposition of H_2O_2 requires activation energy of at least 48 kcal/mole. Therefore thermal decomposition can proceed only through a catalytic route. In the presence of a substrate that can be oxidized the following reaction can occur.

$$H_2O_2 + substrate \rightarrow oxidized\ product\ of\ substrate + H_2O$$
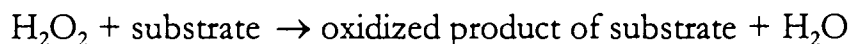
The catalysis of disproportionation of hydrogen peroxide by metal ion or their complexes in homogeneous system have been studied extensively.[7]. They are reported to be very good catalysts for the decomposition of hydrogen peroxide. The catalysis proceeds through successive redox steps.

Metal ions exchanged zeolites show excellent catalytic activity for H_2O_2 decomposition, in a manner similar to that observed in homogeneous systems.

$$2[LM]^{n+} + 2HOO^- \rightarrow 2[LM]^{(n-1)+} + 2HOO$$

$$2[LM]^{(n-1)+} + H_2O_2 \rightarrow 2[LM]^{n+} + 2OH^-$$
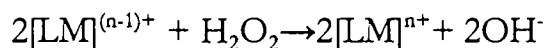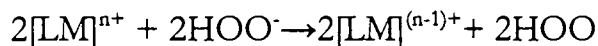
The catalysis of oxidation by hydrogen peroxide has also been investigated extensively. Oxidation of organic substrates using H_2O_2 catalysed by transition metal ions or their complexes having partially filled d-shells has been reported in literature.[8-11] Among all the complexes the

160

complexes of Fe(III) and Cu(II) are known to be most active and they are found in many redox active enzyme systems. The studies carried out on the copper complexes indicate that the redox potential of copper complexes having two nitrogen donors is ideal[12] for a one electron transfer from the peroxide anion to the central metal ion. The standard potential of Cu(II)-Cu(I) couple in water (+ 167 mV) becomes more positive when the water molecules are replaced by nitrogen atom. The ligand must remain coordinated to both cuprous and cupric forms for the redox reaction to occur.

Efforts directed towards understanding the role of copper in the transformation of catechol to o-benzoquinone, has lead to the synthesis of model compounds of copper that would mimic the spectroscopic characteristics as well as the chemical behaviour of tyrosinase[13-15] the biological systems. We have synthesized various supported as well as neat complexes of cobalt(II), nickel(II) and copper(II) complexes and screened their catalytic activity towards the oxidation of catechol to o-benzoquinone. Among these complexes supported copper(II) complex of o-phenylenediamine (YCuOPD) was found to exhibit maximum catalytic activity. It was therefore thought worthwhile to investigate the kinetics and mechanism of catechol oxidation to o-benzoquinone by hydrogen peroxide using the zeolite-encapsulated as well as neat copper complex of o-phenylenediamine as catalyst. We have also studied the kinetics of oxidation of 3,5-di-tert-butylcatechol in the presence of the above two catalysts for comparison. The results of these studies are presented in this chapter.
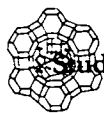
7.2 EXPERIMENTAL

7.2.1 Reagents Used

All the chemicals used were of analytical grade purity. Catechol (Merck), 3,5-di-*tert*-butylcatechol (Aldrich Chem. Co. Ltd.) and H_2O_2 (Merck) were used as purchased. Zeolite encapsulated copper complex of *o*-phenylenediamine (YCuOPD) was synthesized according to the procedure described in Chapter III and it was used as such in the kinetic runs.

7.2.2 Preparation of substrate solution

Catechol $(2.75 \times 10^{-2}$ g) and 3,5-di-*tert*-butylcatechol $(5.78 \times 10^{-2}$ g) respectively were accurately weighed into a 25 ml standard flask and made up using methanol. The resulting solution $(0.01$ mol dm^{-3}) was used as the stock solution. Solutions of substrates were prepared afresh before each set of kinetic runs.

7.2.3 Preparation of stock solution of hydrogen peroxide

For the preparation of stock solution, 1 ml solution of H_2O_2 (30% w/v) solution of was diluted to 100 ml in a standard flask. The concentration of the stock solution was estimated permagnometrically.[16]

7.2.4 Preparation of solution of simple complex

Neat copper complex of *o*-phenylenediamine $(Cu(OPD)_2)$ was prepared according to the literature procedure.[17] The complex $(2.75 \times 10^{-2}$ g) was weighed into a 50 ml standard flask and made up to the mark with methanol. This solution was diluted ten times in a standard flask to obtain the stock solution and characterized in our laboratory.
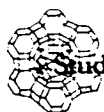
7.2.5 Procedure for screening studies

Prior to carrying out detailed kinetic study, a preliminary study was made in which all the zeolite encapsulated complexes were screened for the catalytic activity towards H_2O_2 oxidation reaction of catechol to *o*-benzoquinone and 3,5-di-*tert*-butylcatechol to 3,5-di-*tert*-butyl-1,2 benzoquinone. These studies were done in 9:1 methanol : water mixtures. The H_2O_2 concentration was 1.0×10^{-2} mol dm^{-3} and the catechol concentration was 1.0×10^{-3} mol dm^{-3}. About 0.01 g of the catalyst was used. Comparison of the activities was made on the basis of percentage conversion after 1 hour. The latter is obtained spectrophotometrically by measuring the absorbance at 419 nm. The total volume of the reaction mixture was 10 ml.

7.2.6 Kinetic procedure

All the kinetic runs were carried out at 30^0C in phosphate buffers, maintaining H_2O_2 concentration at least ten times greater than that of the substrate. The dielectric constant of the reaction mixtures was varied using methanol. The total dielectric constant, D of the reaction mixtures was estimated using the formula $D = (D_1V_1+D_2V_2)/(V_1+V_2)$, where D_1 and D_2 are the individual dielectric constants of water and methanol respectively and V_1 and V_2 are their respective volumes in the reaction mixture. The reaction was initiated with the catalyst and the progress of the reaction was monitored spectrophotometrically (Shimadzu UV-Vis 160A, Japan) by following the absorbance of the respective products. The molar absorption coefficients of the products were determined using Beer-Lambert's method. The reaction was monitored at two different wavelengths, at one wavelength the product of the reaction absorb and at the second wavelength the product does not absorb Any absorbance detected at the

163

latter wavelength corresponds to scattering due to the catalyst particles. Therefore, the difference between the two absorbance values gives corrected absorbance of the product. This method is generally employed in Atomic Absorption Spectroscopy and its use to the UV-visible spectrophotometry is novel. Its pertinency to the latter is obvious from the good reproducibility observed, all the kinetic runs were reproducible within an accuracy of ± 5%. Initial rate method was employed to determine the rate of the reaction from the concentration-time data. Initial rates were obtained by fitting the data into a polynomial of the form

$$[C] = a_o + a_1 t + a_2 t^2 + ...$$

where C and t represent concentration and time respectively and a_0, a_1, a_2 etc. are constants and determining the first derivative from the slope of the plot at t = 0. A software called Microcal Origin 3.54, Microcal Software Inc, USA.

7.3 RESULTS

7.3.1 SCREENING STUDIES

The results of the screening studies are presented in the Table VII.1

Among the various complexes the copper complexes were showing the maximum catalytic activity in the oxidation of catechol and DTBC and least activity was shown by the nickel complexes. The order of activity can be given as, copper > cobalt > nickel. Among the various copper complexes the YCu(OPD) complex gave the highest conversion. A detailed kinetic study using the above complex was carried out.

Table VII.1

Results of the screening studies in the oxidation of catechol and DTBC using the zeolite encapsulated complexes

Catalyst	% Conversion		Catalyst	% Conversion		Catalyst	% Conversion	
	CAT	DTBC		CAT	DTBC		CAT	DTBC
YCuOPD	26.33	30.26	CoYOPD	18.63	24.85	NiYOPD	1.60	9.57
CuYQED	7.20	10.70	CoYQED	5.71	11.66	NiYQED	3.97	5.73
CuYQPD	21.24	26.12	CoYQPD	19.00	22.94	NiYQPD	8.57	11.78
CuYQHD	19.75	18.16	CoYQHD	17.26	17.33	NiYQHD	15.65	18.79
CuYQDT	19.25	19.49	CoYQDT	18.75	24.40	NiYQDT	14.65	18.12

CAT-Catechol   DTBC-3,5-di-*tert*-butylcatechol

7.3.2 KINETIC STUDIES

We have studied the kinetics of the following four reactions.

1. The oxidation of catechol by hydrogen peroxide in the presence of YCuOPD (reaction 1),

2. Oxidation of catechol by hydrogen peroxide in presence of $Cu(OPD)_2$ (reaction 2),

3. Oxidation of DTBC by hydrogen peroxide in the presence of YCuOPD (reaction 3), and

4. Oxidation of DTBC by hydrogen peroxide in the presence of $Cu(OPD)_2$ (reaction 4).

The results obtained in the oxidation of catechol are presented in part I and those of DTBC in part II.

Part I
Kinetics of oxidation of catechol to o-benzoquinone using the zeolite encapsulated as well as the neat copper complexes of o-phenylenediamine

7.3.2.1 Results

a) Order with respect to catechol

When the kinetic runs were carried out in the presence of varying amounts of catechol ranging from 1.0×10^{-4} to 1.0×10^{-3} mol dm^{-3}, a plot of initial rate versus substrate concentration was linear passing through origin for both reactions 1 and 2 (Figure VII.1 a & b). This indicates that the order with respect to catechol was unity in both the reactions. The data obtained in this variation study is presented in Table.VII.2

Table VII.2
Effect of substrate variation on the initial rate for reactions 1 and 2

YCuOPD		Cu(OPD)$_2$	
[substrate] x 10^3 mol dm^{-3}	Initial rate x 10^7 mol dm^{-3} s^{-1}	[substrate] x 10^3 mol dm^{-3}	Initial rate x 10^7 mol dm^{-3} s^{-1}
0.3	0.13	0.4	2.45
0.7	0.23	0.6	3.86
1.0	0.33	0.8	4.76
1.5	0.58	1.0	5.79
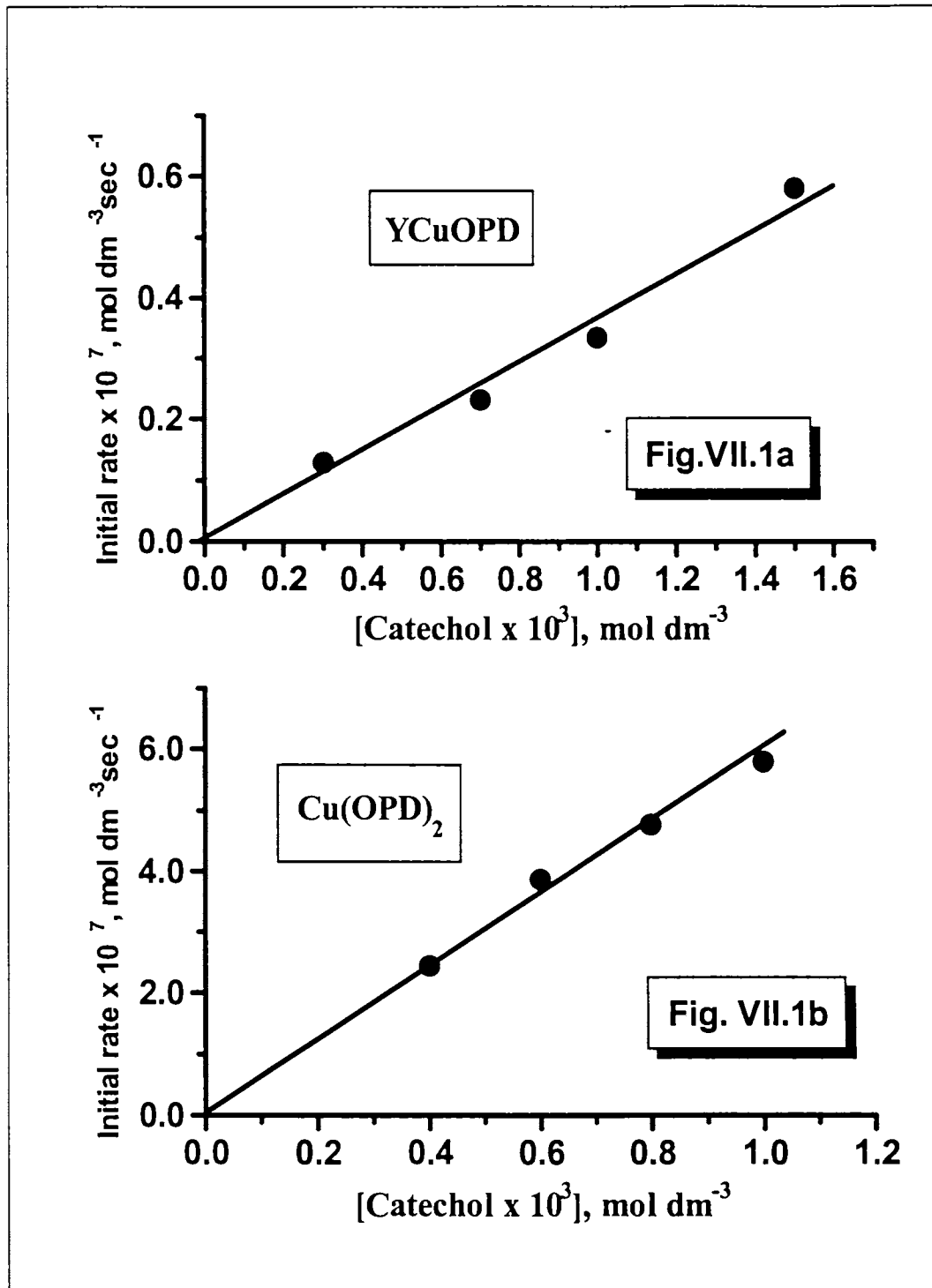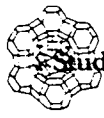
Figure VII. 1a and 1b. Effect of [Catechol] concentration on the initial

rate of reactions 1 and 2

b) Order with respect to H_2O_2

When the kinetic runs were carried out varying the H_2O_2 concentration in the range, 1.0×10^{-3} to 1.0×10^{-2} mol dm^{-3}, the order with respect to H_2O_2 was found to be unity as evident from a plot of initial rate versus $[H_2O_2]$ being linear passing through origin. The kinetic data is presented in Table VII.3

Table VII.3

Effect of $[H_2O_2]$ on the initial rate of reactions 1 and 2

YCuOPD		Cu(OPD)$_2$	
$[H_2O_2] \times 10^2$ mol dm^{-3}	Initial rate $\times 10^7$ mol dm^{-3} s^{-1}	$[H_2O_2] \times 10^2$ mol dm^{-3}	Initial rate $\times 10^7$ mol dm^{-3} s^{-1}
0.5	0.19	0.2	1.42
1	0.33	0.6	3.60
2	0.69	1	5.79
3	1.02	-	-

c) Order with respect to Catalyst

In order to make a comparison of rates of reaction, catalyst variation studies were carried out in such a way that the metal ion concentration of the catalyst in the reaction mixture varies in the same range, $(1.4\text{-}14.3) \times 10^{-5}$ mol dm^{-3}, for the supported as well as the neat complexes. When the initial rates thus obtained were plotted against the metal ion concentration of the catalyst, straight line passing through origin was obtained for both the

catalysts, indicating first with respect to catalyst for both the reactions. The kinetic data is presented in Table VII.4
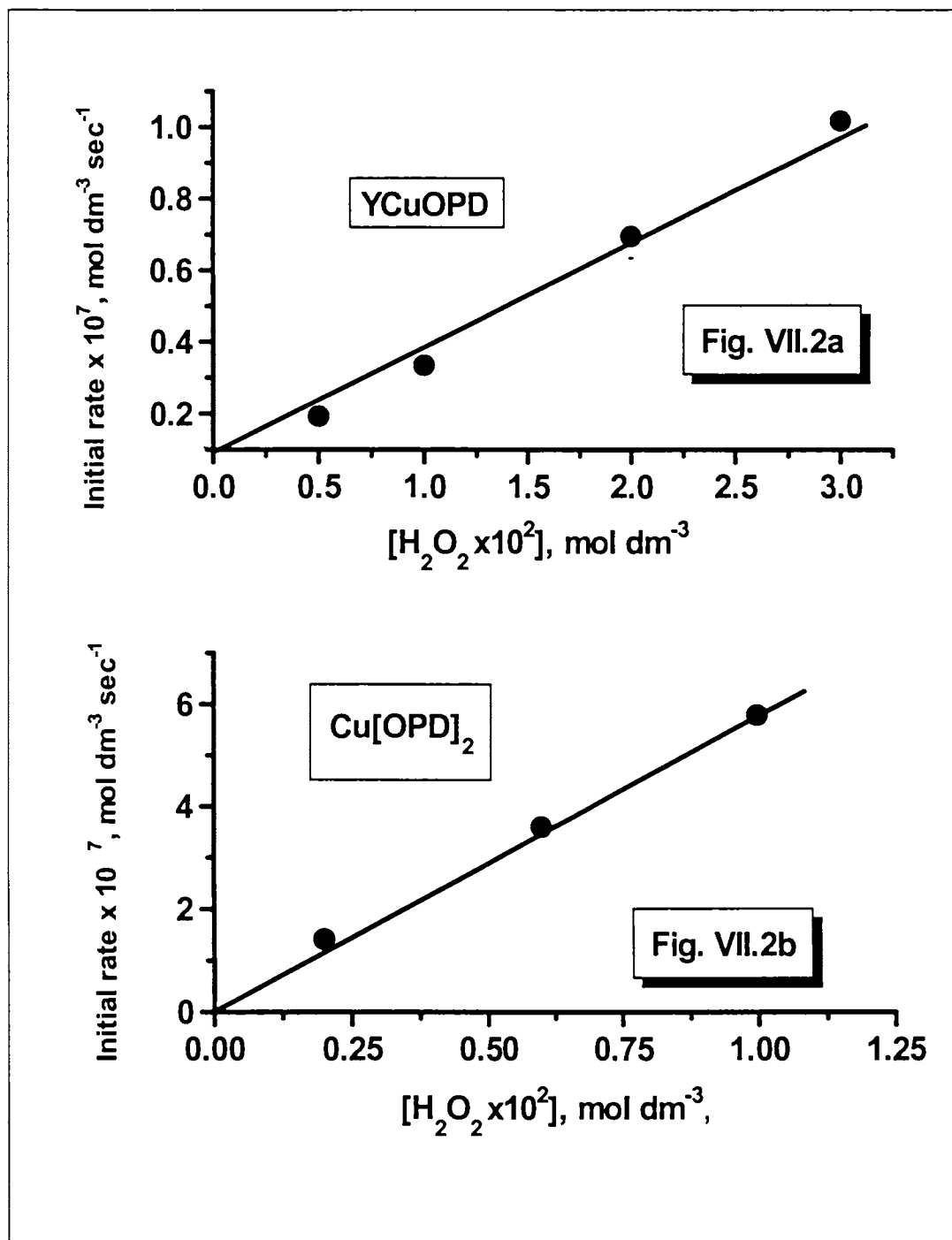

**Figure.VII.2a and 2b.** Effect of $[H_2O_2]$ on the initial rate of reactions 1 and 2
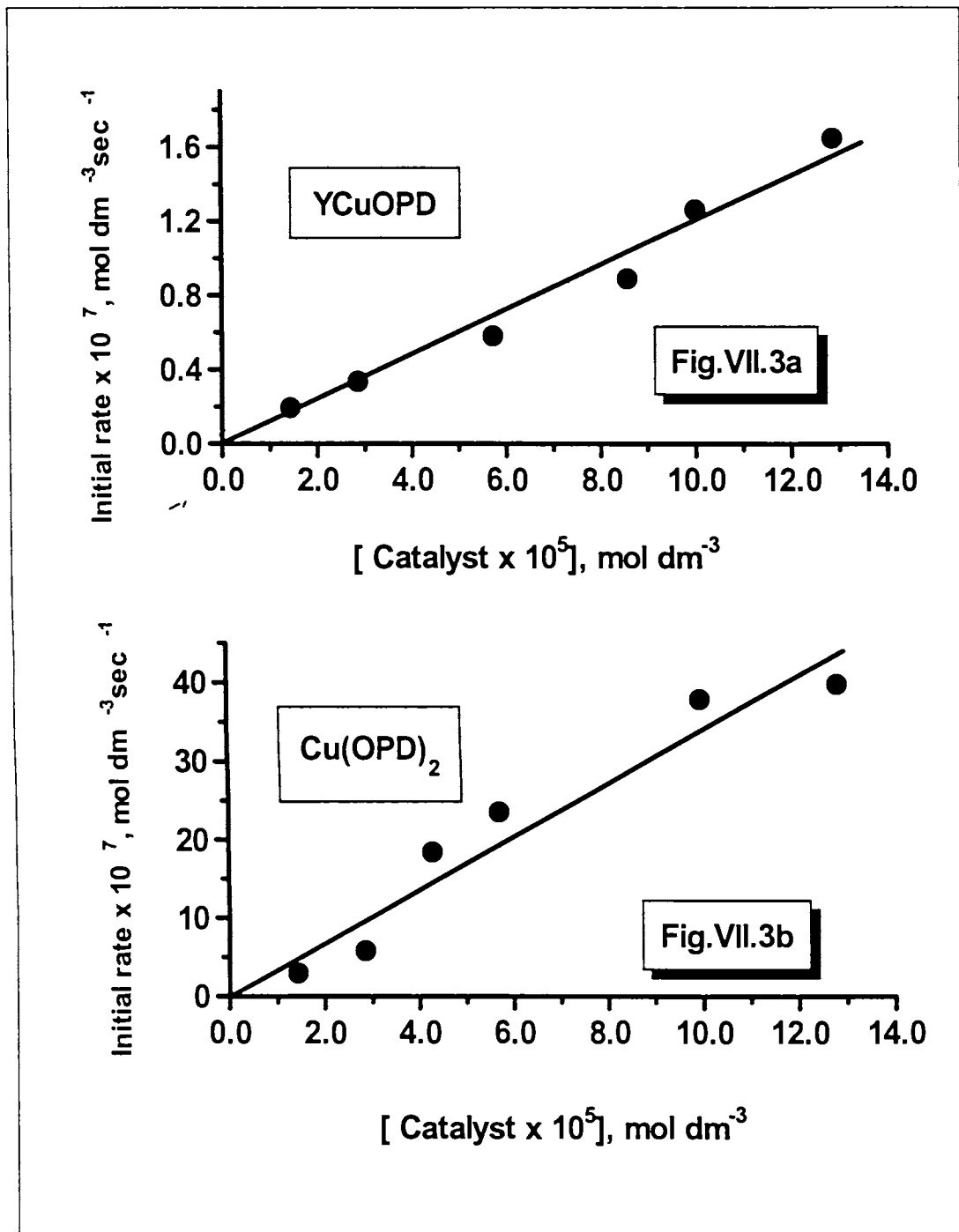
Figure VII. 3a and 3b. Effect of [Catalyst] on the initial rate of
reactions 1 and 2

Table VII.4

Effect of [catalyst] on the initial rate of reactions 1 and 2

YCuOPD		Cu(OPD)$_2$	
[catalyst] x 10^5	Initial rate x 10^7	[catalyst] x 10^5	Initial rate x 10^7
mol dm^{-3}	mol dm^{-3} s^{-1}	mol dm^{-3}	mol dm^{-3} s^{-1}
1.43	0.19	1.43	2.96
2.86	0.33	2.86	5.79
4.29	--	4.29	18.40
5.72	0.58	5.72	23.55
8.58	0.88		--
10.01	1.26	10.01	37.84
12.87	1.65	12.87	39.77

d)   Effect of varying dielectric constant

The influence of dielectric constant of the solvent on the reaction rate was studied by varying methanol to water ratio. When the dielectric constant of the medium is increased, the initial rate remains constant for reaction 1 and decreased for reaction 2. This suggests that a neutral species is involved in the rate determining step of reaction 1 and the active species of reaction 2 are of opposite charge. Kinetic results are presented in the Table VII.5.
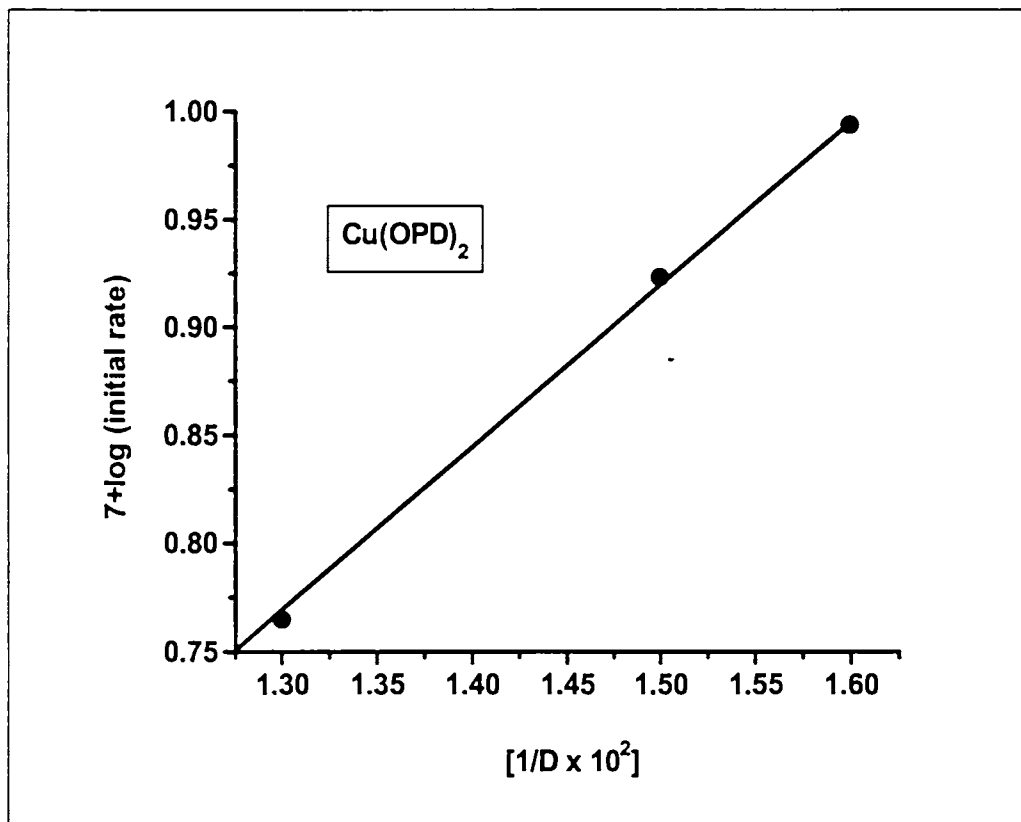
Figure VII.4. Effect of dielectric constant on the rate of reaction 2

Table VII.5

Effect of dielectric constant on the initial rate of reaction 2

D	Initial rate x 10^7 mol dm^{-3} sec^{-1}
0.77	5.81
0.67	8.37
0.63	9.86

e) Effect of varying pH

The pH dependence of the reaction rate in the oxidation of catechol was complex as may be seen from the summary of the results given in the Table VII.6 and plot are given in Figure. VII.5a-5d

Table VII.6.
Effect of pH on the initial rate of reactions 1 and 2

| Reaction	pH	(Initial rate)x 10^7, mol dm^{-3} s^{-1}	Remarks
Reaction 1	5.0	0.33	In the pH range 5-6.5, plot of 1/initial rate versus [H$^+$] is linear with intercept (FigureVII.5a).
	6.0	1.29	
	6.5	2.12	In the pH range 7-8 plot of 1/initial rate versus 1/[H$^+$] linear with intercept .(Figure. VII.5b)
	7.0	1.69	
	7.5	1.54	
	8.0	1.26	
Reaction 2	6.0	4.53	In the pH range 6-6.5, plot of initial rate versus [H$^+$] is linear with intercept (Figure. VII.5c).
	6.2	5.82	
	6.5	8.11	In the pH range 7-8 plot of initial rate versus 1/[H$^+$] linear with intercept (Figure. VII.5d).
	7.0	7.72	
	7.5	5.07	
	8.0	3.89	
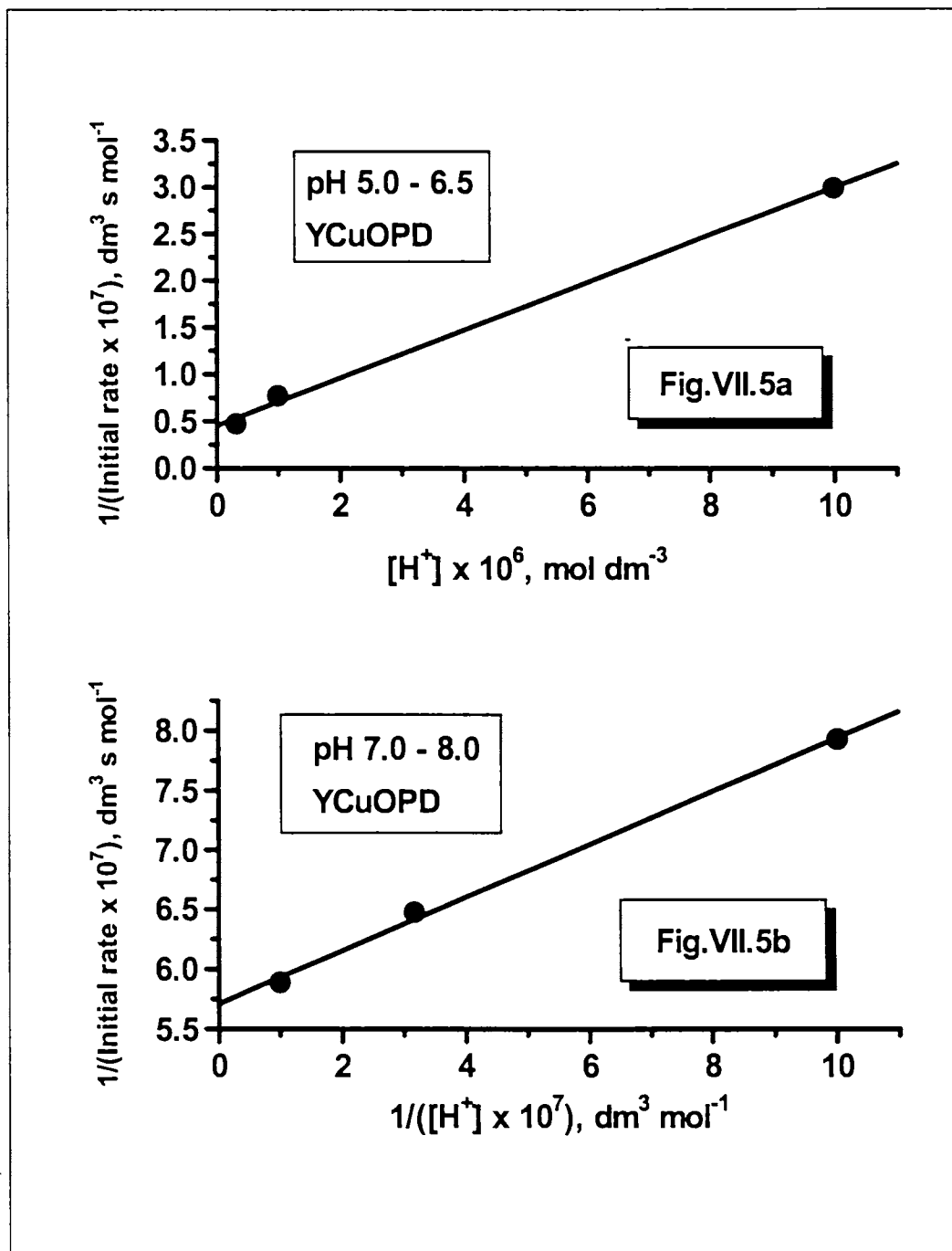
Figure VII.5a and 5b Effect of pH on the initial rate of reaction 1
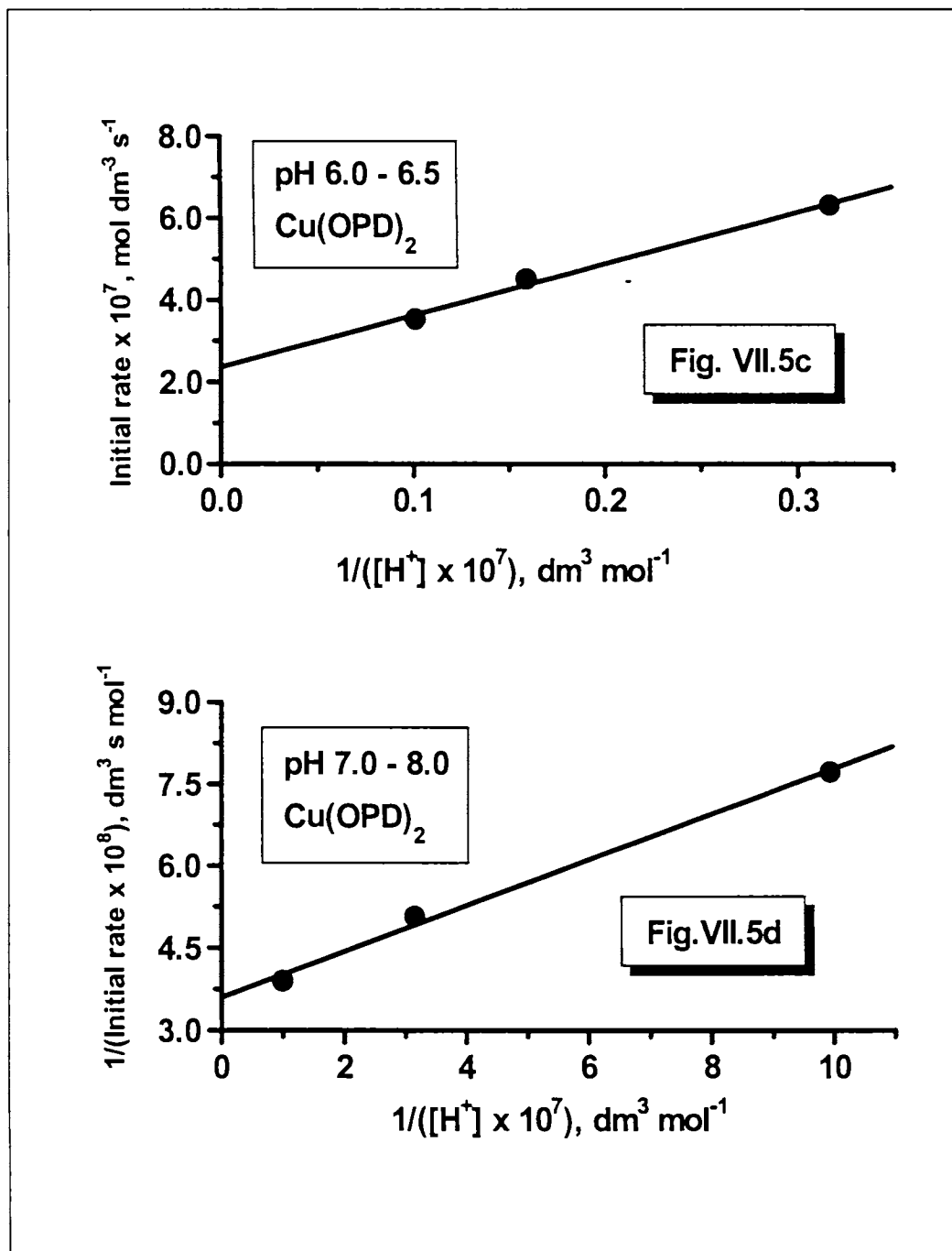
Figure VII. 5c and 5d Effect of pH on the initial rate of reaction 2
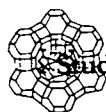
Part II
Kinetics of oxidation of 3,5-di-*tert*-butylcatechol to 3,5-di-*tert*-butyl-o-benzoquinone using the zeolite encapsulated as well as the neat copper complexes of *o*-phenylenediamine

To verify if steric factors can influence catalysis by the zeolite encapsulated as well as the neat complexes, we have studied the kinetics of oxidation of a substituted catechol, i.e., 3,5-di-*tert*-butylcatechol in the presence of the two catalysts. These two reactions are represented as reactions 3 and 4 at the beginning of this section. The observations made in this study are presented below.

7.3.2.2. Results

a)   Order with respect to DTBC

When DTBC concentration was varied in the same range as that of catechol i.e. from 1.0×10^{-3} to 1.0×10^{-2} mol dm^{-3}, a plot of initial rate against substrate concentration (FigureVII.6a & 6b) was linear indicating the order in DTBC to be unity for both the reactions.

Table VII.7
Effect of substrate on the reaction 3 and 4

YCuOPD		Cu(OPD)$_2$	
[substrate] x10^3 mol dm^{-3}	Initial rate x 10^7 mol dm^{-3} s^{-1}	[substrate] x 10^3 mol dm^{-3}	Initial rate x 10^7 mol dm^{-3} s^{-1}
0.2	0.54	0.2	5.53
0.3	0.81	0.4	10.04
0.4	0.80	0.6	12.40
0.5	1.15	0.8	17.52
0.8	1.55	1.0	24.59
1.0	2.29		
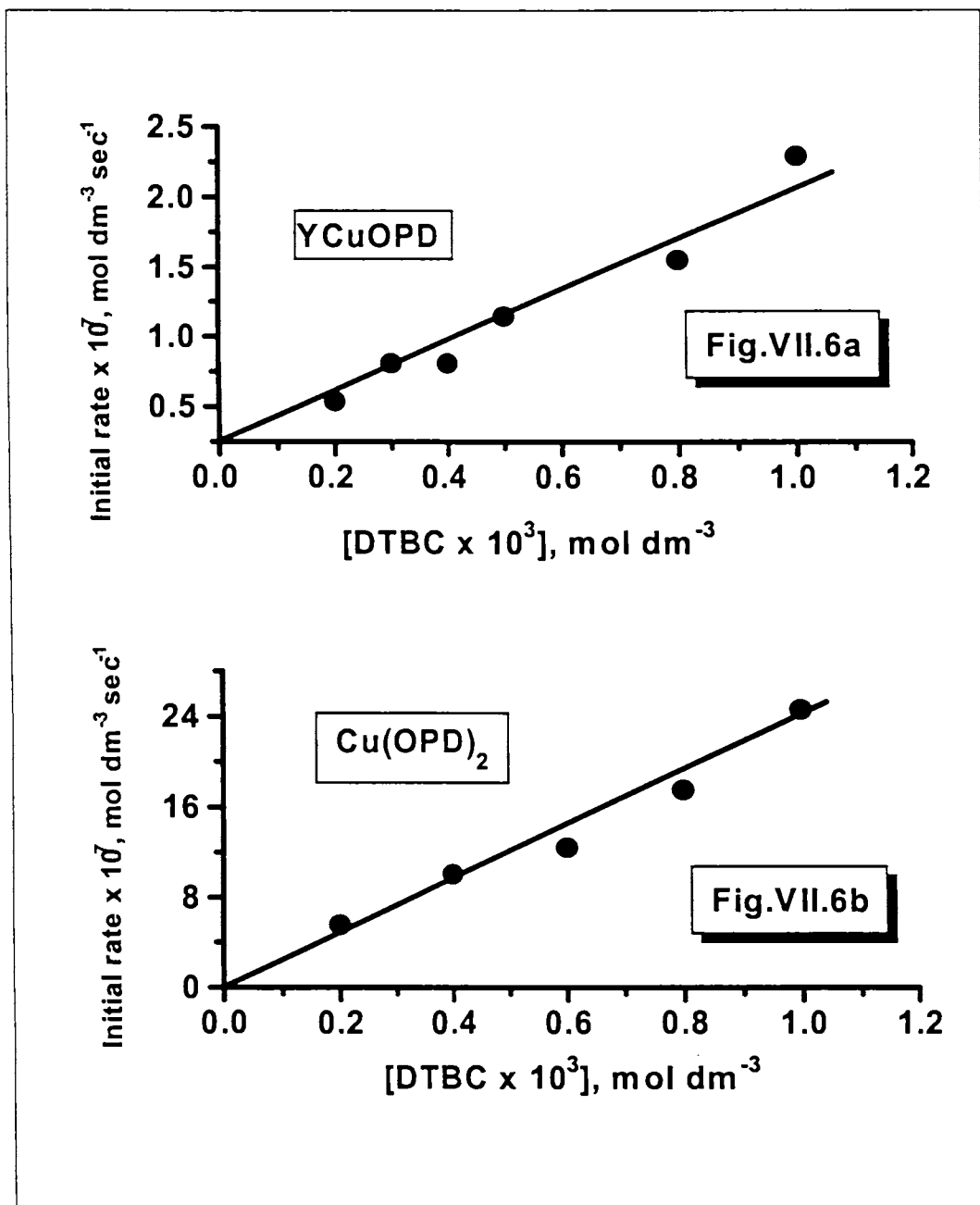
Figure VII.6a and 6b:Effect of [DTBC] on the initial rate of reactions 3 and 4

b)   Order with respect to H₂O₂

The kinetic runs carried out in the presence of varying concentrations of H_2O_2 in the range 0.01 to 0.1 mol dm^{-3} led to the data presented in TableVII.8. From this data, the order in hydrogen peroxide was inferred to be unity since a plot of initial rate versus H_2O_2 concentration was linear for reaction 3 as well as 4(Figure. VII.7a &7b).

Table.VII.8
Effect of H_2O_2 on the rates of reaction 3 and 4

YCuOPD		Cu(OPD)₂	
$[H_2O_2]\times10^3$ mol dm^{-3}	Initial rate x 10^7 mol dm^{-3} s^{-1}	$[H_2O_2]$ x 10^3 mol dm^{-3}	Initial rate x 10^7 mol dm^{-3} s^{-1}
0.2	0.47	0.2	5.39
0.6	1.42	0.4	10.92
0.7	1.68	0.8	20.96
0.8	1.95	1	24.60
1	2.29		

Figure VII. 7a and 7b. Effect of [H$_2$O$_2$] on the initial rate of reactions 3 and 4
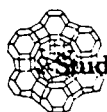
c) Order with respect to Catalyst

A plot of initial rate versus catalyst concentration (FigureVII 8a & 8b)was linear in the catalyst concentration range, $(1.4\text{-}14.3) \times 10^{-5}$ mol dm^{-3} for the encapsulated as well as the neat complex indicating first order with respect to catalyst.

Table.VII.9
Effect of Catalyst on the initial rate of reaction 3 and 4

YCuOPD		Cu(OPD)$_2$	
[Catalyst] x10^5 mol dm^{-3}	Initial rate x 10^7 mol dm^{-3} s^{-1}	[Catalyst] x 10^5 mol dm^{-3}	Initial rate x 10^7 mol dm^{-3} s^{-1}
2.86	2.29	2.86	12.06
4.29	3.17	4.29	21.49
7.15	5.60	5.72	28.98
		7.15	32.35
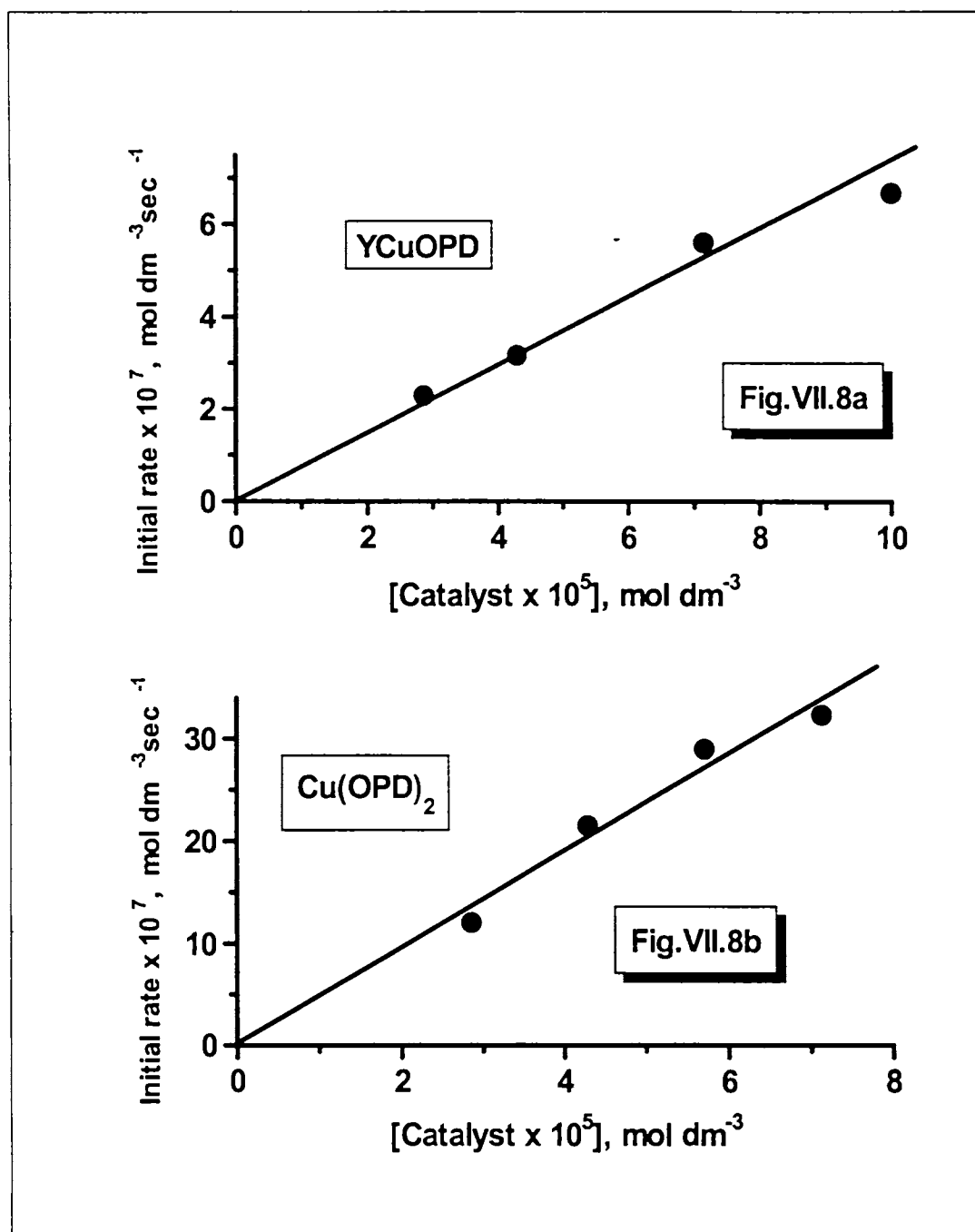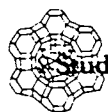
**Figure VII 8a and 8b.** Effect of [Catalyst] on the rate of reactions 3 and 4

d) Dielectric constant variation studies

When the dielectric constant of the medium was varied and the reaction rate was obtained, it was found that the initial rate increases with dielectric constant in the case of zeolite encapsulated complex whereas the rate decreased in the case of simple complexes (Figure. VII.9). Kinetic data is presented in the Table VII.10.

Table.VII.10

Effect of dielectric constant on the rate of the reactions 3 and 4

YCuOPD		Cu(OPD)$_2$	
D	(Initial rate)x10^7 mol dm^{-3} sec^{-1}	D	(Initial rate)x10^7 mol dm^{-3} sec^{-1}
0.77	2.24	0.77	12.04
0.71	1.82	0.71	15.58
0.66	1.45	0.66	21.25
0.63	1.32	0.63	26.76
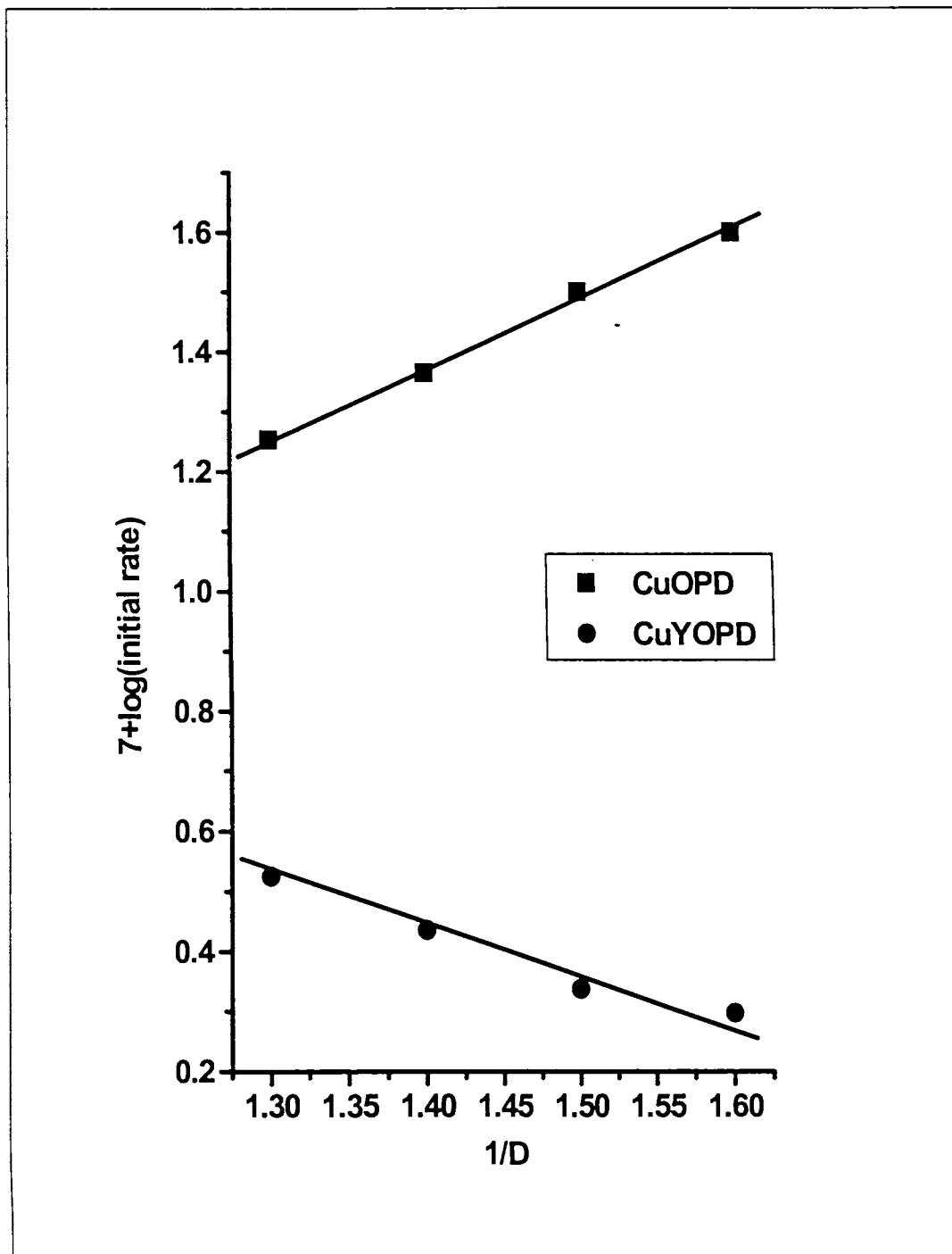
FigureVII.9 Effect of dielectric constant on the initial rate of

reactions 3 and 4

e) pH variation studies

The pH dependence was complex in this case also. The results obtained in this study are given in Table .VII.11.

Table VII.11:

Effect of pH on the reaction 3 and 4

| Reaction	pH	Initial rate x 10^7 mol dm^{-3} s^{-1}	Remarks
Reaction 3	5.0	2.26	In the pH range 5-6.5, plot of
	6.0	1.38	initial rate versus [H$^+$] is linear with intercept (Figure. VII.10a).
	6.5	1.29	In the pH range 7-8 plot of
	7.0	1.23	1/initial rate versus [H$^+$] linear
	7.5	2.61	with intercept(FigureVII.10b).
	8.0	4.09	
Reaction 4	6.0	4.95	From pH 6.5-8, plot of 1/initial
	6.5	12.19	rate versus [H$^+$] is linear with intercept (Figure. VII.10c).
	7.2	20.55	
	7.5	22.71	
	8.0	25.74	

Figure VII. 10a and10b Effect of pH on the initial rate of reaction 3
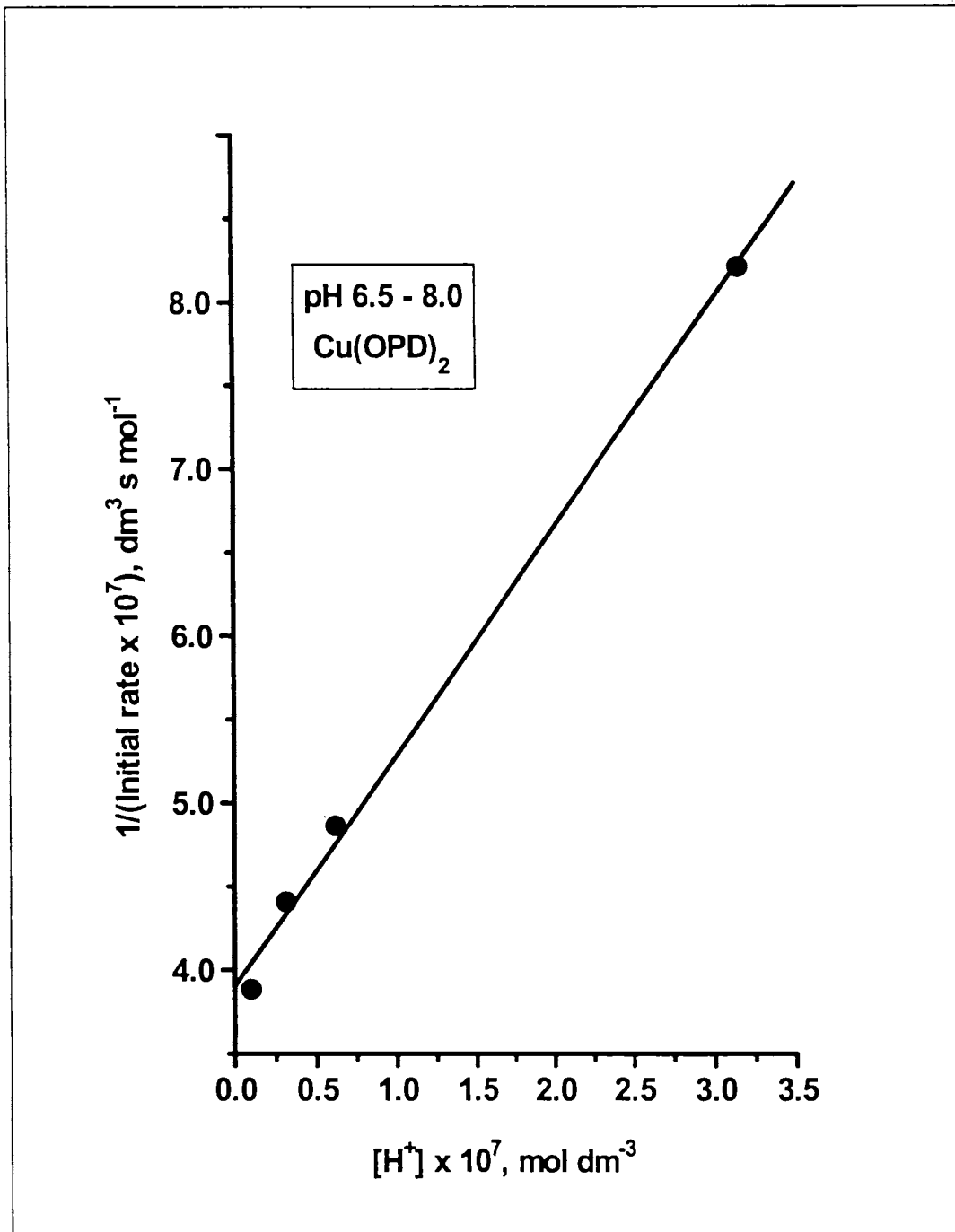
Figure. VII.10c Effect of pH on the initial rate of reaction 4

7.4. MECHANISM OF THE CATALYTIC REACTIONS

Copper catalyzed oxidations by hydrogen peroxide can proceed through either of the following mechanisms.

1. Copper metal is first reduced from +2 state to +1 state by hydrogen peroxide and the +1 state formed oxidizes the substrate.

2. Copper metal in the catalyst is first oxidized by hydrogen peroxide to higher oxidation state, +3. The +3 state formed then is reduced during the oxidation of the substrate.

3. The substrate is first oxidized by copper metal ion in the catalyst, in this process the copper metal ion is reduced. It is then subsequently oxidized by hydrogen peroxide.

The first case is not possible since the Cu^I thus formed cannot oxidize either DTBC or catechol. In the second case, Cu^{III} formed is expected to be unstable hence its reaction with DTBC/catechol is expected to be fast. Therefore, the rate of the reaction should be independent of the substrate concentration which contradicts the observed first order with respect to substrate in both the reactions. Hence, we assume that the oxidation of DTBC as well as catechol is proceeding through the third type of mechanism.

As given in Table 1, in reaction 1 in the pH range 5.0 – 6.5, a plot of 1/rate versus [H$^+$] was found to be linear with an intercept, while in the pH range 7.0 – 8.0, 1/rate versus 1/[H$^+$] plot was linear with an intercept. This shows that at high [H$^+$] the numerator of the rate equation does not bear

[H⁺]-term while at low [H⁺] it is present. This has led to a complex empirical rate equation,

$$\text{Rate} = \frac{a_1[H^+][H_2O_2]_t[\text{Catechol}]_t[YCu^{II}(OPD)_2]_t}{\{b_1 + c_1[H^+]\}\{d_1 + e_1[H^+]\}} \qquad (1)$$

Where it may be assumed that, $b_1 >> c_1[H^+]$ at low [H⁺] and $d_1 << e_1[H^+]$ at high [H⁺]. Equation (1) indicates that both catechol and YCuOPD exist in deprotonation equilibria.

In reaction 3 in the pH range 5.0 - 6.5, initial rate versus [H⁺] plot was linear while in the pH range 7.0 – 8.0, 1/initial rate versus [H⁺] plot is linear. Combining these two we obtain the empirical rate equation for this reaction as

$$\text{rate} = \frac{\{a_3 + b_3[H^+]\}\{c_3 + d_3[H^+]\}[H_2O_2]_t[\text{DTBC}]_t[YCu^{II}(OPD)_2]_t}{\{e_3 + f_3[H^+]\}} \qquad (2)$$

such that at high [H⁺] $e_3 << f_3$ [H⁺] and at low [H⁺], b_3 [H⁺] $<< a_3$ and d_3 [H⁺] $<< c_3$.

By comparing equation (1) and (2), it is easily understood that the term in the denominator of equation 2 arises due to the acid dissociation of YCuOPD, and it is equivalent to the term $\{d_1 + e_1[H^+]\}$ in equation (1). Further, from equation 2 it is understood that the dissociation constant of DTBC is much larger than [H⁺] in the entire pH range studied and therefore it has a magnitude greater than 10^{-6}.

Similar argument leads to empirical rate equations 3 and 4, given below, for reactions 2 and 4 respectively.

$$\text{Rate} = \frac{\{a_2 + b_2[H^+]\}\{c_2 + d_2[H^+]\}[H_2O_2]_t[\text{Catechol}]_t[Cu^{II}(OPD)_2]_t}{\{e_2 + f_2[H^+]\}\{g_2 + h_2[H^+]\}} \quad (3)$$

Where at high $[H^+]$ $g_2 << h_2[H^+]$ and $e_2 + f_2[H^+] = a_2 + b_2[H^+]$ and at low $[H^+]$, $e_2 >> f_2[H^+]$ and $\{g_2 + h_2[H^+]\} = \{c_2 + d_2[H^+]\}$.

$$\text{Rate} = \frac{a_4[H_2O_2]_t[\text{DTBC}]_t[Cu^{II}(OPD)_2]_t}{\{b_4 + c_4[H^+]\}} \quad (4)$$

Equation 3 suggests that all the four species are involved in the rate-determining steps of reaction 2. As has been mentioned earlier, the dissociation constant for the deprotonation of DTBC is much greater than $[H^+]$ and therefore acid term arising from that cannot be observed in the denominator of equation 4. Since no acid term is observed in the numerator of equation 4, it is obvious that unprotonated species of both are participating in the rate determining steps.

When the effect of dielectric constant on the reaction rates is considered, it may be seen that in reaction 1 one of the reactants is non-polar. From the dielectric and pH effects observed for this reaction it is not possible to decide whether the neutral species is that of catechol or the catalyst. However, we assume the neutral species to be that of the catalyst since it is reduced during the reaction. In reaction 2, one of the reactants is positive and the other is negative. It is obvious that both protonated and unprotonated $Cu(OPD)_2$ are positive species. Therefore the negative reactive species is that of catechol. This indicates that the unprotonated reactive species is that of catechol is the predominant reactive species at pH 6.2 where the dielectric effect was studied. In reaction 3, dielectric effect indicates that both the reactive species of DTBC and YCuOPD are

negatively charged at pH 5.0. This indicates that one of the species of YCuOPD is negatively charged. We assume that this species to be the unprotonated one and the protonated one to be neutral. In reaction 4 again the dielectric effect indicates one of the reactive species is positively charged while the other is negatively charged. Since in this case both the reactive species are unprotonated this further confirms that unprotonated $Cu(OPD)_2$ is positively charged.

Although the pH and dielectric effects indicated that the four reactions involve different reactive species, the order with respect to substrate, hydrogen peroxide and the catalyst was unity in all the four reactions suggesting that the mechanism of all these reactions is the same. Since the reaction is third ordered, we assume formation copper(I) intermediate from the catalyst by interaction with the substrate which is subsequently oxidized by hydrogen peroxide. Thus the mechanism of the four reactions may be represented as shown in schemes I, II, III and IV respectively.

$$[YCuOPD] + H_2O \rightleftharpoons [YCuOPD(OH)]^- + H^+$$

$$HCAT \rightleftharpoons CAT^- + H^+$$

$$[YCu^{II}(OPD)_2] + CAT^- \longrightarrow [CAT]^\bullet + [YCu^I(OPD)_2]$$

$$2[YCu^I(OPD)_2] + 2H_2O_2 \xrightarrow{\text{(slow)}} 2[YCu^{II}(OPD)_2] + 2H_2O + O_2$$
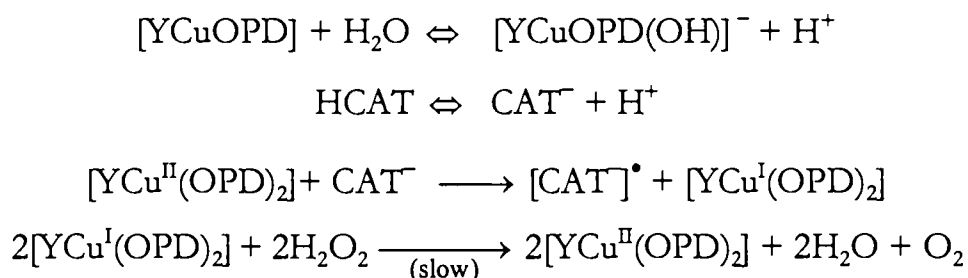
Scheme I : Mechanism of reaction 1

$$[Cu^{II}(OPD)_2]^{2+} + H_2O \Leftrightarrow [Cu^{II}(OPD)_2(OH)]^+ + H^+$$

$$CAT \Leftrightarrow CAT^- + H^+$$

$$[Cu^{II}(OPD)_2]^{2+} + CAT \longrightarrow [CAT^+] + [Cu^{I}(OPD)_2]^+$$

$$[Cu^{II}(OPD)_2(OH)]^+ + CAT \longrightarrow [CAT^+] + [Cu^{I}(OPD)_2(OH)]$$

$$[Cu^{II}(OPD)_2]^{2+} + CAT^- \longrightarrow [CAT]^\bullet + [Cu^{I}(OPD)_2]^+$$

$$[Cu^{II}(OPD)_2(OH)]^+ + CAT^- \longrightarrow [CAT]^\bullet + [Cu^{I}(OPD)_2(OH)]$$

$$2[Cu^{I}(OPD)_2]^+ + 2H_2O_2 \xrightarrow[\text{(slow)}]{} 2[Cu^{II}(OPD)_2]^{2+} + 2H_2O + O_2$$

$$2[Cu^{I}(OPD)_2(OH)] + 2H_2O_2 \xrightarrow[\text{(slow)}]{} 2[Cu^{II}(OPD)_2(OH)]^+ + 2H_2O + O_2$$
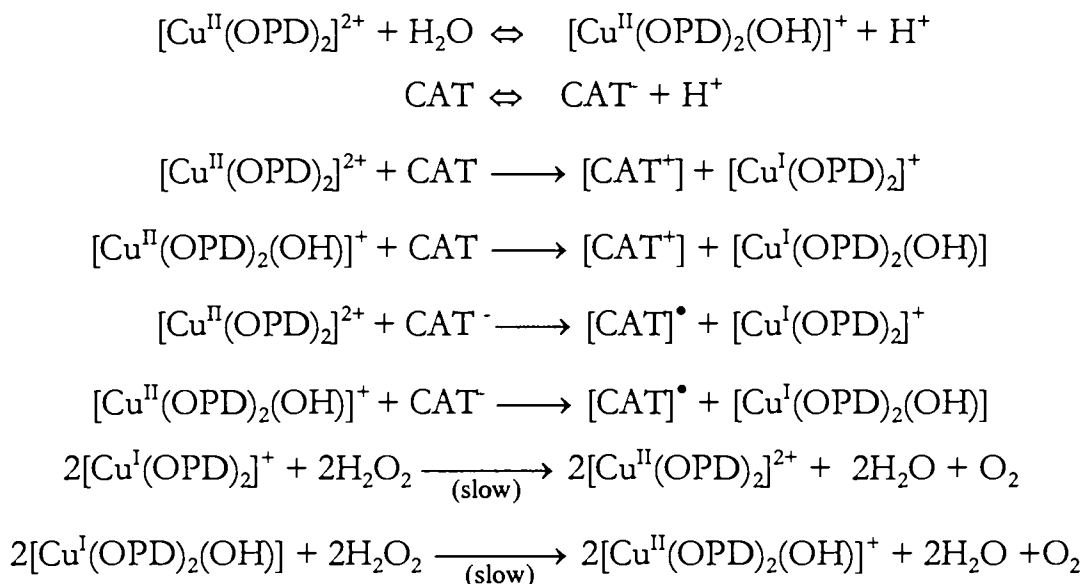
Scheme II : Mechanism of reaction 2

$$[YCu^{II}(OPD)_2] + H_2O \Leftrightarrow [YCu^{II}(OPD)_2(OH)]^- + H^+$$

$$HDTBC \Leftrightarrow DTBC^- + H^+$$

$$[YCu^{II}(OPD)_2] + HDTBC \longrightarrow [HDTBC^+] + [YCu^{I}(OPD)_2]^-$$

$$[YCu^{II}(OPD)_2(OH)]^- + HDTBC \longrightarrow [HDTBC^+] + [YCu^{I}(OPD)_2(OH)]^{2-}$$

$$[YCu^{II}(OPD)_2] + DTBC^- \longrightarrow [DTBC]^\bullet + [YCu^{I}(OPD)_2]^-$$

$$[YCu^{II}(OPD)_2(OH)]^- + DTBC^- \longrightarrow [DTBC]^\bullet + [YCu^{I}(OPD)_2(OH)]^{2-}$$

$$2[YCu^{I}(OPD)_2]^- + 2H_2O_2 \xrightarrow[\text{(slow)}]{} 2[YCu^{II}(OPD)_2] + 2H_2O + O_2$$

$$2[YCu^{I}(OPD)_2(OH)]^{2-} + 2H_2O_2 \xrightarrow[\text{(slow)}]{} 2[YCu^{II}(OPD)_2(OH)]^- + 2H_2O + O_2$$
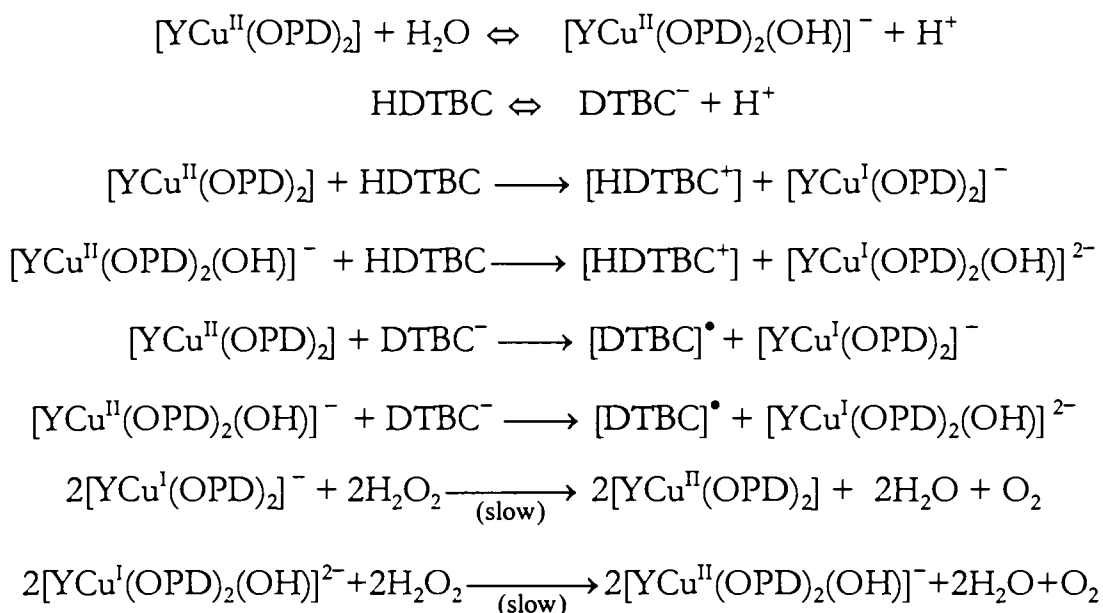
Scheme III : Mechanism of reaction 3

191

$$[Cu(OPD)_2]^{2+} + H_2O \Leftrightarrow [Cu(OPD)_2(OH)]^+ + H^+$$

$$HDTBC \Leftrightarrow DTBC^- + H^+$$

$$[Cu^{II}(OPD)_2(OH)]^+ + DTBC^- \longrightarrow [DTBC]^\bullet + [Cu^I(OPD)_2(OH)]$$

$$2[Cu^I(OPD)_2(OH)] + 2H_2O_2 \xrightarrow[\text{(slow)}]{} 2[Cu^{II}(OPD)_2(OH)]^+ + 2H_2O + O_2$$
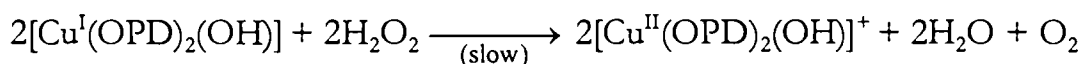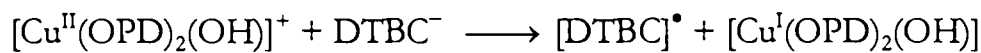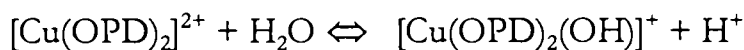
Scheme IV : Mechanism of reaction 4

-

Conclusions

The present study indicated that the mechanism of oxidation of catechol and DTBC by hydrogen peroxide is not altered by the change in the coordination sphere around the metal ion due to encapsulation. This fact suggests outer sphere mechanism for the reactions. However, the catalysis by zeolite encapsulated complex was slower than that by the neat complex. The slowing down of the reaction in the zeolite case is probably due to the constraint imposed by the zeolite framework. The rate of DTBC oxidation was found to be greater than the rate of catechol oxidation. This is obviously due to the electron donating tertiary butyl groups present in the benzene ring.

G78262

REFERENCES

1. L.L. Ingraham, *Arch.Biochem.Biophy.* 81 **(1959)** 309.

2. J.H. Wang, *Acc.Chem.Res.* 3 **(1970)** 90.

3. V.S. Sharma, J. Schubert, *Inorg.Chem* 10 **(1971)** 251.

4. J.R Gillette, D.Walland, G. Kalnilsky, *Biochem Biophy.Acta.*15**(1954)** 520.

5. H. Siegel *Angew.Chem.Int.Ed.Engl.* 18 **(1969)** 3.

6. R.Hollenstein, W.V.Philipsborn, *Helv.chim.Acta.* 56 **(1973)** 320.

7. N.Uri, *Chem.Rev.* 50 **(1952)** 375.

8. J.A. Connon, E.A.V. Ebsworth, *Advance.Inorg.Chemistry and Radiochemistry* 6 **(1964)** 279.

9. H.B. Jonasen, H. Thielmann, *Z.anorg.allg.chem.* 320 **(1963)** 274.

10. J.H. Wang, *J.Am.Chem.Soc.* 77 **(1955)** 4715.

11. B. Kirson, *Bull.Soc.Chim.France* **(1954)**157.

12. A.S. Brill, R.B. Martin, R.J. Williams, *Biochem.Proc.Int.symposium* **(1963)** 519.

13. Allyward Bacon, *Bioinorganic Chemistry,* Boston **(1977)** 218.

14. D.E, Fenton, R.L Lintvedt, *J.Am.Chem.Soc.*100 **(1978)** 6367.

15. D.E Fenton, R.R. Schroeder, R.L Lintvedt, *J.Am.Chem.Soc.* 100 **(1978)** 1931.

16. G.H. Jeffery, J. Bassett, J. Mendham, R.C. Denney, *Vogel's Textbook of Quantitative Inorganic Analysis*-5th Edition-Elbs-Longman Singapore publishers**(1991).**

17. E.J. Duff, *J.chem.Soc.* (A) **(1968)** 434.

SUMMARY AND CONCLUSIONS

The thesis deals with the synthesis, characterization and catalytic activity studies of supported cobalt(II), nickel(II) and copper(II) complexes of *o*-phenylenediamine and Schiff bases derived from 3-hydroxyquinoxaline-2-carboxaldehyde. Zeolite encapsulation and polymer anchoring was employed for supporting the complexes. The characterization techniques proved that the encapsulation as well as polymer supporting has been successfully achieved. The catalytic activity studies revealed that the activity of the simple complexes are improved upon encapsulation.

The thesis is divided into seven chapters. **Chapter I** presents an introduction to the studies on the zeolite encapsulated complexes and polymer supported complexes. The various applications of zeolite encapsulated and polymer supported complexes are also discussed.

Chapter II deals with the brief account on various experimental techniques employed in the present study. Information about the various reagents used for the synthesis of the ligands and complexes and those used for catalytic activity and kinetic study and information about the preparation of Schiff bases of 3-hydroxyqunioxaline-2-carboxaldehyde with ethylenediamine, *o*-phenylenediamine, hydrazine hydrate, diethylenetriamine

and the methods employed for modification of the support to facilitate immobilization are presented in this chapter. The details about various characterization techniques employed for the present study such as chemical analysis, EPR, magnetic measurements, FTIR studies, thermal analysis, electronic spectra, XRD, SEM, surface area, and GC are also given in this chapter.

Chapter III deals with the synthesis and characterization of zeolite encapsulated metal complexes of an aromatic diamine- o-phenylenediamine. Elemental analysis was used to obtain the unit cell composition. The Si/Al ratio of metal exchanged zeolites is same as that of the NaY, indicating that there is no collapse of the framework due to dealumination. The XRD pattern supports this conclusion. Surface area and pore volume studies gave evidence for the encapsulation of metal complexes. The absence of any metal complexes on the outer surface was obtained from SEM studies. FTIR data indicated that the coordination of o-phenylenediamine to the metal is through the nitrogen of the amino group. All the complexes have a tetragonally distorted octahedral structure. TG studies could provide some idea on the relative thermal stability of the various encapsulated complexes.

Chapter IV presents our studies on the synthesis and characterization of Schiff base of 3-hydroxyquinoxaline-2-carboxaldehyde. The Si/Al ratio was same as that in NaY in this case also. The XRD pattern of the complexes indicates the retaining of the framework. The simple complexes of the above Schiff bases were reported to show interesting magnetic properties due to the presence of quinoxaline ring

which is electron deficient. This leads to lesser ligand field splitting. Comparison of structure of the zeolite encapsulated complexes and the simple complexes were done based on the characterization techniques such as EPR, diffuse reflectance and a qualitative magnetic moment study. The simple cobalt complexes of the ligand QED and QHD were reported to be dimers, which become octahedral and square pyramidal when encapsulated. The simple QPD complex, which is square planar and monomeric became tetragonally distorted octahedral in the zeolite. The cobalt complex of the ligand QDT is EPR active and hence assigned a square pyramidal geometry. This is also supported by the electronic spectra. The neat nickel complexes of QED and QHD which were reported to be dimers became tetrahedral and octahedral inside the cages. The YNiQDT and YNiQPD complexes encapsulated in zeolite Y are octahedral. The copper QED complex was pseudotetrahedral and all the other copper complexes were found to have tetragonally distorted octahedral structure.

Chapter V deals with the synthesis and characterization of polymer supported complexes. The cobalt(II), nickel(II), and copper(II) complexes of the ligand, PSOPD and PSHQAD were prepared and characterized. PSOPD was obtained by condensing of polymer bound aldehyde with o-phenylenediamine. PSHQAD was prepared by condensing polymer bound amine with 3-hydroxyqunioxaline-2-carboxaldehyde. The surface area analysis in this case also indicates the formation of the complexes. The FTIR spectroscopy was used to confirm the coordination of azomethine nitrogen to the metal. The EPR and diffuse reflectance UV-Vis studies were used to predict the probable structure of the complexes. The cobalt

complexes of PSOPD are square planar and that of PSHQAD is square pyramidal. The nickel complexes of PSOPD and PSHQAD are octahedral. The complexes, Cu(II)PSOPD and Cu(II)PSHQAD, are octahedral and pseudotetrahedral respectively. TG data indicate that the PSHQAD complexes are more stable than the PSOPD complexes.

Chapter VI deals with catalytic activity studies of the zeolite encapsulated catalysts toward phenol hydroxylation using H_2O_2 as oxidant. The copper complexes are found to be most active. A comparative study of the activity of the simple complexes and encapsulated complexes was carried out. An optimum time of four hours was selected for phenol hydroxylation. Water was found to be the best solvent. Inspite of the higher metal percentage in the simple complexes, the conversion was higher for the zeolite encapsulated complexes. There was greater selectivity towards industrially more useful product, hydroquinone, and there was less tar formation in the case of zeolite encapsulated complexes. The encapsulated complexes were found to retain their catalytic activity even at higher temperature.

Chapter VII deals with a kinetic study of the zeolite encapsulated as well as the neat copper OPD complexes in the oxidation of catechol (CAT) as well as 3,5-di-tert-butylchatechol (DTBC). The present study indicated that the mechanism of oxidation of catechol and DTBC by hydrogen peroxide is not altered by the change in the coordination sphere around the metal ion due to encapsulation. This fact suggests outer sphere mechanism for the reactions. However, the catalytic activity by zeolite encapsulated

complex was found to be slower than that by the neat complex. The slowing down of the reaction in the zeolite case is probably due to the constraint imposed by the zeolite framework. The rate of DTBC oxidation was found to be greater than the rate of catechol oxidation. This is obviously due to the presence of electron donating tertiary butyl groups.

** -

ଔଔଔଔଔ
**